

Distribution Agreement

In presenting this thesis or dissertation as a partial fulfillment of the requirements for an advanced degree from Emory University, I hereby grant to Emory University and its agents the non-exclusive license to archive, make accessible, and display my thesis or dissertation in whole or in part in all forms of media, now or hereafter known, including display on the world-wide web. I understand that I may select some access restrictions as part of the online submission of this thesis or dissertation. I retain all ownership rights to the copyright of the thesis or dissertation. I also retain the right to use in future works (such as articles or books) all or part of this thesis or dissertation.

Signature:

Mary Krista Herrick

Date

The impact of LRRK2 expression and kinase activity in gene by
environment mouse models of Parkinson's disease

By

Mary Krista Herrick
Doctor of Philosophy

Graduate Division of Biological and Biomedical Sciences
Neuroscience Program

Malú G. Tansey, Ph.D.
Advisor

Francisco Alvarez, Ph.D.
Committee Member

W. Michael Caudle, Ph.D.
Committee Member

Ellen Hess, Ph.D.
Committee Member

Jacob Kohlmeier, Ph.D.
Committee Member

Andrew Neish, M.D.
Committee Member

Accepted:

Lisa A. Tedesco, Ph.D.
Dean of the James T. Laney School of Graduate Studies

Date

The impact of LRRK2 expression and kinase activity in gene by
environment mouse models of Parkinson's disease

By

Mary Krista Herrick
B.S., Auburn University, 2013

Advisor: Malú G. Tansey, Ph.D.

An abstract of a
dissertation submitted to the Faculty of the
James T. Laney School of Graduate Studies of Emory University
in partial fulfillment of the requirements for the degree of
Doctor of Philosophy in Neuroscience
2020

ABSTRACT

The impact of LRRK2 expression and kinase activity in gene by environment mouse models of Parkinson's disease

By Mary Krista Herrick

Extensive research has shown that Parkinson's disease (PD) is a multifactorial disease with age, genetics, and environmental factors all contributing to risk for development of PD over an individual's lifespan. The perfect combination of factors creates an environment in which peripheral and brain inflammation shift from protective to deleterious roles and promote PD pathogenesis. However, models exploring the multifaceted components of PD, especially in the context of one of the greatest genetic contributors to PD, Leucine-Rich Repeat Kinase 2 (LRRK2), in the immune system are vastly underexplored given that most PD LRRK2-related research has focused on the neuron. With the knowledge that LRRK2 is highly expressed in immune cells, the question of whether LRRK2 expression and phosphorylation regulates immune cell effector functions that then promote peripheral inflammation associated with PD and other immune diseases has now been brought to the forefront of the PD field.

We hypothesize that LRRK2 functions in immune cells to regulate effector functions and responses to inflammatory stress; but whether LRRK2 activation hastens protective or deleterious inflammatory responses when its levels increase in cells during inflammation remains to be determined, as do the effects of pathogenic LRRK2 mutations that increase risk for PD. To address this knowledge gap, in this doctoral dissertation we have utilized BAC transgenic LRRK2 mouse models overexpressing mouse wildtype LRRK2 or LRRK2 G2019S in all cells that endogenously express LRRK2. The aims of this research were to examine how 1) increased LRRK2 protein and or G2019S-dependent kinase activity affects immune cell profiles *in vivo* as a function of age; and 2) to investigate the extent to which specific environmental factors implicated in PD (bacterial and viral infections, colitis, and pesticides) act as second hits in the LRRK2 mice to promote PD-associated neuroinflammation and neuropathology. Here we report that increased

LRRK2 protein or G2019S-dependent gain-of-function kinase activity does not alter immune cell profiles with aging. Additionally, we report that a second hit in the form of colitis, but not pesticides or bacterial and viral infections, in mice with increased mutant LRRK2 enhance neuroinflammation to promote neurotoxicity in the nigrostriatal pathway, resulting in PD-like neuropathology. Completion of the studies will advance our understanding of the role of LRRK2 in immune cells and alterations in the latter as a consequence of pathogenic mutations; such knowledge is a prerequisite to development of LRRK2-targeted therapeutics that will protect the brain without detrimental or untoward effects on immune system function in the fight against idiopathic and familial forms of PD.

The impact of LRRK2 expression and kinase activity in gene by
environment mouse models of Parkinson's disease

By

Mary Krista Herrick
B.S., Auburn University, 2013

Advisor: Malú G. Tansey, Ph.D.

A dissertation submitted to the Faculty of the
James T. Laney School of Graduate Studies of Emory University
in partial fulfillment of the requirements for the degree of
Doctor of Philosophy in Neuroscience
2020

ACKNOWLEDGEMENTS

First and foremost, I am extremely thankful and grateful to Dr. Malú Tansey for her mentorship and guidance over the years. Her support and mentorship have shaped me into a budding female neuroscientist. I hope that I can carry on her legacy and make her proud no matter where my future takes me. I would like to acknowledge Tansey lab members past and present, as they are the scientific team that has helped me not only in the laboratory but also outside of the laboratory as friends and mentors. Thank you to my committee members for their endless support and guidance in the science as well as my professional development. Lastly and most importantly, I would like to thank my friends and family, whose love and support has shaped me to be the woman I am today and complete this major milestone. This would not have been possible without you.

TABLE OF CONTENTS

CHAPTER 1: BACKGROUND AND LITERATURE REVIEW

1.1: Parkinson's disease.....	1
1.2: PD as a multifactorial disease.....	2
1.2.1: Aging.....	3
1.2.2: Genetics.....	3
1.2.3: Environmental exposures and lifestyles.....	4
1.3: The aging immune system.....	6
1.4: Evidence for the immune system playing a role in PD pathogenesis.....	7
1.4.1: Cellular evidence for inflammation playing a role in PD pathogenesis.....	8
1.4.1.1: Innate immunity – Microglia.....	8
1.4.1.2: Innate immunity – Monocytes.....	10
1.4.1.3: Adaptive immunity – T and B cells.....	11
1.4.2: Epidemiological evidence linking the immune system and PD.....	13
1.4.2.1: PD genetic susceptibility linked to immune-associated genes.....	13
1.4.2.2: Non-steroidal anti-inflammatory drugs.....	14
1.4.2.3: Autoimmune disorders.....	15
1.5: Leucine-Rich Repeat Kinase 2 (LRRK2) in PD.....	16
1.5.1: LRRK2 structure, function, and expression.....	17
1.5.2: LRRK2 animal models.....	24
1.5.3: LRRK2 and the immune system.....	26
1.5.3.1: LRRK2 expression in brain-resident and peripheral blood immune cells.....	27
1.5.3.2: LRRK2 regulation of immune cell function.....	28
1.5.3.3: LRRK2 in inflammation.....	31
1.5.3.4: LRRK2 epidemiologically linked to inflammatory diseases.....	33
1.5.3.5: LRRK2 association with bacterial infection models.....	34

1.5.3.6: LRRK2 and α -synuclein.....	35
1.6: Parkinson's disease and the gastrointestinal system.....	36
1.6.1: Non-motor symptoms linked to GI dysfunction.....	36
1.6.2: GI dysbiosis in PD.....	37
1.6.3: GI α -synuclein pathology in PD.....	38
1.6.4: Epidemiological evidence linking PD and IBD.....	39
1.6.5: Similar phenotypes associated with PD and IBD.....	41
1.6.6: LRRK2: linking PD and CD.....	42
1.6.7: Modeling colitis in animal models.....	45
1.6.8: Evidence linking colitis and PD-associated neuropathology in animal models.....	45
1.6.9: LRRK2 in colitis models.....	48
1.7: Discussion.....	50

CHAPTER 2: LONGITUDINAL DEEP-IMMUNOPROFILING OF PERIPHERAL IMMUNE CELL SUBSETS IN WILDTYPE AND G2019S MUTANT LRRK2 BAC TRANSGENIC MICE

2.1: Abstract.....	52
2.2: Introduction.....	53
2.3: Materials and Methods.....	55
2.4: Results.....	59
2.5: Discussion.....	65

CHAPTER 3: INTESTINAL INFLAMMATION IN LRRK2 G2019S BAC TRANSGENIC MICE PROMOTES NEUROINFLAMMATION AND PD-ASSOCIATED NIGROSTRIATAL PATHOLOGY

3.1: Abstract.....	69
3.2: Introduction.....	70
3.3: Materials and Methods.....	73

3.4: Results.....	83
3.5: Discussion.....	98
CHAPTER 4: THE EFFECTS OF LRRK2 AND CHRONIC PESTICIDE EXPOSURE IN WT OR G2019S OVEREXPRESSING MICE	
4.1: Abstract.....	105
4.2: Introduction.....	106
4.3: Materials and Methods.....	108
4.4: Results.....	116
4.5: Discussion.....	122
4.6: Acknowledgements.....	125
CHAPTER 5: THE EFFECTS OF VIRAL OR BACTERIAL INFECTION EXPOSURE IN WT OR G2019S OVEREXPRESSING MICE	
5.1: Abstract.....	126
5.2: Introduction.....	127
5.3: Materials and Methods.....	129
5.4: Results.....	133
5.5: Discussion.....	139
5.6: Acknowledgements.....	141
CHAPTER 6: DISCUSSION AND FUTURE DIRECTIONS	
6.1: Summary.....	142
6.2: Discussion of results.....	142
6.3: Future directions.....	143
6.4: Conclusions.....	146
REFERENCES.....	148

FIGURES AND TABLES

CHAPTER 1: BACKGROUND AND LITERATURE REVIEW

Figure 1.1: Age-related alterations in immune cell populations and function.....	7
Figure 1.2: LRRK2 structure and phosphorylation activity.....	18
Figure 1.3: Relative human LRRK2 expression.....	24
Figure 1.4: LRRK2 immune cell expression at the interface of PD and CD.....	44

CHAPTER 2: LONGITUDINAL DEEP-IMMUNOPROFILING OF PERIPHERAL IMMUNE CELL SUBSETS IN WILDTYPE AND G2019S MUTANT LRRK2 BAC TRANSGENIC MICE

Figure 2.1: Flow cytometry gating strategy used to analyze mouse PBMC immune cell subsets.....	57
Figure 2.2: Overexpression of WT and G2019S LRRK2 increases LRRK2 levels and LRRK2 autophosphorylation (pSer1292).....	60
Figure 2.3: Similar immune cell profiles in aging WTOE and G2019S non-Tg littermate controls.....	62
Figure 2.4: LRRK2 expression levels and LRRK2 kinase activity levels do not affect aging immune cell profiles.....	63
Figure 2.5: Plasma cytokine levels increase as a function of age.....	64

CHAPTER 3: INTESTINAL INFLAMMATION IN LRRK2 G2019S BAC TRANSGENIC MICE PROMOTES NEUROINFLAMMATION AND PD-ASSOCIATED NIGROSTRIATAL PATHOLOGY

Figure 3.1: Study designs of DSS-induced colitis models.....	74
Table 3.1: Criteria for calculation of disease activity index (DAI) for colitis studies.....	75
Table 3.2: Criteria for calculation of histological score of colon tissue.....	82
Figure 3.2: B6, WTOE, and G2019S water controls exhibit the same peripheral blood, spleen, colon, and brain immunophenotypes.....	84
Figure 3.3: G2019S mice are more susceptible to extended acute DSS.....	85

Figure 3.4: G2019S mice are more susceptible to acute DSS with a slowed recovery.....	88
Figure 3.5: G2019S mice exhibit altered T cell PBMC populations relative to WTOE mice after acute DSS-induced colitis and recovery.....	89
Figure 3.6: Acute DSS causes T cell infiltration in the brain, while both acute and chronic DSS are associated with increased MHCII+ microglia in the brains of G2019S mice.....	91
Figure 3.7: Chronic DSS compromises nigrostriatal pathway integrity.....	94
Figure 3.8: Disease severity in aged mice treated with acute DSS correlates with peripheral inflammation levels.....	96
Figure 3.9: Acute colitis in aged mice causes neuroinflammation and compromises nigrostriatal pathway integrity.....	97
CHAPTER 4: THE EFFECTS OF LRRK2 AND CHRONIC PESTICIDE EXPOSURE IN WT OR G2019S OVEREXPRESSING MICE	
Figure 4.1: G2019S mice display reduced survival in this specific experimental dosing paradigm.....	117
Figure 4.2: Chronic cypermethrin disrupts PBMC subsets and TNF cytokine levels over time, independent of genotype.....	119
Figure 4.3: Brain immune cells and striatal inflammatory gene expression remain unaltered after chronic cypermethrin exposure.....	121
Figure 4.4: The nigrostriatal pathway is unaffected by chronic cypermethrin exposure.....	122
CHAPTER 5: THE EFFECTS OF VIRAL OR BACTERIAL INFECTION EXPOSURE IN WT OR G2019S OVEREXPRESSING MICE	
Figure 5.1: Experimental designs for infection models in LRRK2 BAC mice.....	131
Figure 5.2: Reduced FluNP366+ tetramer CD8 T cells in G2019S influenza-infected spleen and mediastinal lymph node.....	135
Figure 5.3: LRRK2 kinase inhibition alters G2019S weight after LCMV infection and increases early MPECs but decreases tetramer+ CD8 T cells.....	136

Figure 5.4: G2019S mice treated with *L. monocytogenes* exhibit reduced non-inflammatory monocytes.....137

Figure 5.5: Young and aged G2019S mice are protected from sublethal *P. aeruginosa* infection.....138

ABBREVIATIONS

AAV	Adeno-associated virus
AD	Alzheimer's disease
ADP	Adenosine diphosphate
ANOVA	Analysis of variance
α syn	α -synuclein
BAC	Bacterial artificial chromosome
BBB	Blood-brain barrier
CCL2	Chemokine ligand 2
CD	Crohn's disease
CD4	Cluster of differentiation 4
CD8	Cluster of differentiation 8
CD14	Cluster of differentiation 14
CD16	Cluster of differentiation 16
CD19	Cluster of differentiation 19
CNS	Central nervous system
COR	C-terminal of Roc
COX	Cyclooxygenase
CRP	C-reactive protein
CSF	Cerebrospinal fluid
CX3CL1	Fractalkine
CX3CR1	Fractalkine receptor
DA	Dopamine
DSS	Dextran sulfate sodium
EDTA	Ethylenediaminetetraacetic acid
FACS	Fluorescence-activated cell sorting
FADD	Fas-associated protein with death domain
FasL	Fas ligand
FSC	Forward scatter
GFAP	Glial fibrillary acidic protein
GFP	Green fluorescent protein
GI	Gastrointestinal
GWAS	Genome-wide association study
HLA	Human leukocyte antigen
Iba1	Calcium-binding adapter molecule 1
IBD	Inflammatory bowel disease
IBS	Irritable bowel syndrome
IFN γ	Interferon gamma
IgG	Immunoglobulin G
IL-1 β	Interleukin 1 β
IL-2	Interleukin 2
IL-4	Interleukin 4
IL-5	Interleukin 5
IL-6	Interleukin 6
IL-8	Interleukin 8
IL-10	Interleukin 10
KC/GRO (CXCL1)	Keratinocyte chemoattractant human growth-regulated oncogene
L-Dopa	Levodopa
LPS	Lipopolysaccharide
LRR	Leucine-Rich Repeat

LRRK2	Leucine-Rich Repeat Kinase 2
MAPKKK	Mitogen-activated protein kinase kinase kinase
MBP	Myelin basic protein
MCP-1	Monocyte chemoattractant protein-1
MHC	Major histocompatibility complex
MLK	Mixed-lineage kinase
MMP8	Matrix metalloproteinase-8
MPTP	1-methyl-4-phenyl-1,2,3,6-tetrahydropyridine
MTB	<i>Mycobacterium tuberculosis</i>
mTOR	Mammalian target of rapamycin
NFAT	Nuclear factor of activated T cells
NFκB	Nuclear factor kappa-light-chain-enhancer of activated B cells
NGS	Normal goat serum
NOS	Nitric oxide species
NRON	Non-coding repressor of NFAT
NSAID	Nonsteroidal anti-inflammatory drug
PBMC	Peripheral blood mononuclear cell
PD	Parkinson's disease
PDGF	Platelet-derived growth factor
PET	Positron emission tomography
PFA	Paraformaldehyde
PFF	Pre-formed fibril
PKA	Protein kinase A
RBC	Red blood cell
RIPK	Receptor-interacting protein kinase
ROC	Ras of complex
ROS	Reactive oxygen species
SN	Substantia nigra
SNP	Single nucleotide polymorphism
SNpc	Substantia nigra pars compacta
SSC	Side scatter
TB	Tuberculosis
TGFβ	Transforming growth factor beta
TH	Tyrosine hydroxylase
Th17	T-helper 17
TLR4	Toll-like receptor 4
TNF	Tumor necrosis factor
TNSB	Trinitrobenzenesulfonic acid
TPSO	Translocator protein
UC	Ulcerative colitis
VEGF	Vascular endothelial growth factor
V-CAM1	Vascular cell adhesion molecule 1

CHAPTER 1: BACKGROUND AND LITERATURE REVIEW

1.1: Parkinson's disease

Parkinson's disease (PD) is the second most common neurodegenerative disorder next to Alzheimer's disease (AD). By the end of 2020, it is estimated that 930,000 Americans will have PD, and that number is expected to increase in excess of 1.2 million by 2030 (Marras et al., 2018). PD currently affects over 10 million people worldwide but is expected to rise to nearly 13 million people by 2040 (Dorsey & Bloem, 2018), thus placing a huge burden on health care costs and caregivers. It was recently revealed that the economic burden of patients with PD is more than \$51 billion annually in the US alone. These huge burdens from such a debilitating disease collectively warrant the need for research into PD pathophysiology and pathogenesis to develop therapeutics to help mitigate, delay, or prevent the disease.

First described in 1817 by James Parkinson in his "Essay on the Shaking Palsy" (Parkinson, 1922), PD is characterized as a progressive motor disorder with four primary motor symptoms including tremor, rigidity, postural instability and bradykinesia (Gelb, Oliver, & Gilman, 1999). Secondary motor symptoms, including but not limited to shuffling gait or freezing, a mask-like expression, micrographia and speech difficulties, can also occur. Beyond the typical motor symptoms, several non-motor symptoms are associated with PD. Non-motor symptoms can range along a broad spectrum from cognitive and mood changes, such as anxiety, depression, and language and memory difficulties to sleep disorders, such as insomnia or restless leg syndrome, to gastrointestinal (GI) dysfunction, such as constipation or early satiety. Many of these non-motor symptoms often appear decades prior to the first sign of any motor abnormality. Given the vast number of both motor and non-motor symptoms, PD is often hard to diagnose, as patients present with different and varying degrees or severity of symptoms. As of today, there are no specific blood tests available to diagnose PD; so a clinical diagnosis of PD is based on the

presence of bradykinesia and at least one of the three other primary motor symptoms as well as improvement of motor symptoms with dopaminergic medications (Postuma et al., 2015).

Neuropathologically, PD is characterized by two primary hallmarks: progressive loss of dopaminergic neurons in the substantia nigra pars compacta (SNpc) and aggregation of α -synuclein (α syn) leading to Lewy Body formation. Decreased dopamine levels in the nigrostriatal pathway as a result of nigral dopaminergic neuron death or degeneration of their terminals results in the stereotypic motor symptoms associated with PD. In fact, it is estimated that motor symptoms do not appear until at least 50% of SN dopaminergic neurons are lost with more recent reports suggesting symptoms do not appear until after 70% SN dopaminergic neuron loss (Greffard et al., 2006; Lang & Lozano, 1998; S. Y. Ma, Roytta, Rinne, Collan, & Rinne, 1997). Accumulation and aggregation of α syn due to abnormal protein structure or mutations is hypothesized to disrupt neuronal homeostasis and contribute to synaptic dysfunction. More recently, the role of the immune system and neuroinflammation in PD pathogenesis has garnered considerable attention and is now considered another key feature of PD; but it is not yet known how early inflammation starts in PD and whether it is a critical contributor of PD pathogenesis and progression. Evidence and rationale for exploring the immune system and neuroinflammation in the context of PD pathogenesis will be discussed in detail below.

1.2: PD as a multifactorial disease

PD is considered a multifactorial disease with a complex interaction of genetics, aging, and environmental exposures all thought to contribute to pathogenesis. Here, each component as a contributing factor to the pathogenesis of PD will be reviewed.

1.2.1: Aging

The greatest risk factor for PD is aging, with PD affecting 1% of those over the age of 60 and 5% of those over the age of 85 (Bennett et al., 1996; de Lau & Breteler, 2006; Nussbaum & Ellis, 2003; Tanner & Goldman, 1996; Wood-Kaczmar, Gandhi, & Wood, 2006). Aging is considered the most important determinant of PD risk (Collier, Kanaan, & Kordower, 2011; Levy, 2007), with age at the time of onset of disease affecting disease phenotype and severity (Hely et al., 1995). Several reports have suggested that aging alone is sufficient to induce changes in the nigrostriatal pathway. Initial studies showing neurodegeneration in the SN of PD patients also reported neuronal loss in the SN of healthy control subjects (McGeer, Itagaki, Akiyama, & McGeer, 1988; Mortera & Herculano-Houzel, 2012; Stark & Pakkenberg, 2004). Estimates suggest a 7% dopaminergic neuron loss per decade in the SN of healthy controls (McGeer, McGeer, & Suzuki, 1977), suggesting that aging alone contributes to progressive functional decline and neurodegeneration, albeit to lower levels than those associated with development of PD. Studies have also shown that aging can contribute to a decrease in striatal dopamine, which is similarly observed before neuronal degeneration in PD (Carlsson & Winblad, 1976; Kish, Shannak, Rajput, Deck, & Hornykiewicz, 1992; Riederer & Wuketich, 1976). Furthermore, a decrease in nigral cell volume and a loss of neuronal dendrites and dendritic spines have all been associated with aging (Cruz-Sanchez, Cardozo, & Tolosa, 1995; Finch, 1993; Mann & Yates, 1979). All of these typical age-related changes in the nigrostriatal pathway are similarly observed in PD, albeit with higher severity in PD patients, consistent with the hypothesis that PD pathogenesis arises from a complex combination of age, genetics and environmental exposures.

1.2.2: Genetics

Up until the 1990s, it was largely thought that PD was idiopathic with no clear inheritance pattern. Since the 1990s, roughly 23 monogenic genes have been linked to familial PD with approximately 5-10% of PD cases following classical Mendelian inheritance patterns (Lesage &

Brice, 2009). Variants in the genes *SNCA*, *LRRK2*, *GBA*, and *VPS35* have all been linked to dominantly inherited PD, while variants in *PRKN* (*PARK2*), *PARK7* (*DJ-1*), *PINK1*, *ATP13A2*, and *SYNJ1* have all been linked to recessively inherited PD often in the form of early-onset PD for the former three genes or atypical PD for the latter two genes. While these monogenic forms are associated with high risk for development of PD, it is important to note that they are extremely rare, and most have low and incomplete penetrance. However, they do have higher incidences in certain populations, such as those with Ashkenazi Jewish ancestry (X. Liu et al., 2011; van der Brug, Singleton, Gasser, & Lewis, 2015). Over the last two decades, increases in the number of genome-wide association studies (GWAS) have allowed for the identification of several variants that are high in frequency in human population but confer low risk for development of PD (D. Chang et al., 2017; International Parkinson Disease Genomics et al., 2011; Maraganore et al., 2005; Nalls et al., 2014; Satake et al., 2009; Simon-Sanchez et al., 2009). More recently, a GWAS identified 90 risk variants, of which 38 identified as novel, the majority found in the same loci as monogenic forms of PD (Blauwendraat, Nalls, & Singleton, 2020; Nalls et al., 2019). This supports the hypothesis that understanding mechanisms related to genes implicated in monogenic PD may shed light on those mechanisms associated with high-risk variants related to development of idiopathic PD.

1.2.3: Environmental exposures and lifestyles

As individuals age, they are exposed to a number of environmental conditions, develop different kinds of infections, and are engaged in diverse and extremely variable lifestyles. Thus, it is no surprise that incidence of PD has been associated with a slew of environmental factors that either appear to increase or decrease risk for its development. These include, but are not limited to, increased incidence of PD after pesticide exposure, traumatic brain injury, consumption of dairy products, and exposure to certain viral or bacterial infections (Ballard, Tetrad, & Langston, 1985; Langston, 1996; M. Park et al., 2005; Priyadarshi, Khuder, Schaub, & Shrivastava, 2000;

Simon, Tanner, & Brundin, 2020). Interestingly, exposure to the toxin, 1-methyl-4-phenyl-1,2,3,6-tetrahydropyridine (MPTP), after its accidental discovery to have caused dopaminergic neuronal loss in humans during recreational drug use, has become one of the main methods to induce dopaminergic neuronal loss and degeneration in animal models alongside the use of two pesticides that inhibit mitochondrial respiration, paraquat and rotenone (Langston, 1985; Langston & Ballard, 1984; Tanner et al., 2011). Viral or bacterial infections induce worsening of motor symptoms in PD patients while a recent study identified an association between tuberculosis (TB) and PD, suggesting that inflammation or immunological challenges may trigger PD pathogenesis (Brugger et al., 2015; C. H. Shen et al., 2016; Umemura et al., 2014). On the other hand, decreased PD incidence has been associated with increased caffeine consumption and moderate smoking, while increased exercise and the use of nonsteroidal anti-inflammatory drugs (NSAIDs) such as ibuprofen has been associated with reduced incidence of idiopathic PD (Hernan, Takkouche, Caamano-Isorna, & Gestal-Otero, 2002; Kenborg et al., 2015; Ritz et al., 2007; G. W. Ross et al., 2000; F. Yang et al., 2015). Some of these studies have shown associations with occupational hazards through exposure to certain chemicals or metals (Goldman, 2014; Gorell et al., 1997; Priyadarshi, Khuder, Schaub, & Priyadarshi, 2001; Steenland et al., 2006). While a number of other factors have been associated with PD incidence, results are often conflicting. Given the wide variety of environmental exposures and lifestyles and reliance upon self-reported over-the-counter anti-inflammatory drug consumption or occupational exposures, not all studies report these associations. While none of the associations imply causality, the field hypothesizes that the correct combination of these factors can create the perfect storm to enable an environmental trigger to contribute to PD pathogenesis; therefore, all of these immunological and environmental factors are worthy of investigation in future investigations.

1.3: The aging immune system

It is well established that as individuals age, their immune system ages accordingly. Immune aging is characterized by two primary concepts: immunosenescence, the loss of effector function; and inflammaging, the low-level chronic inflammation that persists with age. Inflammaging is characterized by excess production of circulating inflammatory mediators, or cytokines, most notably, C-reactive protein (CRP), interleukin-6 (IL-6), and tumor necrosis factor (TNF) from chronically activated innate and adaptive immune cells (Figure 1.1) (Bruunsgaard et al., 2003; Frasca & Blomberg, 2016). Both the innate and adaptive immune systems are affected with aging as their respective immune responses are decreased with age. Human studies have shown a reduction in lymphoid cells but an increase in myeloid immune cells with age (Figure 1.1) (Goronzy, Li, Yang, & Weyand, 2013; Hearps et al., 2012; Lages et al., 2008; M. Li et al., 2019; Seidler, Zimmermann, Bartneck, Trautwein, & Tacke, 2010). The aging adaptive immune system is impaired as naïve T and B cell populations as well as T and B cell receptor diversity are reduced with age (Figure 1.1) (Franceschi, Bonafe, & Valensin, 2000; Franceschi, Valensin, Fagnoni, Barbi, & Bonafe, 1999; Goronzy et al., 2013). Furthermore, T cell receptor sensitivity is decreased in response to stimuli and there is a failure of self-tolerance and production of autoantibodies (Goronzy et al., 2013). Collectively, these processes in the immune system typical of aging contribute to an increase in susceptibility to infection and autoimmunity in the elderly.

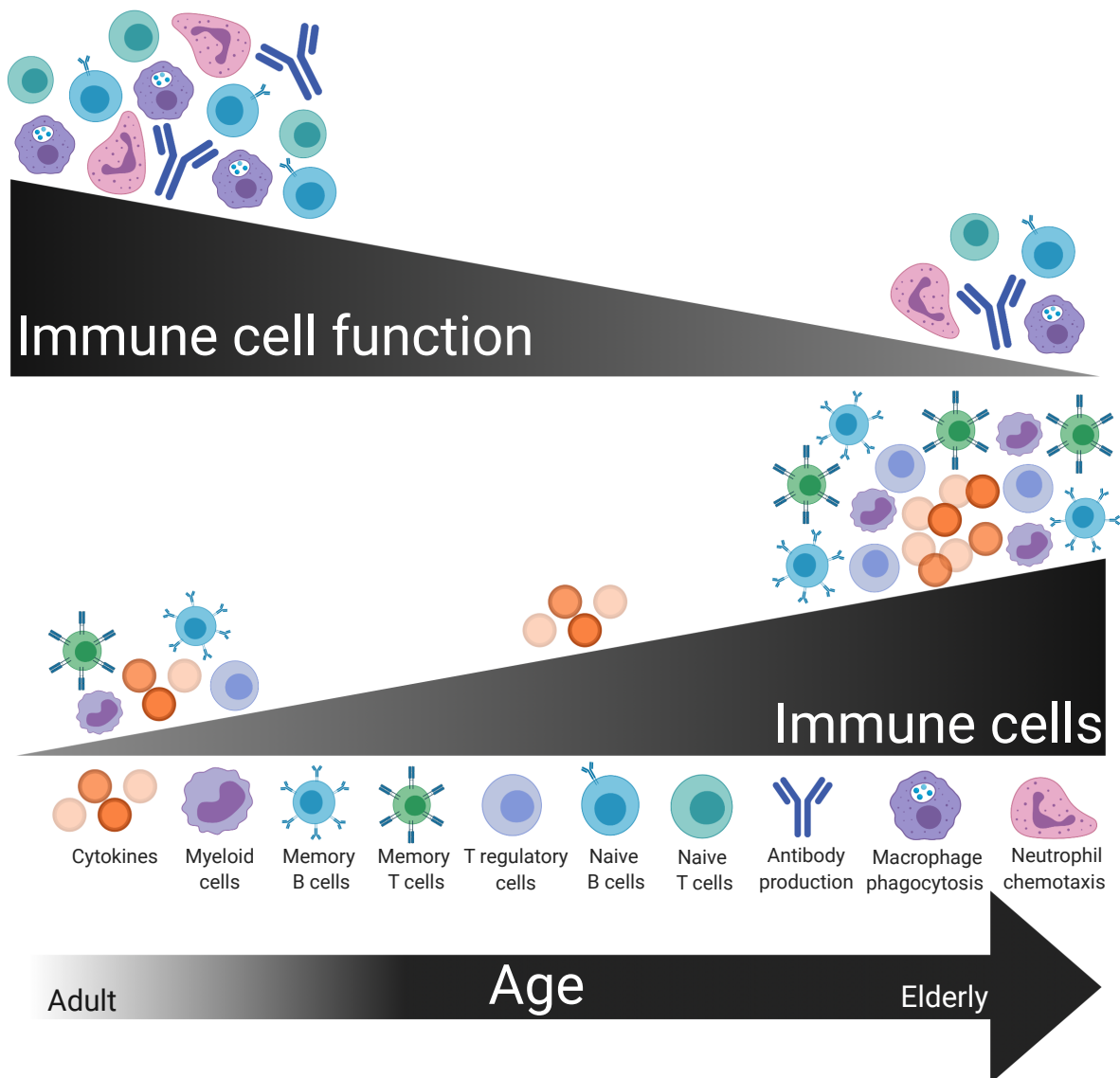


Figure 1.1: Age-related alterations in immune cell populations and function. As a person ages, cytokines and certain immune cell populations (myeloid, memory T and B, and T regulatory cells) are increased, while others are decreased (naïve T and B cells). Immune cell function is decreased (chemotaxis, phagocytosis and antibody production).

1.4: Evidence for the immune system playing a role in PD pathogenesis

The central nervous system (CNS) was initially considered to be immunologically inert for a number of reasons, including the presence of immunoincompetent microglia as brain resident

immune cells, a lack of draining lymphatics, and complete isolation from the peripheral immune system with the blood brain barrier (BBB) physically separating the two (Barker & Billingham, 1977). However, recent discoveries support the idea that the CNS is “immune specialized” rather than “immune privileged” and that it is not as isolated as originally described. The idea that the CNS lacked a lymphatic system was disproven with the discovery of a lymphatics system in the meninges of humans and rodent models that is responsible for draining cerebrospinal fluid (CSF) into the bloodstream (Absinta et al., 2017; Aspelund et al., 2015; Louveau et al., 2015). Although the BBB physically separates the brain and the peripheral immune system, it does allow crosstalk between the two as it is a highly selective semipermeable membrane allowing nutrients in and preventing the entrance of potentially toxic molecules, which is necessary to maintain the proper functioning of the CNS (Carson, Doose, Melchior, Schmid, & Ploix, 2006). Impaired BBB integrity can result in an influx of cytokine and chemokine signaling, debris, microbial pathogens, and peripheral immune cells, all of which can activate microglia and promote neuroinflammation, which has been shown to be cytotoxic or protective depending on the circumstances (Carson et al., 2006; Engelhardt & Ransohoff, 2012; More, Kumar, Kim, Song, & Choi, 2013). Neuroinflammation, peripheral inflammation, and the immune system play a role in several neurodegenerative disorders. Cellular and epidemiological evidence that inflammation and the immune system contributes to PD pathogenesis will be reviewed in detail below.

1.4.1: Cellular evidence for inflammation playing a role in PD pathogenesis

1.4.1.1: Innate immunity - Microglia

Microglia are considered brain resident immune cells or “brain macrophages” that are responsible for a number of functions, including synaptic remodeling and pruning for proper brain function, clearance of debris, and bi-directional communication with neurons for neuronal homeostasis and maintenance. Although similar in function to bone marrow-derived macrophages, microglia are derived from yolk sac progenitors (Ginhoux & Prinz, 2015; Saijo &

Glass, 2011). In a resting state, microglia scavenge the parenchyma until signals, including but not limited to α syn, pesticides, environmental toxins, viral or bacterial antigens, cytokines or antibodies direct them to a site of injury. Microglia morphology shifts from a highly ramified one into an amoeboid shape as they become activated, and they begin to proliferate. They secrete immunomodulatory mediators and cytokines, such as TNF, to promote a pro-inflammatory environment, to which dopaminergic neurons in the midbrain are particularly sensitive (McGuire et al., 2001; Mount et al., 2007; Tansey & Goldberg, 2010). Microglia are densely populated in the SN and striatum of the brain, areas that are both affected in PD. One of the first pieces of evidence showing neuroinflammation in the brains of PD patients came in 1988 when McGeer and colleagues showed human leukocyte antigen (HLA) immunoreactive microglia in SN *post mortem* tissue from PD patients (McGeer, Itagaki, Boyes, & McGeer, 1988). The number of HLA-DR-positive microglia was found to increase with neuronal degeneration throughout the nigrostriatal pathway (Imamura et al., 2003). Activated microglia, which express TNF, IL-6, and interleukin 1 beta (IL-1 β) are partially responsible for the elevated levels of TNF, IL-1 β , IL-6, transforming growth factor beta (TGF β), reactive oxygen species (ROS), nitric oxide species (NOS) and proapoptotic proteins found in the SN, striatum, CSF, and serum of PD patients (Blum-Degen et al., 1995; Eidson et al., 2017; Imamura et al., 2003; Mogi, Harada, Kondo, et al., 1994; Mogi, Harada, Riederer, et al., 1994; Nagatsu, Mogi, Ichinose, & Togari, 2000).

To further understand the role of microglia in PD pathogenesis, studies have used positron emission tomography (PET) ligands to measure and trace neuroinflammation in the human brain. The use of ligands, such as [11C](R)-PK11195, that binds translocator protein (TPSO, formerly known as the peripheral benzodiazepine receptor), which was originally thought to be selectively expressed on activated microglia, showed microglial activation in the brains of PD patients, but the levels of microglia activation did not correlate with clinical severity (Banati, 2002; Bartels et al., 2010; Gerhard et al., 2006). Usage of this first-generation PET ligand has allowed researchers

to conclude that microglia are activated early in the disease process, leaving them to promote neuroinflammation in vulnerable PD associated brain regions. However, the accuracy of this particular ligand may be influenced by a number of issues, such as TPSO genetic polymorphisms that influence binding affinity of the PET ligand, low brain density and expression in multiple cell types, including infiltrating cells from the periphery (Tronel et al., 2017); therefore, new accurate targets must be identified for development of PET ligands to ensure these are faithful reporters of microglia number and activation state.

1.4.1.2: Innate immunity - Monocytes

In addition to brain resident microglia, evidence also suggests a role for peripheral monocytes in PD pathogenesis. Classical monocytes are elevated in PD patients and display an altered transcriptome profile relative to monocytes from healthy controls with a distinct gene expression noted in PD patients early on in disease stage (Grozdanov et al., 2014; Kannarkat et al., 2015; Schlachetzki et al., 2018). Furthermore, monocytes from PD patients displayed higher proliferative rates and contrasting responses to specific stimulation paradigms with some reports suggesting increased while others decreased pro-inflammatory cytokine production (Grozdanov et al., 2014; Nissen et al., 2019; Reale, Iarlori, et al., 2009). The chemokine, CCL2, is upregulated in PD patients suggesting the potential for an increase in CNS recruitment of monocytes and enhanced inflammation, both of which are hypothesized to contribute to neurodegeneration in PD (Gao et al., 2015; Grozdanov et al., 2014; Parillaud et al., 2017; Xie et al., 2017). In fact, pathogenic α syn has been shown to induce alterations in PD monocytes, including hyperactivation, impaired cytokine release and decreased phagocytosis noted in primary cells from both human and animal models, suggesting that monocytes display a dysregulated inflammatory response to α syn (Gardai et al., 2013; Grozdanov et al., 2019). Finally, LRRK2, one of the genes implicated in idiopathic and familial PD, displays increased expression in monocyte

populations and has therefore been postulated to contribute to monocyte dysregulation (Bliederauser et al., 2016; Cook et al., 2017). To this end, levels of LRRK2 in peripheral monocytes may serve as a potential biomarker for PD.

1.4.1.3: Adaptive immunity - T and B cells

Beyond innate immunity contributing to inflammation in PD, there has also been ample evidence to suggest a role for adaptive immunity in PD pathogenesis. In the same study showing HLA-DR positive microglia in the brains of PD patients, McGeer and colleagues also showed that T cells infiltrate the brains of PD patients, which has been replicated in other human studies and animal models (Brochard et al., 2009; McGeer, Itagaki, Boyes, et al., 1988). Subsequent studies have looked more specifically at T cell subsets in the brain and periphery to try to understand their role in the inflammatory component of PD pathogenesis. Interestingly, HLA-DR⁺ T cells and memory T cells have been shown to be increased in PD patients relative to healthy controls, while naïve T cells, cluster of differentiation 4 (CD4) positive, and regulatory T cells are reduced (Bas et al., 2001; Chiba et al., 1995; Fiszer, Mix, Fredrikson, Kostulas, & Link, 1994). Furthermore, CD4⁺, forkhead box P3 (FOXP3)-positive regulatory T cells have increased suppressive activity in PD patients, which correlates with a finding that dopamine lowers regulatory T cell function (Kipnis et al., 2004; Rosenkranz et al., 2007). Similar to observations in the brain, levels of pro-inflammatory cytokines, TNF, interferon gamma (IFN γ), IL-1 β , IL-6, interleukin 2 (IL-2), interleukin 8 (IL-8), and monocyte chemoattractant protein-1 (MCP-1), are also dysregulated in the serum of PD patients and some of their levels correlate with disease severity and disability (Brodacki et al., 2008; Koziorowski, Tomasiuk, Szlufik, & Friedman, 2012; Reale, Iarlori, et al., 2009). This may be a consequence of altered lymphocyte populations that contribute to immune cell dysregulation as higher levels of IFN γ -producing T cells relative to interleukin 4 (IL-4) producing T cells have been identified, which is in accordance with a reduced CD4:CD8 T cell ratio in the periphery of

PD patients (Baba, Kuroiwa, Uitti, Wszolek, & Yamada, 2005). T cell dysregulation in PD patients has been suggested as T cells exhibit increased TNF receptor expression (Bongioanni, Castagna, Maltinti, Boccardi, & Dadone, 1997). In 2017, a groundbreaking study by Sulzer and colleagues was the first to suggest that specific T cell subsets, mainly CD4+ T cells, recognized certain α syn peptides in PD patients (Sulzer et al., 2017) further supporting a role of adaptive immunity in PD pathogenesis. While there are discrepancies between findings in T cell populations, dysregulation and understanding the role of T cells in PD pathogenesis, one thing is clear – dysregulation in immune cell traffic from the periphery to the CNS is likely to promote a pro-inflammatory environment that can contribute to the progressive neuronal cell death associated with PD.

Less understood, the role of B cells in PD is still being explored as reports suggest B cells are reduced in the blood of PD patients relative to controls (Bas et al., 2001; Stevens et al., 2012). Immunoglobulin G (IgG) antibody deposits have been found on dopaminergic neurons in the brain and IgG receptors have been found on activated microglia suggesting humoral immunity may play a role in neuroinflammation and neurodegeneration (Orr, Rowe, Mizuno, Mori, & Halliday, 2005). Autoantibodies, antibodies against an individual's own proteins, such as α syn, dopamine, and melanin are present in the sera and CSF of PD patients, and in some cases are elevated relative to controls (Caggiu et al., 2016; Carvey et al., 1991; Double et al., 2009; M. Han, Nagele, DeMarshall, Acharya, & Nagele, 2012; Papachroni et al., 2007; Yanamandra et al., 2011). Levels of α syn autoantibodies in patients with mild and moderate PD have been correlated in CSF and plasma, supporting the hypothesis that α syn autoantibodies could serve as a potential biomarker for PD (Horvath, Iashchishyn, Forsgren, & Morozova-Roche, 2017)

Collectively, cellular data from the innate and adaptive immune systems provides evidence that immune dysregulation in both the periphery and brain can cause upregulation of pro-inflammatory cytokines that activate microglia and initiate a cascade of pro-inflammatory

signaling ultimately resulting in progressive neurotoxicity and neurodegeneration associated with PD.

1.4.2: Epidemiological evidence linking the immune system and PD

1.4.2.1: PD genetic susceptibility linked to immune-associated genes

Interestingly, several of the histological markers and key cytokines upregulated in PD patients have also been genetically linked to increased risk for PD, further supporting a link between inflammation and PD (Bialecka et al., 2008; D. Li et al., 2012; O. A. Ross et al., 2004; Wahner, Sinsheimer, Bronstein, & Ritz, 2007). GWAS have identified HLA-DR as a genetic risk factor for late on-set PD, while an interaction between IL-6 and estrogen receptor polymorphisms have been linked to increased risk for early onset PD (Hakansson et al., 2005; Hamza et al., 2010). *IL-1 β* polymorphisms are more abundant in PD patients relative to healthy controls and may affect the onset of disease similarly to how *TNF* genetic variants affect it (Nishimura, Kuno, Kaji, Yasuno, & Kawakami, 2005; Schulte et al., 2002). Polymorphisms in the *TNF* gene have been associated with increased incidence of PD with certain single nucleotide polymorphisms (SNPs) correlated to earlier disease onset (Chu, Zhou, & Luo, 2012; Nishimura et al., 2001; Yu et al., 2011). Despite not being a risk factor for PD, allelic distribution of *IFN γ* is significantly different between early-onset and late-onset PD (Mizuta et al., 2001), perhaps further implicating a role of T cells in PD pathogenesis as T cells are major producers of *IFN γ* . To further support this hypothesis, pathway analysis has implicated genes involved in the 'regulation of leukocyte/lymphocyte activity' as conferring an increased susceptibility to PD (Holmans et al., 2013). Therefore, future therapeutics to target the immune system may help delay or mitigate the inflammatory milieu that contributes to PD pathogenesis or disease progression.

1.4.2.2: Non-steroidal anti-inflammatory drugs

Given that NSAIDs have been shown to reduce the risk of other neurodegenerative diseases, it is no surprise that similar findings have been observed in PD. One of the first reports linking NSAIDs and PD identified ibuprofen, acetaminophen, and aspirin as capable of reducing the loss of dopamine neurons in culture by promoting dopaminergic neuronal integrity (Casper, Yaparpalvi, Rempel, & Werner, 2000). Furthermore, the NSAIDs, sodium salicylate, aspirin, and meloxicam, have been shown to protect against MPTP-induced dopaminergic neurotoxicity in animal models (Aubin, Curet, Deffois, & Carter, 1998; Fergert, Teismann, Earl, Kuschinsky, & Oertel, 1999; Sairam, Saravanan, Banerjee, & Mohanakumar, 2003). Following these initial reports in animal models, an epidemiological study found patients who regularly consumed non-aspirin NSAIDs (two or more tablets per day) had a lower risk of developing PD relative to nonregular NSAID users (H. Chen et al., 2003). This was further supported by a follow up study showing that ibuprofen users, but not acetaminophen or aspirin users, had a 35% lower risk of developing PD than nonusers, highlighting the fact that only certain NSAIDs appeared to be associated with protective benefits (H. Chen et al., 2005). These protective properties may be based on the well-known cyclooxygenase (COX) inhibition of NSAIDs but also their inhibitory effects on NOS and ROS, to which dopaminergic neurons are particularly susceptible (Asanuma, Nishibayashi-Asanuma, Miyazaki, Kohno, & Ogawa, 2001). In 2006, a controversial study reported that non-aspirin NSAIDs reduced the risk for PD by 20% in men but increased the incidence in women by 20%, one of the first to link sex differences with NSAID use and PD incidence (Hernan, Logroscino, & Garcia Rodriguez, 2006). More recent studies have tried to evaluate the link in more defined populations, with one study reporting no association between PD risk and NSAID use in an elderly population, while another study claims no links between PD risk and incremental increase use of NSAIDs despite finding an association between non-aspirin use and PD risk (Poly, Islam, Yang, & Li, 2019; Ren et al., 2018). While not all studies have been able to demonstrate positive findings linking incidence of PD and NSAID use, they have

suggested that patients with PD have a higher rate of immediate-type hypersensitivity (asthma, hay fever, or allergic rhinitis), thus providing further evidence for an inflammatory link in the pathogenesis of PD and the need to effectively evaluate the effects of NSAID on the development of PD (Bower, Maraganore, Peterson, Ahlskog, & Rocca, 2006; Ton et al., 2006).

1.4.2.3: Autoimmune disorders

With overwhelming evidence for a role of inflammation in PD pathogenesis, epidemiological studies have focused on identifying genetic overlap or pleiotropic loci between PD and autoimmune disorders to identify a potential common genetic pathway. PD has been epidemiologically linked to several autoimmune disorders, ranging from organ-specific to multi-organ autoimmune disorders. These disorders include but are not limited to multiple sclerosis, psoriasis, amyotrophic lateral sclerosis, Graves's disease (hyperthyroidism), lupus, Hashimoto's disease (hypothyroidism), and the grouped autoimmune rheumatic diseases that affect joints and muscles. Patients with one of the following autoimmune disorders, multiple sclerosis, amyotrophic lateral sclerosis, Graves's disease (hyperthyroidism), Hashimoto's disease (hypothyroidism), pernicious anemia, or polymyalgia rheumatica have a 33% increased incidence of PD and risk appears to increase after hospitalization due to the autoimmune disorder (X. Li, Sundquist, & Sundquist, 2012). Those with autoimmune rheumatic diseases have a 30% greater incidence of PD relative to those without an autoimmune disease (Chang et al., 2018). More specifically, those with rheumatoid arthritis or psoriasis appear to have a significantly higher risk of developing PD (C. C. Chang et al., 2018; Ertan, Fresko, Apaydin, Ozekmekci, & Yazici, 1999; Kogure, Tatsumi, Kaneko, & Okamoto, 2008; Sheu, Wang, Lin, & Huang, 2013). However, one study has noted no association between autoimmune disease and risk for PD and also noted that those with rheumatoid arthritis had a 30% decreased risk for PD (Rugbjerg et al., 2009), which may be due to chronic use of anti-inflammatory regimens. These discrepancies may be due to differences in study design and analysis or inaccuracy of diagnoses. Regardless of the reason, there are even

more studies that have linked autoimmune diseases and PD risk with a recent GWAS identifying 17 shared loci between PD and 7 autoimmune diseases, including type 1 diabetes, Crohn's disease (CD), ulcerative colitis (UC), rheumatoid arthritis, celiac disease, psoriasis, and multiple sclerosis (Witoelar et al., 2017). Collectively the autoimmune diseases represent a group of disorders in which the peripheral immune system is activated and increases peripheral inflammatory mediators in circulation that could trigger neuroinflammation in vulnerable brain regions to promote PD pathogenesis. Therefore, these studies support the idea that PD pathogenesis may evolve from a combination of several immunological challenges and/or environmental exposures with the immune system under attack and awry as individuals age.

1.5: Leucine-Rich Repeat Kinase 2 (LRRK2) in PD

The *LRRK2* gene has been implicated in both sporadic and familial PD. Monogenic forms of the gene are associated with high risk, but low incidence whereas *LRRK2* SNPs are associated with low risk, but high incidence for PD. In 2002, the PARK8 locus on chromosome 12 was identified in a Japanese family with autosomal dominant PD (Funayama et al., 2002). In 2004, missense autosomal dominant mutations in *LRRK2* were identified as a causative form of dominantly inherited PD (Paisan-Ruiz et al., 2004; Zimprich et al., 2004). Since then, it has been shown that mutations in *LRRK2* account for 1-2% of idiopathic and 5-6% of familial PD cases worldwide (Gilks et al., 2005). They are particularly prevalent in individuals of Ashkenazi Jewish (29.7%) and North African Arab ancestry (41%) (Lesage et al., 2005; Ozelius et al., 2006; Thaler, Ash, Gan-Or, Orr-Urtreger, & Giladi, 2009). The most prevalent *LRRK2* mutation, G2019S, results in a glycine to serine substitution at position 2019 that causes a 2-3-fold increase in kinase activity, suggesting that gain-of-function *LRRK2* kinase activity may be involved in PD pathogenesis (Greggio et al., 2006; A. B. West et al., 2005; A. B. West et al., 2007). While hard to exactly pinpoint, penetrance of the G2019S mutation is extremely low with estimations of penetrance to be 28% at 59 years, 51% at 69 years, and 74% at 79 years, further supporting the hypothesis that

environmental factors are critical determinants of risk for PD (Healy et al., 2008). Interestingly, *LRRK2* mutation carriers develop similar clinical symptoms as non-*LRRK2* mutation carriers with PD (Aasly et al., 2005; Haugarvoll et al., 2008; O. A. Ross et al., 2006). This suggests that there are likely to be common mechanisms between inherited and idiopathic PD and highlights the importance of understanding *LRRK2* both in the context of immune responses and inflammation and in the context of PD. The current understanding of *LRRK2* in the neurodegeneration field is reviewed below.

1.5.1: LRRK2 structure, function, and expression

Containing 51 exons that encode a 2527-amino acid protein (~286kDa), *LRRK2* is a rather large protein (Guo et al., 2007; Mata, Wedemeyer, Farrer, Taylor, & Gallo, 2006). As a member of the ROCO protein family of G proteins, *LRRK2* contains two functional domains – a Ras of complex (ROC) with intrinsic GTPase domain and a serine/threonine kinase domain (Figure 1.2). Many of the pathogenic mutations reside in these functional domains, including N1437H, R1441G/C/H, and Y1699C in the ROC and COR (C-terminal of Roc) domains and I2012T, G2019S, and I2020T in the kinase domain (Figure 1.2), and generally result in decreased GTPase activity or increased kinase activity, respectively. This suggests that PD pathogenesis may be closely linked to various *LRRK2* functions. Beside functional domains, *LRRK2* also contains several different protein-protein interacting domains, including a leucine-rich repeat (LRR) domain, a C-terminal WD40 repeat domain, and armadillo and ankyrin repeat domains, all of which contribute to its ability to act as a signaling scaffold protein (Gilsbach et al., 2012; Guo et al., 2007). Interestingly, genetic variants in both the functional and protein-interacting domains have been associated with increased incidence of PD (R1628P, N2081D, and G2385R) or decreased incidence of PD (N551K and R1398H) (Figure 1.2) (Farrer et al., 2007; Heckman et al., 2013; K. Li et al., 2015; O. A. Ross et al., 2011; O. A. Ross et al., 2008; Tan et al., 2010).

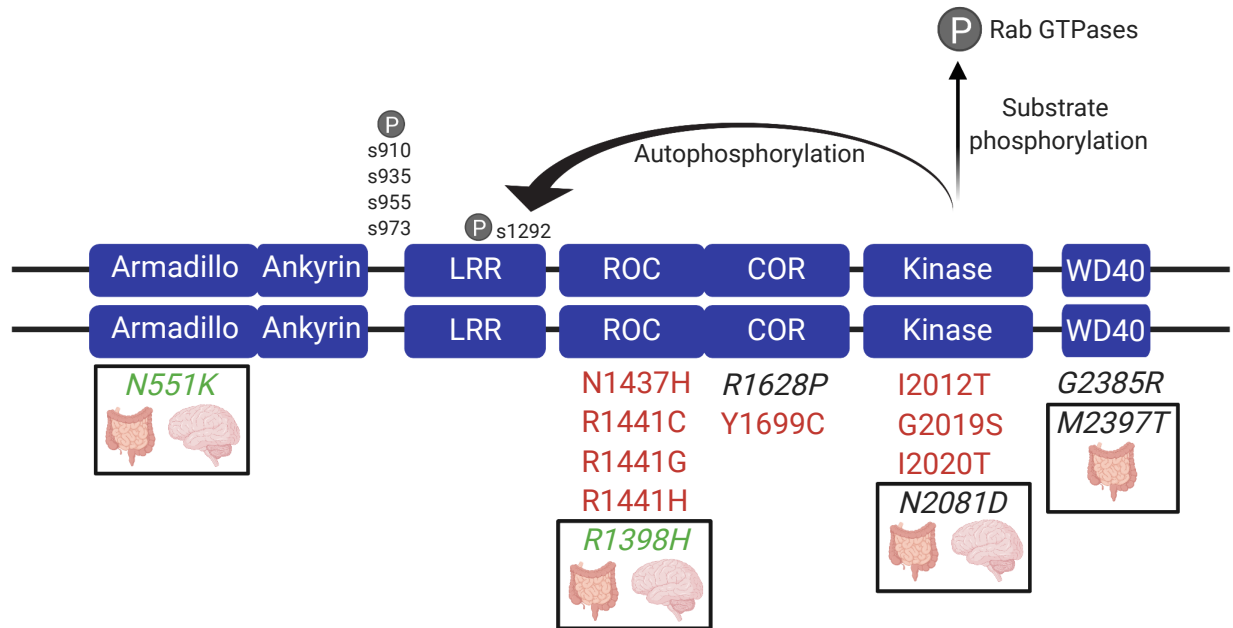


Figure 1.2: LRRK2 structure and phosphorylation activity. The LRRK2 structure encompasses several functional (ROC/COR, and kinase) and protein-protein interacting domains (armadillo, ankyrin, leucine-rich repeats, and WD40). Many of the pathogenic mutations associated with PD, indicated in red, fall in the functional domains. Although less studied, variants associated with increased incidence of PD are denoted in black. Variants associated with decreased incidence of PD (brain) and Crohn's disease (CD) are denoted in green. N2081D and M2397T variants are associated with increased incidence of CD (intestine). LRRK2 is phosphorylated by upstream kinases at s910, 935, 955, and 973 (indirect readouts of kinase activity) or autophosphorylated at s1292 (direct kinase activity readout). The kinase domain phosphorylates the *bona fide* substrates of LRRK2, the Rab GTPases.

Based on the close homology of its protein kinase domain to that of the mixed-lineage kinases, LRRK2 is classified as a mixed-lineage kinase (MLK), belonging in particular to the subfamily mitogen-activated protein kinase kinase kinases (MAPKKKs) (Marin, 2006; Mata et al., 2006). Although its structure resembles both tyrosine kinase and serine/threonine kinases,

LRRK2 has largely been shown to function as a serine/threonine kinase that can autophosphorylate and to be devoid of tyrosine kinase activity (Manning, Whyte, Martinez, Hunter, & Sudarsanam, 2002; A. B. West et al., 2005; A. B. West et al., 2007). Insight into the structure of the LRRK2 kinase domain has been gained from its similarity to Roco4, another serine/threonine kinase that belongs to the ROCO family. Like most conserved kinases, the LRRK2 kinase consists of a two-lobed structure with an adenine nucleotide bound in the binding pocket (Gilsbach & Kortholt, 2014). Classically in ROCO proteins, the C-terminal lobe contains the activation loop with a conserved DFG (aspartic acid, phenylalanine, glycine) motif that is responsible for catalysis; however, in LRRK2 this motif is changed to DYG (aspartic acid, tyrosine, glycine) in the activation loop (**ADYGIAQYCC**), and this is where the most pathogenic LRRK2 mutation, G2019S, resides (Ray & Liu, 2012). While not fully understood, the DYG conformation is apparently more flexible which allows for easy switching between the active and inactive states of the kinase (Ray & Liu, 2012). The G2019S mutation causes a shift in the DYG motif to DYS (aspartic acid, tyrosine, serine) and promotes an active kinase resulting in a substantial increase in kinase activity that has been shown to be cytotoxic (Greggio et al., 2006; M. Liu et al., 2011; Plowey, Cherra, Liu, & Chu, 2008; Ray & Liu, 2012; A. B. West et al., 2005; Yao et al., 2010).

Aside from autophosphorylation, a number of other mechanisms have been proposed to regulate LRRK2 kinase activity including intramolecular regulation and phosphorylation by upstream regulators. Recent insight into the structural model suggests LRRK2 dimerizes into a compact structure that is hypothesized to be responsible for the intramolecular mechanism controlling LRRK2 enzymatic activity, in particular LRRK2 kinase activity (Berger, Smith, & Lavoie, 2010; Greggio et al., 2008; Guaitoli et al., 2016; Leandrou et al., 2019; P. Zhang et al., 2019). The kinase and GTPase domains are considered to be intrinsically regulated with the ability of the kinase domain to phosphorylate the ROC domain and alter GTPase activity and vice versa (Gloeckner et al., 2010; Greggio et al., 2009; A. B. West et al., 2007). In an inactive state, with GDP bound, the GTPase is inactive and results in decreased kinase activity, while an active state

with GTP bound results in increased kinase activity (Ray & Liu, 2012). Furthermore, pathogenic mutations in the ROC/COR domains, R1441C/G and Y1699C, have been shown to increase GTP binding resulting in increased kinase activity while the opposite effect is observed with the T1348N variant that decreases GTP binding (Guo et al., 2007; Ito et al., 2007; Lewis et al., 2007; A. B. West et al., 2007). Given that all currently identified pathogenic mutations localize to the kinase or GTPase domains, LRRK2 kinase inhibitors or GTP modulators have been the focus of therapeutic development for the PD clinic (A. B. West, 2017).

A number of constitutive sites (ser910, ser935, ser955, ser973 to name a few) mainly in the LRR domain have been identified to be phosphorylated by other kinases as an indirect readout of LRRK2 kinase activity; however, an increase in available resources has recently allowed the identification of the ser1292 site as the *bona fide* autophosphorylation site of LRRK2 and a direct readout of LRRK2 kinase activity (Figure 1.2) (Dzamko et al., 2010; Gloeckner et al., 2010; Nichols et al., 2009; Sheng et al., 2012). Several upstream regulators, including casein kinase 1 α , inhibitor of nuclear factor κ B kinase subunits (IKK α and β), and protein kinase A (PKA) to name a few, have been identified to alter LRRK2 kinase activity via ser910 and/or ser935 indirect readouts (De Wit, Baekelandt, & Lobbestael, 2018; Lobbestael, Baekelandt, & Taymans, 2012). Numerous additional upstream regulators have been proposed; however confirmation of their activity has yielded conflicting results and needs further study (Lobbestael et al., 2012).

LRRK2 has been shown to phosphorylate a number of substrates including the mixed-lineage kinases MKK3/6, MKK 4/7, 4E-BP1, moesin, and myelin basic protein (MBP) (Gloeckner, Schumacher, Boldt, & Ueffing, 2009; Hsu et al., 2010; Imai et al., 2008; Jaleel et al., 2007; A. B. West et al., 2005; J. Yang, Zhang, Yu, Yang, & Wang, 2014). However, recent studies have officially identified the *bona fide* substrates of LRRK2 as several members of the Rab GTPase family, that regulate vesicle trafficking (Steger et al., 2017; Steger et al., 2016). LRRK2 phosphorylates Rab3, Rab5, Rab8, Rab10, Rab12, Rab29, Rab35 and Rab43 at a conserved serine or threonine in the switch II domain, and pathogenic LRRK2 mutations have been

associated with increased Rab phosphorylation, while LRRK2 kinase inhibition results in dampened Rab phosphorylation (Bonet-Ponce & Cookson, 2019). While it is unclear how dysregulated LRRK2 phosphorylation of Rab proteins contributes to PD associated neuropathology, hypotheses can be made from our current knowledge of Rab cellular dysfunction in the context of α syn and LRRK2. Rab29 physically interacts with LRRK2 and recruits LRRK2 to the trans-golgi network resulting in increased LRRK2 kinase activity, which consequently causes LRRK2 to phosphorylate other Rab substrates (Z. Liu et al., 2018; Purlyte et al., 2019). This suggests LRRK2 phosphorylation of Rab substrates happens in a Rab29-dependent mechanism. LRRK2 phosphorylation of Rab10 has been implicated in blocking ciliogenesis, while phosphorylation of Rab8A disrupts centrosome positioning, both of which may decrease neurotrophic support (Dhekne et al., 2018; Madero-Perez, Fdez, et al., 2018; Madero-Perez, Fernandez, et al., 2018; Steger et al., 2017). Furthermore, LRRK2 can recruit both Rab8A and Rab10 into lysosomes, promoting premature exocytosis of undegraded materials (Eguchi et al., 2018). Interestingly, phosphorylation of Rab35 by LRRK2 has been shown to increase α syn propagation, while Rab7A, Rab8B, Rab11A and Rab13 have been reported to block α syn aggregation and propagation or to promote α syn clearance (Dinter et al., 2016; Goncalves et al., 2016; Griffin, Yan, Caldwell, & Caldwell, 2018; Steger et al., 2016). While most of the abovementioned studies occurred in cell and rodent models, a recent report suggests phosphorylated Rab10 and LRRK2 kinase activity levels are increased in dopaminergic neurons from the SN of idiopathic PD patients (Di Maio et al., 2018). Collectively, these studies provide a glimpse of the interactions between LRRK2 and Rab proteins and their effects on vesicular trafficking and the autophagy pathway, with more detailed investigations needed, including the possibility of therapeutically targeting this pathway to delay, mitigate or prevent PD.

Given its multiple, highly diverse domains, LRRK2 has been shown to influence several cellular processes although the exact mechanism(s) by which LRRK2 contributes to PD

pathogenesis still remain to be elucidated. Some of the processes dysregulated by LRRK2 include mitochondrial function, autophagy regulation, neurite outgrowth, vesicular trafficking, cytoskeletal maintenance, and immune cell signaling pathways (Berwick & Harvey, 2012; Hongge, Kexin, Xiaojie, Nian, & Jinsha, 2015; Plowey et al., 2008; Ramonet et al., 2011; Schapansky, Nardozzi, Felizia, & LaVoie, 2014). Many of these processes are disrupted by LRRK2 due to physical interactions and changes in LRRK2 localization. Under homeostatic conditions, endogenous LRRK2 typically localizes to the cytoplasm. LRRK2 membrane localization is dependent on its conformation as a dimer, which increases kinase activity of membrane associated LRRK2 relative to that of cytosolic, monomeric LRRK2 (Berger et al., 2010).

One of the first findings to implicate LRRK2 in dysregulation of autophagy resulted from studies in which LRRK2 knockout rodent models were found to exhibit impaired protein degradation and accumulation of lipofuscin in the kidney and lung due to decreased macroautophagy (Baptista et al., 2013; Herzig et al., 2011; Ness et al., 2013; Tong et al., 2010). The effects of LRRK2 on the autophagy pathway are often cell- and context-dependent. Recent studies have shown that lysosomes, with increased LRRK2 kinase activity, increase in size, decrease in number and exhibit lower pH levels, resulting in impaired autophagy in neurons, astrocytes, and fibroblasts (Dehay et al., 2012; Henry et al., 2015). In immune cells, toll like receptor 4 (TLR4) stimulation or target of rapamycin (mTOR) inhibition causes LRRK2 to colocalize with autophagosome membranes resulting in decreased autophagy (Schapansky et al., 2014). Overexpression of wildtype LRRK2 or pathogenic LRRK2 has been associated with induction of autophagy albeit with variable and inconsistent results as G2019S-mediated kinase activity dysregulates autophagy in a neuronal cell line resulting in neurite shortening and neurotoxicity (Gomez-Suaga et al., 2012; Manzoni et al., 2013; Plowey et al., 2008; Schapansky et al., 2018). Interestingly, wildtype LRRK2 protein has been localized to the autophagy pathway in neurons in brains of patients with neurodegenerative diseases and is increased in PD patients,

highlighting the importance of studying LRRK2 in the context of the autophagy pathway as it may be of relevance beyond PD (Higashi et al., 2009).

With mitochondria heavily implicated in PD pathology, there is ample evidence that has supported a link between LRRK2 and mitochondria, often with detrimental effects in the context of pathogenic LRRK2. In both animal models and human tissue, LRRK2 has been shown to contribute to a number of mitochondrial dysfunctions including increased oxidative stress, abnormal fission and fusion, impaired mitophagy, reduced mitochondrial trafficking, decreased ATP production and increased mitochondrial DNA damage (Cherra, Steer, Gusdon, Kiselyov, & Chu, 2013; Cooper et al., 2012; Mortiboys, Johansen, Aasly, & Bandmann, 2010; Niu, Yu, Wang, & Xu, 2012; Sanders et al., 2014; Su & Qi, 2013; X. Wang et al., 2012; Yue et al., 2015). Like many of the situations described above, LRRK2 localizes to a membrane and in the context of mitochondria, specifically the outer mitochondrial membrane. Under normal conditions, LRRK2 forms a complex with the protein Miro, which regulates mitochondria movement and mitophagy, but pathogenic G2019S LRRK2 disrupts this process and delays mitophagy (Hsieh et al., 2016). Rotenone, a pesticide that inhibits mitochondrial complex 1, has been shown to increase reactive oxidative species and decrease mitochondrial membrane potential in G2019S neurons which can be reversed with LRRK2 kinase inhibition (Mendivil-Perez, Velez-Pardo, & Jimenez-Del-Rio, 2016).

In addition to mitochondria, LRRK2 can interact and colocalize with microtubules by binding to β -tubulin, resulting in decreased stability (Caesar et al., 2013; Gandhi, Wang, Zhu, Chen, & Wilson-Delfosse, 2008; Law et al., 2014). Overexpression of LRRK2 or LRRK2 kinase inhibition have also been shown to induce LRRK2 colocalization with filamentous structures on a subset of microtubules (Dzamko et al., 2010; Sheng et al., 2012). Pathogenic mutations altering the GTPase activity enhance LRRK2 microtubule colocalization and impair axonal vesicular transport of mitochondria (Blanca Ramirez et al., 2017; Godena et al., 2014; Kett et al., 2012; Thomas et al., 2016).

LRRK2 is widely expressed in a variety of tissues, including the brain, kidney, lung, intestine, lymph node, prostate gland and ovary (Figure 1.3) (A. B. West, 2017). Within the brain, LRRK2 is expressed in multiple regions with relatively high expression levels in the axons and dendrites of the striatum relative to other brain regions, further linking LRRK2 and the vulnerability of the dopaminergic nigrostriatal pathway to PD pathogenesis, albeit recent research has shown these levels to be lower than peripheral tissues. (Giesert et al., 2013; Higashi et al., 2007; H. Melrose, Lincoln, Tyndall, Dickson, & Farrer, 2006; Simon-Sanchez, Herranz-Perez, Olucha-Bordonau, & Perez-Tur, 2006; A. B. West et al., 2014). Interestingly, LRRK2 expression has been found to be the highest in lymphocytes, most notably neutrophils and monocytes (Fan et al., 2018). LRRK2 in the context of immune cells and the immune system is reviewed in detail below.

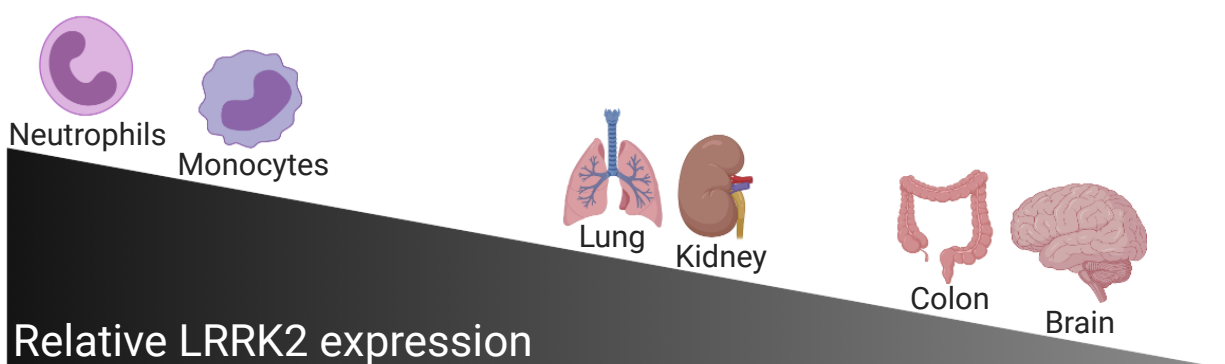


Figure 1.3: Relative human LRRK2 expression. LRRK2 expression is highest in neutrophils and monocytes and relatively low in the brain (adapted from (A. B. West, 2017)).

1.5.2: LRRK2 animal models

Ever since the identification of LRRK2 mutations in idiopathic and familial PD, researchers have developed and utilized several cellular and animal models to elucidate the role of LRRK2 and these have been extensively reviewed (Volta & Melrose, 2017; Xiong, Dawson, & Dawson, 2017). These include but are not limited to *Drosophila*, *Caenorhabditis elegans*, zebrafish, and

BAC transgenic, viral-mediated, knockout and knock-in mouse and rat models. However, none of these models fully recapitulate the phenotypes associated with PD, both behaviorally and neuropathologically. LRRK2 knockout models generally demonstrate a normal nigrostriatal pathway but abnormal peripheral pathology in the lung and kidney due to autophagy defects (Andres-Mateos et al., 2009; Hinkle et al., 2012; Tong et al., 2012; Tong et al., 2010). These effects, while unexpected, are informative given LRRK2 expression is relatively high in the kidney and lung. Early therapeutic interventions targeting LRRK2 levels or kinase activity have also caused on-target effects in the periphery that would not necessarily have been noted without findings from the LRRK2 KO models. Several transgenic LRRK2 rodent models were developed using bacterial artificial chromosome (BAC), knock-in, or tet-inducible technology to express wildtype LRRK2 or pathogenic LRRK2 (G2019S, R1441G/C, I2020T). Using BAC technology, mouse models with human or mouse wildtype, G2019S, or R1441G have been shown to have alterations in extracellular dopamine release, while rat models have been shown to have age-dependent reductions in dopamine release or no differences (Beccano-Kelly et al., 2015; X. Li et al., 2010; Y. Li et al., 2009; H. L. Melrose et al., 2010; Sanchez et al., 2014; Sloan et al., 2016; Volta et al., 2015; Walker et al., 2014). Of those with alterations in dopamine release, behavioral phenotypes ranged from none to mild motor and cognitive deficits (Beccano-Kelly et al., 2015; X. Li et al., 2010; Y. Li et al., 2009; H. L. Melrose et al., 2010; Sanchez et al., 2014; Sloan et al., 2016; Volta et al., 2015; Walker et al., 2014). Some of the rat models with pathogenic LRRK2 mutations have reported to display responsiveness to levodopa (L-Dopa) (Sloan et al., 2016). Knock-in models harboring R1441C/G or G2019S mutations rarely exhibit alterations in the dopamine system or behavioral phenotypes (Herzig et al., 2011; H. F. Liu et al., 2014; Longo, Russo, Shimshek, Greggio, & Morari, 2014; Parisiadou et al., 2014; Tong et al., 2009; Yue et al., 2015). Rodent models using tet-inducible technology under different promoters and enhancers are some of the few models to exhibit locomotor changes and reductions in striatal dopamine or decreased dopamine release (G. Liu et al., 2015; Maekawa et al., 2012; Zhou et al., 2011). Of

note, mutant G2019S mice using the PDGF-B promoter have been shown to develop degeneration at 12 or 20 months of age (C. Y. Chen et al., 2012; Chou et al., 2014). Perhaps some of the most promising models to induce nigrostriatal neurodegenerative phenotypes are from the use of Herpes simplex and adeno-associated viral-mediated gene transfer, in which pathogenic LRRK2 is packed into the viral vectors and is retrogradely transported to the SN after striatal injections, whereby it promotes neurodegeneration (Dusonchet et al., 2011; B. D. Lee et al., 2010; Tsika et al., 2015). These models have been shown to be LRRK2 kinase dependent as LRRK2 kinase-dead mutants did not induce neurodegeneration (B. D. Lee et al., 2010; Tsika et al., 2015).

The use of these different models has permitted the exploration of different questions in the context of LRRK2 biology and provided novel insight into LRRK2 mechanisms regulating inflammation and neurodegeneration. BACs overexpress mutant or wildtype LRRK2 in all tissues that express LRRK2; however, the relevance of these models may be limited as only levels of LRRK2 (not G2019S LRRK2) have been shown to be elevated in subjects with PD (Cook et al., 2017). Knock-in models are thought to more accurately represent LRRK2 PD with point mutations expressed at endogenous levels. However, several differences have been noted between lines, which could be explained by a number of things including genetic background strain effects or vivarium/housing conditions. Given that these models do not fully recapitulate PD phenotypes and LRRK2 mutations have low penetrance, scientists hypothesize that additional factors, such as environmental contributions, are required to promote PD pathology in these animal models, just as is hypothesized to occur in development of sporadic PD and to influence age-at-onset in individuals from the same family with LRRK2 G2019S mutations.

1.5.3: LRRK2 and the immune system

Since the identification of pathogenic mutations in PD, most research has focused on LRRK2 in neurons as LRRK2 gain-of-function kinase activity has been shown to affect neurite

outgrowth (Plowey et al., 2008; Ramonet et al., 2011). However, recent advances into the function of LRRK2 in the context of the immune system have garnered considerable attention, especially given that neuroinflammation is considered a major component of PD pathogenesis. Here the current status of our knowledge of LRRK2 in the context of the immune system and inflammation will be reviewed.

1.5.3.1: LRRK2 expression in brain-resident and peripheral blood immune cells

LRRK2 is most highly expressed in peripheral blood immune cells. In fact, LRRK2 expression in leukocytes has been shown to be much higher than that in neurons (A. B. West, 2017). CD14⁺ monocytes, neutrophils, CD19⁺ B cells, CD4⁺ T cells and CD8⁺ T cells from healthy control peripheral blood mononuclear cells (PBMCs) have all been shown to express LRRK2; however, expression is highest in CD14⁺, CD16⁺ monocytes and neutrophils (Figure 1.3) (Atashrazm et al., 2019; Fan et al., 2018; Hakimi et al., 2011; Thevenet, Pescini Gobert, Hooft van Huijsduijnen, Wiessner, & Sagot, 2011). Following stimulation with lipopolysaccharide (LPS) or IFN γ , LRRK2 expression is increased in myeloid cells from primary monocytes (Gardet et al., 2010; Hakimi et al., 2011), bone-marrow derived macrophages (Hakimi et al., 2011), or human THP-1 monocytic leukemia cell lines (Kuss, Adamopoulou, & Kahle, 2014). Stimulation with IFN γ induces LRRK2 expression in CD14⁺, CD16⁻ monocytes, which causes them transition to CD14⁺ CD16⁺ cells, but LRRK2 kinase inhibition attenuates this process (Thevenet et al., 2011). While LRRK2 expression is relatively low in T cells compared to other immune cell types in peripheral blood, its expression can still be induced by IFN γ stimulation (Gardet et al., 2010; Thevenet et al., 2011). Furthermore, LRRK2 expression at baseline in B cells, T cells and CD16⁺ monocytes from PBMCs of sporadic PD patients is higher relative to healthy controls, and the relationship between monocyte LRRK2 levels and inflammatory activity is significantly different in PD patients as compared to healthy controls (Cook et al., 2017).

The expression of LRRK2 in microglia is variable and often debated. Mouse and rat microglia under homeostatic conditions express very low to no LRRK2 protein; however, expression is increased after stimulation with LPS or TLR4 agonism and restored to basal levels with LRRK2 kinase inhibition, suggesting LRRK2 microglial expression is stimulation-dependent similar to that in peripheral immune cells albeit to lower levels (Moehle et al., 2012). Furthermore, in humans one study suggests LRRK2 expression in microglia is weak; and analyses need to be conducted to ascertain its levels in microglia in idiopathic PD or LRRK2 PD patients (Miklossy et al., 2006). The fact that LRRK2 expression is high in peripheral blood immune cells under homeostatic conditions and further increased upon stimulation suggests its induction is likely to play a regulatory role in their effector functions; therefore, caution should be exercised when targeting LRRK2 as a potential therapeutic intervention in PD as it is still unclear whether the high LRRK2 levels in immune cells are a protective or deleterious mechanism in the immune system.

1.5.3.2: LRRK2 regulation of immune cell function

Beyond the ROCO proteins, LRRK2 is also a member of the receptor-interacting protein kinases (RIPK), a class of serine/threonine kinases that modulate inflammatory responses through apoptosis, necrosis, or direct regulation of intracellular signaling pathways. Given its close structural relation to RIPKs, LRRK2 is also known as RIP7 (Meylan & Tschopp, 2005). RIPKs are involved in the extrinsic pathway of programmed cell death that is initiated by death signals triggered by TNF or Fas ligand (FasL) via binding to their respective receptors (TNFR1 or Fas) and promoting activation of downstream executioner caspases and the nuclear factor kappa-light-chain-enhancer of activated B cells (NF κ B) signaling pathway. LRRK2 interaction with the Fas-associated protein with death domain (FADD) induces neuronal death via caspase-8 activation, and this is LRRK2 kinase dependent, with pathogenic LRRK2 mutations increasing the interaction while LRRK2 kinase inhibition decreasing binding and ensuing neuronal death (C. C. Ho, Rideout, Ribe, Troy, & Dauer, 2009). HEK293T cells expressing green fluorescent protein (GFP)-tagged

LRRK2 I2020T (a mutation that stabilizes the active state conformation and leads to higher LRRK2 kinase activity) display higher cytotoxicity due to enhanced LRRK2 interaction with FADD, further supporting the notion that enhanced TNF signaling downstream by LRRK2 mutations is dependent on its kinase activity (Melachroinou et al., 2016). Further analysis of this interaction, suggests that the armadillo-repeat domain of LRRK2 is specifically responsible for interacting with FADD (Antoniou et al., 2018). In the SH-SY5Y human neuronal cell line, LRRK2 has been shown to phosphorylate p53, a tumor suppressor gene that when activated can induce apoptosis or cell growth arrest and result in enhanced neuroblastoma cell death (D. H. Ho et al., 2015). This has been recapitulated in microglia, showing that LRRK2 can phosphorylate p53 in the BV2 microglial cell line after LPS stimulation, which in turn increases microglia TNF secretion (D. H. Ho, Seol, Eun, & Son, 2017).

A number of functional consequences have been associated with mutant LRRK2 in myeloid cells and microglia, including motility, phagocytosis, and cytokine release. LRRK2 G2019S mouse microglia and bone-marrow derived macrophages display increased phagocytic responses to latex beads or *Escherichia coli* bioparticles, while LRRK2 deficiency decreased phagocytosis in the same cell types (K. S. Kim et al., 2018). However, stimulation of monocytic RAW264.7 and microglial BV2 cell lines with TLR4 agonists results in increased LRRK2 dimerization and translocation to autophagosome membranes with minimal effects on phagocytosis of beads (Schapansky et al., 2014). LRRK2 knockdown results in autophagic deficits, implicating LRRK2 in autophagy regulation. Myeloid cells expressing LRRK2 G2019S exhibit increased chemotaxis due to enhanced association between LRRK2 and actin-regulatory proteins which can be blocked by LRRK2 kinase inhibition (Moehle et al., 2015). On the contrary, LRRK2 G2019S microglia show impaired ADP-induced motility that can be rescued with LRRK2 kinase inhibition (I. Choi et al., 2015). Interestingly, LRRK2-deficient microglia are not only highly motile but exhibit increased CX3CR1, resulting in increased migration towards its ligand fractalkine (CX3CL1). CX3CR1 deficiency restored LRRK2-deficient microglia migration activity

to basal levels (I. Choi et al., 2015; B. Ma et al., 2016). LRRK2 has also been linked to trafficking of monocytes across the BBB as overexpression of wildtype or LRRK2 G2019S increased monocyte attachment to endothelial cells through an upregulation of VCAM-1, a membrane protein that mediates leukocyte-endothelial adhesion and transmigration across the BBB (Hongge et al., 2015). The effects of LRRK2 on motility and migration are opposite in peripheral monocytes versus microglia, further supporting the notion the LRRK2 functions in a cell type-specific and kinase-dependent manner.

In addition to affecting migration, motility, and phagocytosis in myeloid cells, LRRK2 also influences immune cell cytokine production. Primary mouse microglia expressing the LRRK2 R1441G pathogenic mutation exhibit increased expression and secretion of pro-inflammatory cytokines in sera that induced cell death when placed on neuronal cultures (Gillardon, Schmid, & Draheim, 2012). On the contrary, knockdown of LRRK2 in mouse microglia decreased pro-inflammatory gene expression and NF κ B transcriptional activity, but wildtype LRRK2 and LRRK2 mutants increased NF κ B transcriptional activity, suggesting LRRK2 positively regulates inflammation and cytokine production (B. Kim et al., 2012). This idea is supported by another study that confirmed and extended these findings, suggesting that LRRK2 deficiency or kinase inhibition causes increased phosphorylation of the p50 subunit in the NF κ B pathway, resulting in accumulation of p50 in the nucleus, shifting the ratio of p65:p50 subunits, and decreasing the transcription of cytokines (Russo et al., 2015). Furthermore, LRRK2 G2019S-mediated gain-of-function kinase activity in microglia decreases PKA activity leading to a decrease in NF κ B transcription (Russo et al., 2018). Several studies suggest that LRRK2 kinase inhibition dampens microglia cytokine production, thus providing rationale that therapeutically targeting LRRK2 kinase activity in immune cells may dampen PD-associated neuroinflammation (B. Kim et al., 2012; Marker et al., 2012; Moehle et al., 2012; Puccini et al., 2015).

Beyond LRRK2 regulation of signaling pathways in myeloid cells and microglia, LRRK2 has also been implicated in the nuclear factor of activated T cells (NFAT) signaling pathway as a negative regulator. It has been shown that NFAT translocation to the nucleus is blocked through LRRK2 interactions with non-coding repressor of NFAT (NRON). LRRK2-deficient mice showed increased translocation of NFAT to the nucleus in a NRON-dependent manner, thereby resulting in increased NFAT activity (Z. Liu et al., 2011). Additionally, *Aspergillus fumigatus*, an opportunistic fungal pathogen, decreases LRRK2 mRNA and protein levels resulting in upregulation of NFAT translocation, and similar findings have been observed in LRRK2-deficient dendritic cells (Wong et al., 2018). The role of LRRK2 in NFAT signaling in the context of colitis will be detailed in the next chapter.

Collectively, these studies suggest that LRRK2 regulation of immune cell function is cell type-, stimulus-specific and dependent on LRRK2 kinase activity, thereby providing possible explanations for the contrasting reports on its role from various groups. Additional translational studies are needed to fully understand the normal function of LRRK2 in the context of human immune cells, as well as the potential pathogenic role of LRRK2 mutations in immune cells, both of which should be possible with greater access to LRRK2 PD patient blood samples and/or via utilization of human induced pluripotent stem cell-derived macrophages, monocytes and microglia from LRRK2 PD patients (H. Lee, James, & Cowley, 2017; van Wilgenburg, Browne, Vowles, & Cowley, 2013).

1.5.3.3: LRRK2 in inflammation

Given the low penetrance of LRRK2 mutations and low availability of LRRK2 PD samples, human studies examining differences between pathogenic LRRK2 PD patients and sporadic patients have been limited. Nevertheless, one study reports that serum levels of IL-1 β can discriminate between asymptomatic G2019S carriers and controls, while G2019S PD patients have higher levels of serum platelet-derived growth factor (PDGF) and IL-8 and vascular

endothelial growth factor (VEGF) in the CSF relative to sporadic patients (Dzamko, Rowe, & Halliday, 2016). Interestingly, while total LRRK2 levels were not found to be different between G2019S PD, carriers, idiopathic PD and healthy control PBMCs, levels of LRRK2 phosphorylation at ser935 were reduced in G2019S PD patients compared to sporadic PD patients, suggesting that pSer935 may be a potential biomarker for G2019S PD patients (Padmanabhan et al., 2020).

Given that several mutant LRRK2 animal models do not exhibit neurodegenerative phenotypes, studies have examined the effects of LRRK2 mutations in the context of environmental toxins. Mice overexpressing G2019S or wildtype LRRK2 were subjected to the neurotoxin, MPTP, whereby MPTP-treated G2019S mice exhibited greater loss of striatal dopamine and TH neurons in the SN than mice overexpressing wildtype LRRK2 (Karuppagounder et al., 2016). Similar findings were observed in mice overexpressing LRRK2 R1441G mutations subjected to peripheral acute LPS administration, in which mice exhibited neuronal loss in the SN accompanied by neuroinflammation promoted by an immune response from the periphery (Kozina et al., 2018). In yet another study using LPS as a peripheral immune stimulus in aged mice, LRRK2 G2019S mice exhibited similar inflammatory phenotypes relative to wildtype mice with increased glial fibrillary acidic protein (GFAP) positive astrocytes and ionized calcium binding adaptor molecule 1 (Iba1)-positive microglia that were restored to baseline levels with inhibition of matrix metalloproteinase-8 (MMP8), a proteinase responsible for degradation of the extracellular matrix (J. Kim et al., 2017). Using manganese as a stimulus, LRRK2 expression was shown to be upregulated *in vivo* and *in vitro* in conjunction with autophagy dysfunction, which was reversed with LRRK2 kinase inhibition or LRRK2 deletion (J. Chen, Su, Luo, & Chen, 2018; J. Kim et al., 2019). Longitudinal studies in LRRK2 G2019S rats with microglial PET imaging suggest that neuroinflammation increases with age similarly to non-transgenic rats (Walker et al., 2015). Another longitudinal study following LPS-treated G2019S rats with [¹¹C]PBR28 PET imaging showed increased neuroinflammation relative to saline-treated controls, but no dopaminergic neuron degeneration, suggesting that multiple peripheral insults may be necessary for

nigrostriatal neurodegeneration (Schildt et al., 2019). LRRK2 deficiency protects against the toxic herbicide paraquat-induced sickness and inflammation as well as neuronal loss and activated myeloid cells in rats injected with AAV-human α syn (Daher, Volpicelli-Daley, Blackburn, Moehle, & West, 2014; Rudyk, Dwyer, Hayley, & membership, 2019). Collectively, these findings suggest that LRRK2 may regulate inflammatory responses in animal models subjected to environmental factors but in a stimulus-dependent manner.

1.5.3.4: LRRK2 epidemiologically linked to inflammatory diseases

Beyond PD, LRRK2 has been linked to several inflammatory diseases. A recent study identified *LRRK2* as one gene of 17 that overlap between PD and autoimmune diseases (Witoelar et al., 2017). In 2009, a SNP in *LRRK2* was identified to be in weak association for leprosy, an infectious disease caused by *Mycobacterium leprae* that can progressively lead to nerve damage (F. R. Zhang et al., 2009). In 2015, 13 *LRRK2* variants were significantly associated with leprosy in the Han Chinese population (D. Wang et al., 2015). A follow up study identified that 18 *LRRK2* variants were associated with type-1 reactions, excessive pro-inflammatory responses associated with leprosy (Fava et al., 2016). Interestingly, the R1628P genetic variant that is located in the COR domain, exhibits pleiotropic effects with protective association against type-1 reactions but increased incidence of PD (Fava et al., 2019). LRRK2 protein levels have been correlated with the autoimmune disease, systemic lupus erythematosus, disease index and elevated in B cells (M. Zhang et al., 2019). Several GWAS have identified LRRK2 mutations associated with increased incidence of CD (Hui et al., 2018; Michail, Bultron, & Depaolo, 2013; Umeno et al., 2011). The newly identified N2081D variant in *LRRK2* has been reported to be associated with increased incidence of both CD and PD while the N551K variant with reduced incidence of both diseases, suggesting a pleiotropic link between PD and autoimmune disease (Hui et al., 2018; Witoelar et al., 2017). Given these associations and several genetic links between LRRK2, PD,

and inflammatory diseases, therapeutic interventions targeting common mechanisms underlying pathogenesis may help delay onset or mitigate disease progression.

1.5.3.5: LRRK2 association with bacterial infection models

LRRK2 has been linked to several infections by epidemiological studies and in animal and cellular models. Analysis of gene expression from tuberculosis infections identified LRRK2 as being significantly enriched during active infections (Z. Wang, Arat, Magid-Slav, & Brown, 2018). LRRK2 knockout mice showed decreased *Mycobacterium tuberculosis* (MTB) burden early in infection, perhaps with exacerbated inflammation as LRRK2 knockout macrophages treated with MTB exhibited altered innate immune gene expression induced by various mitochondrial stresses (Hartlova et al., 2018; Weindel et al., 2020). Phagosome maturation and bacterial control were increased in human and mouse macrophages treated with LRRK2 kinase inhibitors, suggesting that a lack of LRRK2 kinase activity is protective against MTB (Hartlova et al., 2018). On the other hand, LRRK2 knockout mice infected with *Salmonella typhimurium* exhibited reduced caspase-1 activation and IL-1 β secretion due to inflammasome activation in macrophages, which ultimately impaired clearance of pathogens (W. Liu et al., 2017). A recent study suggested that wildtype LRRK2 is protective from *S. typhimurium* and reovirus infection in a sex-dependent manner with females exhibiting impaired ability to control infection (Shutinoski et al., 2019). Interestingly, LRRK2 G2019S mice controlled *S. typhimurium* infection better, but were more susceptible to reovirus in a LRRK2 kinase-dependent manner (Shutinoski et al., 2019). In another bacterial model, LRRK2 deficiency promotes susceptibility to intestinal but not systemic *Listeria monocytogenes* infection through lysozyme defects and failed recruitment of Rab2a in Paneth cells, a secretory immune cell in the gut responsible for controlling intestinal bacteria (Q. Zhang et al., 2015). Lastly, *Aspergillus fumigatus*, an opportunistic fungal pathogen, decreases LRRK2 mRNA and protein levels, which results in upregulation of NFAT translocation to the nucleus and increased transcription of inflammatory cytokines (Wong et al., 2018). Collectively, these studies

suggest a role for LRRK2 in immunity to control infection burden; however, the mechanism by which LRRK2 controls or contributes to infection is sex-, genotype- and infection-specific which underscores the complexity of LRRK2 signaling and function.

1.5.3.6: LRRK2 and α -synuclein

α syn accumulation is a hallmark of PD pathology and has been shown to promote inflammatory responses, as extracellular α syn can activate microglia and promote NF κ B activation. Given LRRK2 has been associated with phagocytosis and autophagy, recent studies have investigated the interaction between LRRK2 and α syn, particularly in the context of clearance of α syn by immune cells. LRRK2-deficient microglia have dampened cytokine release after exposure to α syn fibrils, while LRRK2 knockout rats exhibited reduced activated microglia after AAV2/1 α syn injection into the SN (Daher et al., 2014; Russo et al., 2015). Furthermore, LRRK2-deficient microglia more effectively take up α syn and in larger amounts relative to wildtype controls due in part to an increase in Rab5 positive endosomes (Maekawa et al., 2016). On the contrary, LRRK2 G2019S transgenic mice subjected to pre-formed fibril (PFF) injection in the striatum displayed increased α syn aggregation, dopaminergic degeneration, and neuroinflammation relative to controls (non-transgenic mice injected with PFFs) (Bieri et al., 2019). G2019S knock-in mice injected with AAV2/9 human A53T synuclein in the SN displayed significantly more dopaminergic loss and higher loads of pSer129 α syn aggregates at 12 months of age relative to wildtype controls injected with AAV2/9 human A53T synuclein (Maekawa et al., 2016; Novello et al., 2018). LRRK2 kinase inhibition is insufficient to attenuate motor defects or reduce α syn accumulation and neuronal loss after PFF injection into the dorsal striatum of wildtype mice (Henderson et al., 2019). These disparate results from studies could be due to differences in α syn PFF batches, α syn conformation (strains) and/or experimental treatment conditions. While the exact mechanism by which LRRK2 interacts with α syn in immune cells still

remains unknown, it could be hypothesized that LRRK2 via its kinase activity alters the autophagy pathway, thereby impairing degradation of α syn, and contributing to its accumulation. This is of particular interest given that the autophagy related proteins p62 and LAMP1 display alterations in *post mortem* SN tissue from LRRK2 G2019S PD patients relative to idiopathic PD patients, and neurons from mice with the LRRK2 G2019S knock-in mutation exhibit altered lysosomal morphology and acidification that result in accumulation of α syn (Mamais et al., 2018; Schapansky et al., 2018). Future investigations need to explore this hypothesis in the context of immune cells as the role of LRRK2 is highly likely to be cell- and context-specific in nature.

1.6: Parkinson's disease and the gastrointestinal system

It is becoming increasingly evident that there are several links between PD pathophysiology and dysfunction in the GI system, a hypothesis first proposed by Braak and colleagues based on α syn staining which he used to stage PD pathology from the periphery to the brain (Braak et al., 2003). Evidence in support of this hypothesis include alterations in gut permeability, gut dysbiosis, and epidemiological evidence linking PD with inflammatory bowel diseases (IBD) which are discussed in detail below.

1.6.1: Non-motor symptoms linked to GI dysfunction

As discussed previously, PD often manifests with several non-motor symptoms that appear earlier than motor impairments, the most prevalent of which includes GI dysfunction. PD patients exhibit more GI-related non-motor symptoms relative to healthy controls (H. Chen et al., 2015; Edwards, Pfeiffer, Quigley, Hofman, & Balluff, 1991). PD-related GI dysfunction includes, but is not limited to dysphagia, early satiety, nausea, vomiting, bloating, fecal incontinence and constipation, which is one of the most common GI symptoms in PD patients (Houser et al., 2018; H. Park et al., 2015). While reports vary depending on population-related demographic variables,

constipation has been reported in as low as 24.6% and as high as 78.7% of PD patients (Edwards et al., 1991; Martinez-Martin et al., 2007; Ueki & Otsuka, 2004). It has also been estimated that constipation can precede the stereotypical clinical PD motor symptoms by decades (Abbott et al., 2003). Furthermore, constipation is associated with a higher incidence of PD, as men with less than one bowel movement per day have over a four-fold increased risk for developing PD relative to men with at least 2 bowel movements per day (Abbott et al., 2001). In conjunction, the severity of constipation has been associated with increased future PD diagnosis in a laxative dose-dependent manner (C. H. Lin, Lin, Liu, Chang, & Wu, 2014).

1.6.2: GI dysbiosis in PD

Changes in intestinal homeostasis and gut microbiota composition have also been linked to increased risk for PD. The relative abundance of certain families of bacteria are notably different between PD patients and healthy controls. While several studies have noted different patterns of changes, fecal levels of *Bifidobacteriaceae*, *Bacteroides*, *Prevotellaceae*, *Christensenellaceae*, *Tissierellaceae*, *Lachnospiraceae*, *Enterobacteriaceae*, *Lactobacillaceae*, *Pasteurellaceae*, and *Verrucomicrobiaceae* amongst others have all been shown to be significantly altered in PD patients relative to healthy controls (Hasegawa et al., 2015; Hill-Burns et al., 2017; Pietrucci et al., 2019). Some of these changes have been shown to be associated with motor symptoms and gut inflammation. The fecal abundance of the family, *Enterobacteriaceae* was positively associated with gait difficulty and postural instability, while decreased levels of *Lachnospiraceae* correlated with motor impairment and disease severity, signifying that alterations in gut composition may be linked to motor symptoms associated with PD (Pietrucci et al., 2019; Scheperjans et al., 2015). Classifying PD patients even further based on constipation symptoms, the abundance of *Prevotellaceae* was found to be reduced in constipated patients relative to non-constipated patients, while diversity of the family *Firmicutes* was increased in constipated patients (L. Zhu et al., 2014). Patients with tremors exhibited relatively higher abundances of fecal

Bacteroides relative to patients without tremors (C. H. Lin et al., 2019). Levels of the anti-inflammatory bacteria from the genera *Blautia*, *Coprococcus*, and *Roseburia* were reduced in the colons of PD patients relative to healthy controls, while levels of the pro-inflammatory bacteria of the genus *Ralstonia* were elevated in PD patients (Keshavarzian et al., 2015). In accordance with these bacterial changes promoting an inflammatory environment in the GI system of PD patients, levels of immune factors, such as Flt1, IL-1 α , and CXCL8 have been shown to be elevated in PD patient stool, (Houser et al., 2018) while levels of *Bacteriodes* and *Verrucomicrobia* have been positively correlated with plasma levels of TNF and IFN γ , respectively (C. H. Lin et al., 2019). Thus, changes in microbiome could potentially be used as biomarkers for disease state or risk. Despite noting several differences in the gut microbiota composition of PD patients relative to healthy controls, the mechanism by which these changes occur or how to effectively target these bacteria as a potential therapeutic to delay or mitigate the pathogenesis of PD still remain unknown. However, this data support the hypothesis that gut dysbiosis could be one of many peripheral perturbations that could promote GI inflammation, which may be one of the key initiating events in PD pathogenesis (Houser & Tansey, 2017).

1.6.3: GI α -synuclein pathology in PD

In 2003, on the basis of α syn immunohistochemistry in post-mortem brain tissue, Braak and colleagues proposed a staging scheme for PD in which pathology in lower brainstem regions occurred first and pathology in higher cortical regions occurred later. This staging scheme formed the basis for the Braak hypothesis which proposes that α syn PD pathology begins in the periphery with an immunogenic antigen entering the nasal or oral cavity that somehow promotes α syn aggregation in the oral and GI systems, upon which α syn can then propagate along the vagus or olfactory nerves to the brainstem and progress to other anterior and dorsal areas of the brain associated with PD neuropathology (Braak et al., 2003; Rietdijk, Perez-Pardo, Garssen, van

Wezel, & Kraneveld, 2017). Consistent with this hypothesis, α syn pathology has been observed throughout the entire GI system of PD patients, with the first study identifying α syn in the myenteric plexus of the colon (Braak, de Vos, Bohl, & Del Tredici, 2006; Kupsky, Grimes, Sweeting, Bertsch, & Cote, 1987; Wakabayashi, Takahashi, Ohama, & Ikuta, 1990; Wakabayashi, Takahashi, Takeda, Ohama, & Ikuta, 1988). More recently, α syn and phosphorylated α syn ($p\alpha$ syn), a proxy for pathological α syn, has been reported in the GI system of nearly all PD patients examined (Beach et al., 2010). In a longitudinal study with routinely obtained biopsies, α syn pathology, $p\alpha$ syn in particular, was present in the GI tract up to 8 years prior to the patient's clinical diagnosis of PD, suggesting GI α syn accumulation may be a potential early biomarker for PD (Hilton et al., 2014). These findings have also been reported in PD patients with pathogenic LRRK2 mutations. Specifically, a small study has shown LRRK2 G2019S patients exhibit α syn pathology in enteric neurons similarly to idiopathic PD patients (Rouaud et al., 2017) promoting the idea that LRRK2 PD patients are clinically indistinguishable from idiopathic PD patients (Kestenbaum & Alcalay, 2017) and supporting the hypothesis that it is the combination of age, genetics and environmental factors that lead to PD pathogenesis. Interestingly, vagotomy at least 5 years prior to a PD clinical diagnosis has been associated with reduced incidence of PD (Gray, Munoz, Schlossmacher, Gray, & Woulfe, 2015; B. Liu et al., 2017).

1.6.4: Epidemiological evidence linking PD and IBD

IBD refers to a group of diseases that include Crohn's disease (CD) or ulcerative colitis (UC), which are collectively characterized by chronic inflammation in the GI tract. Similar to PD, causes of CD and UC are unknown but environmental and genetic factors are hypothesized to contribute to disease pathogenesis. Both diseases seem to affect men and women equally as they present with similar symptoms. CD can affect the entire GI tract, while ulcerative colitis is generally limited to the colon and rectum. Continuous inflammation is common throughout the

colon in UC with the inner most lining of the colon affected. Inflamed areas of the intestine are interspersed between uninflamed, healthy areas in CD. While IBD shares similar symptoms with irritable bowel syndrome (IBS), it is important to note they are very distinct. IBS is defined as a GI condition that affects intestinal behavior and function commonly associated with recurrent abdominal pain and alterations in bowel movements. Furthermore, there is no damage or inflammation in the GI system with IBS.

There are several epidemiological studies that have linked PD and IBD, a group of disorders that exhibit chronic inflammation of the GI tract. Some of the first studies from Taiwanese groups, identified that patients with IBD have a 35% increased incidence of PD (Lai, Liao, Lin, & Sung, 2014; J. C. Lin, Lin, Hsu, Lin, & Kao, 2016). Subsequent studies in the US (Peter et al., 2018), Korea (S. Park et al., 2019) and Sweden (Weimers et al., 2019) looking at associations for the diseases in their respective populations, identified that patients with either CD or UC had increased risk for PD relative to healthy controls; however, a study from Denmark only found an association between UC and PD (Villumsen, Aznar, Pakkenberg, Jess, & Brudek, 2019). Conversely, another study examining this association in Medicare beneficiaries found the opposite association between IBD and PD whereby having IBD was associated with lower incidence of PD (potentially resulting from chronic anti-inflammatory regimens), highlighting how differences between populations and analysis methods are important determinants of how the associations are determined and interpreted (Camacho-Soto, Searles Nielsen, & Racette, 2018). Given these seemingly contradictory results, a systemic review and meta-analysis looking at all studies to date found overall that IBD patients had a 46% increased risk of PD and this increased risk remained when examining patients with CD (28% increased risk) and UC (30% increased risk) separately (F. Zhu et al., 2019). Interestingly, two of the studies that found a positive association between IBD and risk for PD also found that anti-TNF therapy reduced the risk of developing PD, further supporting the hypothesis that inflammation and an awry immune system contribute to PD pathogenesis (S. Park et al., 2019; Peter et al., 2018). Furthermore, these studies

have raised the interesting possibility that anti-TNF therapies used to treat IBD, may be of potential therapeutic benefit to reduce risk for PD or slow its progression. However, additional research is needed to identify causal links between these associations as well as the best therapeutic windows for these and other immunomodulatory drugs, and importantly to determine whether they should be given prophylactically to reduce risk for PD later in life or shortly after the onset of non-motor symptoms to delay or prevent progression of disease and the onset of the disabling motor symptoms typically associated with clinical stages of the disease.

1.6.5: Similar phenotypes associated with PD and IBD

PD and IBD patients exhibit similar peripheral immune phenotypes especially in the context of inflammation and gut permeability. Pro-inflammatory cytokines, including IL-1 β , TNF, IFN γ , IL-2, IL-6, IL-8, are associated with initiation and progression of IBD (Muzes, Molnar, Tulassay, & Sipos, 2012), and many of these are the same cytokines found to be increased in the sera, CSF, and brain of PD patients relative to age-matched healthy controls (Blum-Degen et al., 1995; Eidson et al., 2017; Imamura et al., 2003; Mogi, Harada, Kondo, et al., 1994; Mogi, Harada, Riederer, et al., 1994; Nagatsu et al., 2000). One of the major cytokines increased in PD, TNF, is considered a major contributor to IBD pathogenesis through its pleiotropic effects in a number of signaling cascades (Murch, Braegger, Walker-Smith, & MacDonald, 1993). Similar to IBD patients, PD patients exhibit increased mRNA levels of pro-inflammatory cytokines in the ascending colon relative to healthy controls (Devos et al., 2013). Interestingly, cytokine levels negatively correlated with disease duration, suggesting intestinal inflammation may be a precursor or contribute to initiation of PD pathogenesis but may not remain at high levels throughout the progression of disease (Devos et al., 2013). In addition to similarities in immune cell and inflammatory changes, PD and IBD patients exhibit similar gut permeability phenotypes with both exhibiting increased intestinal permeability due to disruptions and decreased expression

of tight junction proteins (Forsyth et al., 2011; Michielan & D'Inca, 2015). As noted above, these associations should not be taken as proof of a causal association, but as the basis for more mechanism-based studies in animal models (such as those developed for this doctoral thesis) that can interrogate a functional and causal relationship between the two conditions.

1.6.6: LRRK2: linking PD and CD

Several GWAS have identified that the *LRRK2* gene, one of the most common genetic contributors to PD, is a common susceptibility locus for both PD and CD, with some *LRRK2* mutations associated with increased incidence of CD (Barrett et al., 2008; Franke et al., 2010; Hugot et al., 2001; Hui et al., 2018; Michail et al., 2013; Umeno et al., 2011). The M2397T mutation has been associated with increased incidence of CD and type-1 inflammatory reactions associated with leprosy, suggesting that *LRRK2* in the context of the immune system may be the common thread behind these two distinct inflammatory diseases (Fava et al., 2016). Furthermore, the newly identified N2081D variant in the *LRRK2* gene has been shown to be in association with increased risk for both CD and PD while the N551K variant is associated with reduced risk for both diseases (Hui et al., 2018). Similar to PD, *LRRK2* is present in immune cells from CD patients and that expression is upregulated with IFN γ stimulation (Gardet et al., 2010). Additionally, *LRRK2* mRNA is upregulated in inflamed CD tissue relative to uninflamed tissue from the same patient and this was particularly localized to the lamina propria (Gardet et al., 2010). Paneth cells are specialized secretory cells in the small intestine that regulate intestinal microbiome and innate immune response. Interestingly, *LRRK2* M2397T is associated with Paneth cell defects in Japanese CD patients as the number of M2397T alleles negatively correlates with number of normal Paneth cells and pathway analysis suggests this is due to defects in autophagy (T. C. Liu et al., 2017). Interestingly, *LRRK2* shares many similarities with *NOD2*, one of the genes with variants found to be associated with increased incidence of CD. Like *LRRK2*, *NOD2* is expressed in peripheral leukocytes, with highest expression in myeloid cells and is upregulated with bacterial

exposure (Biswas, Petnicki-Ocwieja, & Kobayashi, 2012). NOD2 drives several inflammatory signaling cascades, such as NF κ B and MAPK, and has been shown to play a role in autophagy, yet another similarity with LRRK2 (Cario, 2005; Travassos et al., 2010).

Collectively, these data provide overwhelming evidence for links between PD and pathologies in the GI system. Understanding the similarities in phenotypes between PD and these inflammatory diseases previously not believed to be risk factors for PD may provide insight into PD pathogenesis and underlying disease mechanisms for potential therapeutic intervention that could mitigate risk for multiple inflammatory diseases that increase risk for age-related neuroinflammatory diseases like PD and AD.

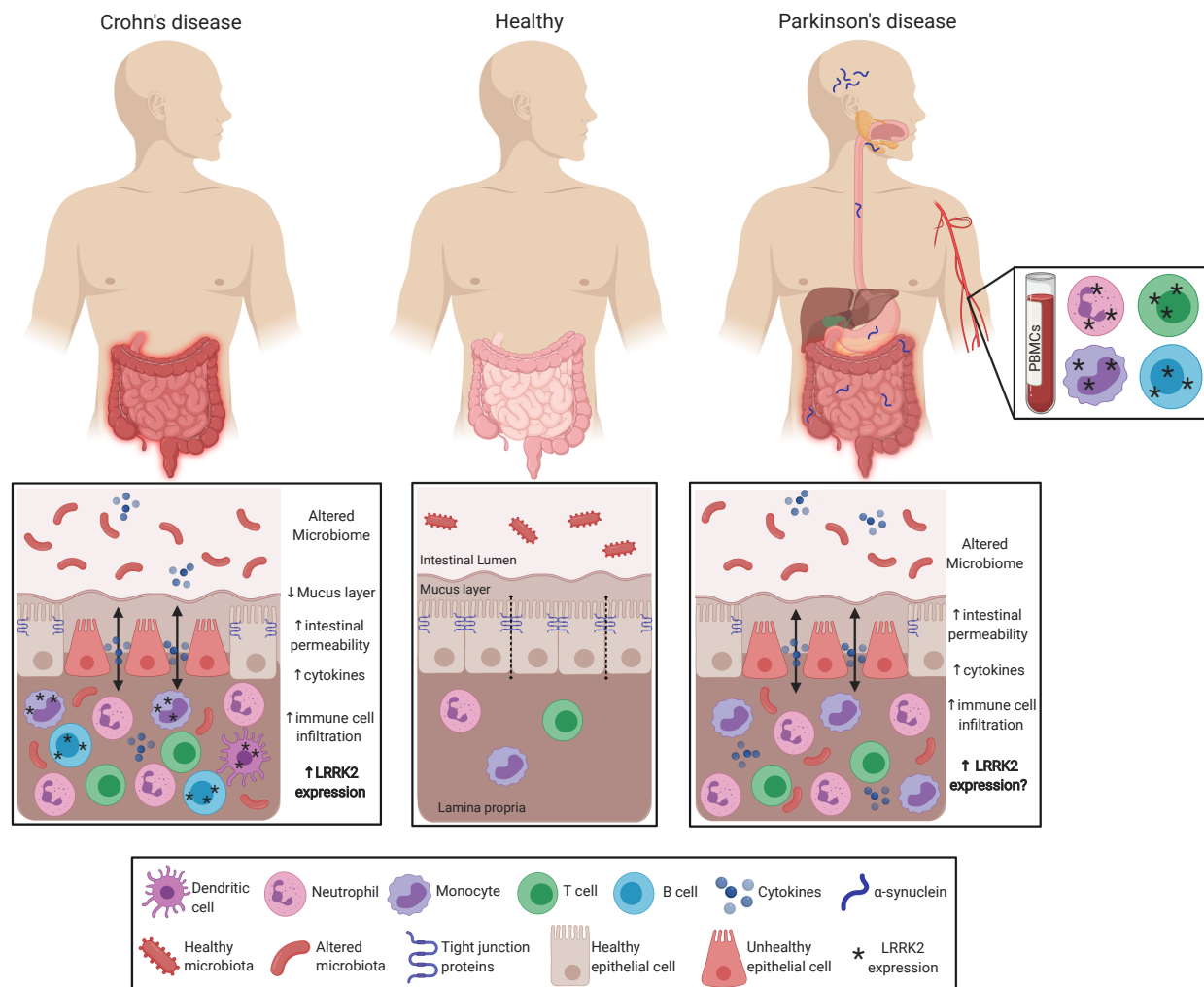


Figure 1.4: LRRK2 immune cell expression at the interface of PD and CD. PD and CD exhibit very similar intestinal phenotypes with altered microbiome, increased intestinal permeability, cytokine secretion, and immune cell infiltration. While LRRK2 expression is increased in specific immune cells in the inflamed intestine in CD, LRRK2 expression in intestinal immune cells from PD patients has not been assessed, but LRRK2 expression is increased in sporadic PD patient PBMCs. We posit that LRRK2 has an important role in regulating inflammatory responses and this is the reason its levels are increased in chronic inflammatory conditions.

1.6.7: Modeling colitis in animal models

The gold standard for studying colitis in rodent models is the use of dextran sodium sulfate salt (DSS) or trinitrobenzenesulfonic acid (TNBS), both of which have been heavily used in the GI field due to their simplicity and reproducibility (Okayasu et al., 1990; Wirtz, Neufert, Weigmann, & Neurath, 2007). The exact molecular mechanisms by which these chemicals induce colitis phenotypes remain unknown, but they basically induce epithelial injury followed by inflammation. While these are particularly useful models, it is important to note they differ in phenotypic presentation order from actual IBD with rodent models subjected to DSS developing intestinal inflammation after destruction of the epithelial lining and increased intestinal permeability whereas the human IBDs result from an imbalance of the immune system in the intestine followed by ensuing microbial dysbiosis and gut alterations (Eichele & Kharbanda, 2017; Kiesler, Fuss, & Strober, 2015). Characteristically included in the drinking water of rodents, DSS paradigms can vary greatly with colitogenic properties dependent on dosage, molecular weight of DSS, and administration length (acute vs chronic). Length of DSS administration should be taken into careful consideration when designing a treatment paradigm as different regimens will answer different questions. Acute paradigms are helpful to assess the peak of inflammation (which is typically 4-7 days after DSS commencement) or recovery rate. Chronic models based on continuous low doses of DSS over a month-long period or relapsing/remitting bouts of colitis more closely mimic the human disease and are helpful to assess overall susceptibility or resilience to colitis (Chassaing, Aitken, Malleshappa, & Vijay-Kumar, 2014; Perse & Cerar, 2012). All of these factors should be considered when assessing and interpreting effects of colitis models on the gut-brain axis and α syn pathology along the Braak highway and in the CNS.

1.6.8: Evidence linking colitis and PD-associated neuropathology in animal models

Although DSS has been comprehensively used to study colitis in terms of the gut and immune cell alterations, there has been some evidence suggesting that intestinal inflammation

induced by DSS can cause alterations in the brain, with even more studies examining this link in recent years. Some of the earliest reports showed that experimental colitis increases the permeability of the BBB evinced by increased leakage of sodium fluorescein in a rabbit model (Hathaway, Appleyard, Percy, & Williams, 1999) and 1-2 days after colitis induction in the hypothalamus of a rat model (Natah, Mouihate, Pittman, & Sharkey, 2005). More specifically, occludin and claudin-5, tight junction proteins that connect epithelial cells to create a closely regulated barrier site, were reduced in the hippocampus of mouse brains after acute colitis, further suggesting impairment of BBB integrity after colitis (Y. Han et al., 2018).

Beyond changes in BBB integrity induced by colitis, changes related to inflammatory cytokines and cytokines associated with peripheral immune cell trafficking to the CNS have been shown to be altered in the brain after colitis induction. Inflammatory IL-6, a pleiotropic cytokine with both pro- and anti-inflammatory properties depending on the physiological state that is highly upregulated in the periphery after colitis, has also been shown to be increased in the brain after DSS- or TNBS-induced colitis, albeit in a temporal manner with increased IL-6 in the cerebral cortex and hypothalamus of rats following colitis induction (Y. Han et al., 2018; K. Wang et al., 2010). Similarly TNF has been shown to be increased in the cortex, while COX-2 mRNA was increased in the hippocampus and hypothalamus but reduced in the amygdala, again suggesting brain region-specific spatiotemporal alterations of inflammatory markers after colitis (Do & Woo, 2018; Y. Han et al., 2018). IL-1 β another pro-inflammatory cytokine that is associated with initiation and progression of colitis, has been shown to be upregulated in the SN of mice after acute and sub-chronic DSS-induced colitis (Garrido-Gil, Rodriguez-Perez, Dominguez-Meijide, Guerra, & Labandeira-Garcia, 2018). Furthermore, endothelial vascular cell adhesion molecule 1 (V-CAM1), a cytokine-inducible molecule that mediates lymphocyte adhesion, is upregulated in the brain of rats and mice after TNBS- or DSS-induced colitis, and this upregulation has been positively correlated with colonic inflammation and colonic V-CAM1 levels (Sans et al., 2001). While V-CAM1 upregulation was not associated with leukocyte infiltration into the brain in the

latter study, it could be hypothesized that it was examined too early in the process and leukocyte infiltration might have been detectable only at a later time point.

More recently, studies have examined other effects of colitis on the brain, specifically in relation to glial cells and specific brain regions. Astrogliosis has been observed in DSS-treated animals, as GFAP mRNA and protein levels were increased in the hippocampus (Do & Woo, 2018). Alterations in microglia phenotypes have been noted in the prefrontal cortex with a shift to a more pro-inflammatory and damage-associated microglia phenotype and this was concomitant with increased peripheral monocyte infiltration in the CNS (Sroor et al., 2019). Similarly, acute DSS increased peripheral monocyte infiltration into the hippocampus of wildtype mice in conjunction with increased peripheral and brain pro-inflammatory cytokine levels (Gampierakis et al., 2020).

Importantly, a few recent studies have reported that colitis is sufficient to induce alterations in the dopaminergic nigrostriatal pathway. A reduction in expression of tyrosine hydroxylase (TH), the rate limiting enzyme in dopamine synthesis, in the SN was observed in a study using acute DSS alone (Gil-Martinez et al., 2019); however, DSS in conjunction with the neurotoxin, MPTP, resulted in enhanced reduction of TH expression in the SN, as well as increases in Iba1+ cells and GFAP+ cells, suggestive of a degenerative phenotype with astrogliosis and increased microglial activation (Gil-Martinez et al., 2019). In a separate study examining different paradigms of DSS induction, it has been reported that an acute model is sufficient to increase nigral IL-1 β suggesting alterations in the inflammatory state of the SN, but insufficient to produce nigrostriatal degenerative phenotypes. Similarly, a sub-chronic paradigm also induced nigral IL-1 β increases; however, unlike the acute paradigm, the sub-chronic induction was sufficient to alter the nigrostriatal pathway with reduced TH expression in the SN and decreased striatal dopamine, suggestive of a neurodegenerative phenotype (Garrido-Gil et al., 2018). A study examining a double-hit model with LPS injected in the SN of rats in conjunction with acute colitis resulted in

exacerbated BBB permeability, peripheral and neuroinflammation, and dopaminergic neuronal loss; and these features were ameliorated with depletion of peripheral macrophages, promoting the idea that brain neuropathology and neuroinflammation are modulated by peripheral inflammation (Villaran et al., 2010).

Finally, this concept has also been explored in animal models subjected to colitis to further explore the Braak hypothesis that α syn pathology can propagate along the vagus nerve from the intestine to the brain. A recent study showed that mice overexpressing A53T human α syn were more susceptible to a low-dose chronic colitis paradigm than wildtype mice and exhibited increased α syn and phosphorylated α syn levels in both the brain and colon after DSS as well as decreased TH+ neuron counts in the SN (Kishimoto, Zhu, Hosoda, Sen, & Mattson, 2019). Similar peripheral phenotypes have been observed in nonhuman primates whereby colitis induced increased inflammatory markers, oxidative stress and phosphorylated α syn in the myenteric plexus, albeit overall levels of α syn were reduced (Resnikoff et al., 2019). This reduction in α syn has also been observed in mice that were treated with acute, but not chronic colitis (Prigent et al., 2019).

Collectively, these data strengthen the links between the gut-brain axis and peripheral circulation and provide evidence that intestinal inflammation or GI perturbations may promote PD pathogenesis.

1.6.9: LRRK2 in colitis models

Although a plethora of evidence suggests a link between PD and IBD with LRRK2 seemingly at the interface between the two diseases, very limited studies have examined LRRK2 in the scope of both diseases. To date, a few studies have been published examining colitis in LRRK2 animal models. In 2011, Liu and colleagues induced colitis in LRRK2 knockout mice using an acute DSS model and reported that LRRK2 knockout mice were more susceptible to DSS-

induced colitis relative to wildtype controls (Z. Liu et al., 2011). The authors hypothesized that there was an exacerbated inflammatory response in the context of LRRK2 deficiency due to increased NFAT activation in macrophages (Z. Liu et al., 2011). In the presence of LRRK2, NFAT transport to the nucleus is blocked by LRRK2 interacting with the NRON scaffolding complex (Jabri & Barreiro, 2011; Z. Liu et al., 2011). On the contrary, LRRK2 deficiency promotes NFAT translocation to the nucleus and triggers IFN γ transcription (Jabri & Barreiro, 2011; X. Shen, Yang, Wu, Zhang, & Jiang, 2017). However, a 2018 study by Takagawa et al. could not replicate these findings, but extended the findings and suggested BAC transgenic mice overexpressing wildtype LRRK2 are more susceptible to acute DSS-induced colitis than wildtype mice due in part to Dectin-1 stimulation in dendritic cells that leads to dysregulated inflammatory signaling through the NF κ B pathway (Takagawa et al., 2018). It was hypothesized that LRRK2 dephosphorylates Beclin-1, preventing the degradation of Beclin-1, thus blocking autophagy and increasing LRRK2 expression, all of which was ameliorated with LRRK2 kinase inhibitors (Takagawa et al., 2018).

While the mechanism by which LRRK2 alters inflammation in the context of colitis models is still being explored, additional studies have suggested other hypotheses related to LRRK2 expression and its kinase activity. LRRK2 phosphorylation has been shown to increase in inflamed colonic mucosa concomitant with IFN γ production after acute colitis, promoting the idea that LRRK2 expression is regulated in an IFN γ -dependent manner (Rodrigues-Sousa et al., 2014). Additionally, LRRK2 may disrupt T-helper 17 (Th17) levels and function. Present in the lamina propria of the intestine, Th17 cells are key orchestrators in mucosal homeostasis and responses to gut pathogens that when dysfunctional are hypothesized to contribute to LRRK2-dependent intestinal inflammation. It is hypothesized that LRRK2 G2019S may suppress Th17 activity and differentiation in the gut due to an increase in immature myeloid cells, which is reversed with LRRK2 kinase inhibition (J. Park et al., 2017). Collectively, studies examining LRRK2 in colitis models have been limited in scope and do not examine the effects of intestinal

inflammation on PD-associated pathology in both the nigrostriatal pathway and GI system as other studies have done in wildtype animal models reviewed above. Given that intestinal inflammation is common in both PD and CD and that intestinal inflammation is hypothesized to contribute to GI pathology (that precedes a PD clinical diagnosis) and PD-like neuropathology, more in-depth studies need to be conducted to further examine the causal links between the two diseases.

1.7: Discussion

Extensive research has shown that PD is a multifactorial disease with age, genetics, and environmental factors all contributing to risk for development of PD over an individual's lifespan. The perfect combination of factors creates an environment in which peripheral and brain inflammation shift from protective to deleterious roles and promote PD pathogenesis. However, models exploring the multifaceted components of PD, especially in the context of LRRK2 in the immune system are vastly underexplored given that most PD LRRK2-related research has focused on the neuron. With the knowledge that LRRK2 is highly expressed in immune cells, the question of whether LRRK2 expression and phosphorylation regulates immune cell effector functions that then promote the peripheral inflammation associated with PD and other immune diseases has now been brought to the forefront of the PD field.

We hypothesize that LRRK2 functions in immune cells to regulate effector functions and responses to inflammatory stress; but whether LRRK2 activation hastens protective or deleterious inflammatory responses when its levels increase in cells during inflammation remains to be determined, as do the effects of pathogenic LRRK2 mutations that increase risk for PD. To address this knowledge gap, in this doctoral dissertation we have utilized BAC transgenic LRRK2 mouse models overexpressing mouse wildtype LRRK2 or LRRK2 G2019S in all cells that endogenously express LRRK2. The aims of this research were to examine how 1) increased LRRK2 protein and/or G2019S-mediated kinase activity affects immune cell profiles *in vivo* as a

function of age; and 2) to investigate the extent to which specific environmental factors implicated in PD (bacterial and viral infections, colitis, and pesticides) act as second hits in the LRRK2 wildtype or G2019S BAC mice to promote PD-associated neuroinflammation and neuropathology. If our hypothesis is correct, we expect to find that increased LRRK2 protein or G2019S-dependent gain-of-function kinase activity will alter immune cell profiles with aging and that second hits in mice with increased protein levels of wildtype or mutant LRRK2 will enhance neuroinflammation to promote neurotoxicity in the nigrostriatal pathway, resulting in PD-like neuropathology. Completion of the studies in this doctoral thesis will advance our understanding of the role of LRRK2 in immune cells and alterations in the latter as a consequence of pathogenic mutations; such knowledge is a prerequisite to development of LRRK2-targeted therapeutics that will protect the brain without detrimental or untoward effects on immune system function in the fight against idiopathic and familial forms of PD.

CHAPTER 2: LONGITUDINAL DEEP-IMMUNOPROFILING OF PERIPHERAL IMMUNE CELL SUBSETS IN WILDTYPE AND G2019S MUTANT LRRK2 BAC TRANSGENIC MICE

2.1: Abstract

Mutations in Leucine-Rich Repeat Kinase 2 (LRRK2) are known as one of the greatest contributors to inherited Parkinson's disease (PD) and are linked to sporadic PD. PD is classified as a neurodegenerative disease with loss of dopaminergic neurons in the substantia nigra pars compacta (SNpc); therefore, most research has focused on the role of gain-of-function LRRK2 mutations in neuronal toxicity. However, PD is also associated with neuroinflammation and LRRK2 is expressed in immune cells, albeit at higher levels than neurons, warranting further investigation into the role of LRRK2 in immune cells. Recent work from our group revealed that LRRK2 levels are increased in peripheral immune cell subsets of PD patients relative to healthy controls. Given that aging is the number one risk factor for PD, the effects of LRRK2 and LRRK2 kinase activity levels on the immune system within the context of aging have been vastly underexplored. Here we report bacterial artificial chromosome (BAC) transgenic mice overexpressing wildtype LRRK2 or mutant G2019S LRRK2 exhibit normal characteristics of inflammaging, immunosenescence and cytokine production across time as they age. Overexpression of wildtype LRRK2 or mutant G2019S LRRK2 alone is insufficient to alter immune cell profiles in aging mouse models. These data support a "multiple-hit" model in which a complex interaction between genetics, aging, and environmental exposures may contribute to PD-like neurodegeneration.

2.2: Introduction

Parkinson's disease (PD) is believed to be a multifactorial disease resulting from a complex interaction of genetics, aging, and environmental exposures all thought to contribute to pathogenesis. Interestingly, the greatest risk factor for PD is age, with PD affecting 1% of those over the age of 60 and 5% of those over the age of 85 (Bennett et al., 1996; de Lau & Breteler, 2006; Nussbaum & Ellis, 2003; Tanner & Goldman, 1996; Wood-Kaczmar, Gandhi, & Wood, 2006). Aging is considered the most important determinant of clinical worsening in PD patients (Collier, Kanaan, & Kordower, 2011; Levy, 2007). Initial studies showing neurodegeneration in the substantia nigra (SN) of patients with PD also reported neuronal loss in the SN of healthy control subjects (McGeer, Itagaki, Akiyama, et al., 1988; Mortera & Herculano-Houzel, 2012; Stark & Pakkenberg, 2004). Studies have shown that aging can contribute to a decrease in striatal dopamine, which is similarly observed before degeneration in PD (Carlsson & Winblad, 1976; Kish et al., 1992; Riederer & Wuketich, 1976).

It is well established that as individuals age, so does their immune system. Immune aging is characterized by two primary concepts: immunosenescence, the loss of effector function; and inflammaging, the low-level chronic inflammation that persists with age. Inflammaging is characterized by excess production of circulating inflammatory mediators or cytokines, most notably C-reactive protein (CRP), interleukin-6 (IL-6), and tumor necrosis factor (TNF) derived from chronically stimulated innate and adaptive immune cells (Bruunsgaard et al., 2003; Frasca & Blomberg, 2016). Both the innate and adaptive immune systems are affected by aging as respective immune responses become impaired with age. An aging adaptive immune system is impaired as naïve T and B cell populations as well as T and B cell receptor diversity are reduced (Franceschi et al., 2000; Franceschi et al., 1999). Furthermore, T cell receptor sensitivity is decreased in response to stimuli (Goronzy et al., 2013). Collectively, these deficiencies contribute to an increase in susceptibility to infection and autoimmunity and a continuous remodeling cycle of the immune system.

In conjunction with aging, genetic mutations contribute to 10-15% of PD cases (K. R. Kumar, Djarmati-Westenberger, & Grunewald, 2011). One of the genes identified as causative for PD, Leucine-Rich Repeat Kinase 2 (LRRK2), results in autosomal dominant PD. While mutations in LRRK2 are one of the most common genetic contributors to familial PD, LRRK2 mutations are also implicated in sporadic PD (Johnson et al., 2007; N. L. Khan et al., 2005; Lesage et al., 2009; Lesage, Durr, & Brice, 2006; Paisan-Ruiz, Nath, Washecka, Gibbs, & Singleton, 2008). This suggests that a common underlying mechanism may link non-LRRK2 PD and LRRK2 PD. Therefore, understanding the role of LRRK2 will not only affect PD patients with a LRRK2 mutation but will also shed light on PD in subjects not carrying a LRRK2 mutation.

The G2019S mutation is the most common pathogenic LRRK2 mutation shown to be causative of PD (Biskup & West, 2009; Monfrini & Di Fonzo, 2017; Paisan-Ruiz et al., 2004; Zimprich et al., 2004). Residing in the kinase domain, the G2019S mutation has been shown to increase LRRK2 kinase activity, which results in neuronal toxicity (Greggio et al., 2006; Jeong et al., 2018; Smith et al., 2006; A. B. West et al., 2005; A. B. West et al., 2007). Given the well-characterized pathological hallmark of PD, dopaminergic neurodegeneration that gives rise to PD motor symptoms, research has heavily focused on the role of LRRK2 and LRRK2-mediated kinase activity in neurons. While the precise physiological function of LRRK2 in cells remains unknown, recent attention has been focused on its role in immune cells. LRRK2 is expressed in all immune cell subsets and in some subsets its expression is increased upon stimulation (Gardet et al., 2010; Gillardon et al., 2012; Kuss et al., 2014; Thevenet et al., 2011). Our group recently identified that LRRK2 levels are increased in peripheral immune cell subsets of sporadic PD patients relative to healthy controls (Cook et al., 2017). While the mechanisms to explain these findings still remain elusive, we are forging forward to investigate the effects of LRRK2 levels and LRRK2 kinase activity in immune cells within the context of an aging immune system.

To examine how increased LRRK2 protein or G2019S-mediated LRRK2 kinase activity affects aging immune cell populations and cytokine production, we immunophenotyped peripheral

blood mononuclear cells (PBMCs) from bacterial artificial chromosome (BAC) transgenic mice overexpressing mutant G2019S LRRK2 or wildtype LRRK2. Mice underwent submandibular bleeds every 2 months until the age of 24 months to assess PBMC immunophenotypes and plasma cytokine and chemokine levels. Here we report on normal age related immunophenotypes observed in mice overexpressing wildtype LRRK2 or G2019S LRRK2.

2.3: Materials and Methods

Animals. Homozygous male *Lrrk2-G2019S* (B6.Cg-Tg(Lrrk2*G2019S)2Yue/J; stock number 012467) and *Lrrk2-WT* (B6.Cg-Tg(Lrrk2)6Yue/J; stock number 012466) mice were purchased from the Jackson Laboratory and bred to hemizygoty at Emory University. Hemizygous male and female BAC transgenic mouse strains overexpressing either mouse mutant G2019S LRRK2 (G2019S) or mouse wildtype LRRK2 (WTOE) were used for experimental procedures with non-transgenic littermates (B6) serving as controls. Genotypes were determined by tail-snip PCR with two sets of primers: Transgene: Forward 5' GAC TAC AAA GAC GAT GAC GAC AAG 3' Reverse 5' CTA CCA CCA CCC AGA TAA TGT C 3'; Internal positive control: Forward 5' CAA ATG TTG CTT GTC TGG TG 3' Reverse 5' GTC AGT CGA GTG CAC AGT TT 3'. Animals were group-housed (maximum 5 mice per cage) and maintained on a 12h/12h light/dark cycle with *ad libitum* access to standard rodent chow and water. Experimental procedures involving use of animals were performed in accordance with the National Institutes of Health Guidelines for Animal Care and Use and approved by the Institutional Animal Care and Use Committee at Emory University School of Medicine.

Plasma and Peripheral blood mononuclear cell (PBMC) isolation. Whole blood was collected from mice via submandibular bleeds with an approximate volume of 200 μ l per mouse collected for each time point. Blood samples were collected beginning at 4 months of age and every 2 months thereafter until mice reached 24 months. Whole blood was collected in

ethylenediaminetetraacetic acid (EDTA) coated tubes (Covidien 8881311248). 50µl of whole blood was treated with 1x red blood cell (RBC) lysis buffer (BioLegend 420301) to lyse RBCs as per the manufacturer's instructions prior to staining PBMCs for flow cytometry. The remaining 150µl of whole blood was centrifuged after which plasma was removed and promptly frozen on dry ice then subsequently stored at -80°C until processing.

Multi-color Flow Cytometry. 50µl of PBMCs were stained for 30 minutes with the following panel: Live/Dead Fixable Aqua (1:2000, Invitrogen L34957), anti-mouse CD16/CD32 (1:100, eBioscience 14-0161-085), anti-mouse CD45 AF700 (1:100, BD Biosciences 560510), anti-mouse CD19 BV785 (1:50, Biolegend 115542), anti-mouse CD3 BV421 (1:50, Biolegend 100227), anti-mouse CD4 BV711 (1:200, Biolegend 100447), anti-mouse CD8 PerCP_Cy5.5 (1:200, Biolegend 100734), anti-mouse CD11b FITC (1:50, eBioscience 11-0112), anti-mouse MHCII PE-eFluor610 (1:100, eBioscience 61-5321-82), anti-mouse Ly6c APC_Cy7 (1:100, Biolegend 128026), anti-mouse CD44 PE (1:200, Biolegend 103007), anti-mouse CD62L PE_Cy7 (1:100, eBioscience 25-0621-81), and anti-mouse CD25 APC (1:50, BD Biosciences 561048) in FACS buffer. Samples were fixed in 1% PFA for 30 minutes. 10µl of counting beads (AccuCheck Counting Beads, Invitrogen PCB100) were added to each sample. Samples were then run on an LSRII (BD Biosciences) and analyzed with FlowJo_V10.

Leukocytes were gated on Side Scatter Area (SSC-A) (granularity) by Forward Scatter Area (FSC-A) (size) and then with Forward Scatter Height (FSC-H) by FSC-A to identify single leukocytes. To identify live, CD45⁺ cells, the Fixable Aqua negative population was selected followed by the CD45⁺ population against FSC-H. CD45⁺ cells were then gated on CD3 by C19, with CD3⁺ cells denoting T cells and CD19⁺ cells denoting B cells. CD3⁺ T cells were then gated for CD4⁺ and CD8⁺ T cells to differentiate T helper cells vs cytotoxic T cells, respectively. CD4⁺ T cells were then gated by CD25 with CD25⁺, CD4⁺ cells signifying regulatory T cells. The CD19 B cell population was then examined for MHCII expression by histogram and geometric mean

fluorescent intensity. The CD3⁻, CD19⁻ population was gated on CD8 vs CD11b. The CD11b⁺, CD8⁻ population was then gated for SSC-A by Ly6C. SSC-A high, Ly6C intermediate cells were identified as neutrophils. The remaining non-neutrophil population was gated on Ly6C and MHCII to differentiate Ly6C⁺, MHCII⁻ monocytes, Ly6C⁺, MHCII⁺ monocytes, Ly6C⁻, MHCII⁺ macrophages, and Ly6C⁻, MHCII⁻ monocytes (Figure 2.1).

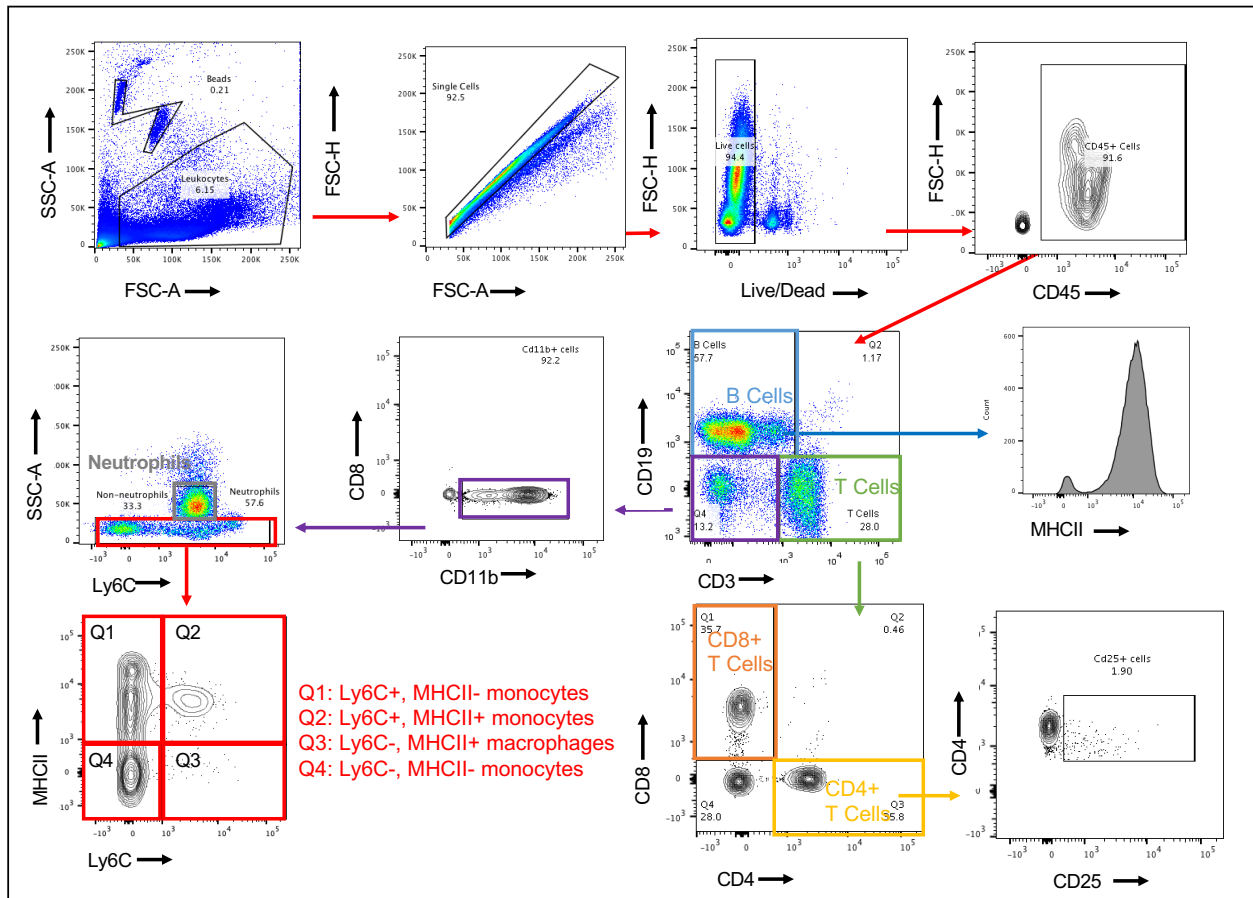


Figure 2.1: Flow cytometry gating strategy used to analyze mouse PBMC immune cell subsets.

Multiplexed Immunoassays. Levels of inflammatory protein were measured in plasma by the Emory Multiplexed Immunoassay Core (EMIC) using a commercially available V-plex Pro-inflammatory Panel 1 Mouse Kit per the manufacturer's instructions on the Meso Scale Discovery

QuickPlex imager (Meso-Scale Discovery, Gaithersburg, MD). Plasma samples were analyzed for cytokines and chemokines (IFN γ , IL-1 β , IL-2, IL-4, IL-5, IL-6, IL-10, IL-12p70, KC/GRO, and TNF) that play key roles in the inflammation response and immune system. Samples were run in replicates of 30 μ l by an experimenter blinded to treatment history and genotype.

Immunoblotting. Immunoblotting was conducted as previously described (Kelly et al., 2018). Splenocytes were sonicated in RIPA lysis buffer (1% Triton-X 100, 50 mM Tris (pH 7.4), 100mM NaCl, 0.1% sodium dodecyl sulfate, 40mM sodium fluoride (NaF), and 1x phosphatase (Roche, 4906845001) and protease inhibitors (Roche, 11697498001)). The bicinchoninic acid (BCA) protein assay (Pierce Scientific, 23225) was used to determine protein concentrations, after which lysates were further diluted 1:1 with 2x Laemmli buffer (BioRad, 1610737) supplemented with 10% DTT and 40mM NaF. Samples were electrophoresed using 4-20% gels (BioRad, 4561096) and transferred to nitrocellulose membranes using a wet transfer system. Membranes were incubated in 5% powdered milk blocking buffer (BioRad, 1706404) for 1 hour before applying primary antibody overnight at 4°C. Primary antibodies included: rabbit anti-LRRK2 antibody MJFF2 (Abcam, ab133474), rabbit anti-Ser(P)-1292 (Abcam, ab203181), or goat anti-GAPDH (Santa Cruz, sc-31915). The following morning, membranes were briefly washed and incubated at room temperature with HRP-conjugated secondary antibodies for 1 hour. Membranes were imaged using Azure Biosystems and analyzed by ImageStudio Lite software. Protein expression was normalized to GAPDH expression or total protein on a Li-Cor Odyssey instrument (Li-Cor #926-11015).

Statistical Analysis. Data from immunophenotyping studies (flow cytometry analysis) and cytokine protein values (Mesoscale analysis) were compared across genotypes and age using a mixed-effects model with GraphPad Prism 8 software. Tukey's multiple comparisons was used

for *post hoc* comparisons within each age. Data from immunoblots were compared across genotypes with a one-way analysis of variance (ANOVA) with Tukey's multiple comparisons for *post hoc* comparisons between genotypes. Significance for all statistical comparisons was set at $p \leq 0.05$. All data are presented as mean \pm SEM.

2.4: Results

Confirmation of LRRK2 overexpression and LRRK2 kinase activity levels in LRRK2 BAC transgenics

Overexpression of wildtype LRRK2 or mutant G2019S LRRK2 was confirmed in splenocyte samples from WTOE and G2019S BACs by immunoblot (Figure 2.2A). By measuring the phosphorylation state at the autophosphorylation site of LRRK2 (pSer1292), G2019S BACs expressed high kinase activity levels associated with the gain-of-function kinase activity promoted by the point mutation, while WTOE mice expressed an intermediary level of kinase activity driven by increased levels of LRRK2 (Figure 2.2B).

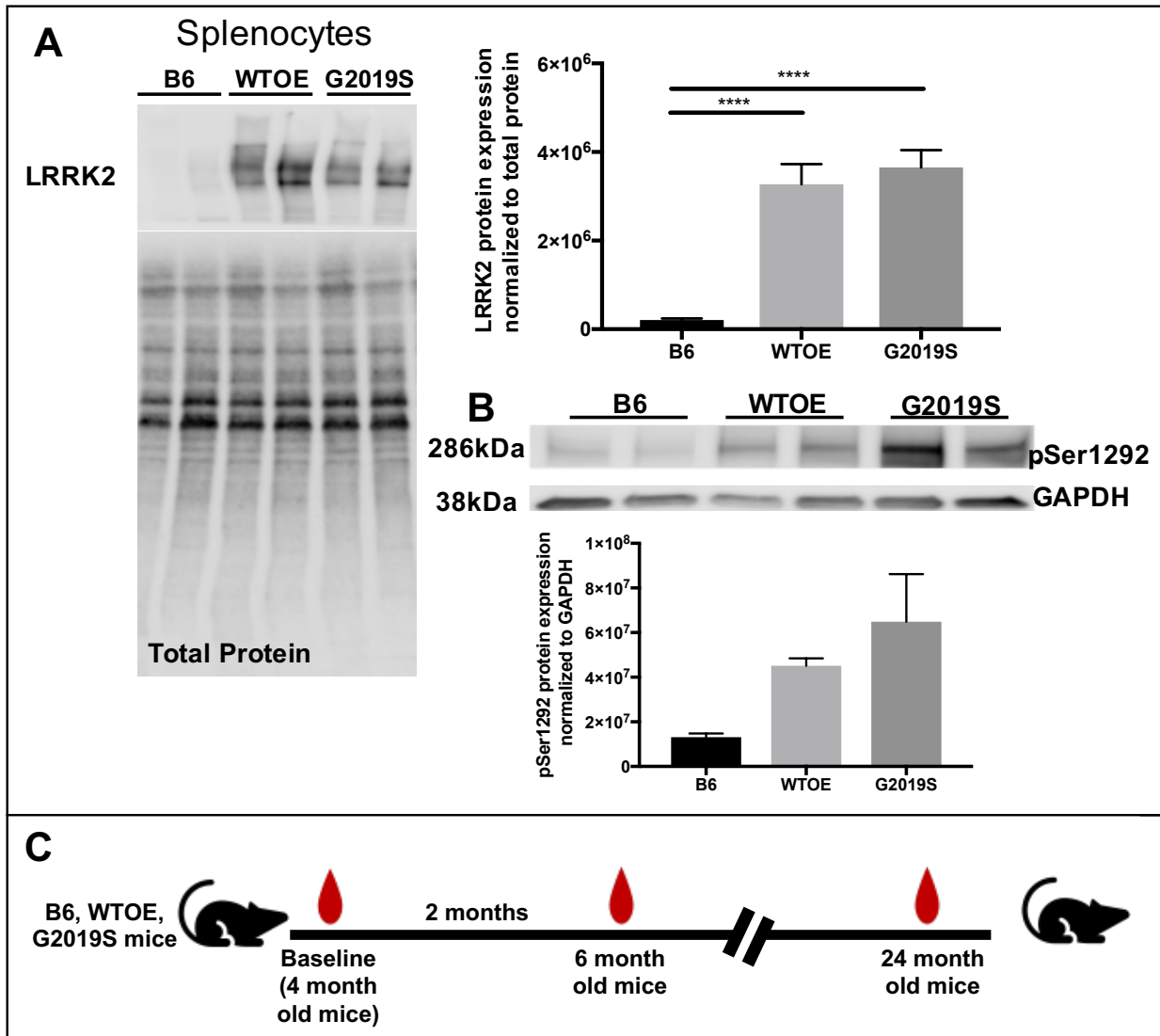


Figure 2.2: Overexpression of WT and G2019S LRRK2 increases LRRK2 levels and LRRK2 autophosphorylation (pSer1292). A) Immunoblot of splenocyte protein with an antibody against LRRK2 confirms elevated levels of LRRK2. B) LRRK2 autophosphorylation as measured by pSer1292 protein expression reveals WTOE mice have an intermediate level of kinase activity while mice with mutant G2019S LRRK2 have gain-of-function kinase activity. C) Immunophenotyping experimental paradigm used to assess immune cell profiles across genotypes as a function of age. One-way ANOVA with Tukey's multiple comparisons. Asterisks (*) signify significant differences between groups ($p < 0.05$).

WTOE and G2019S non-Tg littermate controls exhibit similar immune cell profiles as they age

To determine whether non-Tg littermate controls from WTOE and G2019S strains exhibited different baseline phenotypes, immune cell profiles were analyzed using flow cytometry every two months until 24 months of age (experimental paradigm outlined in Figure 2.2C). Frequencies of CD45+ immune cells decreased with age ($F_{(4.365, 113.1)}=7.097$; $p<0.0001$) but did not differ between the two non-Tg littermate controls (Figure 2.3A). Similarly, frequencies of CD19+ B cells ($F_{(5.159, 118.7)}=3.757$; $p=0.0031$), all T cell populations (CD3+ T cells: $F_{(4.171, 98.02)}=33.31$; $p<0.0001$, CD4+ T cells: $F_{(5.391, 122.9)}=16.97$; $p<0.0001$, CD8+ T cells: $F_{(5.494, 124.7)}=9.562$; $p<0.0001$, CD25+, CD4+ T cells $F_{(5.345, 124)}=14.72$; $p<0.0001$), and two monocyte populations (Ly6C+, MHCII+ monocytes: $F_{(4.72, 118)}=3.85$; $p=0.0035$, Ly6C-, MHCII- monocytes $F_{(5.074, 117.7)}=6.176$; $p<0.0001$) exhibited an effect with age but no genotype effect (Figure 2.3B-D). Frequencies of CD3+ T cells and the subset CD4+ T cells were reduced with age; while CD8+ T cells and regulatory T cells (CD25+, CD4+) were increased with age (Figure 2.3C). An interaction between age and genotype was identified for Ly6C+, MHCII- ($F_{(10, 228)}=2.310$; $p=0.0133$) and Ly6C-, MHCII+ ($F_{(10, 227)}=3.282$; $p=0.0005$) cells, but *post hoc* analysis revealed no significant differences (Figure 2.3D).

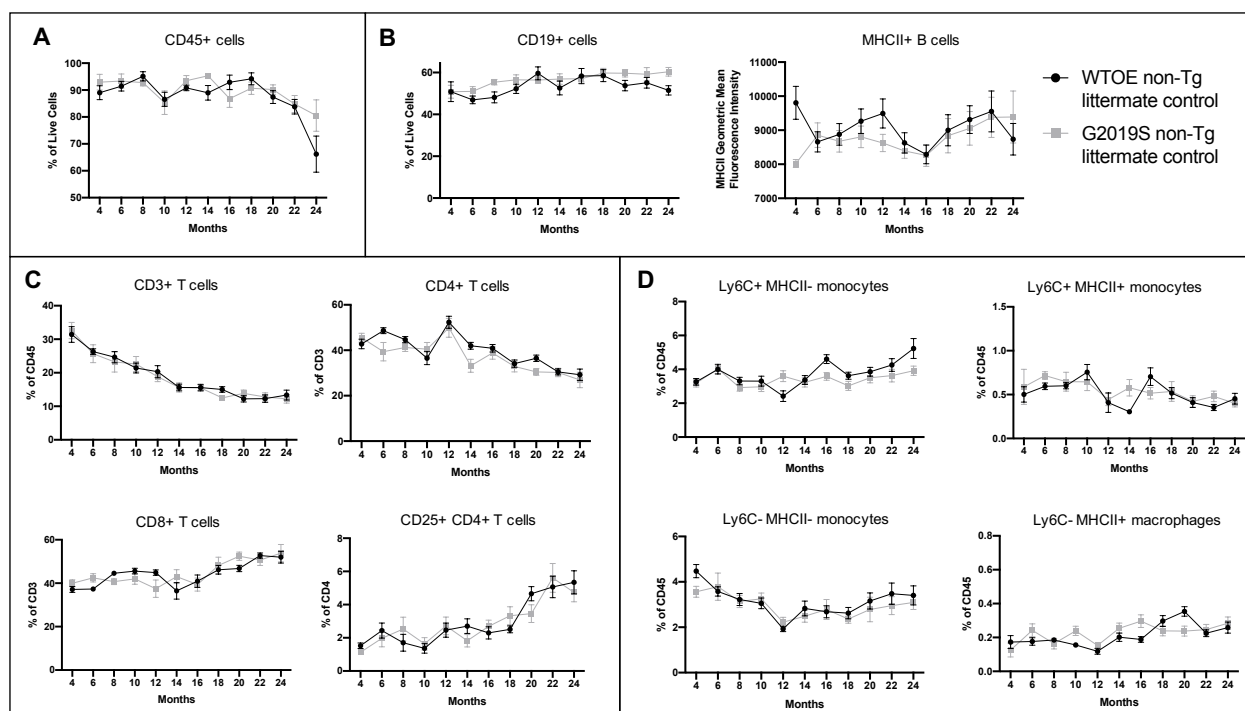


Figure 2.3: Similar immune cell profiles in aging WTOE and G2019S non-Tg littermate controls. By flow cytometry, PBMC populations were measured every two months until 24 months of age. A) Frequencies of CD45+ immune cells reduced with age. B) Alterations in frequencies of B cell populations with age. C) Reduction in frequencies of CD3+ and CD4+ T cells but increases in frequencies of CD8+ and CD25+, CD4+ regulatory T cells with age. D) Alterations in frequencies of monocyte and macrophage populations with age (n=14 per genotype). Data were compared across genotypes and age using a mixed-effects model. Tukey's multiple comparisons was used for *post hoc* comparisons within each age group.

LRRK2 WTOE and G2019S mice exhibit normal aging immune cell populations

To determine whether overexpression of LRRK2 and G2019S-mediated kinase activity affect immune cell profiles as a function of age, PBMCs from B6, WTOE, and G2019S mice were analyzed using flow cytometry every two months until 24 months of age (experimental paradigm outlined in Figure 2.2C). The frequency of CD45+ immune cells as a fraction of total live cells

decreased with age ($F_{(4.219, 220.2)}=18.26$; $p<0.0001$) but did not differ between genotypes (Figure 2.4A). Similarly, frequencies of CD19+ B cells ($F_{(6.976, 375.3)}=12.12$; $p<0.0001$), T cell populations (CD3+ T cells: $F_{(5.742, 311.9)}=69.7$; $p<0.0001$ and CD25+, CD4+ regulatory T cells: $F_{(6.111, 331.2)}=28.25$; $p<0.0001$), Ly6C+, MHCII- monocytes ($F_{(4.614, 246.4)}=14.32$; $p<0.0001$) and Ly6C-, MHCII+ macrophages ($F_{(6.378, 345.7)}=12.02$; $p<0.0001$) exhibited alterations with age but no genotype differences (Figure 2.4B-D). Frequencies of total CD3+ T cells and the subset CD4+ T cells were reduced with age; while frequencies of CD8+ T cells and regulatory T cells (CD25+, CD4+) were increased with age. An interaction between age and genotype was found for the MHCII geometric mean of MHCII+ B cells ($F_{(20, 516)}=2.805$; $p<0.0001$), CD4+ T cells ($F_{(20, 541)}=2.200$; $p=0.0020$), CD8+ T cells ($F_{(20, 530)}=2.180$; $p=0.0023$), Ly6C+, MHCII+ monocytes ($F_{(20, 516)}=1.901$; $p=0.0107$), Ly6C-, MHCII- monocytes ($F_{(20, 539)}=1.969$; $p=0.0074$), but *post hoc* analysis revealed no significant differences.

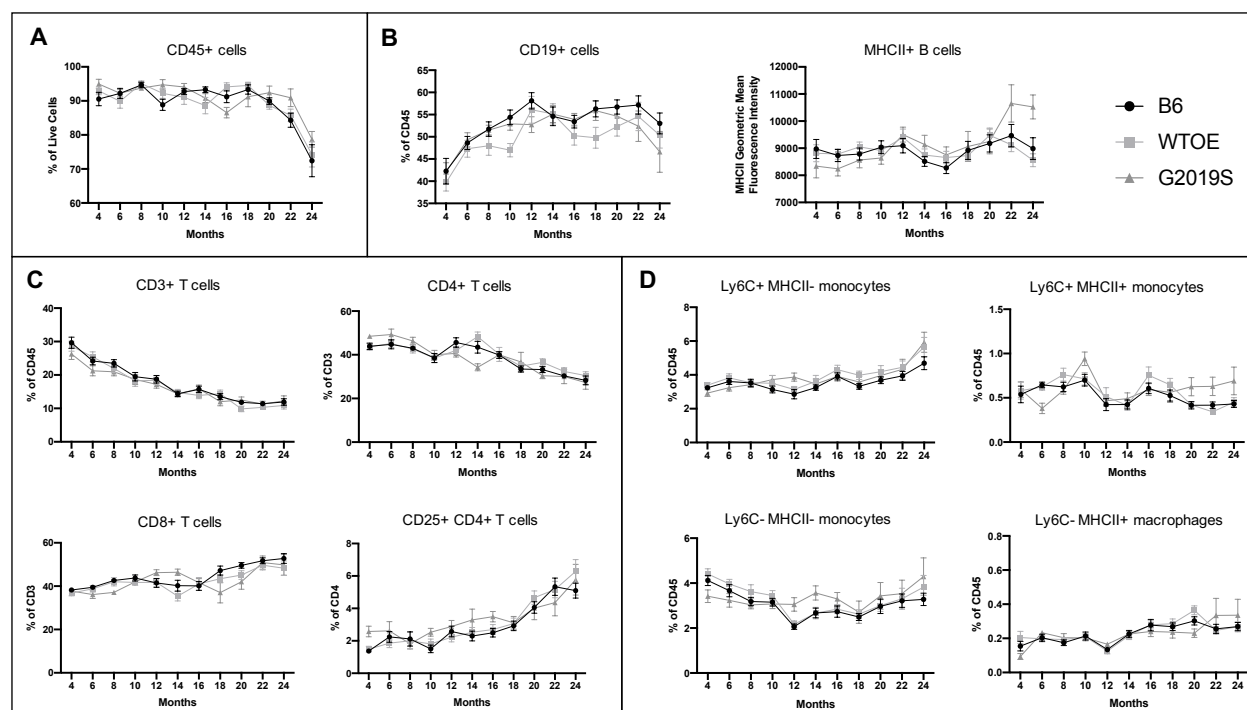


Figure 2.4: LRRK2 expression levels and LRRK2 kinase activity levels do not affect aging immune cell profiles. By flow cytometry, PBMC populations were measured every two months

until 24 months of age to determine if LRRK2 or LRRK2 kinase activity levels alter immune cell profiles. No differences were observed between genotypes, but alterations in immune cell frequencies were observed as a result of age alone. A) Frequencies of CD45+ immune cells reduced with age. B) Alterations in frequencies of B cell populations with age. C) Reduction in frequencies of CD3+ and CD4+ T cells but increases in frequencies of CD8+ and CD25+, CD4+ regulatory T cells with age. D) Alterations in frequencies of monocyte and macrophage populations with age (n=20-28 per genotype). Data were compared across genotypes and age using a mixed-effects model. Tukey's multiple comparisons was used for *post hoc* comparisons within each age. Significance for all statistical comparisons was set at $p \leq 0.05$.

Age-dependent increase in cytokine expression in LRRK2 WTOE and G2019S mice

To further examine the immune system of aging WTOE and G2019S mice, plasma cytokines and chemokines that play major roles in inflammation and immune system function were measured by multiplexed immunoassays. Cytokine levels did not significantly differ between genotypes; however, plasma TNF ($F_{(1.834, 51.35)} = 5.404$; $p=0.0089$), IL-10 ($F_{(2.435, 67.44)} = 5.520$; $p=0.0036$) and KC/GRO ($F_{(4.358, 122)} = 5.082$; $p=0.0006$) expression increased with age in all three genotypes (Figure 2.5 A-C). There were no statistically significant differences observed in $IFN\gamma$, IL-2, IL-5, and IL-6 (data not shown), while IL-4, IL-12p70, and IL-1 β were below the detection limits.

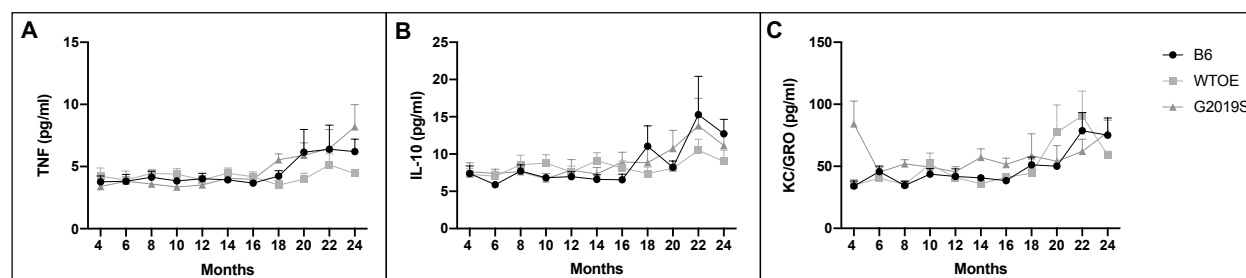


Figure 2.5: Plasma cytokine levels increase as a function of age. There was a main effect of age on A) TNF B) IL-10 and C) KC/GRO plasma levels with aged mice having higher levels of

plasma cytokines regardless of genotype (n=13-18 per genotype). Data was analyzed across genotypes and age using a mixed-effects model. Tukey's multiple comparisons was used for *post hoc* comparisons within each age. Significance for all statistical comparisons was set at $p \leq 0.05$.

2.5: Discussion

Knowledge regarding the effects of increased LRRK2 protein or kinase activity on aging immune cells and inflammation is lacking; and to our knowledge, this is the first in-depth immunoprofiling study of LRRK2 BAC transgenic mice. Given our group's recent finding that LRRK2 protein levels are elevated in peripheral blood immune cell subsets in sporadic PD patients, we posited that LRRK2 regulates inflammatory responses to curb neuroinflammation and reduce the risk for neurodegeneration of vulnerable neuronal populations affected in sporadic PD. To this end, we immunophenotyped PBMCs and measured cytokine and chemokine levels from BAC transgenic mice overexpressing mouse wildtype LRRK2 or mutated G2019S LRRK2 over the course of 24 months.

The transgenic animals were generated using a BAC containing the entire mouse LRRK2 gene, with the G2019S strain modified to include the G2019S mutation (X. Li et al., 2010). The BACs utilized the mouse LRRK2 promoter so that mouse LRRK2 is overexpressed in all cells that endogenously express LRRK2, which is of importance given our interest in investigating LRRK2 in the context of immune cells. Other LRRK2 animal models exist using the human LRRK2 protein; however, using a human protein in a mouse can potentially create unforeseen complications due to interactions. Specifically, mouse immune cells may recognize the human protein as foreign, thus stimulating an unwanted immune response. Importantly, these models do not exhibit the classical hallmarks of PD with no reported evidence of α -synuclein inclusions, motor impairment, or cell loss, thus allowing their use as a tool to examine the effects of increased LRRK2 protein

and G2019S-mediated gain-of-function kinase activity on peripheral and central inflammation as well as brain neurodegenerative phenotypes that may result from second-hit exposures.

According to the 2010 publication from the Yue group reporting the generation and characterization of the LRRK2 BACs, each strain expresses its respective LRRK2 protein 6-fold higher than its non-Tg control (X. Li et al., 2010). To confirm these findings and ensure the BAC transgene was successfully passed through the germline, LRRK2 protein levels were detected by immunoblot in splenocytes, revealing similar overexpression of LRRK2 protein levels in WTOE and G2019S mice. Given that LRRK2 autophosphorylates itself as well as other substrates (Lobbestael et al., 2012), an increase in LRRK2 protein would yield an increase in LRRK2 phosphorylation, which was observed by immunoblot of pSer1292 in the WTOE strain. The G2019S mutation is well known for its gain-of-function kinase activity (Greggio et al., 2006; Jeong et al., 2018; Smith et al., 2006; West et al., 2005; West et al., 2007), which was observed through immunoblot of pSer1292 with higher levels of kinase activity relative to WTOE and B6. These findings support the use of these models as an appropriate tool to examine the effects of LRRK2 protein and kinase activity on immune cells.

To determine whether non-Tg littermate controls from WTOE and G2019S strains were similar and could potentially be grouped as a single control, immune cell subsets were profiled using flow cytometry over 24 months. As expected, changes in immune cell population frequencies were observed with age; but no genotype differences between non-Tg littermate controls from WTOE and G2019S were observed, thus providing rationale for grouping the two non-Tg littermate controls into a single control group (B6) for the remaining analyses.

Similar age-related immunoprofiling results were obtained when comparing all three genotypes and exploring the effects of increased LRRK2 protein levels and G2019S-mediated kinase activity on aging immune cell populations. Despite no genotype differences, changes in frequencies of immune cell populations did occur with age as a factor. Mirroring what is seen in humans, all three genotypes exhibited characteristics of immunosenescence with a reduction in

T cells (CD3 and CD4), a slight increase in CD8 T cells, and a robust increase in regulatory T cells. Given that thymic involution leads to a reduction in output of T cells, it was not surprising to see an overall decrease in the total T cells with age. The reduction in CD4+ T cells and slight increase in CD8+ T cells resulted in a shift in the ratio of T helper subsets relative to cytotoxic T cells. While specific T cell subsets (naïve, effector, and memory) were not measured in the current study, the slight increase in CD8 T cells could be driven largely by an increase in antigen-experienced T cells, while the reduction in CD4 T cells could be largely attributed to a reduction in naïve CD4 T cells (Vescovini et al., 2014). Regulatory T cells (CD25+, CD4+), an immune cell subset that act to suppress an immune response, were increased in all three genotypes with age in accordance with other reports in the literature (Lages et al., 2008; Raynor, Lages, Shehata, Hildeman, & Chougnet, 2012; Rosenkranz et al., 2007). IL-10, which was found to be increased in aged plasma, is an anti-inflammatory cytokine that is responsible for limiting immune cell responses to pathogens. IL-10 dysregulation has been noted in aging, albeit studies have reported opposite findings to ours with age-related decline in expression (Ye & Johnson, 2001). However, overexpression of IL-10 has been shown to induce regulatory T cells, thus the increase in IL-10 seen in the current study could contribute to the observed increase in regulatory T cells (Goudy et al., 2003). This increase in regulatory T cells results in an increase in intensity of immune response, which can also contribute to immune dysfunction (Jagger, Shimojima, Goronzy, & Weyand, 2014).

Monocyte to macrophage transition is commonly referred to as a phase in which monocytes lose Ly6C expression as they enter tissue and upregulate MHCII expression (J. Yang et al., 2014). This transition and cascade were examined in the current study through the gating strategy of the monocyte population, in which we observed an increase in inflammatory monocytes (Ly6C+, MHCII-) with age. The increase in inflammatory monocytes could be one factor contributing to the increase TNF plasma levels, a characteristic of inflammaging.

Collectively, this data supports the idea that inflammaging and immunosenescence are occurring in the LRRK2 BACs and warrants further investigation of aging immune cell function as a risk factor in neurodegeneration as well as further characterization of specific T cell subsets. From these data, we can conclude that increases in LRRK2 protein or G2019S-mediated gain-of-function kinase activity alone are insufficient to alter aging immune cell profiles. In accordance with observations in humans with LRRK2 PD patients presenting clinically with the same features as non-LRRK2 PD patients, we do not see genotype differences in the immune system of these mice that could be dependent on LRRK2 protein levels or G2019S-mediated gain-of-function kinase activity. These data support rationale for a “multiple-hit” model in which a complex interaction between genetics, aging, and environmental exposures contributes to PD pathophysiology.

CHAPTER 3: INTESTINAL INFLAMMATION IN LRRK2 G2019S BAC TRANSGENIC MICE PROMOTES NEUROINFLAMMATION AND PD-ASSOCIATED NIGROSTRIATAL PATHOLOGY

3.1: Abstract

Links between Parkinson's disease (PD) and the gastrointestinal system have become increasingly common. Mutations in Leucine-Rich Repeat Kinase 2 (LRRK2) are one of the greatest genetic contributors to PD and associated with sporadic PD. Interestingly, variants in LRRK2 have also been associated with increased incidence of Crohn's disease (CD). G2019S, the most common LRRK2 pathogenic PD mutation, results in an increased toxic gain-of-function kinase activity. Similarly, the newly identified LRRK2 N2081D SNP that is associated with higher incidence of CD also results in a gain-of-function increase in kinase activity, highlighting the need to further understand the role of LRRK2 in PD and CD. Given LRRK2 apparently sits at the interface between PD and CD, we sought to directly investigate the role of increased LRRK2 protein and increased G2019S-mediated kinase activity on the gut-brain axis. To investigate this, bacterial artificial chromosome (BAC) transgenic mice overexpressing mouse wildtype or G2019S LRRK2 were subjected to acute or chronic DSS-induced colitis and monitored daily for weight loss and disease activity indexes. Data suggest G2019S mice are more susceptible to acute DSS-induced colitis with alterations in peripheral and neuroinflammation. While inflammatory changes were not as profound after chronic colitis compared to acute colitis, changes in the nigrostriatal pathway associated with PD pathology were observed in all three genotypes. In summary, we show that G2019S mice are more susceptible to acute intestinal inflammation thereby resulting in increased neuroinflammation, while chronic colitis is necessary to induce deficits in the nigrostriatal pathway. These studies will advance our understanding of how increased LRRK2 levels and increased gain-of-toxic function kinase activity disrupts the gut-brain axis and may reveal therapeutic opportunities to delay or mitigate gastrointestinal inflammation to lower the risk of brain inflammation and age-related neurodegeneration.

3.2: Introduction

Parkinson's disease (PD) is a progressive movement disorder affecting more than one million Americans and over 10 million people worldwide, making it the second most common neurodegenerative disorder. PD is characterized by aggregation of α -synuclein (α syn) leading to Lewy Body formation and progressive loss of dopaminergic (DA) neurons in the substantia nigra pars compacta (SNpc) (Fahn, 2003). Loss of DA in the nigrostriatal pathway results in stereotypic motor symptoms associated with PD (von Campenhausen et al., 2005; Wirdefeldt, Adami, Cole, Trichopoulos, & Mandel, 2011). Several studies implicate inflammation in the pathophysiology of PD. Late-onset PD has been associated with variations in the human leukocyte antigen (HLA) gene that encodes major histocompatibility complex (MHC) proteins necessary for antigen presentation (Hamza et al., 2010). Reduced CD4:CD8 T cell ratios are present in PD patient blood while T cell infiltration and activated microglia have been identified in the SNpc in PD patients and PD animal models (Baba et al., 2005; McGeer, Itagaki, Boyes, et al., 1988; Saunders et al., 2012; Whitton, 2007). Furthermore, increased inflammatory cytokines (TNF, IFN γ , IL-1 β) have been associated with increased oxidative stress and accelerated DA neurodegeneration in PD (Blum-Degen et al., 1995; Brodacki et al., 2008; Mogi, Harada, Kondo, et al., 1994; Reale, Greig, & Kamal, 2009).

In addition to the stereotypical motor symptoms, PD patients also exhibit non-motor symptoms, with one of the most common identified as gastrointestinal (GI) dysfunction. An estimated 60-80% of PD patients experience GI symptoms (H. Chen et al., 2015; Siddiqui, Rast, Lynn, Auchus, & Pfeiffer, 2002; Ueki & Otsuka, 2004). Moreover, studies suggest chronic constipation manifests in PD patients at least 15 years before diagnosis, making it one of the earliest possible indicators of PD (Abbott et al., 2001; H. Chen et al., 2015; Postuma, Gagnon, Pelletier, & Montplaisir, 2013; Savica et al., 2009). In addition, PD patients exhibit increased intestinal permeability or "leaky gut", with the level of permeability associated with increased

intestinal pro-inflammatory cytokines (Devos et al., 2013; Forsyth et al., 2011). This may be in part due to an infection or sustained exposure to substances resulting in intestinal inflammation (Houser & Tansey, 2017; Mulak & Bonaz, 2015). Therefore, we and others have proposed that intestinal inflammation and altered intestinal permeability contribute to systemic inflammation that in turn promotes neuroinflammation and neurodegeneration associated with PD pathogenesis (Houser & Tansey, 2017; Mulak & Bonaz, 2015).

Interestingly, PD shares several similarities with Crohn's disease (CD), an inflammatory bowel disease characterized by chronic relapsing inflammation of the GI tract. CD risk has been associated with over 160 genetic loci, several of which are related to inflammatory genes (*NOD2*, *TLR4*, *IL-23R*, *HLA*, and *TNF*) (Barrett et al., 2008; Cario & Podolsky, 2000; Duerr et al., 2006; Hugot et al., 2001; Ogura et al., 2001; Wellcome Trust Case Control, 2007). CD results from impaired epithelial barriers and altered immune responses and microbiome. Similar to PD, CD patients exhibit increased levels of circulating pro-inflammatory cytokines (TNF, IFN γ , IL-12) (Daig et al., 1996; Fuss et al., 1996; Murch et al., 1993; Nielsen, Kirman, Rudiger, Hendel, & Vainer, 2003) and altered intestinal permeability that can contribute to intestinal inflammation (Bischoff et al., 2014; Gerova, Stoyanov, Katsarov, & Svinarov, 2011; Petit et al., 2012). Interestingly, patients with CD have a 28% increased risk of PD (F. Zhu et al., 2019). In 2008, studies identified Leucine-Rich Repeat Kinase 2 (LRRK2) as a susceptibility locus for CD (Barrett et al., 2008; Franke et al., 2010). LRRK2 is known as one of the greatest genetic contributors to PD, with the LRRK2 G2019S mutation known as the most prevalent one residing in the kinase domain and resulting in a 2-3-fold increase in toxic gain-of-function kinase activity (Greggio et al., 2006; A. B. West et al., 2005; A. B. West et al., 2007). A recent genome-wide association study (GWAS) identified new LRRK2 variants, N2081D and N551K/R1398H as risk and protective genetic variants, respectively, for both CD and PD (Hui et al., 2018). The N2081D variant resides in the same kinase domain as the G2019S mutation and results in an increase in kinase activity albeit not to the same extent as the G2019S mutation (Hui et al., 2018). LRRK2 protein is expressed in a

variety of tissues and cell types, including immune cells and neurons (A. B. West, 2017). While pathogenic mechanisms underlying LRRK2 mutations are not well understood, LRRK2 has been shown to regulate inflammatory processes, and our group has shown its expression is increased in peripheral blood immune cells from PD patients relative to age- and sex-matched controls (Cook et al., 2017). Interestingly, another group has shown that LRRK2 levels are increased in immune cells in inflamed tissue from CD patients (Gardet et al., 2010). Increased LRRK2 kinase activity due to increased protein expression or the G2019S mutation drives dysregulation resulting in increased inflammatory cytokines (H. Lee et al., 2017; Moehle et al., 2015; Moehle et al., 2012). A handful of studies have examined the role of LRRK2 in experimental models of intestinal inflammation. A recent report suggests bacterial artificial chromosome (BAC) transgenic mice overexpressing wildtype LRRK2 are more susceptible to dextran sodium sulfate (DSS)-induced colitis than wildtype mice, due in part to increases in kinase activity that lead to dysregulated inflammatory signaling (Takagawa et al., 2018). However, studies of LRRK2 in colitis models have been limited in scope and do not examine the effects of intestinal inflammation on PD-like pathology in either the nigrostriatal pathway or GI system. Given that intestinal inflammation is common in both PD and CD and that we hypothesize that intestinal inflammation contributes to GI pathology (that precedes a PD diagnosis) and PD-like neuropathology (Houser & Tansey, 2017), we aimed to explore the effects of increased LRRK2 protein and increased G2019S-mediated kinase activity on the GI system and central nervous system (CNS) in a murine model of intestinal inflammation. We hypothesized that G2019S-mediated kinase activity synergizes with intestinal inflammation to promote GI dysfunction and PD-like neuroinflammation and neuropathology in the CNS. Understanding the effects of LRRK2 and its kinase activity in a model of intestinal inflammation on the CNS and GI system will be critical for development of immunomodulatory neuroprotective therapies to prevent, delay or slow progression of PD pathologies.

3.3: Materials and Methods

Animals. Homozygous male *Lrrk2-G2019S* (B6.Cg-Tg(Lrrk2*G2019S)2Yue/J; stock number 012467) and *Lrrk2-WT* (B6.Cg-Tg(Lrrk2)6Yue/J; stock number 012466) mice were purchased from the Jackson Laboratory and bred to hemizygoty at Emory University. Hemizygous male and female BAC transgenic mouse strains overexpressing either mouse mutant G2019S LRRK2 (G2019S) or mouse wildtype LRRK2 (WTOE) were used for experimental procedures with non-transgenic littermates (B6) serving as controls. Genotypes were determined by tail-snip PCR with two sets of primers: Transgene: Forward 5' GAC TAC AAA GAC GAT GAC GAC AAG 3' Reverse 5' CTA CCA CCA CCC AGA TAA TGT C 3'; Internal positive control: Forward 5' CAA ATG TTG CTT GTC TGG TG 3' Reverse 5' GTC AGT CGA GTG CAC AGT TT 3'. Animals were group-housed (maximum 5 mice per cage) and maintained on a 12h/12h light/dark cycle with *ad libitum* access to standard rodent chow and water. Experimental procedures involving use of animals were performed in accordance with the National Institutes of Health Guidelines for Animal Care and Use and approved by the Institutional Animal Care and Use Committee at Emory University School of Medicine.

Experimental Timeline. Male and female B6, WTOE, and G2019S mice were subjected to different DSS-induction paradigms. For extended acute DSS-induced colitis, 2-3-month-old male and female WTOE and G2019S mice were subjected to 9 days of 2% DSS (Affymetrix 14489) followed by 2 days of autoclaved tap water *ad libitum* (n=6 per genotype) (Figure 3.1A). For acute DSS-induced colitis and recovery, 2-3-month-old male and female B6, WTOE, and G2019S mice were subjected to 5 days of 2% DSS followed by 5 days of autoclaved tap water *ad libitum* (n=18-26 per genotype) (Figure 3.1B). 16-18-month-old B6 and G2019S mice were subjected to the same acute DSS-induced colitis paradigm (n=12-19 per genotype) (Figure 3.1C). For chronic DSS-induced colitis 2-3-month-old male and female B6, WTOE, and G2019S mice were

subjected to 1.5% DSS for 5 days followed by autoclaved tap water for 5 days. This was repeated two consecutive times for a total 30 days (n=19-22 per genotype) (Figure 3.1D). Water controls were placed on autoclaved tap water for their respective study durations. Mice were weighed and assessed for disease activity indexes (DAI) daily for acute paradigms or every other day for the chronic paradigm. DAI scores were calculated based on the sum of weight loss, fecal consistency, and fecal blood scores according to the criteria in Table 3.1. Fecal blood presence was detected using Hemocult II SENSE kits (Beckman Coulter 64152) according to the manufacturer's protocol. Mice were coded so that researchers conducting the experiment were blinded to genotype and treatment groups until after data analyses were completed.

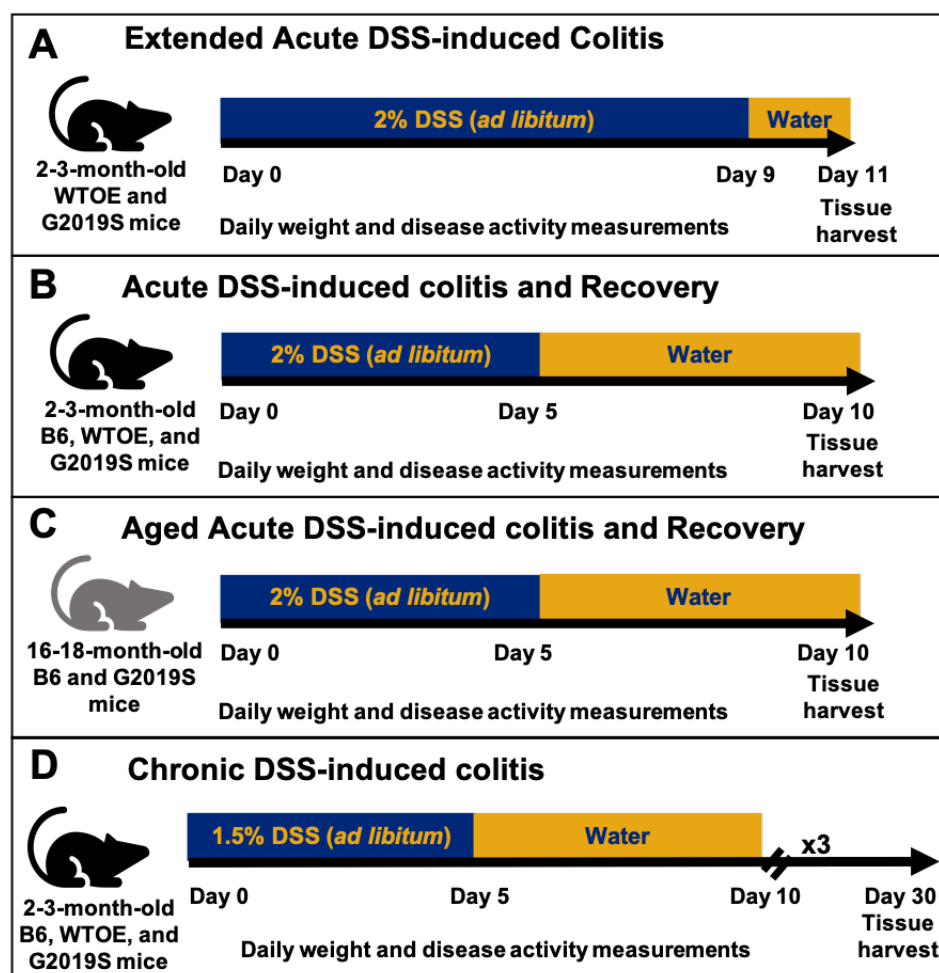


Figure 3.1: Study designs of DSS-induced colitis models.

Score	Weight Loss (% Baseline)	Feces Consistency	Fecal Blood
0	Gain – 1.99%	Firm, dry, well-formed pellets	No blood detected
1	2.0-7.99%	Soft, moist, loose pellets	
2	8-13.99%	Semi-liquid feces, no rectal adherence	Positive hemocult test
3	14-19.99%		Visible blood in fecal smear
4	Over 20%	Liquid feces, rectal adherence	Visible bleeding from the rectum

Table 3.1: Criteria for calculation of disease activity index (DAI) for colitis studies.

Tissue collection. At the end of the paradigm, mice were sacrificed by decapitation. Brain tissue was removed, with the right hemisphere designated for flow cytometry. From the left hemisphere, the striatum, SN, and cortex were dissected, flash frozen and stored in -80°C until processing. For the acute paradigm, caudal tissue from the left hemisphere containing the SN was post-fixed in 4% paraformaldehyde for 24 hours at 4°C for immunohistochemistry.

Plasma and Peripheral blood mononuclear cell (PBMC) isolation. Immediately prior to sacrifice, whole blood was collected by submandibular bleeds with approximately $200\mu\text{l}$ per mouse collected. Whole blood was collected in ethylenediaminetetraacetic acid (EDTA) coated tubes (Covidien 8881311248). $50\mu\text{l}$ of whole blood was treated with 1x red blood cell (RBC) lysis buffer (BioLegend 420301) to lyse RBCs as per the manufacturer's instructions prior to staining PBMCs for flow cytometry. The remaining $150\mu\text{l}$ of whole blood was centrifuged after which plasma was removed and promptly frozen on dry ice then subsequently stored at -80°C until processing.

Brain immune cell isolation. Brain immune cell isolation was performed as previously described with minor modifications (MacPherson et al., 2017). The right hemisphere was minced in 1xHBSS (without calcium, magnesium, and phenol red, Invitrogen, 14175) and transferred to an enzymatic

digestion solution consisting of 1.4U/ml collagenase, type VIII (Sigma, C2139), 1mg/ml DNase 1 (Sigma, DN25) in RPMI1640 medium (ThermoFisher, 11875085). The tissue and enzymatic solution were incubated at 37°C for 15 minutes with shaking every 5 minutes. The solution was then neutralized with 10% FBS (heat inactivated, Atlanta Biologicals, S11150) in RPMI1640 medium and centrifuged to pellet tissue. The remaining tissue pellet was homogenized with glass pipets in ice cold 1x HBSS and then filtered through a 70µM cell strainer. After centrifugation, the remaining pellet was resuspended in 37% Percoll (Sigma, P1644). 70% Percoll was layered below the resuspended pellet while 30% Percoll was layered above. The Percoll gradient was centrifuged for 30 minutes at room temperature without a brake. Immune cells were isolated from the interface between the 37% and 70% layers, washed with 1x HBSS and then stained for flow cytometric analysis.

Multi-color Flow Cytometry. 50µl of PBMCs were stained with BMV109 (1µM, Vergent Bioscience, 40200-100) for 1 hour at 37°C. After a brief wash, PBMCs were then stained for 20 minutes with the following panel: Live/Dead Fixable Red Dead Cell Stain (1:2000, Invitrogen, 23102), anti-mouse CD16/CD32 (1:100, eBioscience, 14-0161-085), anti-mouse CD45 PerCP_Cy5.5 (1:100, eBioscience, 45-0451-80), anti-mouse CD19 BV650 (1:100, Biolegend, 115541), anti-mouse CD3 BV421 (1:50, Biolegend 100227), anti-mouse CD4 V500 (1:100, BD Biosciences, 560783), anti-mouse CD8 BV785 (1:100, Biolegend 100749), anti-mouse CD11b PE_Cy7 (1:200, Biolegend, 101215), anti-mouse MHCII APC_Cy7 (1:200, Biolegend, 107627), anti-mouse CD44 PE (1:200, Biolegend, 103007), anti-mouse Ly6G AF700 (1:100, eBioscience, 56-5931-80), anti-mouse CD11C BV711 (1:200, Biolegend, 117349), and anti-mouse Ly6C AF488 (1:100, Biolegend, 53-5932) in FACS buffer. Samples were fixed in 1% PFA for 30 minutes. 10µl of counting beads (AccuCheck Counting Beads, Invitrogen PCB100) were added

to each sample. Samples were then run on an LSRII cytometer (BD Biosciences) and analyzed with FlowJo_V10 software.

Brain immune cells were stained with BMV109 (1 μ M, Vergent Bioscience, 40200-100) and Pepstatin A, BODIPY FL Conjugate (1 μ g/mL, ThermoFisher Scientific, P12271) for 1 hour at 37°C. After a brief wash, brain immune cells were then stained for 20 minutes with the following panel: Live/Dead Fixable Red Dead Cell Stain (1:2000, Invitrogen, 23102), anti-mouse CD16/CD32 (1:100, eBioscience, 14-0161-085), anti-mouse CD45 PerCP_Cy5.5 (1:100, eBioscience, 45-0451-80), anti-mouse CD3 BV421 (1:50, Biolegend 100227), anti-mouse CD4 V500 (1:100, BD Biosciences, 560783), anti-mouse CD8 PE (1:100, eBioscience, 12-0083-81), anti-mouse CD11b PE_Cy7 (1:200, Biolegend, 101215), anti-mouse MHCII APC_Cy7 (1:200, Biolegend, 107627), anti-mouse Ly6C BV785 (1:100, Biolegend 128041), anti-mouse CD86 BV605 (1:50, Biolegend, 105037), anti-mouse Ly6G AF700 (1:100, eBioscience, 56-5931-80), and anti-mouse CD11C BV711 (1:200, Biolegend, 117349) in FACS buffer. Samples were fixed in 1% PFA for 30 minutes. 10 μ l of counting beads (AccuCheck Counting Beads, Invitrogen PCB100) were added to each sample. Samples were then run on an LSRII cytometer (BD Biosciences) and analyzed with FlowJo_V10 software.

For PBMCs, leukocytes were gated on Side Scatter Area (SSC-A) (granularity) by Forward Scatter Area (FSC-A) (size) and then with Forward Scatter Height (FSC-H) by FSC-A to identify single leukocytes. To identify live CD45⁺ cells, the Fixable Red negative population was selected followed by the CD45⁺ population against FSC-H. CD45⁺ cells were then gated on CD19 by CD3, with CD3⁺ cells denoting T cells. T cells were then gated for CD4⁺ and CD8⁺ T cells to differentiate T helper cells vs cytotoxic T cells, respectively. The CD19⁻ B cell population was examined for MHCII expression by histogram and geometric mean fluorescent intensity. The CD19⁻, CD3⁻ population was gated on CD11b by CD19 to select CD11b⁺ positive cells. That population was then selected and gated for CD11b vs Ly6G to identify neutrophils (CD11b⁺, Ly6G⁺). The non-neutrophil population was then gated for the Ly6C by MHCII cascade that

distinguishes monocyte and macrophage populations (Ly6C⁺, MHCII⁻ monocytes, Ly6C⁺, MHCII⁺ monocytes, Ly6C⁻, MHCII⁺ macrophages, and Ly6C⁻, MHCII⁻ monocytes). In each immune subset, the pan-cathepsin probe, BMV109, were examined for positive cells and geometric mean fluorescent intensity.

For brain immune cells, leukocytes were gated on SSC-A (granularity) by FSC-A (size) and then with FSC-H by FSC-A to identify single leukocytes. To identify live cells, the Fixable Red negative population was selected against FSC-H. From a CD45 by CD11b gate, lymphocytes and mixed monocytes/macrophages were distinguished from microglia populations. The microglia population was further analyzed for MHCII⁺ microglia and CD86⁺ microglia. The geometric mean fluorescent intensity of MHCII⁺ microglia or CD86⁺ microglia was also identified based on the respective antibody. The lymphocyte population was gated on CD3⁺ T cells followed by CD4⁺ and CD8⁺ T cells to differentiate T helper cells vs cytotoxic T cells, respectively. The mixed monocyte/macrophage population was then examined with CD11b by Ly6G to distinguish neutrophils. The non-neutrophil gate was then gated with the Ly6C by MHCII cascade that distinguishes monocyte and macrophage populations (Ly6C⁺, MHCII⁻ monocytes, Ly6C⁺, MHCII⁺ monocytes, Ly6C⁻, MHCII⁺ macrophages, and Ly6C⁻, MHCII⁻ monocytes). In each immune subset, cathepsin probes, BMV109 and Pepstatin A, BODIPY, were examined for positive cells and geometric mean fluorescent intensity (MFI).

Multiplexed Immunoassays. Levels of inflammatory protein were measured in plasma by the Emory Multiplexed Immunoassay Core (EMIC) using a commercially available V-plex Pro-inflammatory Panel 1 Mouse Kit per the manufacturer's instructions on the Meso Scale Discovery QuickPlex (Meso-Scale Discovery, Gaithersburg, MD). Plasma samples were analyzed for cytokines and chemokines (IFN γ , IL-1 β , IL-2, IL-4, IL-5, IL-6, IL-10, IL-12p70, KC/GRO, and TNF) that play key roles in the inflammation response and immune system. Samples were run in replicates of 30 μ l by an experimenter blinded to treatment history and genotype.

RNA extraction and protein isolation. RNA extraction and protein isolation were performed as previously described (de Sousa Rodrigues et al., 2017). Tissue was homogenized in ice-cold TRIzol (Life Technologies, 15596018) using a stainless-steel bead (Qiagen, 69989) and a TissueLyser II (Qiagen, 85300). RNA was then isolated using QIAshredder columns (Qiagen, 79656) and RNeasy mini kits (Qiagen, 74106) according to the manufacturer's protocol. RNA was quantified and purity assessed using a NanoDrop 2000 spectrophotometer (Thermo Fisher Scientific). Protein was isolated from the organic layer of the TRIzol separation method by methanol precipitation. Protein was resuspended in 1% SDS, quantified using a BCA protein assay and then used for immunoblotting.

cDNA synthesis. Following the manufacturer's protocol, RNA was reverse transcribed using SuperScript II Reverse Transcriptase (Life Technologies, 18064014), random hexamers (Integrated DNA Technologies, 51-01-18-25), and dNTPs (Life Technologies, 18427013).

Quantitative real-time polymerase chain reaction (qPCR). qPCR was performed as previously described (de Sousa Rodrigues et al., 2017). Using an ABI Prism 7900 HT Fast Real-time PCR System (Applied Biosystems), 25ng cDNA was analyzed in triplicate with SYBR Green PCR Master Mix and 150nM validated forward and reverse oligonucleotide primers (Integrated DNA Technologies). Cycle of threshold (Ct) values were normalized to the averaged values of the two housekeeping genes, *Gapdh* and cyclophilin (*Ppia*). Relative mRNA expression was obtained by subtracting normalized Ct values from a standard number. Primers used: *Gapdh* – Forward 5' CAA GGT CAT CCA TGA CAA CTT TG 3' Reverse 5'GGC CAT CCA CAG TCT TCT GG 3'; *Tnf* – Forward 5' CTG AGG TCA ATC TGC CCA AGT AC 3' Reverse 5' CTT CAC AGA GCA ATG ACT CCA AAG 3'; *IL-1 β* – Forward 5' CAA CCA ACA AGT GAT ATT CTC CAT G 3' Reverse 5' GAT CCA CAC TCT CCA GCT GCA 3'; *Ptprc* – Forward 5' TCA TGG TCA CAC GAT GTG AAG

A 3' Reverse 5'AGC CCG AGT GCC TTC CT 3'; *Ppia* – Forward 5' TGG AGA GCA CCA AGA CAG ACA 3' Reverse 5' TGC CGG AGT CGA CAA TGA T 3'; *Lcn2* – Forward 5' TGG AAG AAC CAA GGA GCT GT 3' Reverse 5' GGT GGG GAC AGA GAA GAT GA3', *Cd4* – Forward 5' GTG AGC TGG AGA ACA GGA AAG AG 3' Reverse 5' GGC TGG TAC CCG GAC TGA 3'; *Cd8b* – Forward 5' GCT GTC CTT GAT CAT CAC TCT CA 3' Reverse 5' ACT AGC GGC CTG GGA CAT T 3'; *IA-b* – Forward 5' CAG GAG TCA GAA AGG ACC TC 3' Reverse 5' AGT CTG AGA CAG TCA ACT GAG 3'; *Snca* – Forward 5' AAA TGT TGG AGG AGC AGT GG 3' Reverse 5' GAA GGC ATT TCA TAA GCC TCA 3'; *Tjp1* – Forward 5' CCT GAA GGA ATT GAG CAA GA 3' Reverse 5' GCA GAG TTT CAC CTT TCT CT 3'; *Ocln* – Forward 5' GAT TAG GTG ACC AGT GAC ATC 3' Reverse 5' GAT TGG GTT TGA ATT CAT CAG G 3'; *Cldn1* – Forward 5' ATG ATG AGG TGC AGA AGA TG 3' Reverse 5' TCG CCA GAC CTG AAA TTA AA 3'; and *Cldn2* – Forward 5' CAC CCA CAG ATA CTT GTA AGG 3' Reverse 5' AGC CTC TAA TCC CTT ATT TCA C 3'.

Immunoblotting. Immunoblotting was performed as previously described (de Sousa Rodrigues et al., 2017). The bicinchoninic acid (BCA) protein assay (Pierce Scientific, 23225) was used to determine protein concentrations, after which lysates were further diluted 1:1 with 2x Laemmli buffer (BioRad, 1610737) and boiled at 90°C for 5 minutes. Samples (10µg) were electrophoresed using 4-20% Mini-PROTEAN TGX precast gels (BioRad, 4561096) and transferred to 0.45µm PVDF membranes using the Trans-Blot Turbo System (BioRad, 1704150EDU) according to the manufacturer's protocol. Membranes were washed and then incubated in 5% powdered milk blocking buffer (BioRad, 1706404) for 1 hour before applying primary antibody overnight at 4°C. The following morning, membranes were briefly washed and incubated at room temperature with HRP-conjugated secondary antibodies for 1 hour. Membranes were briefly washed and imaged using Azure Biosystems C400 system or a Li-Cor Odyssey Imaging system to detect chemiluminescent signal. Bands were quantified by densitometry using ImageStudio Lite

software. Protein expression was normalized to total protein on a Li-Cor Odyssey instrument (Li-Cor #926-11015).

High-performance liquid chromatography (HPLC). Levels of dopamine and related analytes in the striatum were measured with electrochemical detection by the Emory HPLC Bioanalytical Core (EHBC) as previously published (Song, Fan, Exeter, Hess, & Jinnah, 2012). Analytes were identified by matching retention time and sensor ratio measures to known standards. Levels of dopamine, DOPAC, HVA, L-Dopa, and 3-MT were quantified by comparing peak areas to standards.

RNA sequencing. Total RNA from samples containing the SN was extracted using TRIzol as detailed above. RNA quality, purity, degradation and contamination were assessed by Novogene Corporation (Beijing, China) using a NanoDrop, Agilent 2100, and agarose gel electrophoresis, respectively. cDNA libraries were constructed from RNA samples following the Illumina protocols. Library preparations were sequenced on an Illumina HiSeq 4000 platform at Novogene Corporation.

Immunohistochemistry. Immunohistochemistry was performed as previously published (Caudle et al., 2007; Kline et al., 2019). Upon 24 hours of post-fixation in 4% paraformaldehyde, brain tissue was equilibrated in 30% sucrose in PBS at 4°C. 40µm coronal sections were obtained using a sliding microtome. Floating sections were blocked with 5% normal goat serum (Jackson ImmunoResearch, 005-000-021) for 1 hour at room temperature and then incubated with a goat anti-ionized calcium binding adaptor molecule 1 (Iba1) antibody (Abcam, AB5076) overnight at 4°C. Iba1 signal was amplified using an ABC Elite Kit (Vector Laboratories, PK-6100). Sections were incubated with a biotinylated rabbit anti-goat secondary antibody for 1 hour at 4 °C and then

developed with 3,3'-diaminobenzidine (DAB) tablets (Sigma, D4293) followed by ethanol and xylene dehydration. Tissue was then transferred to microscopy slides. Images were obtained using a THUNDER microscope (Leica) with a DMC4500 digital camera and LAS X 3D analysis and 3D visualization advanced software.

Hematoxylin and eosin (H&E) staining. For histological analysis, colons were removed, cut longitudinally, swiss-rolled and flash frozen in optimal cutting temperature (OCT, Tissue-Tek, 4583) embedding medium. 5 μ M sections were cut on the cryostat and placed on charged glass microscopy slides. H&E staining was performed, and tissue was dehydrated with ethanol and xylene. Images were obtained using a THUNDER microscope (Leica) with a DMC4500 digital camera and LAS X 3D analysis and 3D visualization advanced software. Images were scored in quadrants. Quadrant scores were calculated based on the sum of inflammatory cell infiltration, epithelial changes, and mucosa architecture, fecal consistency, and fecal blood scores according to the criteria in Table 3.2 (adapted from (Erben et al., 2014)). The average of each quadrant score represents the final histological score for each sample.

Score	Inflammatory cell infiltration	Epithelial changes	Mucosa architecture
1	Minimal in the mucosa	Minimal hyperplasia	
2	Mild in the mucosa and sometimes in the submucosa	Mild hyperplasia and goblet cell loss; possible cryptitis and erosion	
3	Moderate in the mucosa and submucosa	Moderate hyperplasia and goblet cell loss; cryptitis and possible crypt abscesses	Ulcerations
4	Marked in the mucosa and submucosa; often transmural	Marked hyperplasia and goblet cell loss; multiple crypt abscesses	Extended ulcerations

Table 3.2: Criteria for calculation of histological score of colon tissue.

Statistical Analysis. Percent body weight changes were analyzed using two-way analysis of variance (ANOVA) or mixed-effects model with repeated measures on GraphPad Prism 8 software. Data were compared across genotype using an unpaired student t-test or one-way ANOVA with Tukey's *post hoc* for multiple comparisons. Data compared across genotype and treatment were analyzed using a two-way ANOVA with Tukey's *post hoc* for multiple comparisons. Significance for all statistical comparisons was set at $p \leq 0.05$. All data are presented as mean \pm SEM. Letters above groups indicate *post hoc* results. Groups sharing the same letter are not significantly different.

3.4: Results

G2019S mice are more susceptible to extended acute DSS

This study utilized several different time courses of DSS induction to assess different questions and parameters. The extended acute DSS model assesses peak inflammation and disease status. From this paradigm, we showed that G2019S mice are more susceptible to intestinal inflammation induced by DSS with a significant loss in body weight and increase in DAI (Figure 3.3B). This was further supported by a reduction in colon weight and length in G2019S mice (Figure 3.3D), as DSS causes the colon to shrink due to loss and damage of epithelial cells. Evidence of alterations in tight junction proteins that may contribute to increased intestinal permeability was also observed. While differences in claudin-1 were not significant (data not shown), G2019S mice exhibited lower levels of claudin-2 and ZO-1 (Figure 3.3F), and evaluation of colonic histology revealed poor crypt health and high levels of ulceration in colons of G2019S mice (Figure 3.3E). Levels of several pro-inflammatory cytokines (TNF, IL-6, IL-1 β , IL-10 (Figure

3.3C) and IL-5 (data not shown)) were increased in the plasma of G2019S mice relative to WTOE, while no significant differences were found in IFN γ , IL-2, IL-4, KC/GRO (data not shown) and IL-12p70 was below detection limits (data not shown).

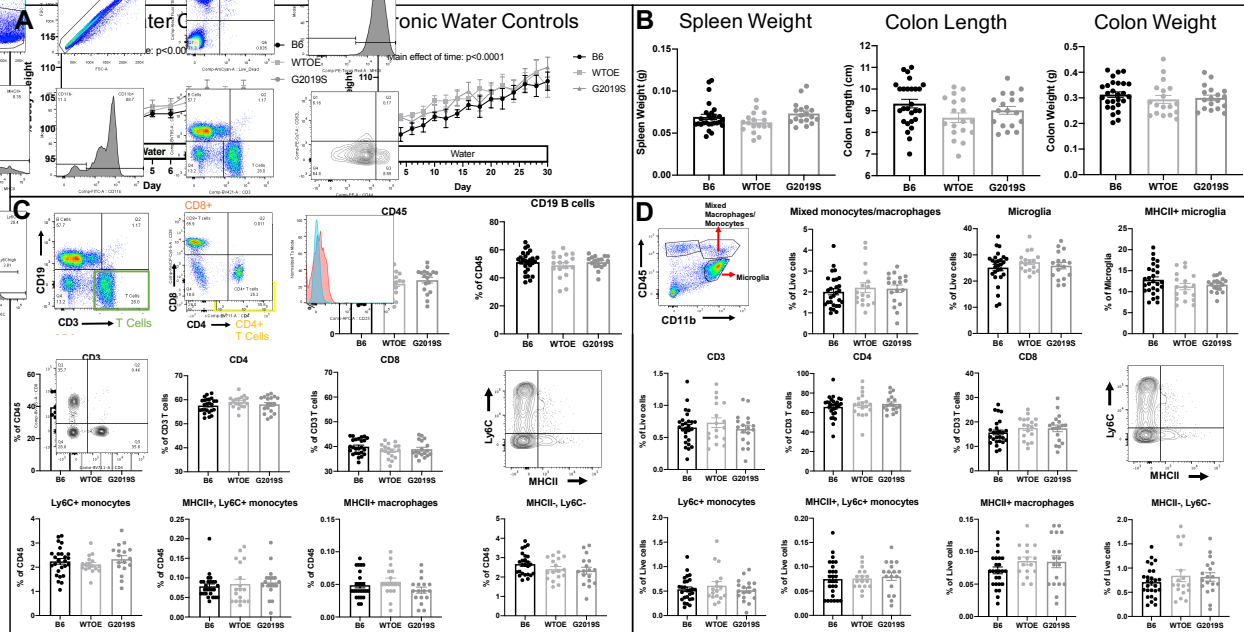


Figure 3.2: B6, WTOE, and G2019S water controls exhibit the same peripheral blood, spleen, colon, and brain immunophenotypes. A) Percent body weight of water controls from acute and chronic paradigms. Data were compared across genotypes and time using a two-way ANOVA with repeated measures. B) Spleen weight (g), colon length (cm), and colon weight (g) from water control samples. C) PBMC and D) brain immunophenotypes (n=18-27 per genotype). Data were compared across genotypes using a one-way ANOVA. Significance for all statistical comparisons was set at $p \leq 0.05$.

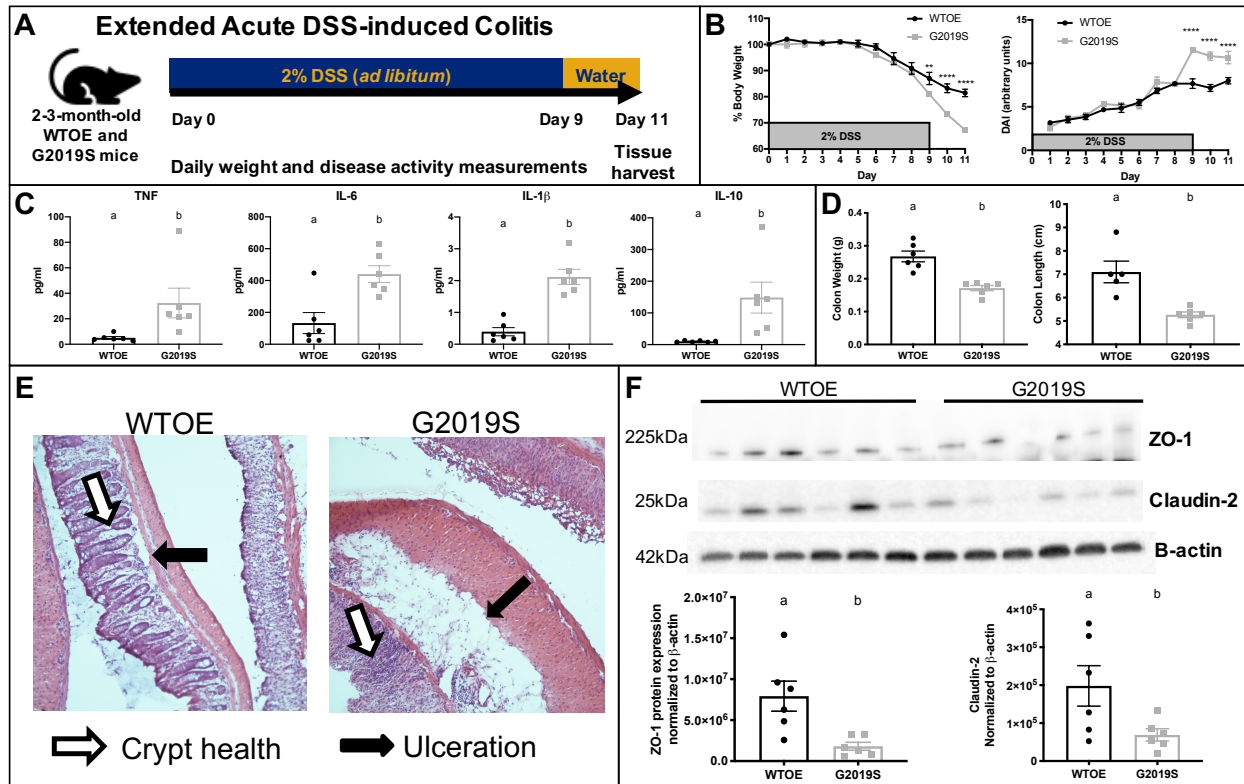


Figure 3.3: G2019S mice are more susceptible to extended acute DSS. A) Experimental design. B) Percent body weight and DAI. Data were compared across genotypes and time using a two-way ANOVA with repeated measures. Asterisks (*) signify differences between WtOE and G2019S groups at that specific time point (** $p < 0.01$, **** $p < 0.0001$). C) Plasma cytokine levels of TNF, IL-6, IL1 β and IL-10. D) Colon weight (g) and colon length (cm). E) Representative H&E colon images visually showing changes in crypt health (white arrow) and levels of ulceration (black arrow). F) Immunoblot and quantification of the tight junction proteins, ZO-1 and Claudin-2, normalized to β -actin ($n=6$ per genotype). Data were compared across genotypes with an unpaired student t-test. Significance for all statistical comparisons was set at $p \leq 0.05$. Groups with the same letter are not significantly different.

G2019S mice exhibit peripheral deficits after acute and chronic colitis with greater inflammatory alterations after acute colitis

Given G2019S mice were severely affected after extended acute DSS, we sought to determine if G2019S mice could recover at the same rate as WTOE; therefore, we assessed mice on an acute paradigm with recovery (Figure 3.4A) as well as a chronic paradigm that resembles the repeated bouts of colitis humans with CD exhibit (Figure 3.4B). No differences were observed between genotypes on water controls in several peripheral and central immunophenotype assessments (Figure 3.2A-D) suggesting that all phenotypes observed are due to DSS-induced colitis. Similar to the extended acute paradigm, G2019S mice exhibited increased susceptibility to the acute and recovery paradigm by body weight loss (Figure 3.4C); however, no differences in body weight (Figure 3.4D) or DAI (data not shown) were observed in mice on the chronic paradigm. Spleen weight was increased in G2019S mice after acute DSS (Figure 3.4C) suggesting that G2019S mice have more inflammation, but no differences in colon weight or colon length were observed (data not shown). While no differences between genotypes were observed in spleen and colon weight after chronic DSS (data not shown), G2019S mice exhibited shorter colons (Figure 3.4D) as DSS causes the colon to shrink due to loss and damage of epithelial cells.

Given that DSS destroys epithelial layers in the colon leading to inflammation, colon integrity and inflammatory status were evaluated. Histological analysis of the colon revealed a higher histological score in G2019S mice relative to WTOE mice after acute DSS (Figure 3.4E) but no differences after chronic DSS (Figure 3.4F). Evaluation of gene expression in the colon after acute DSS revealed elevated levels of *Snca* (which encodes α syn) and *Ptprc* (which encodes CD45, an immune cell marker) in G2019S colons (Figure 3.4G) suggesting that increased inflammation in the colon promotes increased colonic *Snca* levels. Interestingly, *Snca* levels were not significantly different after chronic DSS (Figure 3.4H); however, levels of gene expression related to tight junction proteins, *Cldn1* and *Tjp1*, were significantly lower in G2019S colons (Figure 3.4H) suggestive of an impaired epithelial barrier. No significant differences in

inflammatory gene expression of *Tnf*, *Il1b*, *Lcn2*, or *IA-b* were noted in the colon after acute or chronic DSS (data not shown).

To further assess the systemic inflammatory state of mice after acute and chronic DSS, PBMCs were immunophenotyped by flow cytometry and plasma assessed by multiplexed immunoassays for cytokines and chemokines at sacrifice. No significant differences were observed in frequencies of total CD45+ immune cells, T cells, B cells or monocyte and macrophage populations in the peripheral blood after acute or chronic DSS (data not shown). However, G2019S mice exhibited a shift in T cell ratios relative to WTOE mice with higher frequencies of CD8 cytotoxic T cells and lower frequencies of CD4 T helper cells after acute DSS (Figure 3.5B), but these differences were not observed after chronic DSS (Figure 3.5C). Levels of plasma IL-10 and IL-2 were significantly lower in G2019S mice relative to WTOE mice after acute DSS (Figure 3.5D), but no differences were observed in levels of IFN γ , IL-1 β , IL-4, IL-5, IL-6, KC/GRO, and TNF (data not shown). On the contrary, levels of IFN γ , TNF, and IL-10 were increased in the plasma of G2019S mice relative to WTOE mice after chronic DSS (Figure 3.5E). No significant differences were found in levels of IL-1 β , IL-2, IL-4, IL-5, IL-6, and KC/GRO (data not shown).

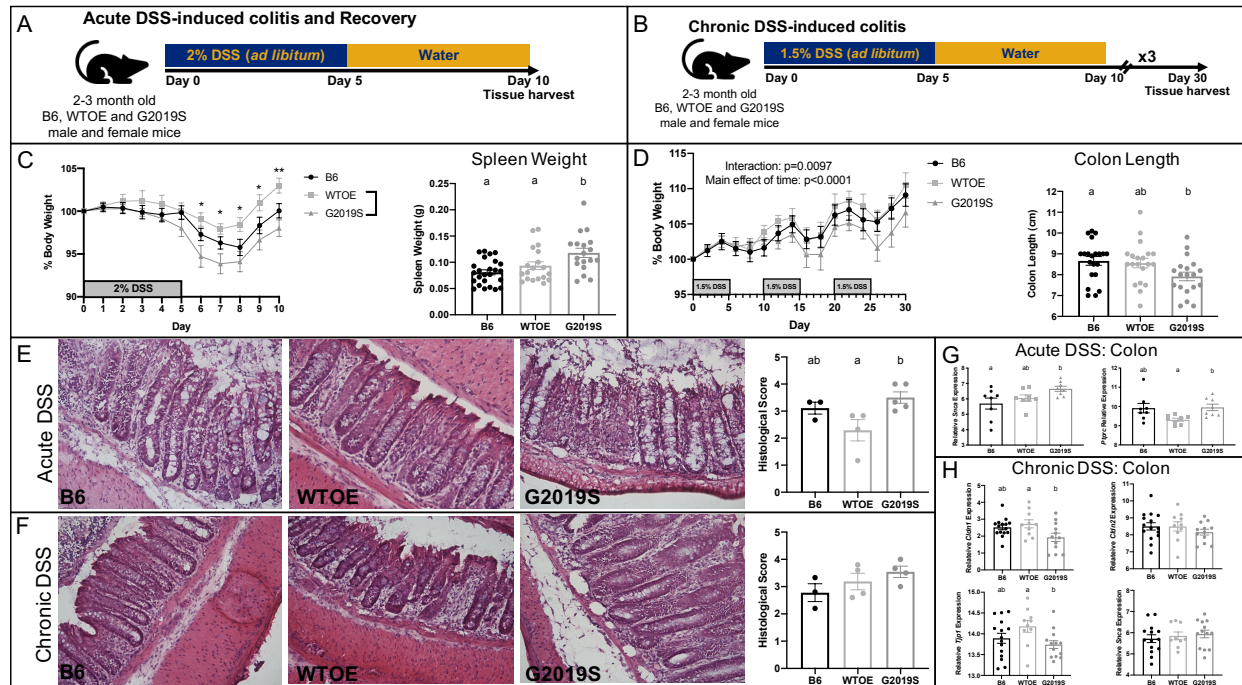


Figure 3.4: G2019S mice are more susceptible to acute DSS with a slowed recovery. A) Experimental design for acute DSS-induced colitis and recovery. B) Experimental design for chronic DSS-induced colitis. C) Percent body weight and spleen weight (g) after acute DSS-induced colitis and recovery (n=14-23 per genotype). D) Percent body weight and colon length (cm) after chronic DSS-induced colitis (n=21-26 per genotype). Representative H&E colon images and histological scoring of colon tissue from samples subjected to E) acute DSS-induced colitis and recovery or F) chronic DSS-induced colitis (n=3-5 per genotype). Relative colonic gene expression of G) *Snca* and *Ptprc* after acute DSS-induced colitis and recovery (n=8 per genotype) or H) *Cldn1*, *Cldn2*, *Tjp1*, and *Snca* after chronic DSS-induced colitis (n=10-15 per genotype). For percent body weight analyses, data were compared across genotypes and time using a mixed-effects model with repeated measures. Asterisks (*) signify differences between WTOE and G2019S groups at that specific time point (* $p<0.05$, ** $p<0.01$). For all remaining analyses, one-

way ANOVA with Tukey's *post hoc* for multiple comparisons was used to compare across genotypes. Significance for all statistical comparisons was set at $p \leq 0.05$. Letters above groups indicate *post hoc* results. Groups with the same letter are not significantly different.

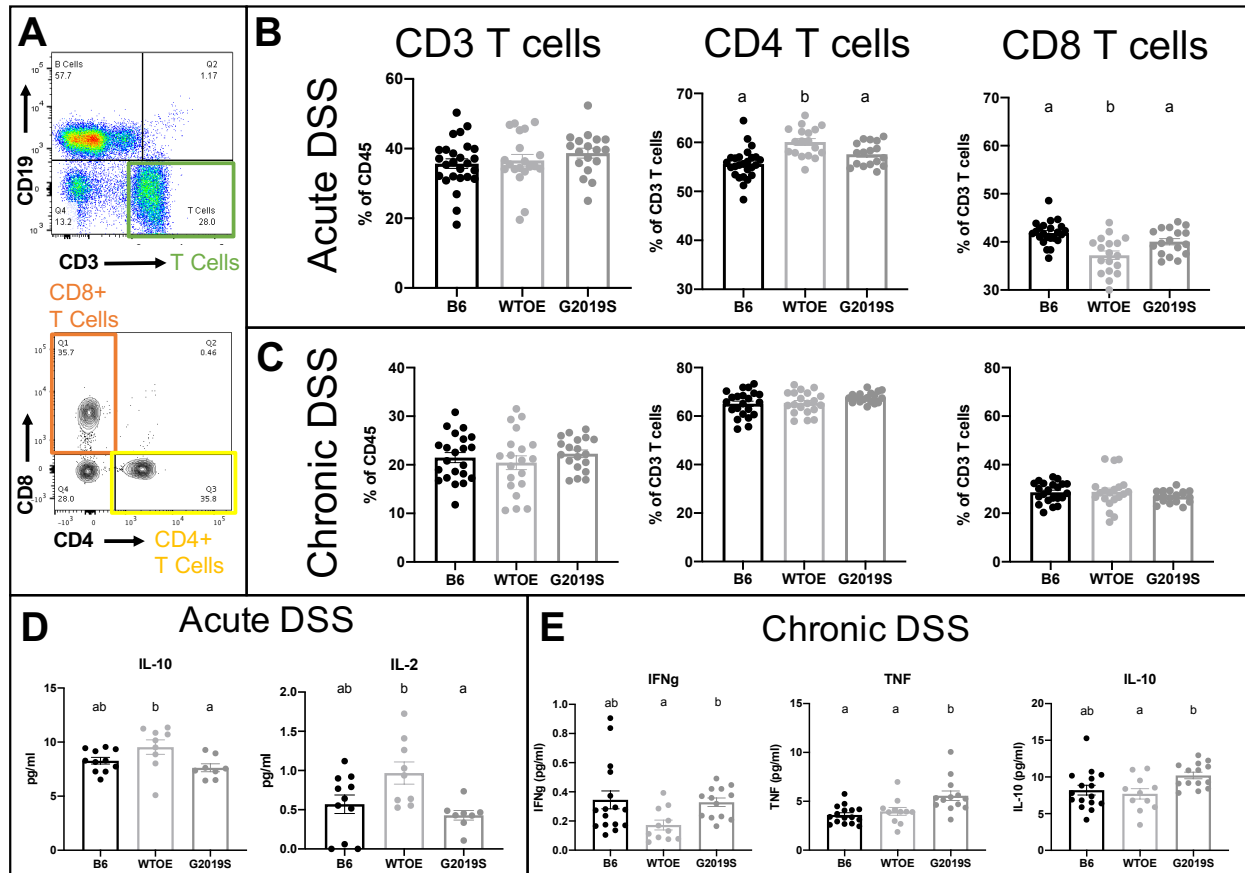


Figure 3.5: G2019S mice exhibit altered T cell PBMC populations relative to WTOE mice after acute DSS-induced colitis and recovery. A) Flow cytometry gating strategy used to identify T cell subsets. Quantification of T cells in PBMCs after B) acute DSS-induced colitis and recovery (n=18-26 per genotype) or C) chronic DSS-induced colitis (n=19-22 per genotype). Plasma cytokine levels of D) IL-10 and IL-2 after acute DSS-induced colitis and recovery (n=8-11

per genotype) or E) IFN γ , TNF, and IL-10 after chronic DSS-induced colitis (n=12-17 per genotype). One-way ANOVA with Tukey's *post hoc* for multiple comparisons was used to compare across genotypes. Significance for all statistical comparisons was set at $p \leq 0.05$. Letters above groups indicate *post hoc* results. Groups with the same letter are not significantly different.

Greater signs of neuroinflammation in brains of G2019S mice after colitis

To assess how LRRK2 expression and G2019S-mediated kinase activity might synergize with colitis to impact neuroinflammation, we assessed brain immunophenotypes by flow cytometry and brain region-specific inflammatory gene expression. While no differences in the overall number of microglia were observed between genotypes by flow cytometry (Figure 3.6B) and confirmed by Iba1 immunohistochemical staining (data not shown), a significant increase in the number of MHCII⁺ microglia was observed in the brains of G2019S mice after both acute and chronic DSS. No differences were observed in infiltrating monocytes, macrophages, and overall T cell populations after acute and chronic DSS (data not shown). Similar to phenotypes observed in PBMCs, G2019S mice exhibited a shift in T cell ratios in the brain relative to WTOE mice with higher frequencies of CD8 cytotoxic T cells and lower frequencies of CD4 T helper cells after acute DSS (Figure 3.6D), but these differences were not observed after chronic DSS (Figure 3.6D). These findings were further corroborated in the striatum with G2019S mice exhibiting higher levels of *Cd8b* gene expression but no differences in *Cd4* after acute DSS (Figure 3.6F). Analysis of RNA sequencing data (adjusted p-value <0.05, |fold change| >0.1) from SN samples

of mice treated with chronic DSS compared to water controls revealed no differentially expressed genes (DEGs) between B6 water and chronic DSS-treated mice (data not shown). However, 28 DEGs were identified between WTOE water and chronic DSS-treated mice, and 13 DEGs were identified between G2019S water and chronic DSS-treated mice, some of which are implicated in inflammatory pathways (Figure 3.6E, red and green dots).

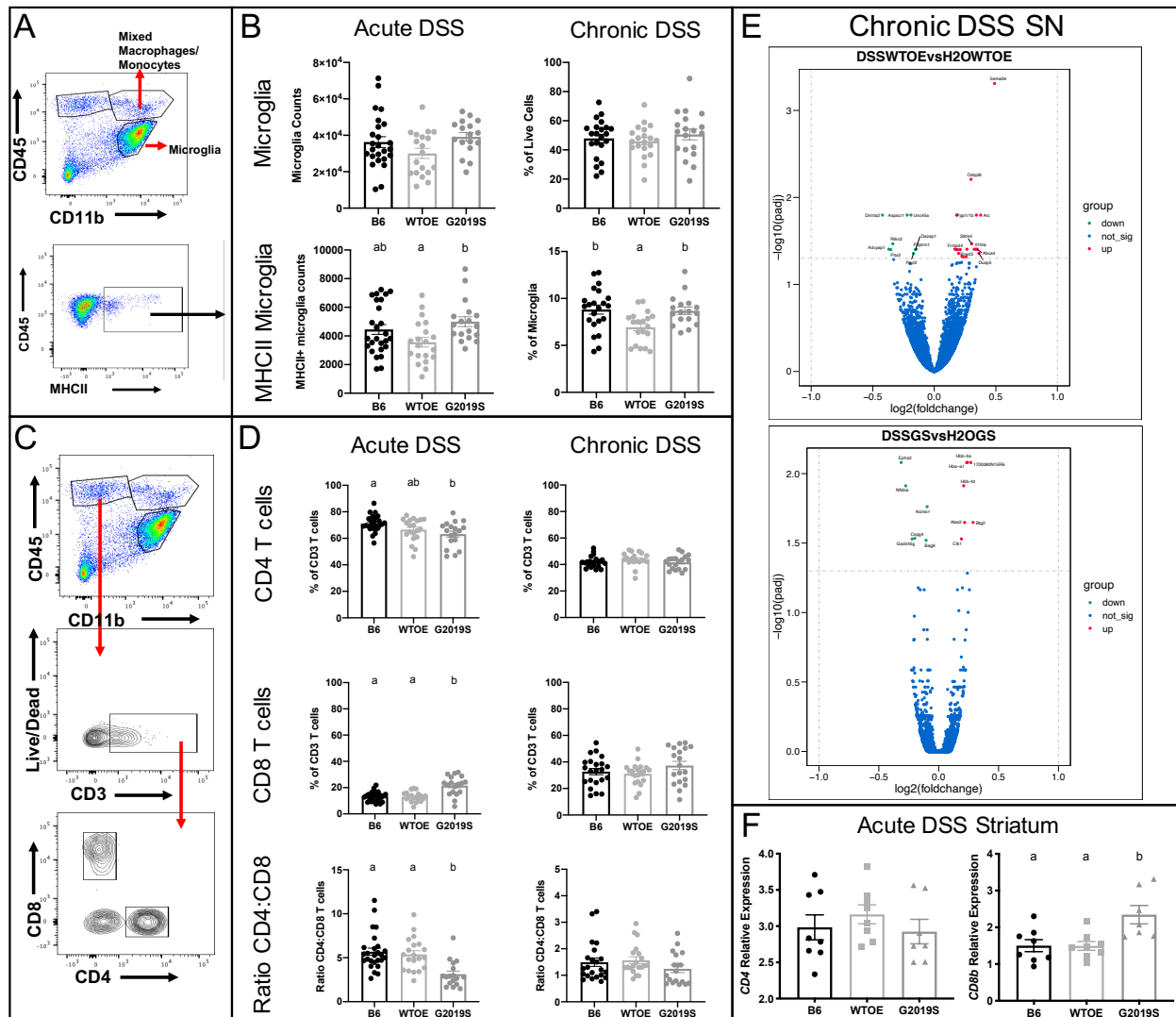


Figure 3.6: Acute DSS causes T cell infiltration in the brain, while both acute and chronic DSS are associated with increased MHCII+ microglia in the brains of G2019S mice. A) Flow

cytometry gating strategy used to identify microglia and MHCII⁺ microglia. B) Quantification of microglia and MHCII⁺ microglia after acute DSS-induced colitis and recovery (n=18-26 per genotype) and chronic DSS-induced colitis (n=19-22 per genotype). C) Flow cytometry gating strategy used to identify T cell populations in the brain. D) Quantification of T cell populations in the brain after acute DSS-induced colitis and recovery (n=18-26 per genotype) and chronic DSS-induced colitis (n=19-22 per genotype). E) Volcano plot showing DEGs in the SN between water and chronic DSS-treated WTOE or G2019S mice (n=5-15 per genotype per treatment). F) Relative striatal gene expression of *Cd4* and *Cd8b* after acute DSS-induced colitis and recovery (n=6-8 per genotype). One-way ANOVA with Tukey's *post hoc* for multiple comparisons was used to compare across genotypes. Significance for all statistical comparisons was set at $p \leq 0.05$. Letters above groups indicate *post hoc* results. Groups with the same letter are not significantly different.

Chronic DSS, but not acute DSS, is sufficient to alter dopaminergic integrity consistent with an impaired nigrostriatal pathway

To evaluate the effects of colitis on the nigrostriatal pathway, immunoblots of proteins associated with the dopaminergic pathway and HPLC to evaluate dopamine metabolites were performed. No differences were identified between genotypes; however, several treatment effects were observed. Analysis of tyrosine hydroxylase (TH), the enzyme that is the rate-limiting step in dopamine synthesis, in the striatum of water controls relative to acute DSS-treated mice revealed no treatment or genotype differences (Figure 3.7A). Furthermore, no differences were noted in

NeuN protein levels, a pan-neuronal marker (data not shown). Interestingly, a trend for a treatment effect for increased α syn protein was noted in the striatum, whereby acute DSS trends to increase α syn levels relative to water controls (Figure 3.7A).

Analysis of the nigrostriatal pathway after chronic DSS revealed several significant treatment effects suggesting that chronic DSS impairs the integrity of dopaminergic neurons. Chronic DSS caused a significant reduction in SN TH protein and an increase in the ratio of phosphorylated TH (pTH) at serine 40 (pSer40) to TH relative to water controls (Figure 3.7B). Phosphorylation of TH at serine 40 is commonly used to assess TH enzymatic activity with the ratio of pTH:TH used as indication of the proportion of active to inactive TH enzyme. In accordance, chronic DSS increased levels of striatal L-3,4-dihydroxyphenylalanine (L-Dopa) the precursor to dopamine, relative to water controls (Figure 3.7C). No treatment or genotype differences were noted in total dopamine levels, but a trend for DSS to increase 3,4-dihydroxyphenylacetic acid (DOPAC, $p=0.0794$), one of the metabolites of dopamine, was noted (Figure 3.7C). No other treatment or genotype differences were observed in other dopaminergic metabolites (homovanillic acid (HVA) or 3-methoxytyramine (3-MT), data not shown). Furthermore, no treatment or genotype differences in levels of α syn, GFAP (a marker of astrocytes), or NeuN levels were noted after chronic DSS (data not shown).

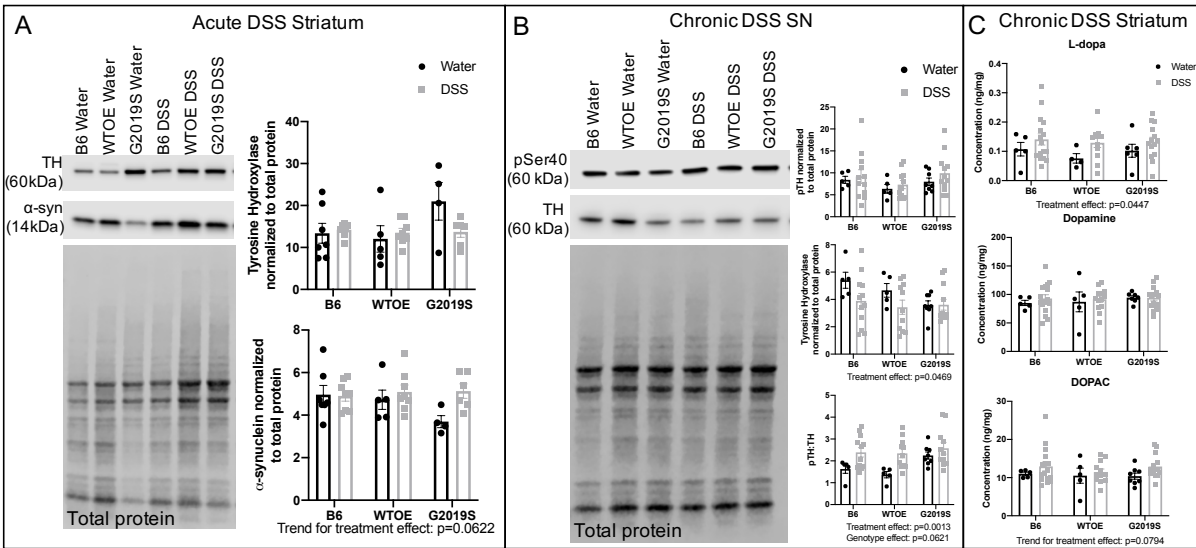


Figure 3.7: Chronic DSS compromises nigrostriatal pathway integrity. A) Immunoblot and quantification of striatal TH and α syn protein levels after acute DSS or water ($n=4-8$ per genotype per treatment). B) Immunoblot and quantification of nigral pSer40 and TH protein levels after chronic DSS or water ($n=5-15$ per genotype per treatment). C) Levels of dopamine and its metabolites as measured by HPLC from the striatum of mice treated with chronic DSS or water ($n=5-15$ per genotype per treatment). Two-way ANOVA with Tukey's *post hoc* for multiple comparisons was used to compare across genotypes and treatments. Significance for all statistical comparisons was set at $p\leq 0.05$.

Acute colitis in aged mice triggers neuroinflammation and compromises nigrostriatal integrity

Given age is the number one risk factor for PD, we sought to assess how G2019S-mediated kinase activity might synergize with colitis in aged mice. We assessed the same

peripheral and CNS parameters as described above in 16-18-month old B6 and G2019S mice treated with acute DSS. While no differences between genotypes were observed in body weight (Figure 3.8A) or DAI (data not shown), a time effect was observed. Spleen weight was increased in aged G2019S mice after acute DSS (Figure 3.8A), but no differences were observed in colon weight or colon length (data not shown). Levels of plasma IL-6 and KC/GRO were significantly higher in aged G2019S mice relative to B6 mice (Figure 3.8B), but no differences were observed in levels of IFN γ , IL-1 β , IL-2, IL-4, IL-5, and TNF (data not shown). A trend for increased plasma IL-10 ($p=0.0531$) levels was determined in aged G2019S mice relative to B6 (Figure 3.8B). Interestingly, TNF, IL-6, or IL-10 plasma levels significantly correlated with disease severity (percent body weight at day 10) in acute DSS-treated groups independent of genotype (Figure 3.8C).

Similar to observations in young mice after acute DSS, aged mice exhibited a treatment effect with acute DSS increasing the frequency of MHCII⁺ microglia independent of genotype (Figure 3.9A). However, unlike young mice, aged mice exhibited increased infiltrating macrophages and monocytes after acute DSS independent of genotype as measured by flow cytometry (Figure 3.9A). No differences between genotype or treatment were noted in T cell populations or total microglia (data not shown).

In accordance with these findings of acute DSS inducing neuroinflammation in aged mice, we also observed alterations in the nigrostriatal pathway. Acute DSS caused a significant reduction in TH and pTH protein levels relative to water controls in the SN of aged mice (Figure 3.9B). This resulted in an increase in the ratio of pTH:TH of DSS-treated mice relative to water

controls (Figure 3.9B). While no differences in dopamine levels were observed, acute DSS decreased the striatal dopamine metabolites, DOPAC and HVA, relative to water controls (Figure 3.9C). Alterations in dopamine turnover were noted with both genotype and treatment effects (Figure 3.9C). Interestingly, dopamine turnover and the DOPAC:dopamine ratio significantly correlated with disease severity (percent body weight at day 10) in acute DSS-treated groups independent of genotype (Figure 3.9D). Levels of 3-MT were not significantly different (data not shown), while levels of L-Dopa were below detection limits.

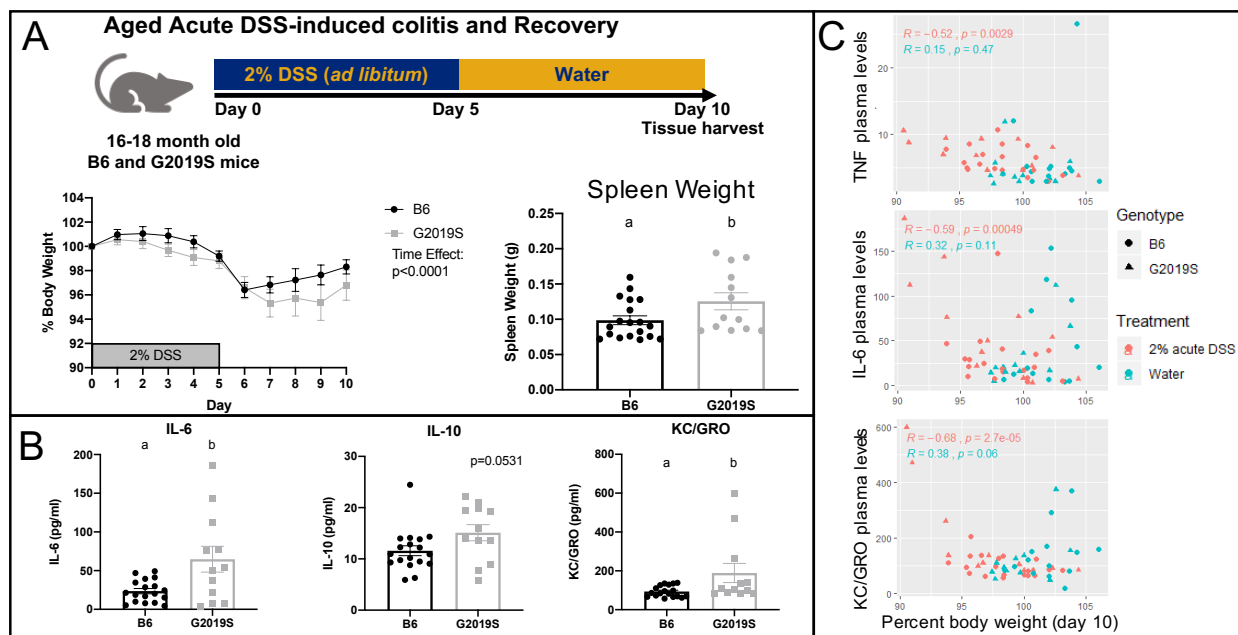


Figure 3.8: Disease severity in aged mice treated with acute DSS correlates with peripheral inflammation levels. A) Experimental design, percent body weight and spleen weight (g) of aged mice on acute DSS. Data were compared across genotypes and time using a two-way ANOVA with repeated measures or across genotypes with an unpaired student t-test ($n=12-19$ per

genotype). B) Plasma cytokine levels of IL-6, IL-10, and KC/GRO of aged mice after acute DSS (n=12-19 per genotype). Data were compared across genotypes with an unpaired student t-test. C) Significant correlation between percent body weight at day 10 as an indication of disease severity and TNF ($p=0.0029$, $R=-0.52$), IL-6 ($p=0.0004$, $R=-0.59$), and KC/GRO ($p<0.0001$, $R=-0.68$) plasma levels in acute DSS-treated groups (peach symbols) but not water controls (teal symbols) (n=22-31 per treatment, Pearson's correlation).

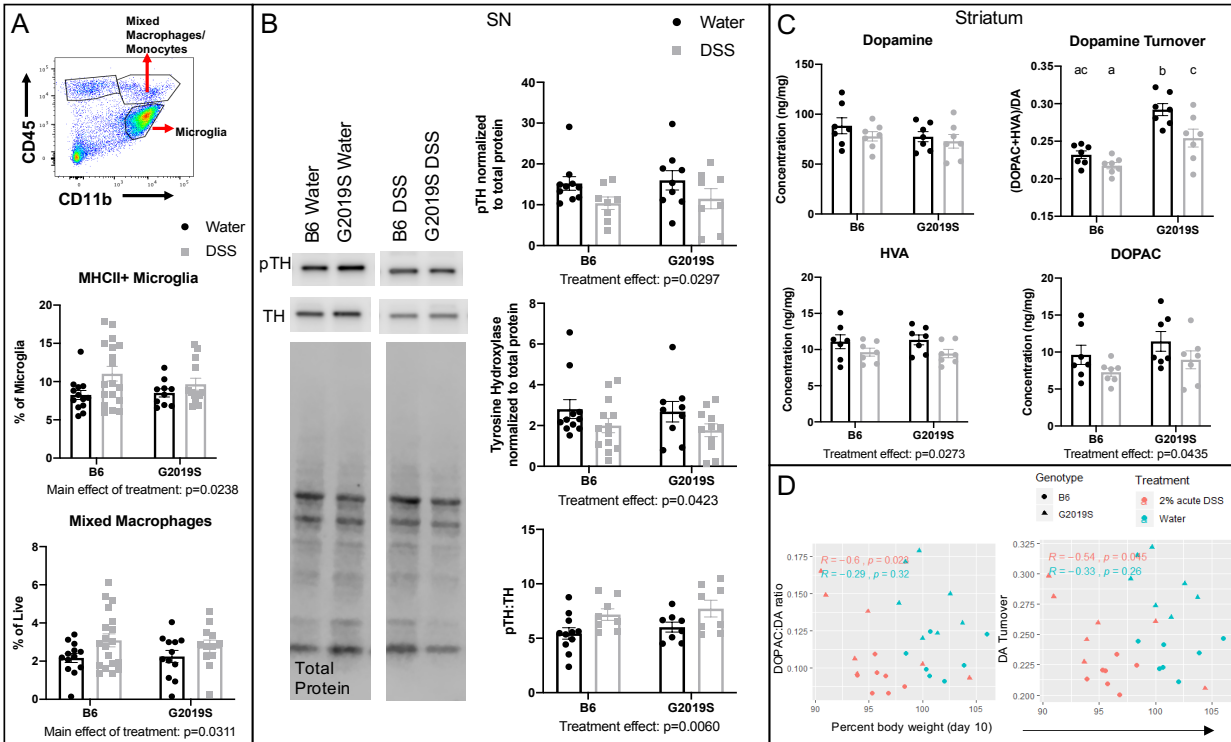


Figure 3.9: Acute colitis in aged mice causes neuroinflammation and compromises nigrostriatal pathway integrity. A) Flow cytometry gating strategy and quantification of MHCII+ microglia and infiltrating monocytes and macrophages (n=12-19 per genotype per treatment). B) Immunoblot and quantification of nigral pSer40 and TH protein levels (8-11 per genotype per

treatment). C) Levels of dopamine, HVA, DOPAC and dopamine turnover, as measured by HPLC from the striatum of aged mice treated with acute DSS or water (n=7 per genotype per treatment). Two-way ANOVA with Tukey's *post hoc* for multiple comparisons was used to compare across genotypes and treatments. Significance for all statistical comparisons was set at $p \leq 0.05$. Letters above groups indicate *post hoc* results. Groups with the same letter are not significantly different. D) Significant correlation between percent body weight at day 10 as an indication of disease severity and DOPAC:DA ratio ($p=0.023$, $R=-0.6$) or DA turnover ($p=0.045$, $R=-0.54$) in acute DSS-treated groups (peach symbols) but not water controls (teal symbols) (n=14 per treatment, Pearson's correlation).

3.5: Discussion

Given that epidemiologically LRRK2 sits at the interface between PD and CD and that studies have shown increased LRRK2 levels in peripheral immune cells of PD patients (Cook et al., 2017) or in inflamed colonic tissue of CD patients (Gardet et al., 2010), this study directly investigates the role of increased LRRK2 protein and increased G2019S-mediated kinase activity in the gut-brain axis on brain inflammation and nigrostriatal pathway integrity. We sought to confirm and extend previous studies investigating how LRRK2 synergizes with intestinal inflammation to promote neuroinflammation and neuropathology associated with PD.

While previous studies have examined the role of LRRK2 deficiency (Z. Liu et al., 2011) and overexpression of wildtype LRRK2 (Takagawa et al., 2018) in colitis models, to our

knowledge this is the first study to describe the role of G2019S-mediated kinase activity in the context of colitis. Mice overexpressing wildtype LRRK2 have been shown to be more susceptible to acute colitis relative to non-transgenic controls (Takagawa et al., 2018); however, G2019S mice were not employed in those studies and the effects of colitis on peripheral and neuropathology were not fully examined in the context of PD. In the current study, we show that mice overexpressing G2019S LRRK2 are more susceptible to extended acute and acute DSS-induced colitis, while mice overexpressing wildtype LRRK2 are protected against colitis-induced phenotypes. Consistent with previous findings from our group showing that overexpression of G2019S or wildtype LRRK2 does not affect immune cell subsets with age, we show here that control WTOE and G2019S mice on autoclaved tap water exhibit similar colon, spleen, and peripheral and neuroinflammatory phenotypes as B6 mice. No differences were observed between genotypes on water controls suggesting that all phenotypes observed are due to DSS-induced colitis.

DSS induces colitis by injuring and stripping away the epithelial barrier and causing a massive inflammatory response with infiltrating immune cells and upregulation of cytokine secretion (Kiesler et al., 2015). We observed that G2019S mice were more susceptible to extended acute and acute DSS paradigms relative to WTOE mice. These findings were supported by examination of the integrity of the colon in which G2019S mice exhibited reductions of tight junction proteins (ZO-1 and Claudin-2) important for maintaining barrier integrity and a worse histological score of the colon after acute DSS. While not directly assessed in the current study, defects observed in tight junction proteins suggest increased intestinal permeability in the G2019S

mice after acute DSS. Interestingly, G2019S mice were not as susceptible to chronic DSS by body weight with no differences observed between genotypes; however, they still exhibited defects in gene expression of tight junction proteins (*Tjp1* and *Cldn1*) further supporting the idea that G2019S mice exhibit increased intestinal permeability after DSS-induced colitis.

With evidence suggestive of a breached colonic epithelial barrier, the chances for elevated systemic inflammation and cytokine signaling in the blood are increased. To examine this, we used flow cytometry and multiplexed immunoassay to measure systemic inflammation. Given the extended acute DSS model assesses peak inflammation levels, G2019S mice exhibited much higher levels of several pro-inflammatory cytokines including TNF, IL-6, IL-10, IL-5, and IL-1 β relative to WTOE mice. However, fewer differences in cytokines were noted after acute DSS and recovery with G2019S mice exhibiting reduced IL-10 and IL-2 plasma levels relative to WTOE mice. IL-10 is known as an anti-inflammatory cytokine that limits inflammatory responses (Couper, Blount, & Riley, 2008). A reduction in IL-10 may be a contributing factor in the dampened recovery rate of G2019S mice. IL-2 regulates immunostimulatory and immunosuppressive responses to inflammation, but is most widely known for its role in T cell growth and CD4 T cell differentiation (Kalia & Sarkar, 2018; Nelson, 2004). The reduction in IL-2 plasma levels in G2019S mice after acute DSS may contribute to the reduced frequency of CD4 T cells in the blood of G2019S mice. The IL-2 levels present may be the driving force in differentiating CD8 T cells, which were increased in the blood of G2019S mice after acute DSS. We did not observe similar cytokine levels or T cell populations after chronic DSS. In fact, levels of IFN γ , TNF, and IL-

10 were all increased in G2019S plasma after chronic DSS suggestive of an exacerbated inflammatory response without alterations in PBMC T cell populations. This is in accordance with studies suggesting that CD8⁺ T cells may act as initiators of the inflammatory process and contribute to epithelial damage early on in CD but not in remitting bouts of colitis (Cheroutre, 2006; Nancey et al., 2006).

α syn is normally expressed in the human enteric nervous system (Bottner et al., 2012; Gray, Munoz, Gray, Schlossmacher, & Woulfe, 2014). Pathological forms (aggregated and phosphorylated) of α syn has been observed throughout the entire GI system of PD patients (Beach et al., 2010) with higher levels of pathological α syn noted in PD patients relative to healthy controls (Gold, Turkalp, & Munoz, 2013; Hilton et al., 2014). Interestingly, we noted an increase in colonic *Snca* gene expression (the gene that encodes α syn) in the colon of G2019S mice after acute DSS but no differences in *Snca* levels between genotypes after chronic DSS. The acute DSS paradigm examines pathology during the recovery phase immediately after the peak of inflammation. Therefore, the increase in *Snca* gene expression in G2019S mice may be a consequence of activation of the peripheral immune system as α syn levels are shown to increase in the mouse colon after intestinal inflammation (J. G. Choi et al., 2018). However, given mouse α syn lacks the aggregation and pathological properties associated with human α syn (Cookson, 2009; Volles & Lansbury, 2007), future studies should explore the effects of LRRK2 in colitis models that can report on human α syn phenotypes.

Our group and others have hypothesized that intestinal perturbations contribute to systemic inflammation and promote neuroinflammation and neurodegeneration associated with PD pathogenesis (Houser & Tansey, 2017). Therefore, we examined the effects of intestinal inflammation induced by DSS on neuroinflammation and neurodegeneration phenotypes in the LRRK2 BACs. Microglia are the brain-resident immune cells. Their activation is measured by upregulation of MHCII expression (Wyss-Coray & Mucke, 2002), which is a common neuroinflammatory response after infection, trauma, or chronic neurodegenerative diseases (McGeer, Itagaki, Boyes, et al., 1988; Schettters, Gomez-Nicola, Garcia-Vallejo, & Van Kooyk, 2017). In the current study, we did not observe differences between genotypes in the number of microglia after acute and chronic DSS. However, we did note that G2019S mice after acute and chronic DSS exhibited an increase in the number of MHCII+ microglia indicating greater levels of neuroinflammation in G2019S brains. Similar to observations in peripheral immune cells, we noted a shift in the ratio of CD4:CD8 T cells in the brain with a higher frequency of CD8 T cells and reduction of CD4 T cells in G2019S mice after acute DSS. However, no genotype differences in T cell populations were noted after chronic DSS. Infiltration of CD8 T cells has been noted in PD patient brains (Brochard et al., 2009). This infiltration of CD8 T cells is associated with dopaminergic neuronal death. However, we did not detect impairments of the nigrostriatal pathway in the acute paradigm. To assess nigrostriatal integrity, key proteins in dopamine synthesis (TH, pTH) were evaluated by immunoblot in conjunction with HPLC analysis to assess striatal levels of dopamine and its metabolites (L-Dopa, 3-MT, HVA, and DOPAC). We did not observe genotype differences after acute or chronic DSS when assessing the nigrostriatal

pathway which is in accordance with the fact that LRRK2 PD patients are clinically indistinguishable from non-LRRK2 PD patients (Kestenbaum & Alcalay, 2017). However, we did observe a treatment effect, whereby chronic, but not acute, DSS impairs dopaminergic neuronal integrity. This is evident by increased pTH:TH ratios after chronic DSS indicative of higher levels of active TH converting tyrosine to L-Dopa, as turnover of active TH controls L-Dopa production (Meiser, Weindl, & Hiller, 2013). These changes at this current time point are not sufficient to decrease dopamine levels, but they are suggestive of the beginning stages of dysfunction and impairment.

Because PD is a multifactorial disease, with age, genetics, and environmental exposures contributing to pathogenesis, we examined the synergistic effects of G2019S-mediated kinase activity on intestinal inflammation in aged mice. Interestingly, we observed several of the same peripheral inflammatory phenotypes as seen in young G2019S mice after acute DSS. These include upregulation of pro-inflammatory cytokines and an increased spleen weight in G2019S mice. Plasma cytokine levels correlated with disease severity as measured by percent of body weight at the end of the paradigm. The more body weight lost (lower percent of initial body weight), the higher the level of plasma cytokines. DSS in aged mice caused an increase in infiltrating monocytes and macrophages and MHCII⁺ microglia independent of genotype suggesting that acute DSS causes increased neuroinflammation. Unlike acute DSS in young mice, aged mice exhibited signs of nigrostriatal impairment independent of genotype, and this correlated with disease severity. The more body weight lost (lower percent of initial body weight), the more DA turnover. While dopamine mechanisms are not fully understood, biochemical data suggests that

increased dopamine turnover might be an early compensatory mechanism in PD (Barrio et al., 1990; Sossi et al., 2002). This suggests that while acute DSS in young mice causes peripheral and neuroinflammatory changes without impairing the nigrostriatal pathway, the changes in aged mice are sufficient to induce impairment in the nigrostriatal pathway.

In conclusion, we have presented a novel study showing that G2019S mice are more susceptible to acute colitis with colonic epithelial destruction, altered T cell ratios in the periphery, and increased MHCII+ microglia relative to WTOE mice. Chronic DSS-induced colitis, but not acute DSS-induced colitis, is sufficient to induce impairment in the nigrostriatal pathway independent of genotype. However, in aged mice, acute DSS causes peripheral and neuroinflammation sufficient to induce impairment in the nigrostriatal pathway. Future studies will explore the extent to which G2019S phenotypes are rescued by LRRK2 kinase inhibition and/or TNF inhibition, based on the reports that anti-TNF therapy reduces the risk of PD in IBD patients by 78% (Peter et al., 2018).

CHAPTER 4: THE EFFECTS OF LRRK2 AND CHRONIC PESTICIDE EXPOSURE IN WT OR G2019S OVEREXPRESSING MICE

4.1: Abstract

Parkinson's disease (PD) is considered a multifactorial disease with an individual's age, genetics, environmental exposures and lifestyle collectively hypothesized to contribute to disease pathogenesis. Exposure to pesticides has been associated with increased incidence of PD. Interestingly, animal models studying the effects of LRRK2, one of the greatest genetic contributors to PD, have found increased susceptibility to toxin exposure especially in the context of LRRK2 G2019S, supporting the idea that genetic predisposition for PD has a complex interplay with environmental interactions to contribute to disease pathogenesis. Cypermethrin is one of the most widely used pyrethroids, a class of pesticides used in homes and agricultural areas to control insects. Studies have shown that long-term exposure to cypermethrin has several health risks for humans and promotes neurotoxicity in animal models. Recent unpublished data from our lab suggests that chronic cypermethrin modifies peripheral T cells to a cytotoxic phenotype and disrupts the nigrostriatal pathway in wildtype mice. Thus, we hypothesized that mice overexpressing mutant G2019S LRRK2 would be more susceptible to chronic cypermethrin exposure with shifts in peripheral and central immunophenotypes that would promote neurodegenerative phenotypes associated with PD. Here we report that BAC transgenic mice overexpressing wildtype LRRK2 or mutant G2019S LRRK2 subjected to chronic cypermethrin exhibit time-dependent peripheral blood immune cell profile changes independent of genotype but no effects on neuroinflammation or enhanced neurodegenerative phenotypes. These data support a model in which several exposures over a lifetime in a genetically susceptible background contributes to PD pathophysiology.

4.2: Introduction

Parkinson's disease (PD) is a progressive movement disorder affecting more than one million Americans and over 10 million people worldwide, making it the second most common neurodegenerative disorder in the US. Characterized by aggregation of α -synuclein leading to Lewy Body formation, the neuropathological hallmark of PD is a loss of nigral dopaminergic neurons in the substantia nigra pars compacta (SNpc) and concomitant reductions in dopamine. This loss of dopamine results in the stereotypic motor symptoms associated with PD. While the exact etiology still remains unknown, PD is considered a multifactorial disease with a complex interaction of genetics, aging, and environmental exposures all thought to contribute to PD pathogenesis. In the 1980s, reports in California surfaced that several patients were presenting with motor symptoms associated with PD but were extremely young for a PD diagnosis (Langston, 2017; Langston, Ballard, Tetud, & Irwin, 1983). The cause was traced back to the patients' use of "synthetic heroin" which contained the neurotoxin, 1-methyl-4-phenyl-1,2,3,6-tetrahydropyridine (MPTP), a byproduct of the synthesis of 1-methyl-4-phenyl-4-propionoxypiperidine (MPPP) (Langston et al., 1983; Langston, Forno, Rebert, & Irwin, 1984; Langston, Irwin, Langston, & Forno, 1984). Since then, MPTP has been used as the gold standard to induce selective degeneration of dopaminergic neurons in animal (rodent and non-human primate) models. Additional toxicants have been identified, including rotenone, a pesticide, and paraquat, an herbicide that shares high structural similarity with MPTP (Fei, McCormack, Di Monte, & Ethell, 2008; Langston, 2017). Given the similarities and wide use of these toxicants, a number of GWAS have found associations between pesticide exposure and incidence of PD, with increased pesticide exposure generally associated with increased incidence of PD (Ascherio et al., 2006; Frigerio et al., 2006; Kamel et al., 2007; Le Couteur, McLean, Taylor, Woodham, & Board, 1999). Collectively, this provides rationale supporting the hypothesis that PD pathogenesis manifests through multiple hits mediated by environmental exposures.

Numerous studies have used the aforementioned toxicants in genetic animal models of PD to study the mechanisms by which these toxicants act and to gain insight into the hypothesis that gene by environment synergistic effects contribute to PD pathogenesis. Several of these studies have used LRRK2 animal models, as LRRK2 is one of the greatest genetic contributors to PD and G2019S mediated kinase activity has been shown to be neurotoxic. A mouse model expressing the human LRRK2 G2019S mutation treated with MPTP resulted in increased neuronal susceptibility and neurotoxicity compared to WT controls (Karuppagounder et al., 2016). Similarly, a recent study identified severe motor impairment and loss of dopaminergic neurons in MPTP-treated mice overexpressing LRRK2 G2019S relative to non-transgenic mice treated with the same dose of MPTP (Arbez et al., 2019). On the other hand, LRRK2 deficiency protects against paraquat-induced sickness and inflammation as well as neuronal loss, suggesting that the presence of LRRK2 may contribute to inflammatory and neurodegenerative phenotypes associated with PD (Rudyk et al., 2019).

Cypermethrin is a class-II synthetic pyrethroid pesticide that is commonly used to control insects in agricultural and household areas and has been associated with a number of human health risks (Azmi et al., 2009; H. Choi et al., 2006; Eadsforth & Baldwin, 1983; Keenan, Vega, & Krieger, 2009; D. A. Khan, Hashmi, Mahjabeen, & Naqvi, 2010). Cypermethrin acts on a number of different pathways but is most commonly known for extending the open time of voltage gated sodium channels leading to neuronal hypopolarization, cell death, insect paralysis and death of the organism (Singh, Tiwari, Prakash, & Singh, 2012). Given that cypermethrin crosses the blood-brain barrier (BBB), it has been shown to affect microglia among other immune cells and several types of neurons, with a preference for dopaminergic neurons, suggesting cypermethrin as an intriguing model for studying PD pathogenesis (Mun, Lee, & Han, 2005; Singh et al., 2011; Singh, Tiwari, Prakash, et al., 2012). A few studies have examined the use of cypermethrin in rats showing that long term exposure in adulthood contributes to nigrostriatal alterations suggestive of a neurodegenerative phenotype (Singh et al., 2011; Singh, Tiwari, Upadhyay, et al., 2012;

Tiwari et al., 2010). Interestingly, cypermethrin has been shown to alter lysosomal homeostasis through activation of autophagosome formation and inhibition of autophagy (Mishra et al., 2018). LRRK2 has also been shown to alter autophagy, thus the convergence of chronic cypermethrin treatment in a LRRK2 context presents as a novel and appealing model in which to study PD pathogenesis.

Furthermore, unpublished data from our lab suggests that chronic cypermethrin promotes peripheral T cells to a cytotoxic phenotype and alters the nigrostriatal pathway in adult wildtype mice. Therefore, we sought to confirm and extend these findings in the context of LRRK2 and its kinase activity. We sought to investigate the extent to which increased mouse LRRK2 protein or increased G2019S-mediated kinase activity in immune cells affects neuronal survival in a chronic cypermethrin model. We hypothesized that when exposed to chronic cypermethrin, LRRK2 G2019S mice would exhibit higher levels of pro-inflammatory and activated central and peripheral immune cells as well as increased infiltrating immune cells to the brain, compared to B6 mice, which will promote dopaminergic cell loss. Here we report that chronic cypermethrin alters peripheral immune cell subsets in a time-dependent manner independent of genotype, but does not contribute to neuroinflammation or neurodegenerative phenotypes associated with PD.

4.3: Materials and Methods

Animals. Homozygous male *Lrrk2-G2019S* (B6.Cg-Tg(Lrrk2*G2019S)2Yue/J; stock number 012467) and *Lrrk2-WT* (B6.Cg-Tg(Lrrk2)6Yue/J; stock number 012466) mice were purchased from the Jackson Laboratory and bred to hemizyosity at Emory University. Hemizygous male and female bacterial artificial chromosome (BAC) transgenic mouse strains overexpressing either mouse mutant G2019S LRRK2 (G2019S) or mouse wildtype LRRK2 (WTOE) were used for experimental procedures with non-transgenic littermates (B6) serving as controls. Genotypes were determined by tail-snip PCR with two sets of primers: Transgene: Forward 5' GAC TAC AAA GAC GAT GAC GAC AAG 3' Reverse 5' CTA CCA CCA CCC AGA TAA TGT C 3'; Internal

positive control: Forward 5' CAA ATG TTG CTT GTC TGG TG 3' Reverse 5' GTC AGT CGA GTG CAC AGT TT 3'. Animals were group housed (maximum 5 mice per cage) and maintained on a 12h/12h light/dark cycle with *ad libitum* access to standard rodent chow and water. Experimental procedures involving use of animals were performed in accordance with the National Institutes of Health Guidelines for Animal Care and Use and approved by the Institutional Animal Care and Use Committee at Emory University School of Medicine.

Experimental Timeline. Male and female B6, WTOE, and G2019S mice were randomly assigned to two treatment groups (vehicle or cypermethrin, n=6-12 per group). As illustrated in figure 4.1A, 7-9-month-old mice were treated with chronic cypermethrin (20mg/kg; Chem Service Inc, N-11545) or vehicle (corn oil) by intraperitoneal injection twice a week for 12 weeks. Every other week mice underwent submandibular bleeds to assess PBMCs and plasma cytokines and chemokines.

Tissue collection. At 12 weeks, animals were sacrificed by decapitation. Brain tissue was removed, with the right hemisphere designated for flow cytometry. From the left hemisphere, the striatum was dissected, flash frozen and stored in -80°C until processing. The remaining caudal tissue from the left hemisphere was post-fixed in 4% paraformaldehyde for 24 hours at 4°C for immunohistochemistry and stereology.

Plasma and Peripheral blood mononuclear cell (PBMC) isolation. Whole blood was collected by submandibular bleeds with approximately 200µl per mouse collected for each time point. Whole blood was collected in ethylenediaminetetraacetic acid (EDTA) coated tubes (Covidien 8881311248). 50µl of whole blood was treated with 1x red blood cell (RBC) lysis buffer (BioLegend 420301) to lyse RBCs as per the manufacturer's instructions prior to staining PBMCs

for flow cytometry. The remaining 150µl of whole blood was centrifuged after which plasma was removed and promptly frozen on dry ice then subsequently stored at -80°C until processing.

Brain immune cell isolation. Brain immune cell isolation was performed as previously described with minor modifications (MacPherson et al., 2017). The right hemisphere was minced in 1xHBSS (without calcium, magnesium, and phenol red, Invitrogen, 14175) and transferred to an enzymatic digestion solution consisting of 1.4U/ml collagenase, type VIII (Sigma, C2139), 1mg/ml DNase 1 (Sigma, DN25) in RPMI1640 medium (ThermoFisher, 11875085). The tissue and enzymatic solution were incubated at 37°C for 15 minutes with shaking every 5 minutes. The solution was then neutralized with 10% FBS (heat inactivated, Atlanta Biologicals, S11150) in RPMI1640 medium and centrifuged to pellet tissue. The remaining tissue pellet was homogenized with glass pipets in ice cold 1x HBSS and then filtered through a 70µM cell strainer. After centrifugation, the remaining pellet was resuspended in 37% Percoll (Sigma, P1644). 70% Percoll was layered below the resuspended pellet while 30% was Percoll layered above. The Percoll gradient was centrifuged for 30 minutes at room temperature without a brake. Immune cells were isolated from the interface between the 37% and 70% layers, washed with 1x HBSS and then stained for flow cytometric analysis.

Multi-color Flow Cytometry. 50µl of PBMCs were stained with BMV109 (1µM, Vergent Bioscience, 40200-100) and Pepstatin A, BODIPY FL Conjugate (1ug/mL, ThermoFisher Scientific, P12271) for 1 hour at 37°C. After a brief wash, PBMCs were then stained for 20 minutes with the following panel: Live/Dead Fixable Red Dead Cell Stain (1:2000, Invitrogen, 23102), anti-mouse CD16/CD32 (1:100, eBioscience, 14-0161-085), anti-mouse CD45 PerCP_Cy5.5 (1:100, eBioscience, 45-0451-80), anti-mouse CD19 BV650 (1:100, Biolegend, 115541), anti-mouse CD3 BV421 (1:50, Biolegend 100227), anti-mouse CD4 V500 (1:100, BD Biosciences, 560783), anti-

mouse CD8 BV785 (1:100, Biolegend 100749), anti-mouse CD11b PE_Cy7 (1:200, Biolegend, 101215), anti-mouse MHCII APC_Cy7 (1:200, Biolegend, 107627), anti-mouse CD44 PE (1:200, Biolegend, 103007), anti-mouse Ly6G AF700 (1:100, eBioscience, 56-5931-80), and anti-mouse CD11c BV711 (1:200, Biolegend, 117349) in FACS buffer. Samples were fixed in 1% PFA for 30 minutes. 10 μ l of counting beads (AccuCheck Counting Beads, Invitrogen PCB100) were added to each sample. Samples were then run on an LSRII cytometer (BD Biosciences) and analyzed with FlowJo_V10 software.

Brain immune cells were stained with BMV109 (1 μ M, Vergent Bioscience, 40200-100) and Pepstatin A, BODIPY FL Conjugate (1 μ g/mL, ThermoFisher Scientific, P12271) for 1 hour at 37°C. After a brief wash, brain immune cells were then stained for 20 minutes with the following panel: Live/Dead Fixable Red Dead Cell Stain (1:2000, Invitrogen, 23102), anti-mouse CD16/CD32 (1:100, eBioscience, 14-0161-085), anti-mouse CD45 PerCP_Cy5.5 (1:100, eBioscience, 45-0451-80), anti-mouse CD3 BV421 (1:50, Biolegend 100227), anti-mouse CD4 V500 (1:100, BD Biosciences, 560783), anti-mouse CD8 PE (1:100, eBioscience, 12-0083-81), anti-mouse CD11b PE_Cy7 (1:200, Biolegend, 101215), anti-mouse MHCII APC_Cy7 (1:200, Biolegend, 107627), anti-mouse Ly6c BV785 (1:100, Biolegend 128041), anti-mouse CD86 PE (1:50, Biolegend, 105037), anti-mouse Ly6G AF700 (1:100, eBioscience, 56-5931-80), and anti-mouse CD11c BV711 (1:200, Biolegend, 117349) in FACS buffer. Samples were fixed in 1% PFA for 30 minutes. 10 μ l of counting beads (AccuCheck Counting Beads, Invitrogen PCB100) were added to each sample. Samples were then run on an LSRII cytometer (BD Biosciences) and analyzed with FlowJo_V10 software.

For PBMCs, leukocytes were gated on Side Scatter Area (SSC-A) (granularity) by Forward Scatter Area (FSC-A) (size) and then with Forward Scatter Height (FSC-H) by FSC-A to identify single leukocytes. To identify live CD45⁺ cells, the Fixable Red negative population was selected followed by the CD45⁺ population against FSC-H. CD45⁺ cells were then gated on CD19 by CD11b, with CD19⁺ cells denoting B cells and CD11b⁺ cells further delineated to identify

populations. CD19-, CD11b- cells were then gated for CD4+ and CD8+ T cells to differentiate T helper cells vs cytotoxic T cells, respectively. The CD19 B cell population was examined for MHCII expression by histogram and geometric mean fluorescent intensity. The CD11b+ population was gated on CD11b vs CD11c to discern dendritic cells (CD11c+ cells). The non-dendritic cell population was then gated for SSC-A by Ly6G. SSC-A high, Ly6G high cells were identified as neutrophils. The SSC-A low, Ly6G low/negative population was identified as monocytes. In each immune subset, cathepsin probes, BMV109 and Pepstatin Bodipy, were examined for positive cells and geometric mean fluorescent intensity.

For brain immune cells, leukocytes were gated on SSC-A (granularity) by FSC-A (size) and then with FSC-H by FSC-A to identify single leukocytes. To identify live cells, the Fixable Red negative population was selected against FSC-H. From a CD45 by CD11b gate, lymphocytes, mixed monocytes/macrophages and microglia populations were discerned. The microglia population was further analyzed for MHCII+ microglia and CD86+ microglia. The geometric mean fluorescent intensity of MHCII+ microglia or CD86+ microglia was also identified based on the respective antibody. The lymphocyte population was gated on CD3+ T cells followed by CD4+ and CD8+ T cells to distinguish T helper cells from cytotoxic T cells, respectively. The mixed monocyte/macrophage population was then examined with CD11b by Ly6G to distinguish neutrophils. The non-neutrophil gate was then gated with the Ly6C by MHCII cascade that distinguishes monocyte and macrophage populations (Ly6C+, MHCII- monocytes, Ly6C+, MHCII+ monocytes, Ly6C-, MHCII+ macrophages, and Ly6C-, MHCII- monocytes). In each immune subset, cathepsin probes, BMV109 and Pepstatin Bodipy, were examined for positive cells and geometric mean fluorescent intensity.

Multiplexed Immunoassays. Levels of inflammatory protein were measured in plasma by the Emory Multiplexed Immunoassay Core (EMIC) using a commercially available V-plex Pro-inflammatory Panel 1 Mouse Kit per the manufacturer's instructions on the Meso Scale Discovery

QuickPlex (Meso-Scale Discovery, Gaithersburg, MD). Plasma samples were analyzed for cytokines and chemokines (IFN γ , IL-1 β , IL-2, IL-4, IL-5, IL-6, IL-10, IL-12p70, KC/GRO, and TNF) that play key roles in the inflammation response and immune system. Samples were run in replicates of 30 μ l by an experimenter blinded to treatment history and genotype.

RNA extraction and protein isolation. RNA extraction and protein isolation were performed as previously described (de Sousa Rodrigues et al., 2017). Striatal tissue was homogenized in ice cold TRIzol (Life Technologies, 15596018) using a stainless-steel bead (Qiagen, 69989) and a TissueLyser II (Qiagen, 85300). RNA was then isolated using QIAshredder columns (Qiagen, 79656) and RNeasy mini kits (Qiagen, 74106) according to the manufacturer's protocol. RNA was quantified and purity assessed using a NanoDrop 2000 spectrophotometer (Thermo Fisher Scientific). Protein was isolated from the organic layer of the TRIzol separation method by methanol precipitation. Protein was resuspended in 1% SDS, quantified using BCA protein assay and then used for immunoblotting.

cDNA synthesis. Following the manufacturer's protocol, RNA was reverse transcribed using SuperScript II Reverse Transcriptase (Life Technologies, 18064014), random hexamers (Integrated DNA Technologies, 51-01-18-25), and dNTPs (Life Technologies, 18427013).

Quantitative real-time polymerase chain reaction (qPCR). qPCR was performed as previously described (de Sousa Rodrigues et al., 2017). Using an ABI Prism 7900 HT Fast Real-time PCR System (Applied Biosystems), 25ng cDNA was analyzed in triplicate with SYBR Green PCR Master Mix and 150nM validated forward and reverse oligonucleotide primers (Integrated DNA Technologies). Cycle of threshold (Ct) values were normalized to the averaged values of the two housekeeping genes, *Gapdh* and cyclophilin (*Ppia*). Relative mRNA expression was obtained by subtracting normalized Ct values from a standard number. Primers used: *Gapdh* – Forward 5'

CAA GGT CAT CCA TGA CAA CTT TG 3' Reverse 5'GGC CAT CCA CAG TCT TCT GG 3'; *Tnf* – Forward 5' CTG AGG TCA ATC TGC CCA AGT AC 3' Reverse 5' CTT CAC AGA GCA ATG ACT CCA AAG 3'; *IL-1 β* – Forward 5' CAA CCA ACA AGT GAT ATT CTC CAT G 3' Reverse 5' GAT CCA CAC TCT CCA GCT GCA 3'; *Ptprc* – Forward 5' TCA TGG TCA CAC GAT GTG AAG A 3' Reverse 5'AGC CCG AGT GCC TTC CT 3'; *Cyclo* – Forward 5' TGG AGA GCA CCA AGA CAG ACA 3' Reverse 5'TGC CGG AGT CGA CAA TGA T 3'; *Lcn2* – Forward 5' TGG AAG AAC CAA GGA GCT GT 3' Reverse 5' GGT GGG GAC AGA GAA GAT GA3'; *Cd4* – Forward 5' GTG AGC TGG AGA ACA GGA AAG AG 3' Reverse 5' GGC TGG TAC CCG GAC TGA 3'; *Cd8b* – Forward 5' GCT GTC CTT GAT CAT CAC TCT CA 3' Reverse 5' ACT AGC GGC CTG GGA CAT T 3'; *IA-b* – Forward 5' CAG GAG TCA GAA AGG ACC TC 3' Reverse 5' AGT CTG AGA CAG TCA ACT GAG 3'.

Immunoblotting. Immunoblotting was performed as previously described (de Sousa Rodrigues et al., 2017). Bicinchoninic acid (BCA) protein assay (Pierce Scientific, 23225) was used to determine protein concentrations, after which lysates were further diluted 1:1 with 2x Laemmli buffer (BioRad, 1610737) and boiled at 90°C for 5 minutes. Samples (10 μ g) were electrophoresed using 4-20% Mini-PROTEAN TGX precast gels (BioRad, 4561096) and transferred to 0.45 μ m PVDF membranes using the Trans-Blot Turbo System (BioRad, 1704150EDU) according to the manufacturer's protocol. Membranes were washed and then incubated in 5% powdered milk blocking buffer (BioRad, 1706404) for 1 hour before applying primary antibody overnight at 4°C. The following morning, membranes were briefly washed and incubated at room temperature with HRP-conjugated secondary antibodies for 1 hour. Membranes were briefly washed and imaged using Azure Biosystems C400 system to detect chemiluminescent signal. Bands were quantified by densitometry using ImageStudio Lite software. Protein expression was normalized to total protein on a Li-Cor Odyssey instrument (Li-Cor #926-11015).

Immunohistochemistry. Immunohistochemistry was performed as previously published (Caudle et al., 2007; Kline et al., 2019). Upon 24 hours of post-fixation in 4% paraformaldehyde, brain tissue was equilibrated in 30% sucrose in PBS at 4°C. 40µm coronal sections were obtained using a sliding microtome. Floating sections were blocked with 5% normal goat serum (Jackson ImmunoResearch, 005-000-021) for 1 hour at room temperature and then incubated with a rabbit anti-tyrosine hydroxylase (TH) antibody (EMD Millipore, AB152) overnight at 4°C. TH signal was amplified using an ABC Elite Kit (Vector Laboratories, PK-6100). Sections were incubated with a biotinylated goat anti-rabbit secondary antibody for 1 hour at 4 °C and then developed with 3,3'-diaminobenzidine (DAB) tablets (Sigma, D4293). Cresyl violet counterstain was performed on tissue using a 0.1% aqueous cresyl violet solution (Poly Scientific R&D, s167c) followed by de-stain and ethanol and xylene dehydration. Tissue was then transferred to microscopy slides. Images were obtained using a THUNDER microscope (Leica) with a DMC4500 digital camera and LAS X 3D analysis and 3D visualization advanced software.

Stereology. Stereology was performed as previously published with minor modifications (Caudle et al., 2007; Kline et al., 2019). Unbiased stereological estimates of dopamine (DA; TH+ cells) and total neuron (cresyl violet+ cells) numbers were performed using StereoInvestigator analysis software (MicroBrightField). Boundaries in the substantia nigra pars compacta (SNpc) were outlined using previously published criteria (M. J. West, Slomianka, & Gundersen, 1991) and cells were counted from 5-6 sections by a blinded investigator.

Statistical Analysis. Survival curves were compared using Kaplan Meier Survival Analysis. Weight, multiplexed immunoassay and PMBC flow data were compared across genotypes and time, while immunoblot, qPCR, brain flow, and stereology data were compared across genotype

and treatment using two-way analysis of variance (ANOVA) or mixed-effects model with GraphPad Prism 8 software. Tukey's multiple comparisons was used for *post hoc* comparisons. Significance for all statistical comparisons was set at $p \leq 0.05$. All data are presented as mean \pm SEM.

4.4: Results

G2019S mice are more susceptible to the experimental paradigm independent of treatment.

Interestingly and unexpectedly, G2019S mice did not survive chronic intraperitoneal dosing with a 50-60% loss of G2019S mice treated with cypermethrin or vehicle, respectively (Figure 4.1B). All WTOE mice survived, while only one B6 mouse was lost during the study. Furthermore, this loss of mice was not contained to a certain timing but occurred throughout the paradigm. In an effort to understand why G2019S mice were more susceptible to the dosing paradigm independent of treatment, body weight was assessed throughout the dosing paradigm with no genotype differences observed. Vehicle-treated mice gained weight in a time-dependent manner similarly to cypermethrin-treated mice (Vehicle-treated mice: $F_{(2.575, 43.34)}=7.847$; $p=0.0005$; cypermethrin-treated mice: $F_{(3.745, 94.25)}=9.417$; $p<0.0001$) (Figure 4.1C).

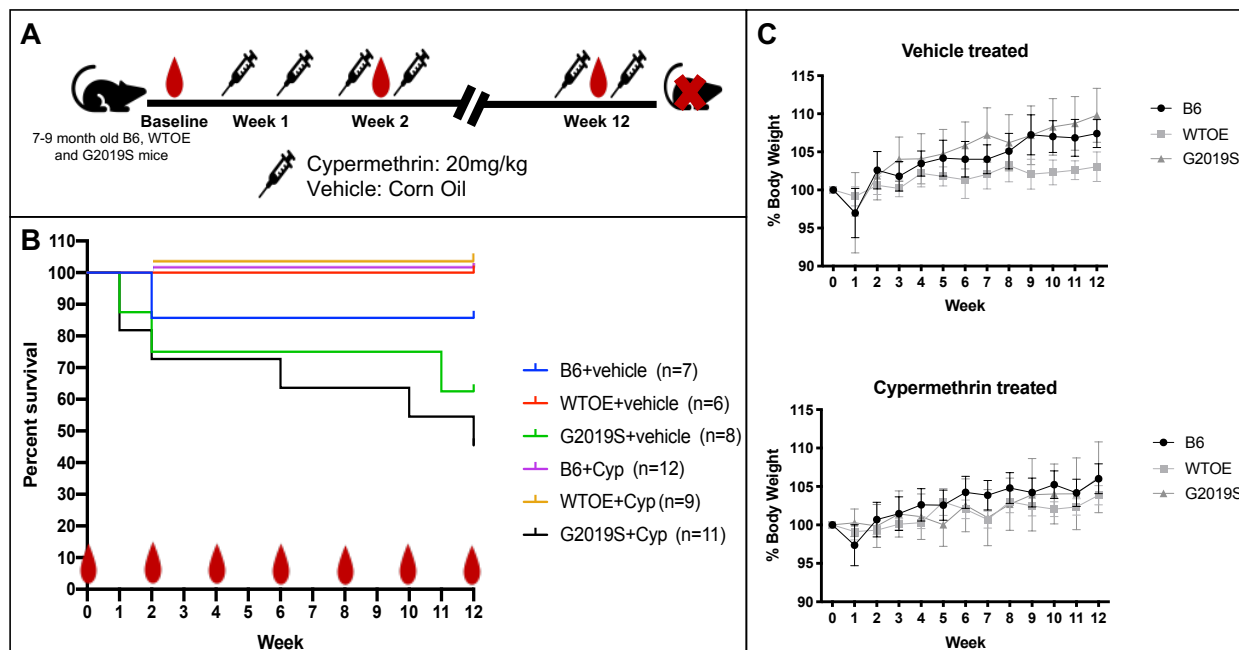


Figure 4.1: G2019S mice display reduced survival in this specific experimental dosing paradigm. A) Experimental timeline for dosing of cypermethrin or corn oil vehicle (denoted by needle) and biweekly submandibular bleeds (denoted by blood drop). B) Survival curve of the experimental groups ($p=0.0025$). Data was analyzed by Kaplan Meier Survival Analysis. C) Percent body weight change of vehicle-treated or cypermethrin-treated mice revealed no genotype differences but suggested increases in weight over time. Data were compared across genotypes and time using a mixed-effects model. Significance for all statistical comparisons was set at $p \leq 0.05$.

Chronic cypermethrin alters peripheral immune cell subsets and plasma TNF over time independent of genotype.

To evaluate the effects of chronic cypermethrin on peripheral inflammation, PBMCs were assessed by flow cytometry and plasma cytokine levels were assessed by multiplexed immunoassay every two weeks during the course of the study. Interestingly, genotype differences were not detected with mostly time effects observed. CD45⁺ immune cells (Time effect: $F_{(4,674)}$,

$_{112,2})=11.12$; $p<0.0001$) (Figure 4.2A), CD4+ T cells (Time effect: $F_{(3,547, 85.12)}=11.28$; $p<0.0001$), and CD8+ T cells (Time effect: $F_{(4,073, 97.75)}=4.786$; $p=0.0013$) (Figure 4.2B) showed time-dependent population alterations with a reduction after initiation of dosing followed by an increase towards the end of the study in cypermethrin-treated mice relative to vehicle-treated mice. Cypermethrin-treated monocyte populations exhibited the opposite effects with initial subtle increases followed by no changes relative to vehicle-treated mice (Interaction effect: $F_{(12, 144)}=2.458$; $p<0.0060$) (Figure 4.2C). Other immune cell subsets (neutrophils, B cells, MHCII+ B cells and MHCII+ monocytes) were assessed but no significant differences were noted (data not shown). To evaluate functional aspects of monocytes during treatment, BMV109 was used to assess pan-cathepsin activity and Pepstatin Bodipy was used to assess cathepsin D, as cypermethrin has been shown to affect lysosomal homeostasis. Interestingly, G2019S cypermethrin-treated mice showed increased BMV109+ monocytes relative to WTOE cypermethrin-treated mice 2 weeks after the start of dosing; however, these effects were not sustained throughout the treatment course (Interaction effect: $F_{(12, 144)}=2.286$; $p=0.0109$) (Figure 4.2C). Geometric mean fluorescent intensity of BMV109 on BMV109+ monocytes increased in all genotypes after treatment initiation and higher intensity levels were maintained until the end of the treatment paradigm, again showing time dependent changes in cypermethrin-treated mice independent of genotype (Time effect: $F_{(3,484, 83.62)}=15.60$; $p<0.0001$) (Figure 4.2C). No differences in Pepstatin Bodipy-positive cells or intensity levels as measured by geometric mean fluorescent intensity were noted (data not shown). Plasma TNF levels were incrementally increased throughout the dosing paradigm in cypermethrin-treated mice relative to vehicle-treated mice independent of genotype (Time effect: $F_{(2,320, 42.33)}=3.825$; $p=0.0244$), while no significant differences were noted in IL-6 and IL-10 levels (Figure 4.2D). Furthermore, no significant differences were observed in IFN γ , IL-2, IL-5, KC/GRO cytokine levels (data not shown), and IL-4, IL-12p70, and IL-1 β levels were below detection limits of the assay.

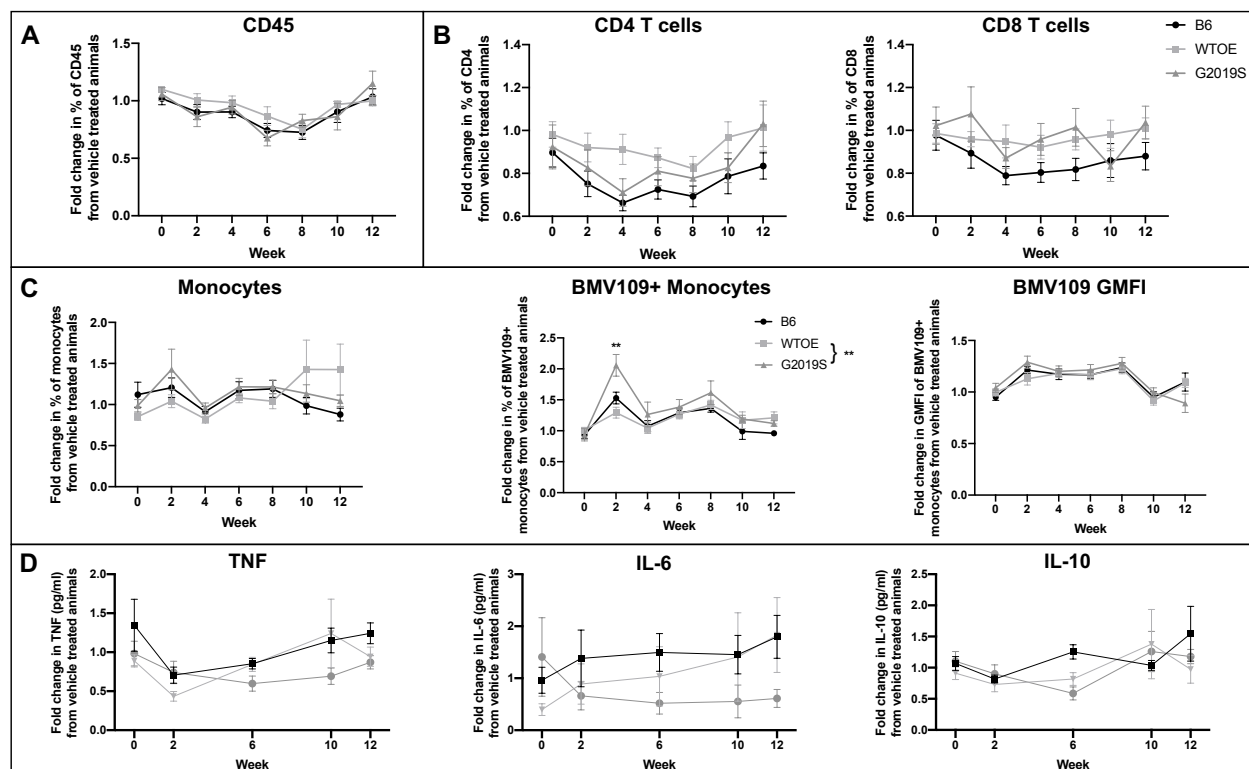


Figure 4.2: Chronic cypermethrin disrupts PBMC subsets and TNF cytokine levels over time, independent of genotype. By flow cytometry or multiplexed immunoassay, PBMC populations or plasma cytokines were measured every two weeks during the experimental paradigm. A) CD45+ immune cells changed with time. B) Alterations in T cell and C) monocyte populations with time. D) TNF time-dependent changes (n=5-12 per genotype per treatment). Data are presented as fold change of cypermethrin-treated mice from vehicle-treated mice at each time point and were compared across genotypes and time using a mixed-effects model. Tukey's multiple comparisons was used for *post hoc* comparisons within each timepoint (**signifies statistically significant differences between two groups at that time point).

Chronic cypermethrin does not trigger neuroinflammation and alter the nigrostriatal pathway.

To evaluate the effects of chronic cypermethrin on neuroinflammation, brain immune cells were assessed by flow cytometry and striatal gene expression assessed by qPCR. Interestingly, no

differences between genotype and treatment were observed in microglia, MHCII⁺ microglia, CD3⁺ T cells, CD4⁺ T cells, and CD8⁺ T cells (Figure 4.3A and B). No differences were observed in potentially brain-infiltrating immune cell populations (monocytes and neutrophils), and functional readouts of cathepsin activity using BMV109 or Pepstatin Bodipy to assess lysosome immune cell homeostasis were not different (data not shown). Given that an entire brain hemisphere was used for flow cytometry analysis, we sought to measure neuroinflammation in a more localized region of the nigrostriatal pathway; therefore, we evaluated inflammatory gene expression in the striatum. Again, no genotype and treatment differences were observed in canonical inflammatory genes in the striatum, further supporting a lack of detectable neuroinflammation in the brain (Figure 4.3C). Additional immune cell and inflammatory markers were assessed by qPCR (*CD8b*, *CD4*, *Lcn2*) but similarly no differences were noted (data not shown).

Although we found no indications of neuroinflammatory changes, nigrostriatal integrity was assessed using stereology of brain sections containing the substantia nigra and protein expression analysis in the striatum. No differences were observed in dopaminergic (TH⁺) and total neuron (cresyl violet ⁺) counts (Figure 4.4A). Similarly, no genotype or treatment effects were noted in DAT, TH, and α syn striatal protein expression (Figure 4.4B), suggesting a lack of nigrostriatal pathology associated with a neurodegenerative phenotype.

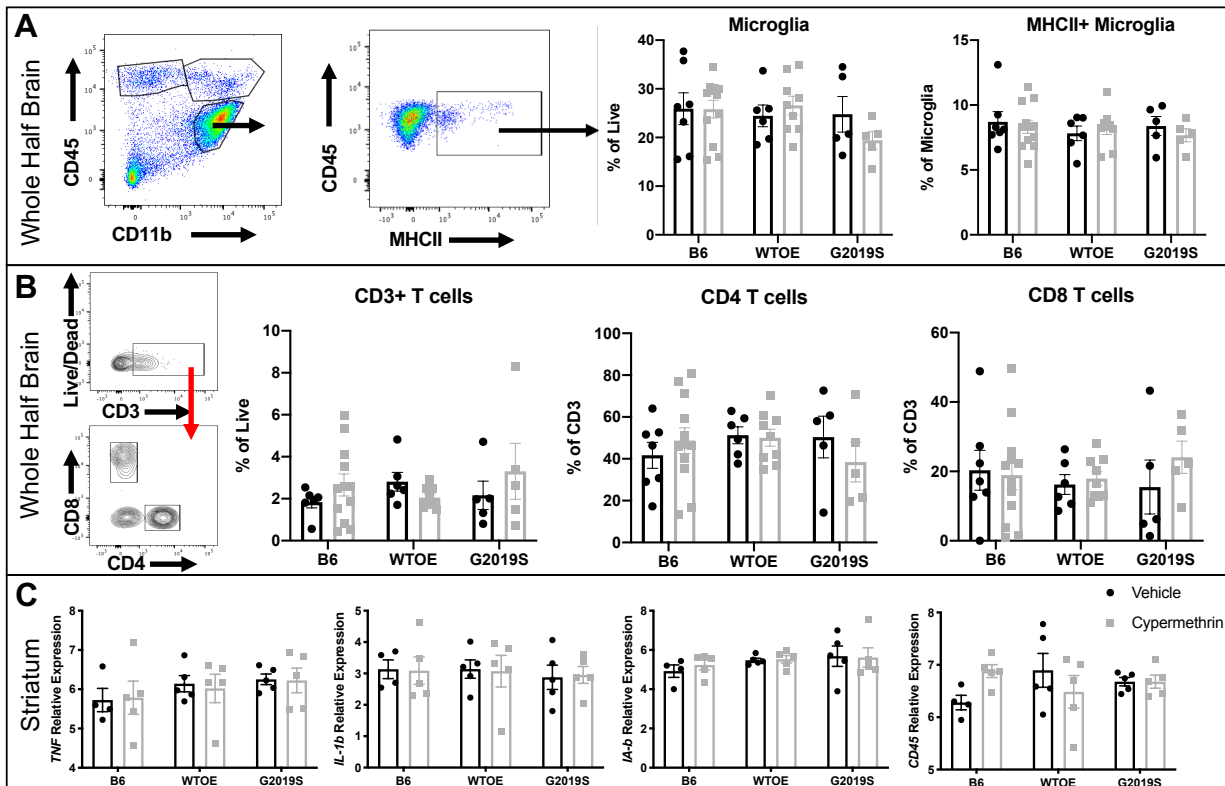


Figure 4.3: Brain immune cells and striatal inflammatory gene expression remain unaltered after chronic cypermethrin exposure. To evaluate immune cells and the inflammatory state in the brain after chronic cypermethrin, brain immune populations were assessed by flow cytometry and gene expression of canonical pro-inflammatory cytokines was assessed by qPCR. A) No differences were observed in microglia, MHCII+ microglia, B) CD3+ T cell, CD4+ T cell or CD8+ T cell populations within the right hemisphere of the brain (n=5-12 per genotype per treatment. C) No differences in *Tnf*, *IL-1 β* , *IA-b*, and *Cd45* striatal inflammatory gene expression (n=4-5 per group per treatment) were observed. Data were compared using a two-way ANOVA with genotype and treatment as factors.

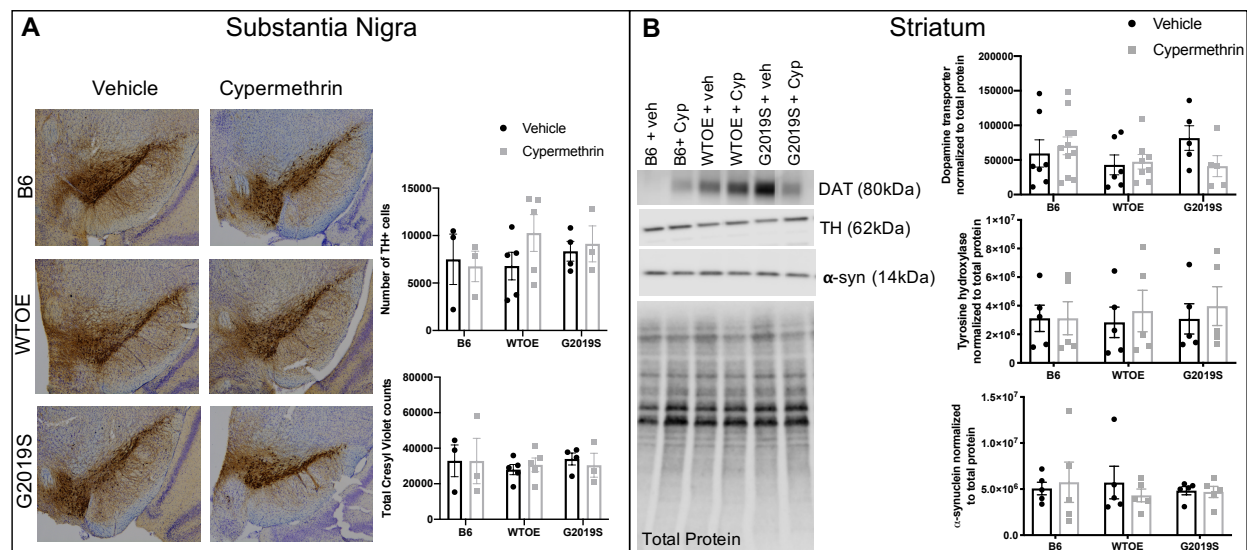


Figure 4.4: The nigrostriatal pathway is unaffected by chronic cypermethrin exposure. To evaluate nigrostriatal integrity after chronic cypermethrin, brain sections containing the substantia nigra were assessed by stereology and striatal protein expression was assessed by immunoblot. A) No differences in dopaminergic (TH+) and total (cresyl violet+) neurons ($n=3-6$ per genotype per treatment). B) No differences in DAT, TH, and α syn striatal protein expression ($n=5-11$ per group per treatment). Data were compared using a two-way ANOVA with genotype and treatment as factors.

4.5: Discussion

In the current study, we sought to investigate the extent to which increased mouse LRRK2 protein (WTOE) or increased G2019S-mediated kinase activity (G2019S) affects inflammation and neuronal survival in a chronic cypermethrin model with the hypothesis that cypermethrin-treated G2019S mice would exhibit exacerbated inflammation and nigrostriatal deficits relative to WTOE and B6 mice. However, our data suggest that chronic cypermethrin alters peripheral immune cell subsets independent of genotype but does not promote impaired nigrostriatal integrity.

Interestingly and unexpectedly, we observed that G2019S mice were more susceptible to the experimental paradigm independent of treatment type. Given that this phenotype was mainly observed in the G2019S strain independent of sex (data not shown) and treatment, we hypothesize that this may be due to an inability of G2019S mice to effectively handle the stress induced by biweekly submandibular bleeds and twice per week intraperitoneal injections. Studies examining the stress axis in LRRK2 G2019S mice are limited; however, a recent study using LRRK2 G2019S transgenic mice subjected to paraquat noted that G2019S mice had higher levels of corticosterone, a glucocorticoid steroid that plays a major role in the stress hypothalamic pituitary adrenal axis, while LRRK2-deficient mice treated with paraquat had reduced corticosterone levels (Rudyk et al., 2019). Although we did not measure stress hormones in the current study; the evidence from the paraquat model along with our data suggests that LRRK2 may be involved in the stress response and warrants further investigation.

Given the surprising lack of cypermethrin-induced changes in the periphery and brain, confirmation of cypermethrin metabolites in the plasma and brain could help explain the observed phenotypes. We did observe time-dependent changes in peripheral immune cell populations in cypermethrin-treated mice relative to vehicle-treated mice, but no differences in brain immune cell populations or inflammatory gene expression. This finding suggests that cypermethrin may not have crossed the BBB in large enough quantities to promote neuroinflammation and neurodegeneration, but this claim should be confirmed and explored in future studies.

Interestingly, in our study we did not observe the same peripheral immune cell phenotypes observed in unpublished data from wildtype cypermethrin-treated mice, with a lack of increased CD8 T cell phenotypes. In fact, we observed the opposite with a reduction of T cell populations and an increase in monocyte populations in cypermethrin-treated mice independent of genotype. A recent report has noted that pyrethroids have high affinity for T and B cell receptors, but the functional consequence of this remains unknown as it hypothesized that this increased affinity could stimulate the immune system, suppress the immune system or cause no alteration (A.

Kumar, Behera, Rangra, Dey, & Kant, 2018). This may explain why we observed decreased T cell populations with initial cypermethrin treatment that was resolved by the end of the study. Furthermore, gene expression in human PBMCs treated *ex vivo* with cypermethrin were largely unchanged, potentially explaining our lack of cypermethrin-induced peripheral immune changes (Mandarapu & Prakhya, 2016). RAW 264.7 murine macrophages are susceptible to cypermethrin through increased oxidative stress and ensuing apoptosis (Huang et al., 2016). We did not observe a reduction of monocyte populations treated with cypermethrin as would be hypothesized; however, future investigations should explore cypermethrin effects on macrophage and monocyte function as this was not examined in-depth the present study.

Cypermethrin has been reported to activate autophagosome formation and to inhibit autophagy in neurons which contributes to impaired degradation of toxic materials (Mishra et al., 2018). Given that LRRK2 has been implicated in similar functions in a kinase-dependent manner, we hypothesized that G2019S mice treated with cypermethrin would have impaired autophagy and lysosomal pathways in neuronal and immune cells. We examined cathepsin activity levels as an orthogonal measure of lysosomal homeostasis in immune cells but observed a lack of changes in lysosomal cathepsin activity as measured by flow cytometry. Future investigations should target the autophagy pathway whereby more effective tools may be used to fully understand the mechanism by which cypermethrin synergizes with LRRK2 to act on the autophagy pathway in immune cells as well as other functional readouts of immune cells.

In conclusion, the current study aimed to examine a role for a gene (LRRK2) by environment (cypermethrin) synergistic effect to promote PD pathogenesis but failed to produce PD-related phenotypes in any genotype examined. Given that humans are typically exposed to pesticides dermally or through inhalation, more relevant models of cypermethrin exposure should be used to identify the mechanisms by which cypermethrin impairs immune cells and poses a risk to human health. Future studies should also examine the synergistic effects of other PD-related

genes, such as VPS35, that also affect the autophagy lysosomal pathway in the context of cypermethrin or other pyrethroid pesticides.

4.6: Acknowledgements

Cypermethrin studies were performed in collaboration with Dr. William M. Caudle's laboratory in the Rollins School of Public Health at Emory University.

CHAPTER 5: THE EFFECTS OF VIRAL OR BACTERIAL INFECTION EXPOSURE IN WT OR G2019S OVEREXPRESSING MICE

5.1: Abstract

Parkinson's disease (PD) is considered a multifactorial disease with an individual's age, genetics, environmental exposures and lifestyle collectively hypothesized to contribute to disease pathogenesis. Increased incidence of PD has been associated with certain viral or bacterial infections, supporting the idea that inflammation may contribute to PD pathogenesis. Animal models studying the effects of LRRK2, one of the greatest genetic contributors to PD, suggest a role for LRRK2 in immunity to control infection burden; however, the mechanism by which LRRK2 controls or contributes to infection remains unknown. Previous studies have examined specific infections in different LRRK2 rodent models with results often suggesting that LRRK2 controls or contributes to infection in a LRRK2 kinase-, sex- and infection-dependent manner. Therefore, we sought to confirm and extend these findings by utilizing viral (lymphocytic choriomeningitis virus (LCMV) and influenza) and bacterial (*Listeria monocytogenes* and *Pseudomonas aeruginosa*) infections in the presence or absence of LRRK2 kinase inhibition (PF-360) in the same BAC transgenic mice overexpressing mouse wildtype LRRK2 or mutated G2019S LRRK2. Utilization of these particular infections in the same LRRK2 mouse models enabled us to assess distinct arms of the immune system with a focus on the role of antibody-mediated immunity (influenza), CD8 T cells (LCMV), and macrophage and monocyte responses to intracellular (*L. monocytogenes*) or extracellular (*P. aeruginosa*) bacteria. Here, we present data that suggests G2019S BACs are protected from *P. aeruginosa* and in contrast minimal immune cell deficits occur after infection with LCMV, influenza, or *L. monocytogenes* supporting the hypothesis that LRRK2 regulates inflammation in a kinase-dependent and antigen-specific manner.

5.2: Introduction

Parkinson's disease (PD) is an aged-related neurodegenerative disease typically classified by α -synuclein aggregation in the substantia nigra (SN) and dopaminergic cell loss that gives rise to the stereotypical motor symptoms. As a multifactorial disease, a complex interaction of genetics, aging, and environmental exposures are all thought to contribute to PD pathogenesis. Importantly, aging is the number one risk factor for PD (Bennett et al., 1996). Humans are exposed to several different viral and bacterial antigens during their lifetime as dampened immune function and increased susceptibility to infection occur with aging. PD incidence has been associated with certain viral or bacterial infections. PD patients with systemic infections or fevers are shown to have worsened clinical motor symptoms (Brugger et al., 2015; Umemura et al., 2014). A recent study identified an association between tuberculosis (TB) patients and PD, as those with newly diagnosed TB had higher incidence of PD, suggesting that inflammation may contribute to PD pathogenesis (C. H. Shen et al., 2016).

Leucine-Rich Repeat Kinase 2 (LRRK2) is one of the greatest known genetic contributors to Parkinson's disease (PD). LRRK2 regulates multiple cellular processes including neurite outgrowth, cytoskeletal maintenance, vesicular trafficking, and autophagy, all of which are disrupted by mutations in LRRK2 (Berwick & Harvey, 2012; Hongge et al., 2015; Plowey et al., 2008; Ramonet et al., 2011; Schapansky et al., 2014). The G2019S mutation within the LRRK2 kinase domain is the most prevalent PD-associated LRRK2 mutation resulting in a gain-of-toxic function and 2-3-fold increase in kinase activity that drives cellular dysfunction (Greggio et al., 2006; A. B. West et al., 2005; A. B. West et al., 2007). To date, most research has focused on the effect of LRRK2 mutations in neurons and the contributions of G2019S-mediated kinase activity to neuronal toxicity, leaving the role of LRRK2 and G2019S-mediated kinase activity in immune cell homeostasis unresolved. Interestingly, LRRK2 expression is higher in immune cells relative to neurons, suggesting LRRK2 has an important role in the immune system (A. B. West, 2017). LRRK2 protein is expressed in adaptive (B and T cells) and innate (dendritic cells,

macrophages, and monocytes) immune cells, and its expression is increased upon stimulation; however, the exact function of LRRK2 in these cell types is unknown (Atashrazm et al., 2019; Fan et al., 2018; Gardet et al., 2010; Hakimi et al., 2011; Thevenet et al., 2011). Intriguingly, a recent study from our group revealed higher levels of LRRK2 in adaptive and innate immune cells of idiopathic PD patients compared with healthy controls, underscoring the importance of investigating the contribution of immune cell LRRK2 activity to PD (Cook et al., 2017).

LRRK2 has been linked to several infections in animal and cellular models. Analysis of gene expression from tuberculosis infections identified LRRK2 as being significantly enriched during active infections (Z. Wang et al., 2018). LRRK2 knockout mice showed decreased *Mycobacterium tuberculosis* burden early in infection, perhaps with exacerbated inflammation as LRRK2 knockout macrophages treated with *M. tuberculosis* exhibited altered innate immune gene expression induced by various mitochondrial stresses (Hartlova et al., 2018; Weindel et al., 2020). Phagosome maturation and bacterial control were increased in human and mouse macrophages treated with LRRK2 kinase inhibitors, suggesting that a lack of LRRK2 kinase activity is protective against *M. tuberculosis* (Hartlova et al., 2018). On the other hand, LRRK2 knockout mice infected with *Salmonella typhimurium* exhibited reduced caspase-1 activation and IL-1 β secretion due to inflammasome activation in macrophages, which ultimately impaired clearance of pathogens (W. Liu et al., 2017). A recent study suggested that wildtype LRRK2 is protective against *S. typhimurium* and reovirus infection in a sex-dependent manner with females exhibiting impaired ability to control infection (Shutinoski et al., 2019). Interestingly, LRRK2 G2019S mice controlled *S. typhimurium* infection better, but were more susceptible to reovirus in a LRRK2 kinase-dependent manner (Shutinoski et al., 2019). Collectively, these studies suggest a role for LRRK2 in immunity to control infection burden; however, the mechanism by which LRRK2 appears to control or contribute to infection is sex-, genotype- and infection-specific and remains to be elucidated, underscoring the complexity of LRRK2 signaling and function.

To further elucidate the role of LRRK2 in immune cell function and regulation and determine whether LRRK2, itself, or its gain-of-function kinase activity alters immune cell function, we utilized bacterial artificial chromosome (BAC) transgenic mice overexpressing mouse wildtype LRRK2 (WTOE) or mutated G2019S LRRK2 (G2019S) and subjected them to viral (lymphocytic choriomeningitis virus (LCMV) and influenza) and bacterial infections (*Listeria monocytogenes* and *Pseudomonas aeruginosa*) in the presence or absence LRRK2 kinase inhibition (PF-360). Utilization of these particular infections in the same LRRK2 mouse models permit assessment of specific arms of the immune system, with a focus on antibody-mediated immunity (influenza), CD8 T cells (LCMV), and macrophage responses to intracellular (*L. monocytogenes*) or extracellular (*P. aeruginosa*) bacterium. Here, we report minimal effects on immune profiles or responses after LCMV, influenza, or *L. monocytogenes* infection, but data suggest that G2019S mice are protected from *P. aeruginosa*, consistent with the hypothesis that LRRK2 regulates inflammation in a kinase-dependent and antigen-specific manner.

5.3: Materials and Methods

Animals. Homozygous male *Lrrk2-G2019S* (B6.Cg-Tg(Lrrk2*G2019S)2Yue/J; stock number 012467) and *Lrrk2-WT* (B6.Cg-Tg(Lrrk2)6Yue/J; stock number 012466) mice were purchased from the Jackson Laboratory and bred to hemizygoty at Emory University. Hemizygous male and female BAC transgenic mouse strains overexpressing either mouse mutant G2019S LRRK2 (G2019S) or mouse wildtype LRRK2 (WTOE) were used for experimental procedures with non-transgenic littermates (B6) serving as controls. Genotypes were determined by tail-snip PCR with two sets of primers: Transgene: Forward 5' GAC TAC AAA GAC GAT GAC GAC AAG 3' Reverse 5' CTA CCA CCA CCC AGA TAA TGT C 3'; Internal positive control: Forward 5' CAA ATG TTG CTT GTC TGG TG 3' Reverse 5' GTC AGT CGA GTG CAC AGT TT 3'. Animals were group housed (maximum 5 mice per cage) and maintained on a 12h/12h light/dark cycle with *ad libitum* access to standard rodent chow and water. Experimental procedures involving use of animals

were performed in accordance with the National Institutes of Health Guidelines for Animal Care and Use and approved by the Institutional Animal Care and Use Committee at Emory University School of Medicine.

Infections. Intranasal inoculation with influenza A/PR/8/34 (H1N1) at 3000 plaque-forming units (PFU) was performed with mice under isoflurane anesthesia (n=12-16 per genotype per treatment). For LCMV infections, mice were infected by intraperitoneal injection with 2×10^5 PFU (strain: Armstrong; n=12-16 per genotype per treatment). For *L. monocytogenes* infections, mice were infected by intravenous injection with 2×10^3 PFU (strain 45231; n=12-16 per genotype per treatment). For all experiments, mice were monitored with daily weighing and euthanized when they reached 25% weight loss. Mice inoculated with influenza, *L. monocytogenes*, or LCMV were treated twice a day by oral gavage with the selective LRRK2 kinase inhibitor, PF-360 (Pfizer, 20mg/kg) or vehicle for 14 days post infection. Early immune cell effector responses were assessed in a cohort sacrificed at 8- or 10-days post infection, while memory responses to LCMV or influenza were assessed in a cohort sacrificed at 30- or 35-days post infection, respectively (Figure 5.1A).

Stock of *P. aeruginosa* was prepared as previously described (Sadikot et al., 2007). For young mice, *P. aeruginosa* was administered in anaesthetized mice with a sublethal dose of PAO.1lux strain (1.75×10^6 colony forming unit (CFU)/mouse, ≤ 0.5 LD₅₀) via intranasal route in a total volume of 20ul (10ul/nostril; n=3-8 per genotype). For aged mice, a sublethal dose of PAO.1lux was administered (4×10^6 CFU/mouse) in a total volume of 20ul (10ul/nostril; n=11-13 per genotype). Mice were scored as follows to assess health: 0-1: normal and active; 2-3: mild-to-moderate symptoms with less activity but responsive to stimuli; 4: obvious symptoms: discharge on eyes and nose, hunched posture, labored breathing but responsive; 5: all symptoms in score 4 and non-responsive to stimuli, which required euthanasia. Young mice were subjected to *in vivo* bioluminescent imaging using the IVIS 24- and 48-hours post infection (Figure 5.1B).

For aged mouse colonization studies, mice were euthanized at 24 hours post-infection and whole lungs were collected aseptically, weighed, and homogenized in 1 mL of phosphate buffered saline (PBS). Tissue homogenates were serially diluted and plated. CFU determinations were made 16-18 hours later.

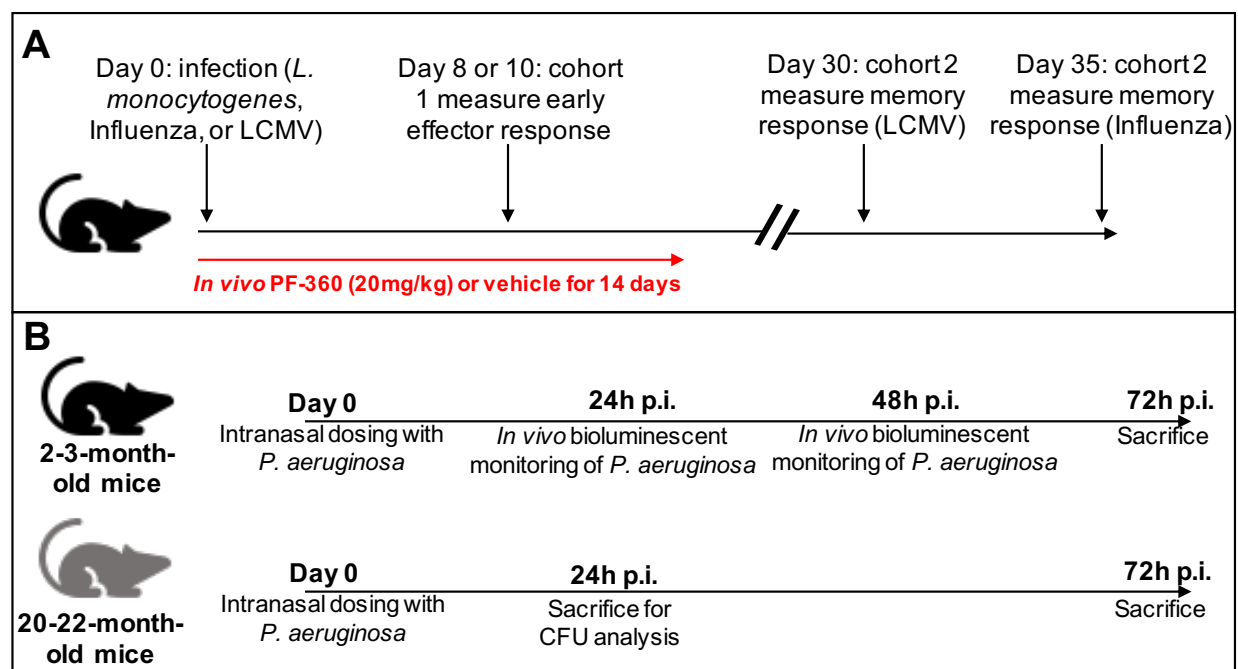


Figure 5.1: Experimental designs for infection models in LRRK2 BAC mice. Experimental timelines for A) *L. monocytogenes*, LCMV, influenza or B) *P. aeruginosa* in young (2-3-month-old) or aged (20-22-month-old) mice.

Tissue collection. At sacrifice, mice were euthanized with avertin (2,2,2-Tribromoethanol, Sigma) and exsanguinated prior to harvest of lung, spleen or mediastinal lymph node. Tissues were collected and single-cell immune cell populations isolated as previously described (Dunbar et al., 2020; Hayward et al., 2020; McMaster, Wilson, Wang, & Kohlmeier, 2015). In sum, bronchoalveolar lavage was performed and the airways were washed five times after which the lungs were harvested into HBSS. Lungs were finely minced and digested by collagenase D

(Roche) for 30 minutes at 37°C followed by purification with centrifugation in a Percoll gradient (40-80%). Splenocytes and immune cells from mediastinal lymph nodes were obtained by mechanical dissociation and straining through nylon mesh. Red blood cells in splenocytes were lysed with buffered ammonium chloride.

Multi-color Flow Cytometry. Single-cell populations from lung, spleen or mediastinal lymph node were stained for flow cytometry to assess immune cell populations. Cells were stained with Live/Dead Zombie Yellow, Ultraviolet or Near Infrared (Biolegend) to differentiate live versus dead cells and Fc blocked with anti-mouse CD16/CD32 (eBioscience). Fluorescently labeled antibodies against surface markers that are commercially available were used to assess immune cell populations. These antibodies include anti-mouse CD11b BV711 (Biolegend), anti-mouse Ly6G BV510 (Biolegend), anti-mouse MHCII PE_Cy7 (Biolegend), anti-mouse Ly6C APC_Cy7 (BD Biosciences), anti-mouse CCR2 APC (R&D), anti-mouse B220 PE_Cy7 (Biolegend), anti-mouse CD3 APC (Biolegend), anti-mouse CD4 APC_Cy7 (eBiosciences), anti-mouse CD8 BV750 (Biolegend), anti-mouse CD44 AF700 (eBiosciences), anti-mouse KLRG-1 BV605 (Biolegend), anti-mouse CD127 PE-CF594 (BD Biosciences), anti-mouse CD62L BV605 (Biolegend), anti-mouse CD69 PE_Cy7 (Biolegend), and anti-mouse CXCR3 BV650 (Biolegend). Tetramers used for detection of antigen-specific cells included H-2K^b Listeria OVA (eBiosciences), H-2D^b Influenza A NP₃₆₆₋₃₇₄ (ASNENMETM), and H-2D^b LCMV GP33 (KAVYNFATM) with the latter two supplied by the NIH tetramer core at Emory. Samples were run on an LSRFortessa or LSRII (BD Biosciences) and analyzed with FlowJo_V10.

Statistical Analysis. Immune cell populations and percent body weights were compared across genotype and treatment using two-way analysis of variance (ANOVA) or mixed-effects model with GraphPad Prism 8 software. Tukey's multiple comparisons was used for *post hoc* comparisons. Survival curves were compared using Kaplan Meier Survival Analysis with Log-rank test to identify

differences in groups. Colonization was compared across genotype using one-way ANOVA with Tukey's multiple comparisons for *post hoc* comparisons. Significance for all statistical comparisons was set at $p \leq 0.05$. All data are presented as mean \pm SEM. Letters above groups signify *post hoc* results. Groups sharing the same letter are not significantly different.

5.4: Results

Minimal immune cell changes after *L. monocytogenes*, LCMV, or influenza

To evaluate the effects of *L. monocytogenes*, LCMV, or influenza in WTOE and G2019S BACs treated in the presence or absence of LRRK2 kinase inhibition (PF-360), body weight and certain immune cell populations were assessed. Body weight changed in a time-dependent manner after each infection (effect of time: $p < 0.0001$ for each comparison), but no differences in body weight between genotypes or treatment were noted with the exception of LCMV-infected G2019S mice (Figures 5.2A-B, 5.3A-B, 5.4A-B). PF-360-treated G2019S mice exhibited a greater loss in body weight after infection with LCMV relative to vehicle treated mice, in particular 6-days post infection (Figure 5.3B).

To assess immune cell responses, mice were sacrificed at early (8- or 10-days post infection) or late (30- or 35-days post infection) time points to assess immunologic memory against the particular viral or bacterial antigen. Immune cells were stained with infection-specific major histocompatibility complex (MHC) tetramers, which are effective tools used to identify antigen-specific T cells. LRRK2 kinase inhibition had no effect on influenza-exposed B6 or G2019S mice, but G2019S mice exhibited reduced FluNP366 tetramer + CD8 T cells in the spleen 10-days post infection (genotype effect: $F_{(1, 12)} = 5.274$; $p = 0.0404$) and in the mediastinal lymph node 35-days post infection (genotype effect: $F_{(1, 12)} = 5.556$; $p = 0.0362$) (Figure 5.2D-E). A trend was identified for reduced FluNP366 tetramer + CD8 T cells in G2019S mediastinal lymph node 10-days post infection although it did not reach statistical significance (Figure 5.2D). No

differences were observed in FluNP366 tetramer+ CD8 T cells from the lung at either time point (data not shown).

While no significant differences were observed in LCMV tetramer (GP33)+ CD8 T cells in the spleen at 8-days post infection, an interaction between genotype and drug was identified at 30-days post infection (interaction effect: $F_{(1, 13)}=20.70$; $p=0.0005$) (Figure 5.3D-E). Interestingly, 8-days post LCMV infection, PF-360 increased CD8 memory precursor effector cells (MPECs) independent of genotype (drug effect: $F_{(1, 16)}=6.201$; $p=0.0241$) (Figure 5.3D). After an infection, naïve CD8 T cells proliferate and differentiate into effector cells to clear pathogens. MPECs represent a small percentage of those cells that do not undergo apoptosis and survive to form long-term memory cells (Yuzefpolskiy, Baumann, Kalia, & Sarkar, 2015). Unlike LCMV, no differences were observed in tetramer-specific CD8 T cells or MPECs after infection with *L. monocytogenes* 8-days post infection in the spleen (Figure 5.4D). However, given that *L. monocytogenes* is internalized by antigen-presenting cells such as monocytes or macrophages to control pathogen clearance, it was noted that G2019S mice independent of treatment exhibited decreased non-inflammatory (non-classical) monocytes in the spleen 8-days after *L. monocytogenes* infection (genotype effect: $F_{(1, 15)}=13.17$; $p=0.0025$) with no genotype differences in inflammatory (classical) monocytes (Figure 5.4C).

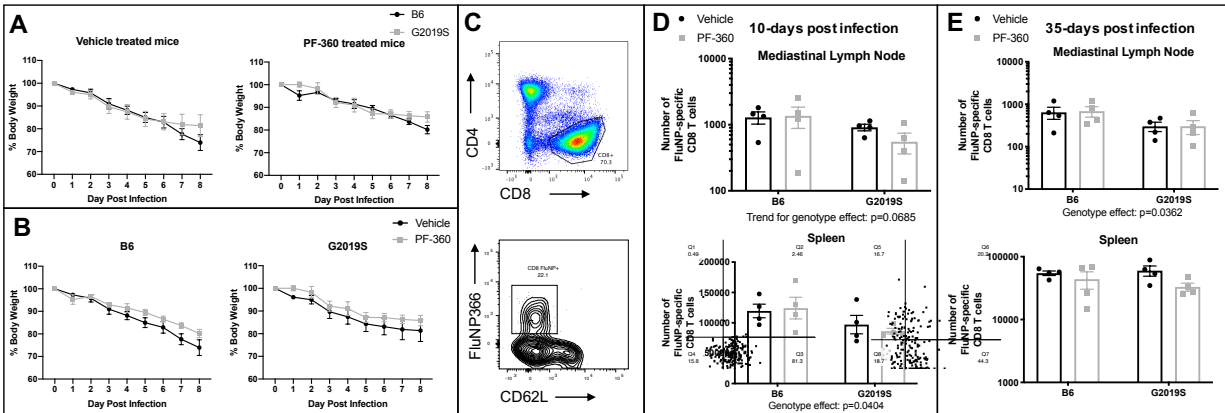


Figure 5.2: Reduced FluNP366+ tetramer CD8 T cells in G2019S influenza-infected spleen and mediastinal lymph node. A) Percent body weight of vehicle (effect of time: $F_{(8, 56)}=36.44$; $p<0.0001$) and PF-360-treated influenza inoculated mice compared across genotypes until 8-days post infection (effect of time: $F_{(8, 64)}=54.31$; $p<0.0001$). B) Percent body weight of B6 (effect of time: $F_{(8, 56)}=66.50$; $p<0.0001$) and G2019S (effect of time: $F_{(8, 64)}=31.57$; $p<0.0001$) influenza inoculated mice compared across treatment until 8-days post infection. C) Gating strategy used to identify influenza antigen-specific T cells (FluNP366+ CD8+ T cells). Number of influenza antigen-specific T cells in the mediastinal lymph node and spleen at D) 10- or E) 35-days post infection to measure early and memory responses, respectively.

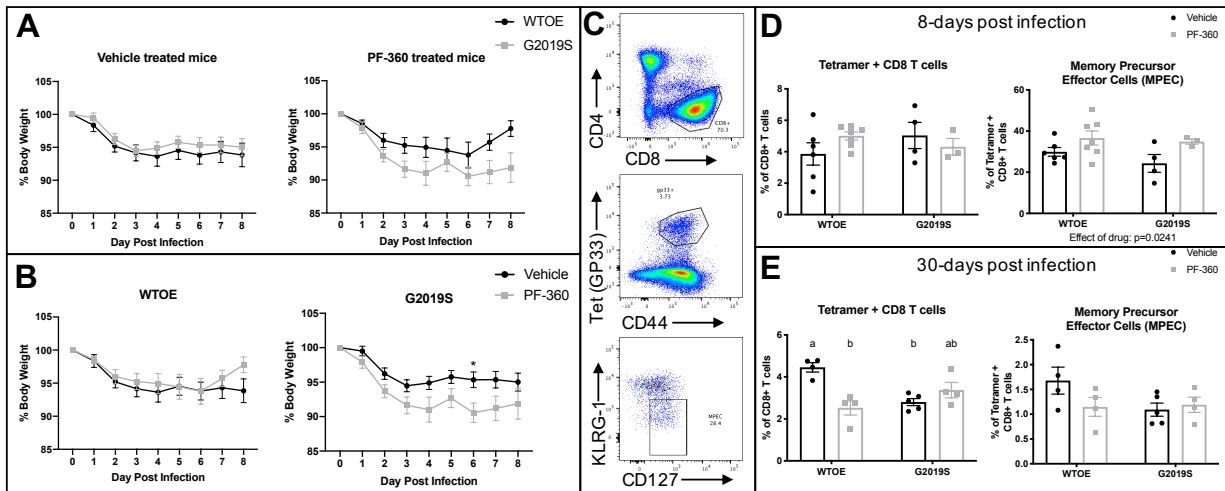


Figure 5.3: LRRK2 kinase inhibition alters G2019S weight after LCMV infection and increases early MPECs but decreases tetramer+ CD8 T cells. A) Percent body weight of vehicle (effect of time: $F_{(8, 223)}=18.69$; $p<0.0001$) and PF-360-treated LCMV inoculated mice compared across genotypes until 8-days post infection (effect of time: $F_{(8, 214)}=20.59$; $p<0.0001$). B) Percent body weight of WT0E (effect of time: $F_{(8, 235)}=14.60$; $p<0.0001$) and G2019S (interaction effect: $F_{(8, 202)}=2.173$; $p=0.0309$) LCMV-inoculated mice compared across treatment until 8-days post infection. Asterisk (*) signifies a statistically significant difference between vehicle and PF-360-treated G2019S mice at that time point (day 6). C) Gating strategy used to identify LCMV antigen-specific T cells (TetGP33+ CD8+ T cells) and MPECs (KLRG-1-, CD127+). Number of LCMV antigen-specific T cells or MPECs in spleen at D) 8- or E) 30-days post infection to measure early and memory responses, respectively.

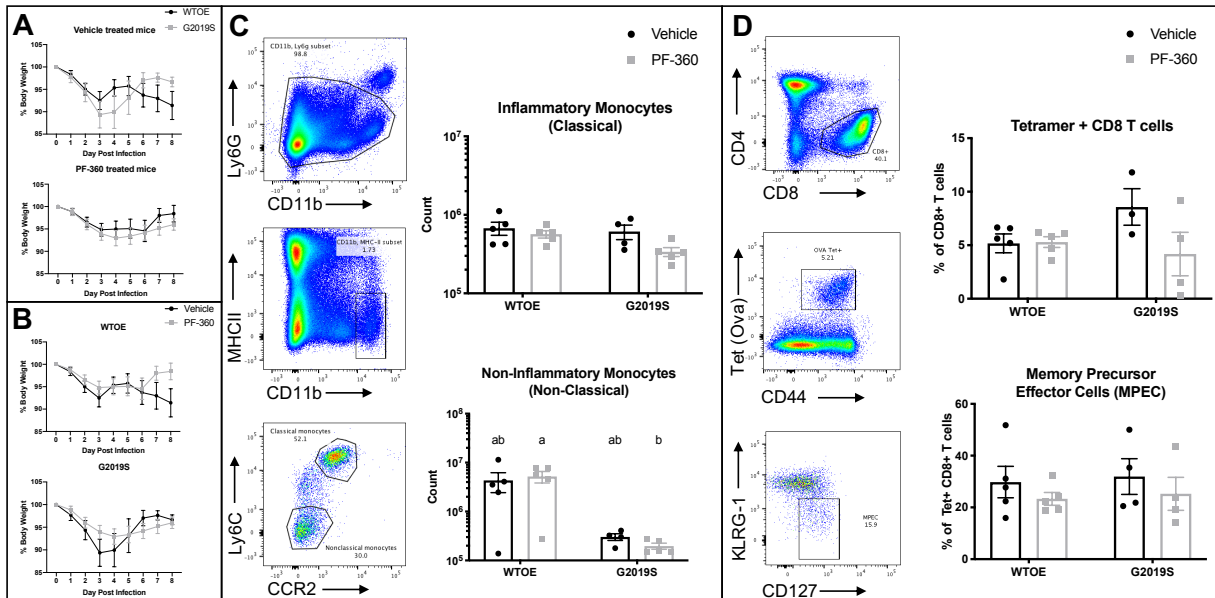


Figure 5.4: G2019S mice treated with *L. monocytogenes* exhibit reduced non-inflammatory monocytes. A) Percent body weight of vehicle (effect of time: $F_{(8, 169)}=8.760$; $p<0.0001$) and PF-360-treated *L. monocytogenes* inoculated mice compared across genotypes until 8-days post infection (effect of time: $F_{(8, 240)}=14.02$; $p<0.0001$). B) Percent body weight of WTOE (effect of time: $F_{(8, 215)}=8.499$; $p<0.0001$) and G2019S (effect of time: $F_{(8, 194)}=14.58$; $p<0.0001$) *L. monocytogenes* inoculated mice compared across treatment until 8-days post infection. Gating strategy and quantification of C) inflammatory and non-inflammatory monocytes or D) antigen-specific T cells (Tet OVA⁺, CD8⁺ T cells) and MPECs (KLRG-1⁻, CD127⁺) in the spleen 8-days post infection.

G2019S mice are protected from sublethal *P. aeruginosa* infection

Given the immune system undergoes a number of changes with age, young and aged mice were infected with sublethal *P. aeruginosa*. Interestingly, G2019S mice at both ages survived the longest relative to B6 mice, suggesting that G2019S mice may be protected or better able to control pathogen load (Figure 5.5A&C). This was further supported by *in vivo* bioluminescent imaging of young mice infected with *P. aeruginosa* that showed G2019S mice had

lower luminescent signal intensity indicative of less bacteria at 48 hours post infection (Figure 5.5B). In aged mice, bacterial colonization in the lungs was assessed 24 hours after infection and revealed that both WTOE and G2019S mice had decreased bacterial colonization levels (Figure 5.5D).

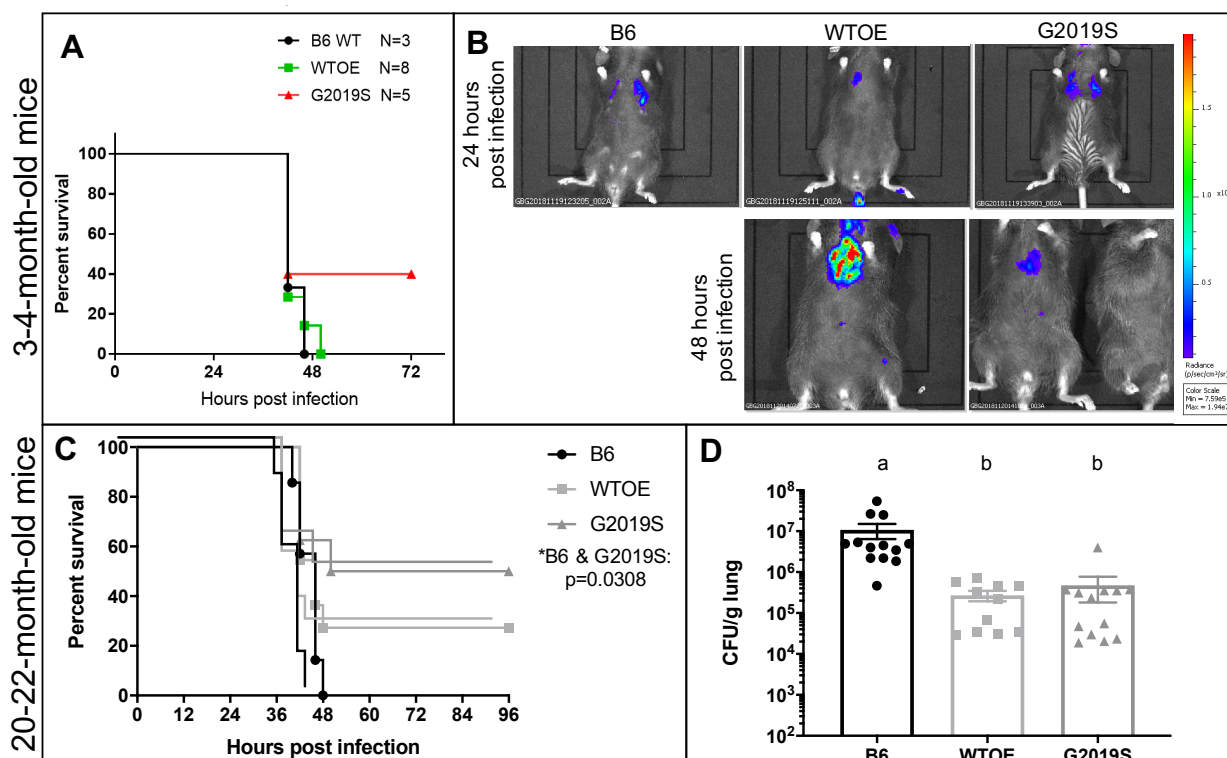


Figure 5.5: Young and aged G2019S mice are protected from sublethal *P. aeruginosa* infection. A) Survival analysis of 3-4-month old mice infected with 1.75×10^6 CFU/mouse PAO.1 lux strain of *P. aeruginosa*. Mice were monitored for up to 3-days post infection. Results are represented by Kaplan Meier survival curves. B) *In vivo* bioluminescent imaging of *P. aeruginosa* bacteria in airways with the IVIS imaging system 24- and 48-hours post infection. The intensity of the luminescent signal is indicated by the color bar with red and blue serving as high and low signals, respectively. C) Survival analysis of 20-22-month old mice infected with 4×10^6 CFU/mouse PAO.1 lux of *P. aeruginosa*. Mice were monitored for up to 3-days post infection. Results are represented by Kaplan Meier survival curves. Significant differences were calculated

by Log-rank test by comparing each group (B6 vs. G2019S, $p=0.0308$). D) Bacterial burden recovered from aged mice at 24-hours post infection. Results were analyzed by one-way ANOVA and Tukey's *post hoc* analysis for multiple comparisons. Letters above groups signify *post hoc* results. Groups sharing the same letter are not significantly different.

5.5: Discussion

In the current study, we sought to investigate the extent to which increased mouse LRRK2 protein (WTOE) or increased G2019S-mediated kinase activity (G2019S) affect immune cells and infection control in response to specific viral or bacterial infections each of which target a different arm of the immune system. Based on the literature, we hypothesized that LRRK2 kinase activity would play a role in infection burden and subsequent immune cell responses to specific infections. To evaluate LRRK2 kinase activity, we utilized G2019S BAC mice that have increased gain-of-function kinase activity, WTOE mice that have an intermediate kinase activity between B6 wildtype mice and G2019S BAC mice, and wildtype B6 with endogenous levels of mouse LRRK2. We then evaluated the effects of the selective LRRK2 kinase inhibitor PF-360 that has been shown to effectively reduce LRRK2 kinase activity without altering LRRK2 protein levels (data not shown). Surprisingly, robust immune cell phenotype changes were not observed after LCMV, influenza, or *L. monocytogenes* infections.

Influenza is known to induce massive inflammation and lung damage. In the murine model, influenza infection initiates a substantial adaptive immune response in the lung and promotes antigen presenting cell migration to the draining lymph nodes of the lung (mediastinal lymph nodes) to induce CD8 T cell activation, proliferation, and viral clearance. CD8 T cells are critical for controlling infection, thus our study focused on assessing this population in secondary lymphoid organs. Interestingly, no difference in FluNP366 tetramer specific CD8 T cells was noted in the primary site of infection in the lung. However, a reduction in the number of FluNP366 tetramer specific CD8 T cells was found in G2019S mice in the spleen and a trend was identified

in the mediastinal lymph node 10-days post infection but became significantly different 35-days post infection. This genotype difference may suggest that the immune system of G2019S mice failed to encounter and build a response to the influenza antigen or alternatively, that a less robust immune response was required to contain the virus. To further explore this, future immunophenotyping studies could examine a model in which G2019S mice are re-challenged with influenza infection or treated with an influenza vaccine.

LCMV is one of the best-studied viral infection models in rodents often employed to understand immune responses, especially for the study of antigen-specific CD8 T cells (Miller et al., 2002). Similar to influenza, a host mounts an immune response to LCMV in the form of CD8 T cells recognizing antigenic peptides from LCMV with a large memory response needed to prevent persistent infection (Bocharov, Argilaguet, & Meyerhans, 2015). In the current study, we showed that G2019S mice treated with PF-360 after inoculation of LCMV exhibited decreased body weight. Furthermore, LCMV infection was regulated in a kinase-dependent manner with kinase inhibition increasing MPECs 8-days post infection, suggesting that LRRK2 kinase inhibition aids in producing memory against LCMV.

L. monocytogenes is a gram-positive intracellular bacterium that invades the cytosol of infected cells. Antigen presenting cells internalize the bacteria into phagosomes, and toll-like receptors activate NF κ B and ensuing cytokine production (Pamer, 2004). The innate immune system is critical for response to *L. monocytogenes* as mice lacking T and B cell immunity are resistant to infection early on but unable to control it long-term (Bancroft, Schreiber, & Unanue, 1991; Nickol & Bonventre, 1977). CD8 T cells are necessary to protect against re-infection and provide a memory response (Soudja, Ruiz, Marie, & Lauvau, 2012). In our study we did not detect any differences in tetramer-specific CD8 T cells or MPECs at 8-days post infection. However, we observed a decrease in non-inflammatory monocytes in G2019S mice independent of treatment which suggests an impaired response to *L. monocytogenes* that could be further explored with longer timepoints. We did not observe any other indication of susceptibility of the LRRK2 mice in

our model of *L. monocytogenes* infection; however, this is in agreement with another study showing that LRRK2 deficiency promotes susceptibility to intestinal but not systemic *L. monocytogenes* infection (Q. Zhang et al., 2015). Therefore, future investigations could examine the differences of LRRK2-mediated kinase activity in enteric versus systemic *L. monocytogenes* infection.

P. aeruginosa is a gram-negative extracellular bacterium that can cause both acute and chronic infections, with the chronic form often complicating cystic fibrosis due to compromised pulmonary function. The current study with *P. aeruginosa* yielded some of the most interesting data suggesting that young and aged G2019S mice are protected from infection, as they survive longer and have better bacterial clearance similar to G2019S mice subjected to *S. typhimurium*, another gram-negative bacterium (Shutinoski et al., 2019). Given that study suggested this was due to G2019S-mediated kinase activity in myeloid cells, future studies should examine LRRK2 kinase inhibitors in the context of *P. aeruginosa* infection. Furthermore, effects of LRRK2 kinase activity should be explored in individual innate immune cell subsets by examining neutrophils and myeloid cells given the large innate immune system response to infection.

Collectively, the data here supports the hypothesis that LRRK2 regulates inflammation in a kinase-dependent and antigen-specific manner but warrant further investigation into specific mechanisms of regulation. Future studies with peripheral immune cells *ex vivo* collected from individuals carrying the G2019S LRRK2 mutation plus or minus PD are expected to shed light on the relevance of our findings to immune function in humans.

5.6: Acknowledgements

Influenza, LCMV, and *L. monocytogenes* infections were performed in collaboration with Paul Dunbar in the Kohlmeier and Boss labs at Emory University. *P. aeruginosa* infection studies were performed in collaboration with Dina Moustafa in the Goldberg lab at Emory University.

CHAPTER 6: DISCUSSION AND FUTURE DIRECTIONS

6.1: Summary

Extensive research has shown that Parkinson's disease (PD) is a multifactorial disease with age, genetics, and environmental factors all contributing to risk for development of PD over an individual's lifespan. The perfect combination of factors creates an environment in which peripheral and brain inflammation shift from protective to deleterious roles and promote PD pathogenesis. However, models exploring the multifaceted components of PD, especially in the context of LRRK2, one of the greatest genetic contributors to PD, in the immune system are vastly underexplored given that most PD LRRK2-related research has focused on the neuron. With the knowledge that LRRK2 is highly expressed in immune cells, the question of whether LRRK2 expression and phosphorylation regulates immune cell effector functions that then promote peripheral inflammation associated with PD and other immune diseases has now been brought to the forefront of the PD field. In the previous chapters, we described in detail the impact of increased LRRK2 protein and G2019S-mediated kinase activity on aging immune cells and in several second-hit models (colitis, pesticides, and bacterial and viral infections) implicated in PD.

6.2: Discussion of results

Over fifteen years after the identification of mutations in LRRK2 as causative for PD, most LRRK2 research has focused on the neurotoxicity of its kinase activity, especially due to its mutant form (Greggio et al., 2006; M. Liu et al., 2011; Plowey et al., 2008; Ray & Liu, 2012; A. B. West et al., 2005; Yao et al., 2010). Given the fact that inflammation plays an important role in PD pathogenesis and LRRK2 expression is much higher in immune cells relative to neurons, the importance of understanding the role of LRRK2 and its kinase activity in immune cell regulation should be underscored and is the focus of this doctoral thesis. Here, we have shown that increased wildtype LRRK2 and G2019S-mediated kinase activity do not significantly disrupt peripheral blood immune profiles as a function of age. While these results were a bit surprising,

they are consistent with the current knowledge that individuals carrying the G2019S mutation have not been reported to develop immunological abnormalities at a young age. If the G2019S mutation alone disrupted immunity, one might expect that individuals carrying this mutation would become immunocompromised and display increased susceptibility to infection. However, to date studies suggest that LRRK2 PD patients present with the same clinical features as non-LRRK2 PD patients (Aasly et al., 2005; Haugarvoll et al., 2008; O. A. Ross et al., 2006). Yet individuals of Ashkenazi-Jewish ancestry do appear to have a higher incidence of CD which is an inflammatory autoimmune condition (Kenny et al., 2012); therefore, additional immunological studies are merited and are underway within our research group to look into the possibility that individuals with the LRRK2 G2019S mutation have alterations in immune function that could predispose them to development of PD .

We have also shown a link between intestinal inflammation and PD-related phenotypes in a mouse model that overexpresses mutant G2019S LRRK2; whereby, G2019S mice exhibit increased susceptibility to intestinal inflammation and PD-associated pathology. While G2019S-mediated kinase activity increased susceptibility to colitis, we have also shown that G2019S-mediated kinase activity may be protective in some other environmental models (*Pseudomonas aeruginosa*). This is in accordance with another study suggesting a protective mechanism for LRRK2 G2019S to control infection burden (Shutinoski et al., 2019); however, the mechanism by which LRRK2 controls or contributes to inflammation is sex-, genotype-, and antigen-specific which underscores the complexity of LRRK2 signaling and function. Therefore, additional studies are merited and are underway to investigate the molecular pathways within cells that contribute to these differences.

6.3: Future directions

The data described in previous chapters further link LRRK2 in the immune system to CD and other autoimmune diseases with mutated LRRK2 increasing susceptibility to intestinal

inflammation induced by DSS and the capacity to promote PD-associated pathology. Interestingly, two of the epidemiological studies that found a positive association between IBD and incidence of PD also found that anti-TNF therapy was associated with reduced incidence of PD in IBD patients by at least 78%, further supporting the hypothesis that chronic inflammation and awry immune responses contribute to PD pathogenesis (S. Park et al., 2019; Peter et al., 2018). Furthermore, these studies have raised the interesting possibility that anti-TNF therapies used to treat IBD may be of potential therapeutic benefit to reduce risk for PD or slow its progression. However, none of these studies have examined anti-TNF therapy in the context of LRRK2. Therefore, selective inhibition of soluble TNF with XPro1595 versus inhibition of both membrane and soluble TNF with Etanercept, which is already approved for treatment of IBD, are warranted and ongoing in the LRRK2 colitis models to determine if TNF inhibition rescues G2019S phenotypes. Completion of these studies may reveal therapeutic opportunities for the use of TNF inhibitors to delay or mitigate GI inflammation to lower the risk of brain inflammation and age-related neurodegeneration.

Given the ability of LRRK2 to act as a GTPase and a protein kinase and that most pathogenic mutations identified to date localize to the kinase or GTPase domains, LRRK2 kinase inhibitors or GTP modulators have been the primary focus of therapeutic development for the PD clinic. While these functional domains are rational targets, complete LRRK2 kinase inhibition or GTPase modulation may cause deleterious effects such as those observed in on-target effects of LRRK2 kinase inhibition in the lung of non-human primates (Fuji et al., 2015). Therefore, it may be sensible to consider alternatives to inhibition of LRRK2 activity in future investigations, such as targeting LRRK2 in a cell type-specific way or some of its downstream phosphorylation substrates. In addition, other approaches that selectively knockdown LRRK2 levels in specific cells (neurons versus glia) and/or in specific compartments (brain versus peripheral immune cells) by using LRRK2 anti-sense oligonucleotides, would be helpful to advance our fundamental understanding of the biological role of LRRK2 in different tissues and cells. Our data herein

suggest that peripheral immune cells are infiltrating the brains of mice as a result of colitis-driven inflammation. Therefore, one potential question for the future is whether selective LRRK2 kinase inhibition or protein knockdown in the peripheral compartment can rescue colitis-induced phenotypes in G2019S mice; or whether a combination therapy with anti-TNF inhibition is better. As an orthogonal tool to investigate the role of peripheral immune cell infiltration into the CNS after colitis, fingolimod, a currently approved sphingosine-1 phosphate receptor modulator that keeps lymphocytes sequestered in the lymph node and out of the brain in individuals with multiple sclerosis, could be used. Furthermore, studies such as these will help determine whether interventions should be given prophylactically to reduce risk for PD later in life or shortly after the onset of non-motor symptoms to delay or prevent progression of disease and the onset of the disabling motor symptoms typically associated with later clinical stages of the disease.

While PD is commonly associated with loss of dopaminergic neurons and α -synuclein (α syn) pathology; the LRRK2 BAC transgenic mouse models used in the studies herein express endogenous mouse α syn and are therefore not suitable for assessing the effects of colitis on gut or brain α syn aggregation, propagation, or pathology. While we did observe increased α syn colonic mRNA levels, unlike human α syn, mouse α syn is not prone to misfolding or aggregation (Cookson, 2009; Volles & Lansbury, 2007); therefore, the potential pathogenic effects of increased LRRK2 protein expression and/or G2019S-mediated kinase activity coupled with colitis should be explored in mouse models with human α syn pathology. One option would be compound transgenics between LRRK2 BAC mice and human α syn transgenic mice. Another would be the use of AAV-hAsyn or injection of pre-formed fibrils (PFFs) into the gut of LRRK2 BAC mice to investigate if there is propagation from the periphery and aggregation of the injected human α syn in response to chronic inflammation induced by colitis, gut infections, pesticides, or dysbiosis. Furthermore, LRRK2 BACs could be crossed with a new DBH-hSNCA mouse line developed in our laboratory that uses the dopamine beta-hydroxylase promoter to drive wildtype human α syn

in locus coeruleus neurons, the degeneration of which is associated with the non-motor symptoms of PD (Butkovich et al., 2019).

Collectively, our data from infection studies in LRRK2 mice suggest that G2019S mice failed to encounter and build a response to a specific antigen or less of an immune response is required to contain the infection, consistent with the hypothesis that LRRK2 regulates inflammation in a protein kinase-dependent and antigen-specific manner; but further investigations into specific mechanisms of regulation are warranted. To further explore this, future studies could re-challenge the LRRK2 BAC mice, as is commonplace with humans exposed to infections multiple times throughout their lifespan. Such a study may advance our understanding of how LRRK2 and LRRK2 kinase activity affect immunologic memory. Additionally, LRRK2 transgenic mice or humans carrying LRRK2 pathogenic mutations could be evaluated pre and post vaccination to viral infections, such as seasonal influenza, to further understand the role of LRRK2 and LRRK2 kinase activity in immune cell regulation and response to antigens. Rodent models are critical pre-clinical tools and have advanced our understanding of the potential mechanisms related to PD pathogenesis; but all of these findings should be further explored in human populations using primary immune cells from peripheral blood of PD and non-PD age- and sex-matched individuals with and without LRRK2 mutations to enable cross-correlation and comparison with pre-clinical model findings. Additionally, studies to measure LRRK2 expression and kinase activity in the periphery (PBMCs and immune cells in the GI tract) in patients with PD and IBD may help establish its potential as a biomarker for these diseases.

6.4: Conclusions

LRRK2 expression is relatively high in immune cells of PD patients and our knowledge of its role in regulation of inflammation is vastly underexplored. In the studies herein, overexpression of LRRK2 expression and G2019S-mediated kinase activity were explored in aging immune cells and second-hit models (colitis, pesticides, and bacterial and viral infections) implicated in PD

pathogenesis. Taken together, the results suggest that increased LRRK2 protein or LRRK2 G2019S do not affect aging immunophenotypes, but G2019S-mediated kinase activity may be protective in some environmental models (*Pseudomonas aeruginosa*) while in others (colitis) it is deleterious and increases susceptibility to PD-associated pathology. The exact mechanism by which LRRK2 G2019S confers protection or susceptibility remains unknown and may turn out to be stimulus specific. Future efforts to enhance our understanding of the complexity of LRRK2 signaling and function in immune cells will provide key insights into PD pathogenesis and progression. The long-term goal of the studies undertaken here and those planned for the future will shed light on the relationship between PD and autoimmune IBD disorders and may reveal therapeutic opportunities for the use of LRRK2 kinase inhibitors to delay or mitigate peripheral inflammation to lower the risk of brain inflammation and age-related neurodegeneration.

REFERENCES

- Aasly, J. O., Toft, M., Fernandez-Mata, I., Kachergus, J., Hulihan, M., White, L. R., & Farrer, M. (2005). Clinical features of LRRK2-associated Parkinson's disease in central Norway. *Ann Neurol*, *57*(5), 762-765. doi:10.1002/ana.20456
- Abbott, R. D., Petrovitch, H., White, L. R., Masaki, K. H., Tanner, C. M., Curb, J. D., . . . Ross, G. W. (2001). Frequency of bowel movements and the future risk of Parkinson's disease. *Neurology*, *57*(3), 456-462. doi:10.1212/wnl.57.3.456
- Abbott, R. D., Ross, G. W., White, L. R., Sanderson, W. T., Burchfiel, C. M., Kashon, M., . . . Petrovitch, H. (2003). Environmental, life-style, and physical precursors of clinical Parkinson's disease: recent findings from the Honolulu-Asia Aging Study. *J Neurol*, *250* Suppl 3, III30-39. doi:10.1007/s00415-003-1306-7
- Absinta, M., Ha, S. K., Nair, G., Sati, P., Luciano, N. J., Palisoc, M., . . . Reich, D. S. (2017). Human and nonhuman primate meninges harbor lymphatic vessels that can be visualized noninvasively by MRI. *Elife*, *6*. doi:10.7554/eLife.29738
- Andres-Mateos, E., Mejias, R., Sasaki, M., Li, X., Lin, B. M., Biskup, S., . . . Dawson, V. L. (2009). Unexpected lack of hypersensitivity in LRRK2 knock-out mice to MPTP (1-methyl-4-phenyl-1,2,3,6-tetrahydropyridine). *J Neurosci*, *29*(50), 15846-15850. doi:10.1523/JNEUROSCI.4357-09.2009
- Antoniou, N., Vlachakis, D., Memou, A., Leandrou, E., Valkimadi, P. E., Melachroinou, K., . . . Rideout, H. J. (2018). A motif within the armadillo repeat of Parkinson's-linked LRRK2 interacts with FADD to hijack the extrinsic death pathway. *Sci Rep*, *8*(1), 3455. doi:10.1038/s41598-018-21931-8
- Arbez, N., He, X., Huang, Y., Ren, M., Liang, Y., Nucifora, F. C., . . . Ross, C. A. (2019). G2019S-LRRK2 mutation enhances MPTP-linked Parkinsonism in mice. *Hum Mol Genet*. doi:10.1093/hmg/ddz271
- Asanuma, M., Nishibayashi-Asanuma, S., Miyazaki, I., Kohno, M., & Ogawa, N. (2001). Neuroprotective effects of non-steroidal anti-inflammatory drugs by direct scavenging of nitric oxide radicals. *J Neurochem*, *76*(6), 1895-1904. doi:10.1046/j.1471-4159.2001.00205.x
- Ascherio, A., Chen, H., Weisskopf, M. G., O'Reilly, E., McCullough, M. L., Calle, E. E., . . . Thun, M. J. (2006). Pesticide exposure and risk for Parkinson's disease. *Ann Neurol*, *60*(2), 197-203. doi:10.1002/ana.20904
- Aspelund, A., Antila, S., Proulx, S. T., Karlsen, T. V., Karaman, S., Detmar, M., . . . Alitalo, K. (2015). A dural lymphatic vascular system that drains brain interstitial fluid and macromolecules. *J Exp Med*, *212*(7), 991-999. doi:10.1084/jem.20142290
- Atashrazm, F., Hammond, D., Perera, G., Bolliger, M. F., Matar, E., Halliday, G. M., . . . Dzamko, N. (2019). LRRK2-mediated Rab10 phosphorylation in immune cells from Parkinson's disease patients. *Mov Disord*, *34*(3), 406-415. doi:10.1002/mds.27601
- Aubin, N., Curet, O., Deffois, A., & Carter, C. (1998). Aspirin and salicylate protect against MPTP-induced dopamine depletion in mice. *J Neurochem*, *71*(4), 1635-1642. doi:10.1046/j.1471-4159.1998.71041635.x
- Azmi, M. A., Naqvi, S. N., Akhtar, K., Moinuddin, Parveen, S., Parveen, R., & Aslam, M. (2009). Effect of pesticide residues on health and blood parameters of farm workers from rural Gadap, Karachi, Pakistan. *J Environ Biol*, *30*(5), 747-756. Retrieved from <https://www.ncbi.nlm.nih.gov/pubmed/20136060>
- Baba, Y., Kuroiwa, A., Uitti, R. J., Wszolek, Z. K., & Yamada, T. (2005). Alterations of T-lymphocyte populations in Parkinson disease. *Parkinsonism Relat Disord*, *11*(8), 493-498. doi:10.1016/j.parkreldis.2005.07.005

- Ballard, P. A., Tetrud, J. W., & Langston, J. W. (1985). Permanent human parkinsonism due to 1-methyl-4-phenyl-1,2,3,6-tetrahydropyridine (MPTP): seven cases. *Neurology*, *35*(7), 949-956. doi:10.1212/wnl.35.7.949
- Banati, R. B. (2002). Visualising microglial activation in vivo. *Glia*, *40*(2), 206-217. doi:10.1002/glia.10144
- Bancroft, G. J., Schreiber, R. D., & Unanue, E. R. (1991). Natural immunity: a T-cell-independent pathway of macrophage activation, defined in the scid mouse. *Immunol Rev*, *124*, 5-24. doi:10.1111/j.1600-065x.1991.tb00613.x
- Baptista, M. A., Dave, K. D., Frasier, M. A., Sherer, T. B., Greeley, M., Beck, M. J., . . . Fiske, B. K. (2013). Loss of leucine-rich repeat kinase 2 (LRRK2) in rats leads to progressive abnormal phenotypes in peripheral organs. *PLoS One*, *8*(11), e80705. doi:10.1371/journal.pone.0080705
- Barker, C. F., & Billingham, R. E. (1977). Immunologically privileged sites. *Adv Immunol*, *25*, 1-54. Retrieved from <https://www.ncbi.nlm.nih.gov/pubmed/345773>
- Barrett, J. C., Hansoul, S., Nicolae, D. L., Cho, J. H., Duerr, R. H., Rioux, J. D., . . . Daly, M. J. (2008). Genome-wide association defines more than 30 distinct susceptibility loci for Crohn's disease. *Nat Genet*, *40*(8), 955-962. doi:10.1038/ng.175
- Barrio, J. R., Huang, S. C., Melega, W. P., Yu, D. C., Hoffman, J. M., Schneider, J. S., . . . Phelps, M. E. (1990). 6-[¹⁸F]fluoro-L-dopa probes dopamine turnover rates in central dopaminergic structures. *J Neurosci Res*, *27*(4), 487-493. doi:10.1002/jnr.490270408
- Bartels, A. L., Willemsen, A. T., Doorduyn, J., de Vries, E. F., Dierckx, R. A., & Leenders, K. L. (2010). [¹¹C]-PK11195 PET: quantification of neuroinflammation and a monitor of anti-inflammatory treatment in Parkinson's disease? *Parkinsonism Relat Disord*, *16*(1), 57-59. doi:10.1016/j.parkreldis.2009.05.005
- Bas, J., Calopa, M., Mestre, M., Mollevi, D. G., Cutillas, B., Ambrosio, S., & Buendia, E. (2001). Lymphocyte populations in Parkinson's disease and in rat models of parkinsonism. *J Neuroimmunol*, *113*(1), 146-152. doi:10.1016/s0165-5728(00)00422-7
- Beach, T. G., Adler, C. H., Sue, L. I., Vedders, L., Lue, L., White lli, C. L., . . . Arizona Parkinson's Disease, C. (2010). Multi-organ distribution of phosphorylated alpha-synuclein histopathology in subjects with Lewy body disorders. *Acta Neuropathol*, *119*(6), 689-702. doi:10.1007/s00401-010-0664-3
- Beccano-Kelly, D. A., Volta, M., Munsie, L. N., Paschall, S. A., Tatarnikov, I., Co, K., . . . Milnerwood, A. J. (2015). LRRK2 overexpression alters glutamatergic presynaptic plasticity, striatal dopamine tone, postsynaptic signal transduction, motor activity and memory. *Hum Mol Genet*, *24*(5), 1336-1349. doi:10.1093/hmg/ddu543
- Bennett, D. A., Beckett, L. A., Murray, A. M., Shannon, K. M., Goetz, C. G., Pilgrim, D. M., & Evans, D. A. (1996). Prevalence of parkinsonian signs and associated mortality in a community population of older people. *N Engl J Med*, *334*(2), 71-76. doi:10.1056/NEJM199601113340202
- Berger, Z., Smith, K. A., & Lavoie, M. J. (2010). Membrane localization of LRRK2 is associated with increased formation of the highly active LRRK2 dimer and changes in its phosphorylation. *Biochemistry*, *49*(26), 5511-5523. doi:10.1021/bi100157u
- Berwick, D. C., & Harvey, K. (2012). LRRK2 functions as a Wnt signaling scaffold, bridging cytosolic proteins and membrane-localized LRP6. *Hum Mol Genet*, *21*(22), 4966-4979. doi:10.1093/hmg/dds342
- Bialecka, M., Klodowska-Duda, G., Kurzawski, M., Slawek, J., Gorzkowska, A., Opala, G., . . . Drozdik, M. (2008). Interleukin-10 (IL10) and tumor necrosis factor alpha (TNF) gene polymorphisms in Parkinson's disease patients. *Parkinsonism Relat Disord*, *14*(8), 636-640. doi:10.1016/j.parkreldis.2008.02.001

- Bieri, G., Brahic, M., Bousset, L., Couthouis, J., Kramer, N. J., Ma, R., . . . Gitler, A. D. (2019). LRRK2 modifies alpha-syn pathology and spread in mouse models and human neurons. *Acta Neuropathol*, *137*(6), 961-980. doi:10.1007/s00401-019-01995-0
- Bischoff, S. C., Barbara, G., Buurman, W., Ockhuizen, T., Schulzke, J. D., Serino, M., . . . Wells, J. M. (2014). Intestinal permeability--a new target for disease prevention and therapy. *BMC Gastroenterol*, *14*, 189. doi:10.1186/s12876-014-0189-7
- Biskup, S., & West, A. B. (2009). Zeroing in on LRRK2-linked pathogenic mechanisms in Parkinson's disease. *Biochim Biophys Acta*, *1792*(7), 625-633. doi:10.1016/j.bbadis.2008.09.015
- Biswas, A., Petnicki-Ocwieja, T., & Kobayashi, K. S. (2012). Nod2: a key regulator linking microbiota to intestinal mucosal immunity. *J Mol Med (Berl)*, *90*(1), 15-24. doi:10.1007/s00109-011-0802-y
- Blanca Ramirez, M., Lara Ordonez, A. J., Fdez, E., Madero-Perez, J., Gonnelli, A., Drouyer, M., . . . Hilfiker, S. (2017). GTP binding regulates cellular localization of Parkinson's disease-associated LRRK2. *Hum Mol Genet*, *26*(14), 2747-2767. doi:10.1093/hmg/ddx161
- Blauwendraat, C., Nalls, M. A., & Singleton, A. B. (2020). The genetic architecture of Parkinson's disease. *Lancet Neurol*, *19*(2), 170-178. doi:10.1016/S1474-4422(19)30287-X
- Bliederhaeuser, C., Zondler, L., Grozdanov, V., Ruf, W. P., Brenner, D., Melrose, H. L., . . . Danzer, K. M. (2016). LRRK2 contributes to monocyte dysregulation in Parkinson's disease. *Acta Neuropathol Commun*, *4*(1), 123. doi:10.1186/s40478-016-0396-2
- Blum-Degen, D., Muller, T., Kuhn, W., Gerlach, M., Przuntek, H., & Riederer, P. (1995). Interleukin-1 beta and interleukin-6 are elevated in the cerebrospinal fluid of Alzheimer's and de novo Parkinson's disease patients. *Neurosci Lett*, *202*(1-2), 17-20. doi:10.1016/0304-3940(95)12192-7
- Bocharov, G., Argilaguet, J., & Meyerhans, A. (2015). Understanding Experimental LCMV Infection of Mice: The Role of Mathematical Models. *J Immunol Res*, *2015*, 739706. doi:10.1155/2015/739706
- Bonet-Ponce, L., & Cookson, M. R. (2019). The role of Rab GTPases in the pathobiology of Parkinson' disease. *Curr Opin Cell Biol*, *59*, 73-80. doi:10.1016/j.ceb.2019.03.009
- Bongioanni, P., Castagna, M., Maltinti, S., Boccardi, B., & Dadone, F. (1997). T-lymphocyte tumor necrosis factor-alpha receptor binding in patients with Parkinson's disease. *J Neurol Sci*, *149*(1), 41-45. doi:10.1016/s0022-510x(97)05382-3
- Bottner, M., Zorenkov, D., Hellwig, I., Barrenschee, M., Harde, J., Fricke, T., . . . Wedel, T. (2012). Expression pattern and localization of alpha-synuclein in the human enteric nervous system. *Neurobiol Dis*, *48*(3), 474-480. doi:10.1016/j.nbd.2012.07.018
- Bower, J. H., Maraganore, D. M., Peterson, B. J., Ahlskog, J. E., & Rocca, W. A. (2006). Immunologic diseases, anti-inflammatory drugs, and Parkinson disease: a case-control study. *Neurology*, *67*(3), 494-496. doi:10.1212/01.wnl.0000227906.99570.cc
- Braak, H., de Vos, R. A., Bohl, J., & Del Tredici, K. (2006). Gastric alpha-synuclein immunoreactive inclusions in Meissner's and Auerbach's plexuses in cases staged for Parkinson's disease-related brain pathology. *Neurosci Lett*, *396*(1), 67-72. doi:10.1016/j.neulet.2005.11.012
- Braak, H., Del Tredici, K., Rub, U., de Vos, R. A., Jansen Steur, E. N., & Braak, E. (2003). Staging of brain pathology related to sporadic Parkinson's disease. *Neurobiol Aging*, *24*(2), 197-211. doi:10.1016/s0197-4580(02)00065-9
- Brochard, V., Combadiere, B., Prigent, A., Laouar, Y., Perrin, A., Beray-Berthet, V., . . . Hunot, S. (2009). Infiltration of CD4+ lymphocytes into the brain contributes to neurodegeneration in a mouse model of Parkinson disease. *J Clin Invest*, *119*(1), 182-192. doi:10.1172/JCI36470
- Brodacki, B., Staszewski, J., Toczylowska, B., Kozłowska, E., Drela, N., Chalimoniuk, M., & Stepien, A. (2008). Serum interleukin (IL-2, IL-10, IL-6, IL-4), TNFalpha, and INFgamma

- concentrations are elevated in patients with atypical and idiopathic parkinsonism. *Neurosci Lett*, 441(2), 158-162. doi:10.1016/j.neulet.2008.06.040
- Brugger, F., Erro, R., Balint, B., Kagi, G., Barone, P., & Bhatia, K. P. (2015). Why is there motor deterioration in Parkinson's disease during systemic infections-a hypothetical view. *NPJ Parkinsons Dis*, 1, 15014. doi:10.1038/npjparkd.2015.14
- Bruunsgaard, H., Ladelund, S., Pedersen, A. N., Schroll, M., Jorgensen, T., & Pedersen, B. K. (2003). Predicting death from tumour necrosis factor-alpha and interleukin-6 in 80-year-old people. *Clin Exp Immunol*, 132(1), 24-31. doi:10.1046/j.1365-2249.2003.02137.x
- Butkovich, L., Houser, M., Chalermphanupap, T., Porter-Stransky, K., Eidson, L., De Sousa Rodrigues, M., . . . Tansey, M. (2019). Transgenic mice expressing human alpha-synuclein in noradrenergic neurons develop locus coeruleus pathology and non-motor features of Parkinson's disease. *bioRxiv*, 857987. doi:10.1101/857987
- Caesar, M., Zach, S., Carlson, C. B., Brockmann, K., Gasser, T., & Gillardon, F. (2013). Leucine-rich repeat kinase 2 functionally interacts with microtubules and kinase-dependently modulates cell migration. *Neurobiol Dis*, 54, 280-288. doi:10.1016/j.nbd.2012.12.019
- Caggiu, E., Paulus, K., Arru, G., Piredda, R., Sechi, G. P., & Sechi, L. A. (2016). Humoral cross reactivity between alpha-synuclein and herpes simplex-1 epitope in Parkinson's disease, a triggering role in the disease? *J Neuroimmunol*, 291, 110-114. doi:10.1016/j.jneuroim.2016.01.007
- Camacho-Soto, A., Searles Nielsen, S., & Racette, B. A. (2018). Inflammatory bowel disease and risk of Parkinson's disease in medicare beneficiaries. *Parkinsonism Relat Disord*, 57, 77. doi:10.1016/j.parkreldis.2018.06.028
- Cario, E. (2005). Bacterial interactions with cells of the intestinal mucosa: Toll-like receptors and NOD2. *Gut*, 54(8), 1182-1193. doi:10.1136/gut.2004.062794
- Cario, E., & Podolsky, D. K. (2000). Differential alteration in intestinal epithelial cell expression of toll-like receptor 3 (TLR3) and TLR4 in inflammatory bowel disease. *Infect Immun*, 68(12), 7010-7017. doi:10.1128/iai.68.12.7010-7017.2000
- Carlsson, A., & Winblad, B. (1976). Influence of age and time interval between death and autopsy on dopamine and 3-methoxytyramine levels in human basal ganglia. *J Neural Transm*, 38(3-4), 271-276. doi:10.1007/bf01249444
- Carson, M. J., Doose, J. M., Melchior, B., Schmid, C. D., & Ploix, C. C. (2006). CNS immune privilege: hiding in plain sight. *Immunol Rev*, 213, 48-65. doi:10.1111/j.1600-065X.2006.00441.x
- Carvey, P. M., McRae, A., Lint, T. F., Ptak, L. R., Lo, E. S., Goetz, C. G., & Klawans, H. L. (1991). The potential use of a dopamine neuron antibody and a striatal-derived neurotrophic factor as diagnostic markers in Parkinson's disease. *Neurology*, 41(5 Suppl 2), 53-58; discussion 59-60. doi:10.1212/wnl.41.5_suppl_2.53
- Casper, D., Yaparpalvi, U., Rempel, N., & Werner, P. (2000). Ibuprofen protects dopaminergic neurons against glutamate toxicity in vitro. *Neurosci Lett*, 289(3), 201-204. doi:10.1016/s0304-3940(00)01294-5
- Caudle, W. M., Richardson, J. R., Wang, M. Z., Taylor, T. N., Guillot, T. S., McCormack, A. L., . . . Miller, G. W. (2007). Reduced vesicular storage of dopamine causes progressive nigrostriatal neurodegeneration. *J Neurosci*, 27(30), 8138-8148. doi:10.1523/JNEUROSCI.0319-07.2007
- Chang, C. C., Lin, T. M., Chang, Y. S., Chen, W. S., Sheu, J. J., Chen, Y. H., & Chen, J. H. (2018). Autoimmune rheumatic diseases and the risk of Parkinson disease: a nationwide population-based cohort study in Taiwan. *Ann Med*, 50(1), 83-90. doi:10.1080/07853890.2017.1412088
- Chang, D., Nalls, M. A., Hallgrimsdottir, I. B., Hunkapiller, J., van der Brug, M., Cai, F., . . . Graham, R. R. (2017). A meta-analysis of genome-wide association studies identifies 17 new Parkinson's disease risk loci. *Nat Genet*, 49(10), 1511-1516. doi:10.1038/ng.3955

- Chassaing, B., Aitken, J. D., Malleshappa, M., & Vijay-Kumar, M. (2014). Dextran sulfate sodium (DSS)-induced colitis in mice. *Curr Protoc Immunol*, 104, 15 25 11-15 25 14. doi:10.1002/0471142735.im1525s104
- Chen, C. Y., Weng, Y. H., Chien, K. Y., Lin, K. J., Yeh, T. H., Cheng, Y. P., . . . Wang, H. L. (2012). (G2019S) LRRK2 activates MKK4-JNK pathway and causes degeneration of SN dopaminergic neurons in a transgenic mouse model of PD. *Cell Death Differ*, 19(10), 1623-1633. doi:10.1038/cdd.2012.42
- Chen, H., Jacobs, E., Schwarzschild, M. A., McCullough, M. L., Calle, E. E., Thun, M. J., & Ascherio, A. (2005). Nonsteroidal antiinflammatory drug use and the risk for Parkinson's disease. *Ann Neurol*, 58(6), 963-967. doi:10.1002/ana.20682
- Chen, H., Zhang, S. M., Hernan, M. A., Schwarzschild, M. A., Willett, W. C., Colditz, G. A., . . . Ascherio, A. (2003). Nonsteroidal anti-inflammatory drugs and the risk of Parkinson disease. *Arch Neurol*, 60(8), 1059-1064. doi:10.1001/archneur.60.8.1059
- Chen, H., Zhao, E. J., Zhang, W., Lu, Y., Liu, R., Huang, X., . . . Peddada, S. (2015). Meta-analyses on prevalence of selected Parkinson's nonmotor symptoms before and after diagnosis. *Transl Neurodegener*, 4(1), 1. doi:10.1186/2047-9158-4-1
- Chen, J., Su, P., Luo, W., & Chen, J. (2018). Role of LRRK2 in manganese-induced neuroinflammation and microglial autophagy. *Biochem Biophys Res Commun*, 498(1), 171-177. doi:10.1016/j.bbrc.2018.02.007
- Cheroutre, H. (2006). In IBD eight can come before four. *Gastroenterology*, 131(2), 667-670. doi:10.1053/j.gastro.2006.06.041
- Cherra, S. J., 3rd, Steer, E., Gusdon, A. M., Kiselyov, K., & Chu, C. T. (2013). Mutant LRRK2 elicits calcium imbalance and depletion of dendritic mitochondria in neurons. *Am J Pathol*, 182(2), 474-484. doi:10.1016/j.ajpath.2012.10.027
- Chiba, S., Matsumoto, H., Saitoh, M., Kasahara, M., Matsuya, M., & Kashiwagi, M. (1995). A correlation study between serum adenosine deaminase activities and peripheral lymphocyte subsets in Parkinson's disease. *J Neurol Sci*, 132(2), 170-173. doi:10.1016/0022-510x(95)00136-p
- Choi, H., Moon, J. K., Liu, K. H., Park, H. W., Ihm, Y. B., Park, B. S., & Kim, J. H. (2006). Risk assessment of human exposure to cypermethrin during treatment of mandarin fields. *Arch Environ Contam Toxicol*, 50(3), 437-442. doi:10.1007/s00244-005-1050-3
- Choi, I., Kim, B., Byun, J. W., Baik, S. H., Huh, Y. H., Kim, J. H., . . . Joe, E. H. (2015). LRRK2 G2019S mutation attenuates microglial motility by inhibiting focal adhesion kinase. *Nat Commun*, 6, 8255. doi:10.1038/ncomms9255
- Choi, J. G., Kim, N., Ju, I. G., Eo, H., Lim, S. M., Jang, S. E., . . . Oh, M. S. (2018). Oral administration of *Proteus mirabilis* damages dopaminergic neurons and motor functions in mice. *Sci Rep*, 8(1), 1275. doi:10.1038/s41598-018-19646-x
- Chou, J. S., Chen, C. Y., Chen, Y. L., Weng, Y. H., Yeh, T. H., Lu, C. S., . . . Wang, H. L. (2014). (G2019S) LRRK2 causes early-phase dysfunction of SNpc dopaminergic neurons and impairment of corticostriatal long-term depression in the PD transgenic mouse. *Neurobiol Dis*, 68, 190-199. doi:10.1016/j.nbd.2014.04.021
- Chu, K., Zhou, X., & Luo, B. Y. (2012). Cytokine gene polymorphisms and Parkinson's disease: a meta-analysis. *Can J Neurol Sci*, 39(1), 58-64. doi:10.1017/s0317167100012695
- Collier, T. J., Kanaan, N. M., & Kordower, J. H. (2011). Ageing as a primary risk factor for Parkinson's disease: evidence from studies of non-human primates. *Nat Rev Neurosci*, 12(6), 359-366. doi:10.1038/nrn3039
- Cook, D. A., Kannarkat, G. T., Cintron, A. F., Butkovich, L. M., Fraser, K. B., Chang, J., . . . Tansey, M. G. (2017). LRRK2 levels in immune cells are increased in Parkinson's disease. *NPJ Parkinsons Dis*, 3, 11. doi:10.1038/s41531-017-0010-8
- Cookson, M. R. (2009). alpha-Synuclein and neuronal cell death. *Mol Neurodegener*, 4, 9. doi:10.1186/1750-1326-4-9

- Cooper, O., Seo, H., Andrabi, S., Guardia-Laguarta, C., Graziotto, J., Sundberg, M., . . . Isacson, O. (2012). Pharmacological rescue of mitochondrial deficits in iPSC-derived neural cells from patients with familial Parkinson's disease. *Sci Transl Med*, 4(141), 141ra190. doi:10.1126/scitranslmed.3003985
- Couper, K. N., Blount, D. G., & Riley, E. M. (2008). IL-10: the master regulator of immunity to infection. *J Immunol*, 180(9), 5771-5777. doi:10.4049/jimmunol.180.9.5771
- Cruz-Sanchez, F. F., Cardozo, A., & Tolosa, E. (1995). Neuronal changes in the substantia nigra with aging: a Golgi study. *J Neuropathol Exp Neurol*, 54(1), 74-81. doi:10.1097/00005072-199501000-00009
- Daher, J. P., Volpicelli-Daley, L. A., Blackburn, J. P., Moehle, M. S., & West, A. B. (2014). Abrogation of alpha-synuclein-mediated dopaminergic neurodegeneration in LRRK2-deficient rats. *Proc Natl Acad Sci U S A*, 111(25), 9289-9294. doi:10.1073/pnas.1403215111
- Daig, R., Andus, T., Aschenbrenner, E., Falk, W., Scholmerich, J., & Gross, V. (1996). Increased interleukin 8 expression in the colon mucosa of patients with inflammatory bowel disease. *Gut*, 38(2), 216-222. doi:10.1136/gut.38.2.216
- de Lau, L. M., & Breteler, M. M. (2006). Epidemiology of Parkinson's disease. *Lancet Neurol*, 5(6), 525-535. doi:10.1016/S1474-4422(06)70471-9
- de Sousa Rodrigues, M. E., Bekhbat, M., Houser, M. C., Chang, J., Walker, D. I., Jones, D. P., . . . Tansey, M. G. (2017). Chronic psychological stress and high-fat high-fructose diet disrupt metabolic and inflammatory gene networks in the brain, liver, and gut and promote behavioral deficits in mice. *Brain Behav Immun*, 59, 158-172. doi:10.1016/j.bbi.2016.08.021
- De Wit, T., Baekelandt, V., & Lobbestael, E. (2018). LRRK2 Phosphorylation: Behind the Scenes. *Neuroscientist*, 24(5), 486-500. doi:10.1177/1073858418756309
- Dehay, B., Martinez-Vicente, M., Ramirez, A., Perier, C., Klein, C., Vila, M., & Bezdard, E. (2012). Lysosomal dysfunction in Parkinson disease: ATP13A2 gets into the groove. *Autophagy*, 8(9), 1389-1391. doi:10.4161/auto.21011
- Devos, D., Lebouvier, T., Lardeux, B., Biraud, M., Rouaud, T., Pouclet, H., . . . Derkinderen, P. (2013). Colonic inflammation in Parkinson's disease. *Neurobiol Dis*, 50, 42-48. doi:10.1016/j.nbd.2012.09.007
- Dhekne, H. S., Yanatori, I., Gomez, R. C., Tonelli, F., Diez, F., Schule, B., . . . Pfeffer, S. R. (2018). A pathway for Parkinson's Disease LRRK2 kinase to block primary cilia and Sonic hedgehog signaling in the brain. *Elife*, 7. doi:10.7554/eLife.40202
- Di Maio, R., Hoffman, E. K., Rocha, E. M., Keeney, M. T., Sanders, L. H., De Miranda, B. R., . . . Greenamyre, J. T. (2018). LRRK2 activation in idiopathic Parkinson's disease. *Sci Transl Med*, 10(451). doi:10.1126/scitranslmed.aar5429
- Dinter, E., Saridaki, T., Nippold, M., Plum, S., Diederichs, L., Komnig, D., . . . Falkenburger, B. H. (2016). Rab7 induces clearance of alpha-synuclein aggregates. *J Neurochem*, 138(5), 758-774. doi:10.1111/jnc.13712
- Do, J., & Woo, J. (2018). From Gut to Brain: Alteration in Inflammation Markers in the Brain of Dextran Sodium Sulfate-induced Colitis Model Mice. *Clin Psychopharmacol Neurosci*, 16(4), 422-433. doi:10.9758/cpn.2018.16.4.422
- Dorsey, E. R., & Bloem, B. R. (2018). The Parkinson Pandemic-A Call to Action. *JAMA Neurol*, 75(1), 9-10. doi:10.1001/jamaneurol.2017.3299
- Double, K. L., Rowe, D. B., Carew-Jones, F. M., Hayes, M., Chan, D. K., Blackie, J., . . . Halliday, G. M. (2009). Anti-melanin antibodies are increased in sera in Parkinson's disease. *Exp Neurol*, 217(2), 297-301. doi:10.1016/j.expneurol.2009.03.002
- Duerr, R. H., Taylor, K. D., Brant, S. R., Rioux, J. D., Silverberg, M. S., Daly, M. J., . . . Cho, J. H. (2006). A genome-wide association study identifies IL23R as an inflammatory bowel disease gene. *Science*, 314(5804), 1461-1463. doi:10.1126/science.1135245

- Dunbar, P. R., Cartwright, E. K., Wein, A. N., Tsukamoto, T., Tiger Li, Z. R., Kumar, N., . . . Kohlmeier, J. E. (2020). Pulmonary monocytes interact with effector T cells in the lung tissue to drive TRM differentiation following viral infection. *Mucosal Immunol*, *13*(1), 161-171. doi:10.1038/s41385-019-0224-7
- Dusonchet, J., Kochubey, O., Stafa, K., Young, S. M., Jr., Zufferey, R., Moore, D. J., . . . Aebischer, P. (2011). A rat model of progressive nigral neurodegeneration induced by the Parkinson's disease-associated G2019S mutation in LRRK2. *J Neurosci*, *31*(3), 907-912. doi:10.1523/JNEUROSCI.5092-10.2011
- Dzamko, N., Deak, M., Hentati, F., Reith, A. D., Prescott, A. R., Alessi, D. R., & Nichols, R. J. (2010). Inhibition of LRRK2 kinase activity leads to dephosphorylation of Ser(910)/Ser(935), disruption of 14-3-3 binding and altered cytoplasmic localization. *Biochem J*, *430*(3), 405-413. doi:10.1042/BJ20100784
- Dzamko, N., Rowe, D. B., & Halliday, G. M. (2016). Increased peripheral inflammation in asymptomatic leucine-rich repeat kinase 2 mutation carriers. *Mov Disord*, *31*(6), 889-897. doi:10.1002/mds.26529
- Eadsforth, C. V., & Baldwin, M. K. (1983). Human dose-excretion studies with the pyrethroid insecticide, cypermethrin. *Xenobiotica*, *13*(2), 67-72. doi:10.3109/00498258309052238
- Edwards, L. L., Pfeiffer, R. F., Quigley, E. M., Hofman, R., & Balluff, M. (1991). Gastrointestinal symptoms in Parkinson's disease. *Mov Disord*, *6*(2), 151-156. doi:10.1002/mds.870060211
- Eguchi, T., Kuwahara, T., Sakurai, M., Komori, T., Fujimoto, T., Ito, G., . . . Iwatsubo, T. (2018). LRRK2 and its substrate Rab GTPases are sequentially targeted onto stressed lysosomes and maintain their homeostasis. *Proc Natl Acad Sci U S A*, *115*(39), E9115-E9124. doi:10.1073/pnas.1812196115
- Eichele, D. D., & Kharbanda, K. K. (2017). Dextran sodium sulfate colitis murine model: An indispensable tool for advancing our understanding of inflammatory bowel diseases pathogenesis. *World J Gastroenterol*, *23*(33), 6016-6029. doi:10.3748/wjg.v23.i33.6016
- Eidson, L. N., Kannarkat, G. T., Barnum, C. J., Chang, J., Chung, J., Caspell-Garcia, C., . . . Tansey, M. G. (2017). Candidate inflammatory biomarkers display unique relationships with alpha-synuclein and correlate with measures of disease severity in subjects with Parkinson's disease. *J Neuroinflammation*, *14*(1), 164. doi:10.1186/s12974-017-0935-1
- Engelhardt, B., & Ransohoff, R. M. (2012). Capture, crawl, cross: the T cell code to breach the blood-brain barriers. *Trends Immunol*, *33*(12), 579-589. doi:10.1016/j.it.2012.07.004
- Erben, U., Loddenkemper, C., Doerfel, K., Spieckermann, S., Haller, D., Heimesaat, M. M., . . . Kuhl, A. A. (2014). A guide to histomorphological evaluation of intestinal inflammation in mouse models. *Int J Clin Exp Pathol*, *7*(8), 4557-4576. Retrieved from <https://www.ncbi.nlm.nih.gov/pubmed/25197329>
- Ertan, S., Fresko, I., Apaydin, H., Ozekmekci, S., & Yazici, H. (1999). Extraparalytic rigidity in rheumatoid arthritis. *Rheumatology (Oxford)*, *38*(7), 627-630. doi:10.1093/rheumatology/38.7.627
- Fahn, S. (2003). Description of Parkinson's disease as a clinical syndrome. *Ann N Y Acad Sci*, *991*, 1-14. doi:10.1111/j.1749-6632.2003.tb07458.x
- Fan, Y., Howden, A. J. M., Sarhan, A. R., Lis, P., Ito, G., Martinez, T. N., . . . Sammler, E. M. (2018). Interrogating Parkinson's disease LRRK2 kinase pathway activity by assessing Rab10 phosphorylation in human neutrophils. *Biochem J*, *475*(1), 23-44. doi:10.1042/BCJ20170803
- Farrer, M. J., Stone, J. T., Lin, C. H., Dachsel, J. C., Hulihan, M. M., Haugarvoll, K., . . . Wu, R. M. (2007). Lrrk2 G2385R is an ancestral risk factor for Parkinson's disease in Asia. *Parkinsonism Relat Disord*, *13*(2), 89-92. doi:10.1016/j.parkreldis.2006.12.001
- Fava, V. M., Manry, J., Cobat, A., Orlova, M., Van Thuc, N., Ba, N. N., . . . Canadian Lrrk2 in Inflammation, T. (2016). A Missense LRRK2 Variant Is a Risk Factor for Excessive

- Inflammatory Responses in Leprosy. *PLoS Negl Trop Dis*, 10(2), e0004412. doi:10.1371/journal.pntd.0004412
- Fava, V. M., Xu, Y. Z., Lettre, G., Van Thuc, N., Orlova, M., Thai, V. H., . . . Schurr, E. (2019). Pleiotropic effects for Parkin and LRRK2 in leprosy type-1 reactions and Parkinson's disease. *Proc Natl Acad Sci U S A*, 116(31), 15616-15624. doi:10.1073/pnas.1901805116
- Fei, Q., McCormack, A. L., Di Monte, D. A., & Ethell, D. W. (2008). Paraquat neurotoxicity is mediated by a Bak-dependent mechanism. *J Biol Chem*, 283(6), 3357-3364. doi:10.1074/jbc.M708451200
- Ferger, B., Teismann, P., Earl, C. D., Kuschinsky, K., & Oertel, W. H. (1999). Salicylate protects against MPTP-induced impairments in dopaminergic neurotransmission at the striatal and nigral level in mice. *Naunyn Schmiedebergs Arch Pharmacol*, 360(3), 256-261. doi:10.1007/s002109900079
- Finch, C. E. (1993). Neuron atrophy during aging: programmed or sporadic? *Trends Neurosci*, 16(3), 104-110. doi:10.1016/0166-2236(93)90134-8
- Fiszer, U., Mix, E., Fredrikson, S., Kostulas, V., & Link, H. (1994). Parkinson's disease and immunological abnormalities: increase of HLA-DR expression on monocytes in cerebrospinal fluid and of CD45RO+ T cells in peripheral blood. *Acta Neurol Scand*, 90(3), 160-166. doi:10.1111/j.1600-0404.1994.tb02699.x
- Forsyth, C. B., Shannon, K. M., Kordower, J. H., Voigt, R. M., Shaikh, M., Jaglin, J. A., . . . Keshavarzian, A. (2011). Increased intestinal permeability correlates with sigmoid mucosa alpha-synuclein staining and endotoxin exposure markers in early Parkinson's disease. *PLoS One*, 6(12), e28032. doi:10.1371/journal.pone.0028032
- Franceschi, C., Bonafe, M., & Valensin, S. (2000). Human immunosenescence: the prevailing of innate immunity, the failing of clonotypic immunity, and the filling of immunological space. *Vaccine*, 18(16), 1717-1720. doi:10.1016/s0264-410x(99)00513-7
- Franceschi, C., Valensin, S., Fagnoni, F., Barbi, C., & Bonafe, M. (1999). Biomarkers of immunosenescence within an evolutionary perspective: the challenge of heterogeneity and the role of antigenic load. *Exp Gerontol*, 34(8), 911-921. doi:10.1016/s0531-5565(99)00068-6
- Franke, A., McGovern, D. P., Barrett, J. C., Wang, K., Radford-Smith, G. L., Ahmad, T., . . . Parkes, M. (2010). Genome-wide meta-analysis increases to 71 the number of confirmed Crohn's disease susceptibility loci. *Nat Genet*, 42(12), 1118-1125. doi:10.1038/ng.717
- Frasca, D., & Blomberg, B. B. (2016). Inflammaging decreases adaptive and innate immune responses in mice and humans. *Biogerontology*, 17(1), 7-19. doi:10.1007/s10522-015-9578-8
- Frigerio, R., Sanft, K. R., Grossardt, B. R., Peterson, B. J., Elbaz, A., Bower, J. H., . . . Rocca, W. A. (2006). Chemical exposures and Parkinson's disease: a population-based case-control study. *Mov Disord*, 21(10), 1688-1692. doi:10.1002/mds.21009
- Fuji, R. N., Flagella, M., Baca, M., Baptista, M. A., Brodbeck, J., Chan, B. K., . . . Watts, R. J. (2015). Effect of selective LRRK2 kinase inhibition on nonhuman primate lung. *Sci Transl Med*, 7(273), 273ra215. doi:10.1126/scitranslmed.aaa3634
- Funayama, M., Hasegawa, K., Kowa, H., Saito, M., Tsuji, S., & Obata, F. (2002). A new locus for Parkinson's disease (PARK8) maps to chromosome 12p11.2-q13.1. *Ann Neurol*, 51(3), 296-301. doi:10.1002/ana.10113
- Fuss, I. J., Neurath, M., Boirivant, M., Klein, J. S., de la Motte, C., Strong, S. A., . . . Strober, W. (1996). Disparate CD4+ lamina propria (LP) lymphokine secretion profiles in inflammatory bowel disease. Crohn's disease LP cells manifest increased secretion of IFN-gamma, whereas ulcerative colitis LP cells manifest increased secretion of IL-5. *J Immunol*, 157(3), 1261-1270. Retrieved from <https://www.ncbi.nlm.nih.gov/pubmed/8757634>
- Gampierakis, I. A., Koutmani, Y., Semitekolou, M., Morianos, I., Charalampopoulos, I., Xanthou, G., . . . Karalis, K. P. (2020). Hippocampal neural stem cells and microglia response to

- experimental inflammatory bowel disease (IBD). *Mol Psychiatry*. doi:10.1038/s41380-020-0651-6
- Gandhi, P. N., Wang, X., Zhu, X., Chen, S. G., & Wilson-Delfosse, A. L. (2008). The Roc domain of leucine-rich repeat kinase 2 is sufficient for interaction with microtubules. *J Neurosci Res*, *86*(8), 1711-1720. doi:10.1002/jnr.21622
- Gao, L., Brenner, D., Llorens-Bobadilla, E., Saiz-Castro, G., Frank, T., Wieghofer, P., . . . Martin-Villalba, A. (2015). Infiltration of circulating myeloid cells through CD95L contributes to neurodegeneration in mice. *J Exp Med*, *212*(4), 469-480. doi:10.1084/jem.20132423
- Gardai, S. J., Mao, W., Schule, B., Babcock, M., Schoebel, S., Lorenzana, C., . . . Johnston, J. A. (2013). Elevated alpha-synuclein impairs innate immune cell function and provides a potential peripheral biomarker for Parkinson's disease. *PLoS One*, *8*(8), e71634. doi:10.1371/journal.pone.0071634
- Gardet, A., Benita, Y., Li, C., Sands, B. E., Ballester, I., Stevens, C., . . . Podolsky, D. K. (2010). LRRK2 is involved in the IFN-gamma response and host response to pathogens. *J Immunol*, *185*(9), 5577-5585. doi:10.4049/jimmunol.1000548
- Garrido-Gil, P., Rodriguez-Perez, A. I., Dominguez-Meijide, A., Guerra, M. J., & Labandeira-Garcia, J. L. (2018). Bidirectional Neural Interaction Between Central Dopaminergic and Gut Lesions in Parkinson's Disease Models. *Mol Neurobiol*, *55*(9), 7297-7316. doi:10.1007/s12035-018-0937-8
- Gelb, D. J., Oliver, E., & Gilman, S. (1999). Diagnostic criteria for Parkinson disease. *Arch Neurol*, *56*(1), 33-39. doi:10.1001/archneur.56.1.33
- Gerhard, A., Pavese, N., Hotton, G., Turkheimer, F., Es, M., Hammers, A., . . . Brooks, D. J. (2006). In vivo imaging of microglial activation with [¹¹C](R)-PK11195 PET in idiopathic Parkinson's disease. *Neurobiol Dis*, *21*(2), 404-412. doi:10.1016/j.nbd.2005.08.002
- Gerova, V. A., Stoynov, S. G., Katsarov, D. S., & Svinarov, D. A. (2011). Increased intestinal permeability in inflammatory bowel diseases assessed by iohexol test. *World J Gastroenterol*, *17*(17), 2211-2215. doi:10.3748/wjg.v17.i17.
- Giesert, F., Hofmann, A., Burger, A., Zerle, J., Kloos, K., Hafen, U., . . . Wurst, W. (2013). Expression analysis of Lrrk1, Lrrk2 and Lrrk2 splice variants in mice. *PLoS One*, *8*(5), e63778. doi:10.1371/journal.pone.0063778
- Gil-Martinez, A. L., Estrada, C., Cuenca, L., Cano, J. A., Valiente, M., Martinez-Caceres, C. M., . . . Herrero, M. T. (2019). Local Gastrointestinal Injury Exacerbates Inflammation and Dopaminergic Cell Death in Parkinsonian Mice. *Neurotox Res*, *35*(4), 918-930. doi:10.1007/s12640-019-0010-z
- Gilks, W. P., Abou-Sleiman, P. M., Gandhi, S., Jain, S., Singleton, A., Lees, A. J., . . . Wood, N. W. (2005). A common LRRK2 mutation in idiopathic Parkinson's disease. *Lancet*, *365*(9457), 415-416. doi:10.1016/S0140-6736(05)17830-1
- Gillardon, F., Schmid, R., & Draheim, H. (2012). Parkinson's disease-linked leucine-rich repeat kinase 2(R1441G) mutation increases proinflammatory cytokine release from activated primary microglial cells and resultant neurotoxicity. *Neuroscience*, *208*, 41-48. doi:10.1016/j.neuroscience.2012.02.001
- Gilsbach, B. K., Ho, F. Y., Vetter, I. R., van Haastert, P. J., Wittinghofer, A., & Kortholt, A. (2012). Roco kinase structures give insights into the mechanism of Parkinson disease-related leucine-rich-repeat kinase 2 mutations. *Proc Natl Acad Sci U S A*, *109*(26), 10322-10327. doi:10.1073/pnas.1203223109
- Gilsbach, B. K., & Kortholt, A. (2014). Structural biology of the LRRK2 GTPase and kinase domains: implications for regulation. *Front Mol Neurosci*, *7*, 32. doi:10.3389/fnmol.2014.00032
- Ginhoux, F., & Prinz, M. (2015). Origin of microglia: current concepts and past controversies. *Cold Spring Harb Perspect Biol*, *7*(8), a020537. doi:10.1101/cshperspect.a020537

- Gloeckner, C. J., Boldt, K., von Zweyendorf, F., Helm, S., Wiesent, L., Sarioglu, H., & Ueffing, M. (2010). Phosphopeptide analysis reveals two discrete clusters of phosphorylation in the N-terminus and the Roc domain of the Parkinson-disease associated protein kinase LRRK2. *J Proteome Res*, 9(4), 1738-1745. doi:10.1021/pr9008578
- Gloeckner, C. J., Schumacher, A., Boldt, K., & Ueffing, M. (2009). The Parkinson disease-associated protein kinase LRRK2 exhibits MAPKKK activity and phosphorylates MKK3/6 and MKK4/7, in vitro. *J Neurochem*, 109(4), 959-968. doi:10.1111/j.1471-4159.2009.06024.x
- Godena, V. K., Brookes-Hocking, N., Moller, A., Shaw, G., Oswald, M., Sancho, R. M., . . . De Vos, K. J. (2014). Increasing microtubule acetylation rescues axonal transport and locomotor deficits caused by LRRK2 Roc-COR domain mutations. *Nat Commun*, 5, 5245. doi:10.1038/ncomms6245
- Gold, A., Turkalp, Z. T., & Munoz, D. G. (2013). Enteric alpha-synuclein expression is increased in Parkinson's disease but not Alzheimer's disease. *Mov Disord*, 28(2), 237-240. doi:10.1002/mds.25298
- Goldman, S. M. (2014). Environmental toxins and Parkinson's disease. *Annu Rev Pharmacol Toxicol*, 54, 141-164. doi:10.1146/annurev-pharmtox-011613-135937
- Gomez-Suaga, P., Luzon-Toro, B., Churamani, D., Zhang, L., Bloor-Young, D., Patel, S., . . . Hilfiker, S. (2012). Leucine-rich repeat kinase 2 regulates autophagy through a calcium-dependent pathway involving NAADP. *Hum Mol Genet*, 21(3), 511-525. doi:10.1093/hmg/ddr481
- Goncalves, S. A., Macedo, D., Raquel, H., Simoes, P. D., Giorgini, F., Ramalho, J. S., . . . Outeiro, T. F. (2016). shRNA-Based Screen Identifies Endocytic Recycling Pathway Components That Act as Genetic Modifiers of Alpha-Synuclein Aggregation, Secretion and Toxicity. *PLoS Genet*, 12(4), e1005995. doi:10.1371/journal.pgen.1005995
- Gorell, J. M., Johnson, C. C., Rybicki, B. A., Peterson, E. L., Kortsha, G. X., Brown, G. G., & Richardson, R. J. (1997). Occupational exposures to metals as risk factors for Parkinson's disease. *Neurology*, 48(3), 650-658. doi:10.1212/wnl.48.3.650
- Goronzy, J. J., Li, G., Yang, Z., & Weyand, C. M. (2013). The janus head of T cell aging - autoimmunity and immunodeficiency. *Front Immunol*, 4, 131. doi:10.3389/fimmu.2013.00131
- Goudy, K. S., Burkhardt, B. R., Wasserfall, C., Song, S., Campbell-Thompson, M. L., Brusko, T., . . . Atkinson, M. A. (2003). Systemic overexpression of IL-10 induces CD4+CD25+ cell populations in vivo and ameliorates type 1 diabetes in nonobese diabetic mice in a dose-dependent fashion. *J Immunol*, 171(5), 2270-2278. doi:10.4049/jimmunol.171.5.2270
- Gray, M. T., Munoz, D. G., Gray, D. A., Schlossmacher, M. G., & Woulfe, J. M. (2014). Alpha-synuclein in the appendiceal mucosa of neurologically intact subjects. *Mov Disord*, 29(8), 991-998. doi:10.1002/mds.25779
- Gray, M. T., Munoz, D. G., Schlossmacher, M. G., Gray, D. A., & Woulfe, J. M. (2015). Protective effect of vagotomy suggests source organ for Parkinson disease. *Ann Neurol*, 78(5), 834-835. doi:10.1002/ana.24501
- Greffard, S., Verny, M., Bonnet, A. M., Beinis, J. Y., Gallinari, C., Meaume, S., . . . Duyckaerts, C. (2006). Motor score of the Unified Parkinson Disease Rating Scale as a good predictor of Lewy body-associated neuronal loss in the substantia nigra. *Arch Neurol*, 63(4), 584-588. doi:10.1001/archneur.63.4.584
- Greggio, E., Jain, S., Kingsbury, A., Bandopadhyay, R., Lewis, P., Kaganovich, A., . . . Cookson, M. R. (2006). Kinase activity is required for the toxic effects of mutant LRRK2/dardarin. *Neurobiol Dis*, 23(2), 329-341. doi:10.1016/j.nbd.2006.04.001
- Greggio, E., Taymans, J. M., Zhen, E. Y., Ryder, J., Vancraenenbroeck, R., Beilina, A., . . . Cookson, M. R. (2009). The Parkinson's disease kinase LRRK2 autophosphorylates its

- GTPase domain at multiple sites. *Biochem Biophys Res Commun*, 389(3), 449-454. doi:10.1016/j.bbrc.2009.08.163
- Greggio, E., Zambrano, I., Kaganovich, A., Beilina, A., Taymans, J. M., Daniels, V., . . . Cookson, M. R. (2008). The Parkinson disease-associated leucine-rich repeat kinase 2 (LRRK2) is a dimer that undergoes intramolecular autophosphorylation. *J Biol Chem*, 283(24), 16906-16914. doi:10.1074/jbc.M708718200
- Griffin, E. F., Yan, X., Caldwell, K. A., & Caldwell, G. A. (2018). Distinct functional roles of Vps41-mediated neuroprotection in Alzheimer's and Parkinson's disease models of neurodegeneration. *Hum Mol Genet*, 27(24), 4176-4193. doi:10.1093/hmg/ddy308
- Grozdanov, V., Bliederhaeuser, C., Ruf, W. P., Roth, V., Fundel-Clemens, K., Zondler, L., . . . Danzer, K. M. (2014). Inflammatory dysregulation of blood monocytes in Parkinson's disease patients. *Acta Neuropathol*, 128(5), 651-663. doi:10.1007/s00401-014-1345-4
- Grozdanov, V., Bousset, L., Hoffmeister, M., Bliederhaeuser, C., Meier, C., Madiona, K., . . . Danzer, K. M. (2019). Increased Immune Activation by Pathologic alpha-Synuclein in Parkinson's Disease. *Ann Neurol*, 86(4), 593-606. doi:10.1002/ana.25557
- Guaitoli, G., Raimondi, F., Gilsbach, B. K., Gomez-Llorente, Y., Deyaert, E., Renzi, F., . . . Gloeckner, C. J. (2016). Structural model of the dimeric Parkinson's protein LRRK2 reveals a compact architecture involving distant interdomain contacts. *Proc Natl Acad Sci U S A*, 113(30), E4357-4366. doi:10.1073/pnas.1523708113
- Guo, L., Gandhi, P. N., Wang, W., Petersen, R. B., Wilson-Delfosse, A. L., & Chen, S. G. (2007). The Parkinson's disease-associated protein, leucine-rich repeat kinase 2 (LRRK2), is an authentic GTPase that stimulates kinase activity. *Exp Cell Res*, 313(16), 3658-3670. doi:10.1016/j.yexcr.2007.07.007
- Hakansson, A., Westberg, L., Nilsson, S., Buervenich, S., Carmine, A., Holmberg, B., . . . Nissbrandt, H. (2005). Interaction of polymorphisms in the genes encoding interleukin-6 and estrogen receptor beta on the susceptibility to Parkinson's disease. *Am J Med Genet B Neuropsychiatr Genet*, 133B(1), 88-92. doi:10.1002/ajmg.b.30136
- Hakimi, M., Selvanantham, T., Swinton, E., Padmore, R. F., Tong, Y., Kabbach, G., . . . Schlossmacher, M. G. (2011). Parkinson's disease-linked LRRK2 is expressed in circulating and tissue immune cells and upregulated following recognition of microbial structures. *J Neural Transm (Vienna)*, 118(5), 795-808. doi:10.1007/s00702-011-0653-2
- Hamza, T. H., Zabetian, C. P., Tenesa, A., Laederach, A., Montimurro, J., Yearout, D., . . . Payami, H. (2010). Common genetic variation in the HLA region is associated with late-onset sporadic Parkinson's disease. *Nat Genet*, 42(9), 781-785. doi:10.1038/ng.642
- Han, M., Nagele, E., DeMarshall, C., Acharya, N., & Nagele, R. (2012). Diagnosis of Parkinson's disease based on disease-specific autoantibody profiles in human sera. *PLoS One*, 7(2), e32383. doi:10.1371/journal.pone.0032383
- Han, Y., Zhao, T., Cheng, X., Zhao, M., Gong, S. H., Zhao, Y. Q., . . . Zhu, L. L. (2018). Cortical Inflammation is Increased in a DSS-Induced Colitis Mouse Model. *Neurosci Bull*, 34(6), 1058-1066. doi:10.1007/s12264-018-0288-5
- Hartlova, A., Herbst, S., Peltier, J., Rodgers, A., Bilkei-Gorzo, O., Fearn, A., . . . Gutierrez, M. G. (2018). LRRK2 is a negative regulator of Mycobacterium tuberculosis phagosome maturation in macrophages. *EMBO J*, 37(12). doi:10.15252/embj.201798694
- Hasegawa, S., Goto, S., Tsuji, H., Okuno, T., Asahara, T., Nomoto, K., . . . Hirayama, M. (2015). Intestinal Dysbiosis and Lowered Serum Lipopolysaccharide-Binding Protein in Parkinson's Disease. *PLoS One*, 10(11), e0142164. doi:10.1371/journal.pone.0142164
- Hathaway, C. A., Appleyard, C. B., Percy, W. H., & Williams, J. L. (1999). Experimental colitis increases blood-brain barrier permeability in rabbits. *Am J Physiol*, 276(5), G1174-1180. doi:10.1152/ajpgi.1999.276.5.G1174
- Haugarvoll, K., Rademakers, R., Kachergus, J. M., Nuytemans, K., Ross, O. A., Gibson, J. M., . . . Wszolek, Z. K. (2008). Lrrk2 R1441C parkinsonism is clinically similar to sporadic

- Parkinson disease. *Neurology*, 70(16 Pt 2), 1456-1460. doi:10.1212/01.wnl.0000304044.22253.03
- Hayward, S. L., Scharer, C. D., Cartwright, E. K., Takamura, S., Li, Z. T., Boss, J. M., & Kohlmeier, J. E. (2020). Environmental cues regulate epigenetic reprogramming of airway-resident memory CD8(+) T cells. *Nat Immunol*, 21(3), 309-320. doi:10.1038/s41590-019-0584-x
- Healy, D. G., Falchi, M., O'Sullivan, S. S., Bonifati, V., Durr, A., Bressman, S., . . . International, L. C. (2008). Phenotype, genotype, and worldwide genetic penetrance of LRRK2-associated Parkinson's disease: a case-control study. *Lancet Neurol*, 7(7), 583-590. doi:10.1016/S1474-4422(08)70117-0
- Hearps, A. C., Martin, G. E., Angelovich, T. A., Cheng, W. J., Maisa, A., Landay, A. L., . . . Crowe, S. M. (2012). Aging is associated with chronic innate immune activation and dysregulation of monocyte phenotype and function. *Aging Cell*, 11(5), 867-875. doi:10.1111/j.1474-9726.2012.00851.x
- Heckman, M. G., Soto-Ortolaza, A. I., Aasly, J. O., Abahuni, N., Annesi, G., Bacon, J. A., . . . Genetic Epidemiology of Parkinson's Disease, C. (2013). Population-specific frequencies for LRRK2 susceptibility variants in the Genetic Epidemiology of Parkinson's Disease (GEO-PD) Consortium. *Mov Disord*, 28(12), 1740-1744. doi:10.1002/mds.25600
- Hely, M. A., Morris, J. G., Reid, W. G., O'Sullivan, D. J., Williamson, P. M., Broe, G. A., & Adena, M. A. (1995). Age at onset: the major determinant of outcome in Parkinson's disease. *Acta Neurol Scand*, 92(6), 455-463. doi:10.1111/j.1600-0404.1995.tb00480.x
- Henderson, M. X., Sengupta, M., McGeary, I., Zhang, B., Olufemi, M. F., Brown, H., . . . Lee, V. M. Y. (2019). LRRK2 inhibition does not impart protection from alpha-synuclein pathology and neuron death in non-transgenic mice. *Acta Neuropathol Commun*, 7(1), 28. doi:10.1186/s40478-019-0679-5
- Henry, A. G., Aghamohammadzadeh, S., Samaroo, H., Chen, Y., Mou, K., Needle, E., & Hirst, W. D. (2015). Pathogenic LRRK2 mutations, through increased kinase activity, produce enlarged lysosomes with reduced degradative capacity and increase ATP13A2 expression. *Hum Mol Genet*, 24(21), 6013-6028. doi:10.1093/hmg/ddv314
- Hernan, M. A., Logroscino, G., & Garcia Rodriguez, L. A. (2006). Nonsteroidal anti-inflammatory drugs and the incidence of Parkinson disease. *Neurology*, 66(7), 1097-1099. doi:10.1212/01.wnl.0000204446.82823.28
- Hernan, M. A., Takkouche, B., Caamano-Isorna, F., & Gestal-Otero, J. J. (2002). A meta-analysis of coffee drinking, cigarette smoking, and the risk of Parkinson's disease. *Ann Neurol*, 52(3), 276-284. doi:10.1002/ana.10277
- Herzig, M. C., Kolly, C., Persohn, E., Theil, D., Schweizer, T., Hafner, T., . . . Shimshek, D. R. (2011). LRRK2 protein levels are determined by kinase function and are crucial for kidney and lung homeostasis in mice. *Hum Mol Genet*, 20(21), 4209-4223. doi:10.1093/hmg/ddr348
- Higashi, S., Biskup, S., West, A. B., Trinkaus, D., Dawson, V. L., Faull, R. L., . . . Emson, P. C. (2007). Localization of Parkinson's disease-associated LRRK2 in normal and pathological human brain. *Brain Res*, 1155, 208-219. doi:10.1016/j.brainres.2007.04.034
- Higashi, S., Moore, D. J., Yamamoto, R., Minegishi, M., Sato, K., Togo, T., . . . Iseki, E. (2009). Abnormal localization of leucine-rich repeat kinase 2 to the endosomal-lysosomal compartment in lewy body disease. *J Neuropathol Exp Neurol*, 68(9), 994-1005. doi:10.1097/NEN.0b013e3181b44ed8
- Hill-Burns, E. M., Debelius, J. W., Morton, J. T., Wissemann, W. T., Lewis, M. R., Wallen, Z. D., . . . Payami, H. (2017). Parkinson's disease and Parkinson's disease medications have distinct signatures of the gut microbiome. *Mov Disord*, 32(5), 739-749. doi:10.1002/mds.26942
- Hilton, D., Stephens, M., Kirk, L., Edwards, P., Potter, R., Zajicek, J., . . . Carroll, C. (2014). Accumulation of alpha-synuclein in the bowel of patients in the pre-clinical phase of

- Parkinson's disease. *Acta Neuropathol*, 127(2), 235-241. doi:10.1007/s00401-013-1214-6
- Hinkle, K. M., Yue, M., Behrouz, B., Dachsel, J. C., Lincoln, S. J., Bowles, E. E., . . . Melrose, H. L. (2012). LRRK2 knockout mice have an intact dopaminergic system but display alterations in exploratory and motor co-ordination behaviors. *Mol Neurodegener*, 7, 25. doi:10.1186/1750-1326-7-25
- Ho, C. C., Rideout, H. J., Ribe, E., Troy, C. M., & Dauer, W. T. (2009). The Parkinson disease protein leucine-rich repeat kinase 2 transduces death signals via Fas-associated protein with death domain and caspase-8 in a cellular model of neurodegeneration. *J Neurosci*, 29(4), 1011-1016. doi:10.1523/JNEUROSCI.5175-08.2009
- Ho, D. H., Kim, H., Kim, J., Sim, H., Ahn, H., Kim, J., . . . Seol, W. (2015). Leucine-Rich Repeat Kinase 2 (LRRK2) phosphorylates p53 and induces p21(WAF1/CIP1) expression. *Mol Brain*, 8, 54. doi:10.1186/s13041-015-0145-7
- Ho, D. H., Seol, W., Eun, J. H., & Son, I. H. (2017). Phosphorylation of p53 by LRRK2 induces microglial tumor necrosis factor alpha-mediated neurotoxicity. *Biochem Biophys Res Commun*, 482(4), 1088-1094. doi:10.1016/j.bbrc.2016.11.163
- Holmans, P., Moskvina, V., Jones, L., Sharma, M., International Parkinson's Disease Genomics, C., Vedernikov, A., . . . Williams, N. M. (2013). A pathway-based analysis provides additional support for an immune-related genetic susceptibility to Parkinson's disease. *Hum Mol Genet*, 22(5), 1039-1049. doi:10.1093/hmg/ddt492
- Hongge, L., Kexin, G., Xiaojie, M., Nian, X., & Jinsha, H. (2015). The role of LRRK2 in the regulation of monocyte adhesion to endothelial cells. *J Mol Neurosci*, 55(1), 233-239. doi:10.1007/s12031-014-0312-9
- Horvath, I., Iashchishyn, I. A., Forsgren, L., & Morozova-Roche, L. A. (2017). Immunochemical Detection of alpha-Synuclein Autoantibodies in Parkinson's Disease: Correlation between Plasma and Cerebrospinal Fluid Levels. *ACS Chem Neurosci*, 8(6), 1170-1176. doi:10.1021/acschemneuro.7b00063
- Houser, M. C., Chang, J., Factor, S. A., Molho, E. S., Zabetian, C. P., Hill-Burns, E. M., . . . Tansey, M. G. (2018). Stool Immune Profiles Evince Gastrointestinal Inflammation in Parkinson's Disease. *Mov Disord*, 33(5), 793-804. doi:10.1002/mds.27326
- Houser, M. C., & Tansey, M. G. (2017). The gut-brain axis: is intestinal inflammation a silent driver of Parkinson's disease pathogenesis? *NPJ Parkinsons Dis*, 3, 3. doi:10.1038/s41531-016-0002-0
- Hsieh, C. H., Shaltouki, A., Gonzalez, A. E., Bettencourt da Cruz, A., Burbulla, L. F., St Lawrence, E., . . . Wang, X. (2016). Functional Impairment in Mito Degradation and Mitophagy Is a Shared Feature in Familial and Sporadic Parkinson's Disease. *Cell Stem Cell*, 19(6), 709-724. doi:10.1016/j.stem.2016.08.002
- Hsu, C. H., Chan, D., Greggio, E., Saha, S., Guillily, M. D., Ferree, A., . . . Wolozin, B. (2010). MKK6 binds and regulates expression of Parkinson's disease-related protein LRRK2. *J Neurochem*, 112(6), 1593-1604. doi:10.1111/j.1471-4159.2010.06568.x
- Huang, F., Liu, Q., Xie, S., Xu, J., Huang, B., Wu, Y., & Xia, D. (2016). Cypermethrin Induces Macrophages Death through Cell Cycle Arrest and Oxidative Stress-Mediated JNK/ERK Signaling Regulated Apoptosis. *Int J Mol Sci*, 17(6). doi:10.3390/ijms17060885
- Hugot, J. P., Chamaillard, M., Zouali, H., Lesage, S., Cezard, J. P., Belaiche, J., . . . Thomas, G. (2001). Association of NOD2 leucine-rich repeat variants with susceptibility to Crohn's disease. *Nature*, 411(6837), 599-603. doi:10.1038/35079107
- Hui, K. Y., Fernandez-Hernandez, H., Hu, J., Schaffner, A., Pankratz, N., Hsu, N. Y., . . . Peter, I. (2018). Functional variants in the LRRK2 gene confer shared effects on risk for Crohn's disease and Parkinson's disease. *Sci Transl Med*, 10(423). doi:10.1126/scitranslmed.aai7795

- Imai, Y., Gehrke, S., Wang, H. Q., Takahashi, R., Hasegawa, K., Oota, E., & Lu, B. (2008). Phosphorylation of 4E-BP by LRRK2 affects the maintenance of dopaminergic neurons in *Drosophila*. *EMBO J*, *27*(18), 2432-2443. doi:10.1038/emboj.2008.163
- Imamura, K., Hishikawa, N., Sawada, M., Nagatsu, T., Yoshida, M., & Hashizume, Y. (2003). Distribution of major histocompatibility complex class II-positive microglia and cytokine profile of Parkinson's disease brains. *Acta Neuropathol*, *106*(6), 518-526. doi:10.1007/s00401-003-0766-2
- International Parkinson Disease Genomics, C., Nalls, M. A., Plagnol, V., Hernandez, D. G., Sharma, M., Sheerin, U. M., . . . Wood, N. W. (2011). Imputation of sequence variants for identification of genetic risks for Parkinson's disease: a meta-analysis of genome-wide association studies. *Lancet*, *377*(9766), 641-649. doi:10.1016/S0140-6736(10)62345-8
- Ito, G., Okai, T., Fujino, G., Takeda, K., Ichijo, H., Katada, T., & Iwatsubo, T. (2007). GTP binding is essential to the protein kinase activity of LRRK2, a causative gene product for familial Parkinson's disease. *Biochemistry*, *46*(5), 1380-1388. doi:10.1021/bi061960m
- Jabri, B., & Barreiro, L. B. (2011). Don't move: LRRK2 arrests NFAT in the cytoplasm. *Nat Immunol*, *12*(11), 1029-1030. doi:10.1038/ni.2139
- Jagger, A., Shimojima, Y., Goronzy, J. J., & Weyand, C. M. (2014). Regulatory T cells and the immune aging process: a mini-review. *Gerontology*, *60*(2), 130-137. doi:10.1159/000355303
- Jaleel, M., Nichols, R. J., Deak, M., Campbell, D. G., Gillardon, F., Knebel, A., & Alessi, D. R. (2007). LRRK2 phosphorylates moesin at threonine-558: characterization of how Parkinson's disease mutants affect kinase activity. *Biochem J*, *405*(2), 307-317. doi:10.1042/BJ20070209
- Jeong, G. R., Jang, E. H., Bae, J. R., Jun, S., Kang, H. C., Park, C. H., . . . Lee, B. D. (2018). Dysregulated phosphorylation of Rab GTPases by LRRK2 induces neurodegeneration. *Mol Neurodegener*, *13*(1), 8. doi:10.1186/s13024-018-0240-1
- Johnson, J., Paisan-Ruiz, C., Lopez, G., Crews, C., Britton, A., Malkani, R., . . . Singleton, A. B. (2007). Comprehensive screening of a North American Parkinson's disease cohort for LRRK2 mutation. *Neurodegener Dis*, *4*(5), 386-391. doi:10.1159/000105160
- Kalia, V., & Sarkar, S. (2018). Regulation of Effector and Memory CD8 T Cell Differentiation by IL-2-A Balancing Act. *Front Immunol*, *9*, 2987. doi:10.3389/fimmu.2018.02987
- Kamel, F., Tanner, C., Umbach, D., Hoppin, J., Alavanja, M., Blair, A., . . . Sandler, D. (2007). Pesticide exposure and self-reported Parkinson's disease in the agricultural health study. *Am J Epidemiol*, *165*(4), 364-374. doi:10.1093/aje/kwk024
- Kannarkat, G. T., Cook, D. A., Lee, J. K., Chang, J., Chung, J., Sandy, E., . . . Tansey, M. G. (2015). Common Genetic Variant Association with Altered HLA Expression, Synergy with Pyrethroid Exposure, and Risk for Parkinson's Disease: An Observational and Case-Control Study. *NPJ Parkinsons Dis*, *1*. doi:10.1038/npjparkd.2015.2
- Karuppagounder, S. S., Xiong, Y., Lee, Y., Lawless, M. C., Kim, D., Nordquist, E., . . . Dawson, V. L. (2016). LRRK2 G2019S transgenic mice display increased susceptibility to 1-methyl-4-phenyl-1,2,3,6-tetrahydropyridine (MPTP)-mediated neurotoxicity. *J Chem Neuroanat*, *76*(Pt B), 90-97. doi:10.1016/j.jchemneu.2016.01.007
- Keenan, J. J., Vega, H., & Krieger, R. I. (2009). Potential exposure of children and adults to cypermethrin following use of indoor insecticide foggers. *J Environ Sci Health B*, *44*(6), 538-545. doi:10.1080/03601230902997733
- Kelly, K., Wang, S., Boddu, R., Liu, Z., Moukha-Chafiq, O., Augelli-Szafran, C., & West, A. B. (2018). The G2019S mutation in LRRK2 imparts resiliency to kinase inhibition. *Exp Neurol*, *309*, 1-13. doi:10.1016/j.expneurol.2018.07.012
- Kenborg, L., Rugbjerg, K., Lee, P. C., Ravnskjaer, L., Christensen, J., Ritz, B., & Lassen, C. F. (2015). Head injury and risk for Parkinson disease: results from a Danish case-control study. *Neurology*, *84*(11), 1098-1103. doi:10.1212/WNL.0000000000001362

- Kenny, E. E., Pe'er, I., Karban, A., Ozelius, L., Mitchell, A. A., Ng, S. M., . . . Peter, I. (2012). A genome-wide scan of Ashkenazi Jewish Crohn's disease suggests novel susceptibility loci. *PLoS Genet*, *8*(3), e1002559. doi:10.1371/journal.pgen.1002559
- Keshavarzian, A., Green, S. J., Engen, P. A., Voigt, R. M., Naqib, A., Forsyth, C. B., . . . Shannon, K. M. (2015). Colonic bacterial composition in Parkinson's disease. *Mov Disord*, *30*(10), 1351-1360. doi:10.1002/mds.26307
- Kestenbaum, M., & Alcalay, R. N. (2017). Clinical Features of LRRK2 Carriers with Parkinson's Disease. *Adv Neurobiol*, *14*, 31-48. doi:10.1007/978-3-319-49969-7_2
- Kett, L. R., Boassa, D., Ho, C. C., Rideout, H. J., Hu, J., Terada, M., . . . Dauer, W. T. (2012). LRRK2 Parkinson disease mutations enhance its microtubule association. *Hum Mol Genet*, *21*(4), 890-899. doi:10.1093/hmg/ddr526
- Khan, D. A., Hashmi, I., Mahjabeen, W., & Naqvi, T. A. (2010). Monitoring health implications of pesticide exposure in factory workers in Pakistan. *Environ Monit Assess*, *168*(1-4), 231-240. doi:10.1007/s10661-009-1107-2
- Khan, N. L., Jain, S., Lynch, J. M., Pavese, N., Abou-Sleiman, P., Holton, J. L., . . . Wood, N. W. (2005). Mutations in the gene LRRK2 encoding dardarin (PARK8) cause familial Parkinson's disease: clinical, pathological, olfactory and functional imaging and genetic data. *Brain*, *128*(Pt 12), 2786-2796. doi:10.1093/brain/awh667
- Kiesler, P., Fuss, I. J., & Strober, W. (2015). Experimental Models of Inflammatory Bowel Diseases. *Cell Mol Gastroenterol Hepatol*, *1*(2), 154-170. doi:10.1016/j.jcmgh.2015.01.006
- Kim, B., Yang, M. S., Choi, D., Kim, J. H., Kim, H. S., Seol, W., . . . Joe, E. H. (2012). Impaired inflammatory responses in murine Lrrk2-knockdown brain microglia. *PLoS One*, *7*(4), e34693. doi:10.1371/journal.pone.0034693
- Kim, J., Jeong, Y. H., Lee, E. J., Park, J. S., Seo, H., & Kim, H. S. (2017). Suppression of neuroinflammation by matrix metalloproteinase-8 inhibitor in aged normal and LRRK2 G2019S Parkinson's disease model mice challenged with lipopolysaccharide. *Biochem Biophys Res Commun*, *493*(2), 879-886. doi:10.1016/j.bbrc.2017.09.129
- Kim, J., Pajarillo, E., Rizzor, A., Son, D. S., Lee, J., Aschner, M., & Lee, E. (2019). LRRK2 kinase plays a critical role in manganese-induced inflammation and apoptosis in microglia. *PLoS One*, *14*(1), e0210248. doi:10.1371/journal.pone.0210248
- Kim, K. S., Marcogliese, P. C., Yang, J., Callaghan, S. M., Resende, V., Abdel-Messih, E., . . . Park, D. S. (2018). Regulation of myeloid cell phagocytosis by LRRK2 via WAVE2 complex stabilization is altered in Parkinson's disease. *Proc Natl Acad Sci U S A*, *115*(22), E5164-E5173. doi:10.1073/pnas.1718946115
- Kipnis, J., Cardon, M., Avidan, H., Lewitus, G. M., Mordechay, S., Rolls, A., . . . Schwartz, M. (2004). Dopamine, through the extracellular signal-regulated kinase pathway, downregulates CD4+CD25+ regulatory T-cell activity: implications for neurodegeneration. *J Neurosci*, *24*(27), 6133-6143. doi:10.1523/JNEUROSCI.0600-04.2004
- Kish, S. J., Shannak, K., Rajput, A., Deck, J. H., & Hornykiewicz, O. (1992). Aging produces a specific pattern of striatal dopamine loss: implications for the etiology of idiopathic Parkinson's disease. *J Neurochem*, *58*(2), 642-648. doi:10.1111/j.1471-4159.1992.tb09766.x
- Kishimoto, Y., Zhu, W., Hosoda, W., Sen, J. M., & Mattson, M. P. (2019). Chronic Mild Gut Inflammation Accelerates Brain Neuropathology and Motor Dysfunction in alpha-Synuclein Mutant Mice. *Neuromolecular Med*, *21*(3), 239-249. doi:10.1007/s12017-019-08539-5
- Kline, E. M., Butkovich, L. M., Bradner, J. M., Chang, J., Gelbard, H., Goodfellow, V., . . . Tansey, M. G. (2019). The second generation mixed lineage kinase-3 (MLK3) inhibitor CLFB-1134 protects against neurotoxin-induced nigral dopaminergic neuron loss. *Exp Neurol*, *318*, 157-164. doi:10.1016/j.expneurol.2019.05.002

- Kogure, T., Tatsumi, T., Kaneko, Y., & Okamoto, K. (2008). Rheumatoid arthritis accompanied by Parkinson disease. *J Clin Rheumatol*, *14*(3), 192-193. doi:10.1097/RHU.0B013E318178825f
- Kozina, E., Sadasivan, S., Jiao, Y., Dou, Y., Ma, Z., Tan, H., . . . Smeyne, R. J. (2018). Mutant LRRK2 mediates peripheral and central immune responses leading to neurodegeneration in vivo. *Brain*, *141*(6), 1753-1769. doi:10.1093/brain/awy077
- Koziorowski, D., Tomasiuk, R., Szlufik, S., & Friedman, A. (2012). Inflammatory cytokines and NT-proCNP in Parkinson's disease patients. *Cytokine*, *60*(3), 762-766. doi:10.1016/j.cyto.2012.07.030
- Kumar, A., Behera, P. C., Rangra, N. K., Dey, S., & Kant, K. (2018). Computational tool for immunotoxic assessment of pyrethroids toward adaptive immune cell receptors. *Pharmacogn Mag*, *14*(53), 124-128. doi:10.4103/pm.pm_62_17
- Kumar, K. R., Djarmati-Westenberger, A., & Grunewald, A. (2011). Genetics of Parkinson's disease. *Semin Neurol*, *31*(5), 433-440. doi:10.1055/s-0031-1299782
- Kupsky, W. J., Grimes, M. M., Sweeting, J., Bertsch, R., & Cote, L. J. (1987). Parkinson's disease and megacolon: concentric hyaline inclusions (Lewy bodies) in enteric ganglion cells. *Neurology*, *37*(7), 1253-1255. doi:10.1212/wnl.37.7.1253
- Kuss, M., Adamopoulou, E., & Kahle, P. J. (2014). Interferon-gamma induces leucine-rich repeat kinase LRRK2 via extracellular signal-regulated kinase ERK5 in macrophages. *J Neurochem*, *129*(6), 980-987. doi:10.1111/jnc.12668
- Lages, C. S., Suffia, I., Velilla, P. A., Huang, B., Warshaw, G., Hildeman, D. A., . . . Chougnet, C. (2008). Functional regulatory T cells accumulate in aged hosts and promote chronic infectious disease reactivation. *J Immunol*, *181*(3), 1835-1848. doi:10.4049/jimmunol.181.3.1835
- Lai, S. W., Liao, K. F., Lin, C. L., & Sung, F. C. (2014). Irritable bowel syndrome correlates with increased risk of Parkinson's disease in Taiwan. *Eur J Epidemiol*, *29*(1), 57-62. doi:10.1007/s10654-014-9878-3
- Lang, A. E., & Lozano, A. M. (1998). Parkinson's disease. Second of two parts. *N Engl J Med*, *339*(16), 1130-1143. doi:10.1056/NEJM199810153391607
- Langston, J. W. (1985). MPTP neurotoxicity: an overview and characterization of phases of toxicity. *Life Sci*, *36*(3), 201-206. doi:10.1016/0024-3205(85)90059-1
- Langston, J. W. (1996). The etiology of Parkinson's disease with emphasis on the MPTP story. *Neurology*, *47*(6 Suppl 3), S153-160. doi:10.1212/wnl.47.6_suppl_3.153s
- Langston, J. W. (2017). The MPTP Story. *J Parkinsons Dis*, *7*(s1), S11-S19. doi:10.3233/JPD-179006
- Langston, J. W., & Ballard, P. (1984). Parkinsonism induced by 1-methyl-4-phenyl-1,2,3,6-tetrahydropyridine (MPTP): implications for treatment and the pathogenesis of Parkinson's disease. *Can J Neurol Sci*, *11*(1 Suppl), 160-165. doi:10.1017/s0317167100046333
- Langston, J. W., Ballard, P., Tetrud, J. W., & Irwin, I. (1983). Chronic Parkinsonism in humans due to a product of meperidine-analog synthesis. *Science*, *219*(4587), 979-980. doi:10.1126/science.6823561
- Langston, J. W., Forno, L. S., Rebert, C. S., & Irwin, I. (1984). Selective nigral toxicity after systemic administration of 1-methyl-4-phenyl-1,2,5,6-tetrahydropyridine (MPTP) in the squirrel monkey. *Brain Res*, *292*(2), 390-394. doi:10.1016/0006-8993(84)90777-7
- Langston, J. W., Irwin, I., Langston, E. B., & Forno, L. S. (1984). The importance of the '4-5' double bond for neurotoxicity in primates of the pyridine derivative MPTP. *Neurosci Lett*, *50*(1-3), 289-294. doi:10.1016/0304-3940(84)90501-9
- Law, B. M., Spain, V. A., Leinster, V. H., Chia, R., Beilina, A., Cho, H. J., . . . Harvey, K. (2014). A direct interaction between leucine-rich repeat kinase 2 and specific beta-tubulin isoforms regulates tubulin acetylation. *J Biol Chem*, *289*(2), 895-908. doi:10.1074/jbc.M113.507913

- Le Couteur, D. G., McLean, A. J., Taylor, M. C., Woodham, B. L., & Board, P. G. (1999). Pesticides and Parkinson's disease. *Biomed Pharmacother*, *53*(3), 122-130. doi:10.1016/S0753-3322(99)80077-8
- Leandrou, E., Markidi, E., Memou, A., Melachroinou, K., Greggio, E., & Rideout, H. J. (2019). Kinase activity of mutant LRRK2 manifests differently in hetero-dimeric vs. homo-dimeric complexes. *Biochem J*, *476*(3), 559-579. doi:10.1042/BCJ20180589
- Lee, B. D., Shin, J. H., VanKampen, J., Petrucelli, L., West, A. B., Ko, H. S., . . . Dawson, T. M. (2010). Inhibitors of leucine-rich repeat kinase-2 protect against models of Parkinson's disease. *Nat Med*, *16*(9), 998-1000. doi:10.1038/nm.2199
- Lee, H., James, W. S., & Cowley, S. A. (2017). LRRK2 in peripheral and central nervous system innate immunity: its link to Parkinson's disease. *Biochem Soc Trans*, *45*(1), 131-139. doi:10.1042/BST20160262
- Lesage, S., & Brice, A. (2009). Parkinson's disease: from monogenic forms to genetic susceptibility factors. *Hum Mol Genet*, *18*(R1), R48-59. doi:10.1093/hmg/ddp012
- Lesage, S., Condroyer, C., Lannuzel, A., Lohmann, E., Troiano, A., Tison, F., . . . French Parkinson's Disease Genetics Study, G. (2009). Molecular analyses of the LRRK2 gene in European and North African autosomal dominant Parkinson's disease. *J Med Genet*, *46*(7), 458-464. doi:10.1136/jmg.2008.062612
- Lesage, S., Durr, A., & Brice, A. (2006). [LRRK2 is a major gene in North African parkinsonism]. *Med Sci (Paris)*, *22*(5), 470-471. doi:10.1051/medsci/2006225470
- Lesage, S., Ibanez, P., Lohmann, E., Pollak, P., Tison, F., Tazir, M., . . . French Parkinson's Disease Genetics Study, G. (2005). G2019S LRRK2 mutation in French and North African families with Parkinson's disease. *Ann Neurol*, *58*(5), 784-787. doi:10.1002/ana.20636
- Levy, G. (2007). The relationship of Parkinson disease with aging. *Arch Neurol*, *64*(9), 1242-1246. doi:10.1001/archneur.64.9.1242
- Lewis, P. A., Greggio, E., Beilina, A., Jain, S., Baker, A., & Cookson, M. R. (2007). The R1441C mutation of LRRK2 disrupts GTP hydrolysis. *Biochem Biophys Res Commun*, *357*(3), 668-671. doi:10.1016/j.bbrc.2007.04.006
- Li, D., He, Q., Li, R., Xu, X., Chen, B., & Xie, A. (2012). Interleukin-10 promoter polymorphisms in Chinese patients with Parkinson's disease. *Neurosci Lett*, *513*(2), 183-186. doi:10.1016/j.neulet.2012.02.033
- Li, K., Tang, B. S., Liu, Z. H., Kang, J. F., Zhang, Y., Shen, L., . . . Guo, J. F. (2015). LRRK2 A419V variant is a risk factor for Parkinson's disease in Asian population. *Neurobiol Aging*, *36*(10), 2908 e2911-2905. doi:10.1016/j.neurobiolaging.2015.07.012
- Li, M., Yao, D., Zeng, X., Kasakovski, D., Zhang, Y., Chen, S., . . . Xu, L. (2019). Age related human T cell subset evolution and senescence. *Immun Ageing*, *16*, 24. doi:10.1186/s12979-019-0165-8
- Li, X., Patel, J. C., Wang, J., Avshalumov, M. V., Nicholson, C., Buxbaum, J. D., . . . Yue, Z. (2010). Enhanced striatal dopamine transmission and motor performance with LRRK2 overexpression in mice is eliminated by familial Parkinson's disease mutation G2019S. *J Neurosci*, *30*(5), 1788-1797. doi:10.1523/JNEUROSCI.5604-09.2010
- Li, X., Sundquist, J., & Sundquist, K. (2012). Subsequent risks of Parkinson disease in patients with autoimmune and related disorders: a nationwide epidemiological study from Sweden. *Neurodegener Dis*, *10*(1-4), 277-284. doi:10.1159/000333222
- Li, Y., Liu, W., Oo, T. F., Wang, L., Tang, Y., Jackson-Lewis, V., . . . Li, C. (2009). Mutant LRRK2(R1441G) BAC transgenic mice recapitulate cardinal features of Parkinson's disease. *Nat Neurosci*, *12*(7), 826-828. doi:10.1038/nn.2349
- Lin, C. H., Chen, C. C., Chiang, H. L., Liou, J. M., Chang, C. M., Lu, T. P., . . . Wu, M. S. (2019). Altered gut microbiota and inflammatory cytokine responses in patients with Parkinson's disease. *J Neuroinflammation*, *16*(1), 129. doi:10.1186/s12974-019-1528-y

- Lin, C. H., Lin, J. W., Liu, Y. C., Chang, C. H., & Wu, R. M. (2014). Risk of Parkinson's disease following severe constipation: a nationwide population-based cohort study. *Parkinsonism Relat Disord*, *20*(12), 1371-1375. doi:10.1016/j.parkreldis.2014.09.026
- Lin, J. C., Lin, C. S., Hsu, C. W., Lin, C. L., & Kao, C. H. (2016). Association Between Parkinson's Disease and Inflammatory Bowel Disease: a Nationwide Taiwanese Retrospective Cohort Study. *Inflamm Bowel Dis*, *22*(5), 1049-1055. doi:10.1097/MIB.0000000000000735
- Liu, B., Fang, F., Pedersen, N. L., Tillander, A., Ludvigsson, J. F., Ekbom, A., . . . Wirdefeldt, K. (2017). Vagotomy and Parkinson disease: A Swedish register-based matched-cohort study. *Neurology*, *88*(21), 1996-2002. doi:10.1212/WNL.00000000000003961
- Liu, G., Sgobio, C., Gu, X., Sun, L., Lin, X., Yu, J., . . . Cai, H. (2015). Selective expression of Parkinson's disease-related Leucine-rich repeat kinase 2 G2019S missense mutation in midbrain dopaminergic neurons impairs dopamine release and dopaminergic gene expression. *Hum Mol Genet*, *24*(18), 5299-5312. doi:10.1093/hmg/ddv249
- Liu, H. F., Lu, S., Ho, P. W., Tse, H. M., Pang, S. Y., Kung, M. H., . . . Ho, S. L. (2014). LRRK2 R1441G mice are more liable to dopamine depletion and locomotor inactivity. *Ann Clin Transl Neurol*, *1*(3), 199-208. doi:10.1002/acn3.45
- Liu, M., Kang, S., Ray, S., Jackson, J., Zaitsev, A. D., Gerber, S. A., . . . Glicksman, M. A. (2011). Kinetic, mechanistic, and structural modeling studies of truncated wild-type leucine-rich repeat kinase 2 and the G2019S mutant. *Biochemistry*, *50*(43), 9399-9408. doi:10.1021/bi201173d
- Liu, T. C., Naito, T., Liu, Z., VanDussen, K. L., Haritunians, T., Li, D., . . . Stappenbeck, T. S. (2017). LRRK2 but not ATG16L1 is associated with Paneth cell defect in Japanese Crohn's disease patients. *JCI Insight*, *2*(6), e91917. doi:10.1172/jci.insight.91917
- Liu, W., Liu, X., Li, Y., Zhao, J., Liu, Z., Hu, Z., . . . Kang, Z. (2017). LRRK2 promotes the activation of NLRC4 inflammasome during Salmonella Typhimurium infection. *J Exp Med*, *214*(10), 3051-3066. doi:10.1084/jem.20170014
- Liu, X., Cheng, R., Verbitsky, M., Kisselev, S., Browne, A., Mejia-Sanatana, H., . . . Lee, J. H. (2011). Genome-wide association study identifies candidate genes for Parkinson's disease in an Ashkenazi Jewish population. *BMC Med Genet*, *12*, 104. doi:10.1186/1471-2350-12-104
- Liu, Z., Bryant, N., Kumaran, R., Beilina, A., Abeliovich, A., Cookson, M. R., & West, A. B. (2018). LRRK2 phosphorylates membrane-bound Rabs and is activated by GTP-bound Rab7L1 to promote recruitment to the trans-Golgi network. *Hum Mol Genet*, *27*(2), 385-395. doi:10.1093/hmg/ddx410
- Liu, Z., Lee, J., Krummey, S., Lu, W., Cai, H., & Lenardo, M. J. (2011). The kinase LRRK2 is a regulator of the transcription factor NFAT that modulates the severity of inflammatory bowel disease. *Nat Immunol*, *12*(11), 1063-1070. doi:10.1038/ni.2113
- Lobbestael, E., Baekelandt, V., & Taymans, J. M. (2012). Phosphorylation of LRRK2: from kinase to substrate. *Biochem Soc Trans*, *40*(5), 1102-1110. doi:10.1042/BST20120128
- Longo, F., Russo, I., Shimshek, D. R., Greggio, E., & Morari, M. (2014). Genetic and pharmacological evidence that G2019S LRRK2 confers a hyperkinetic phenotype, resistant to motor decline associated with aging. *Neurobiol Dis*, *71*, 62-73. doi:10.1016/j.nbd.2014.07.013
- Louveau, A., Smirnov, I., Keyes, T. J., Eccles, J. D., Rouhani, S. J., Peske, J. D., . . . Kipnis, J. (2015). Structural and functional features of central nervous system lymphatic vessels. *Nature*, *523*(7560), 337-341. doi:10.1038/nature14432
- Ma, B., Xu, L., Pan, X., Sun, L., Ding, J., Xie, C., . . . Cai, H. (2016). LRRK2 modulates microglial activity through regulation of chemokine (C-X3-C) receptor 1 -mediated signalling pathways. *Hum Mol Genet*, *25*(16), 3515-3523. doi:10.1093/hmg/ddw194

- Ma, S. Y., Roytta, M., Rinne, J. O., Collan, Y., & Rinne, U. K. (1997). Correlation between neuromorphometry in the substantia nigra and clinical features in Parkinson's disease using disector counts. *J Neurol Sci*, *151*(1), 83-87. doi:10.1016/s0022-510x(97)00100-7
- MacPherson, K. P., Sompol, P., Kannarkat, G. T., Chang, J., Sniffen, L., Wildner, M. E., . . . Tansey, M. G. (2017). Peripheral administration of the soluble TNF inhibitor XPro1595 modifies brain immune cell profiles, decreases beta-amyloid plaque load, and rescues impaired long-term potentiation in 5xFAD mice. *Neurobiol Dis*, *102*, 81-95. doi:10.1016/j.nbd.2017.02.010
- Madero-Perez, J., Fdez, E., Fernandez, B., Lara Ordonez, A. J., Blanca Ramirez, M., Gomez-Suaga, P., . . . Hilfiker, S. (2018). Parkinson disease-associated mutations in LRRK2 cause centrosomal defects via Rab8a phosphorylation. *Mol Neurodegener*, *13*(1), 3. doi:10.1186/s13024-018-0235-y
- Madero-Perez, J., Fernandez, B., Lara Ordonez, A. J., Fdez, E., Lobbestael, E., Baekelandt, V., & Hilfiker, S. (2018). RAB7L1-Mediated Relocalization of LRRK2 to the Golgi Complex Causes Centrosomal Deficits via RAB8A. *Front Mol Neurosci*, *11*, 417. doi:10.3389/fnmol.2018.00417
- Maekawa, T., Mori, S., Sasaki, Y., Miyajima, T., Azuma, S., Ohta, E., & Obata, F. (2012). The I2020T Leucine-rich repeat kinase 2 transgenic mouse exhibits impaired locomotive ability accompanied by dopaminergic neuron abnormalities. *Mol Neurodegener*, *7*, 15. doi:10.1186/1750-1326-7-15
- Maekawa, T., Sasaoka, T., Azuma, S., Ichikawa, T., Melrose, H. L., Farrer, M. J., & Obata, F. (2016). Leucine-rich repeat kinase 2 (LRRK2) regulates alpha-synuclein clearance in microglia. *BMC Neurosci*, *17*(1), 77. doi:10.1186/s12868-016-0315-2
- Mamais, A., Manzoni, C., Nazish, I., Arber, C., Sonustun, B., Wray, S., . . . Bandopadhyay, R. (2018). Analysis of macroautophagy related proteins in G2019S LRRK2 Parkinson's disease brains with Lewy body pathology. *Brain Res*, *1701*, 75-84. doi:10.1016/j.brainres.2018.07.023
- Mandarapu, R., & Prakhya, B. M. (2016). Exposure to cypermethrin and mancozeb alters the expression profile of THBS1, SPP1, FEZ1 and GPNMB in human peripheral blood mononuclear cells. *J Immunotoxicol*, *13*(4), 463-473. doi:10.3109/1547691X.2015.1130088
- Mann, D. M., & Yates, P. O. (1979). The effects of ageing on the pigmented nerve cells of the human locus caeruleus and substantia nigra. *Acta Neuropathol*, *47*(2), 93-97. doi:10.1007/bf00717030
- Manning, G., Whyte, D. B., Martinez, R., Hunter, T., & Sudarsanam, S. (2002). The protein kinase complement of the human genome. *Science*, *298*(5600), 1912-1934. doi:10.1126/science.1075762
- Manzoni, C., Mamais, A., Dihanich, S., McGoldrick, P., Devine, M. J., Zerle, J., . . . Lewis, P. A. (2013). Pathogenic Parkinson's disease mutations across the functional domains of LRRK2 alter the autophagic/lysosomal response to starvation. *Biochem Biophys Res Commun*, *441*(4), 862-866. doi:10.1016/j.bbrc.2013.10.159
- Maraganore, D. M., de Andrade, M., Lesnick, T. G., Strain, K. J., Farrer, M. J., Rocca, W. A., . . . Ballinger, D. G. (2005). High-resolution whole-genome association study of Parkinson disease. *Am J Hum Genet*, *77*(5), 685-693. doi:10.1086/496902
- Marin, I. (2006). The Parkinson disease gene LRRK2: evolutionary and structural insights. *Mol Biol Evol*, *23*(12), 2423-2433. doi:10.1093/molbev/msl114
- Marker, D. F., Puccini, J. M., Mockus, T. E., Barbieri, J., Lu, S. M., & Gelbard, H. A. (2012). LRRK2 kinase inhibition prevents pathological microglial phagocytosis in response to HIV-1 Tat protein. *J Neuroinflammation*, *9*, 261. doi:10.1186/1742-2094-9-261

- Marras, C., Beck, J. C., Bower, J. H., Roberts, E., Ritz, B., Ross, G. W., . . . Parkinson's Foundation, P. G. (2018). Prevalence of Parkinson's disease across North America. *NPJ Parkinsons Dis*, 4, 21. doi:10.1038/s41531-018-0058-0
- Martinez-Martin, P., Schapira, A. H., Stocchi, F., Sethi, K., Odin, P., MacPhee, G., . . . Chaudhuri, K. R. (2007). Prevalence of nonmotor symptoms in Parkinson's disease in an international setting; study using nonmotor symptoms questionnaire in 545 patients. *Mov Disord*, 22(11), 1623-1629. doi:10.1002/mds.21586
- Mata, I. F., Wedemeyer, W. J., Farrer, M. J., Taylor, J. P., & Gallo, K. A. (2006). LRRK2 in Parkinson's disease: protein domains and functional insights. *Trends Neurosci*, 29(5), 286-293. doi:10.1016/j.tins.2006.03.006
- McGeer, P. L., Itagaki, S., Akiyama, H., & McGeer, E. G. (1988). Rate of cell death in parkinsonism indicates active neuropathological process. *Ann Neurol*, 24(4), 574-576. doi:10.1002/ana.410240415
- McGeer, P. L., Itagaki, S., Boyes, B. E., & McGeer, E. G. (1988). Reactive microglia are positive for HLA-DR in the substantia nigra of Parkinson's and Alzheimer's disease brains. *Neurology*, 38(8), 1285-1291. doi:10.1212/wnl.38.8.1285
- McGeer, P. L., McGeer, E. G., & Suzuki, J. S. (1977). Aging and extrapyramidal function. *Arch Neurol*, 34(1), 33-35. doi:10.1001/archneur.1977.00500130053010
- McGuire, S. O., Ling, Z. D., Lipton, J. W., Sortwell, C. E., Collier, T. J., & Carvey, P. M. (2001). Tumor necrosis factor alpha is toxic to embryonic mesencephalic dopamine neurons. *Exp Neurol*, 169(2), 219-230. doi:10.1006/exnr.2001.7688
- McMaster, S. R., Wilson, J. J., Wang, H., & Kohlmeier, J. E. (2015). Airway-Resident Memory CD8 T Cells Provide Antigen-Specific Protection against Respiratory Virus Challenge through Rapid IFN-gamma Production. *J Immunol*, 195(1), 203-209. doi:10.4049/jimmunol.1402975
- Meiser, J., Weindl, D., & Hiller, K. (2013). Complexity of dopamine metabolism. *Cell Commun Signal*, 11(1), 34. doi:10.1186/1478-811X-11-34
- Melachroinou, K., Leandrou, E., Valkimadi, P. E., Memou, A., Hadjigeorgiou, G., Stefanis, L., & Rideout, H. J. (2016). Activation of FADD-Dependent Neuronal Death Pathways as a Predictor of Pathogenicity for LRRK2 Mutations. *PLoS One*, 11(11), e0166053. doi:10.1371/journal.pone.0166053
- Melrose, H., Lincoln, S., Tyndall, G., Dickson, D., & Farrer, M. (2006). Anatomical localization of leucine-rich repeat kinase 2 in mouse brain. *Neuroscience*, 139(3), 791-794. doi:10.1016/j.neuroscience.2006.01.017
- Melrose, H. L., Dachsel, J. C., Behrouz, B., Lincoln, S. J., Yue, M., Hinkle, K. M., . . . Farrer, M. J. (2010). Impaired dopaminergic neurotransmission and microtubule-associated protein tau alterations in human LRRK2 transgenic mice. *Neurobiol Dis*, 40(3), 503-517. doi:10.1016/j.nbd.2010.07.010
- Mendivil-Perez, M., Velez-Pardo, C., & Jimenez-Del-Rio, M. (2016). Neuroprotective Effect of the LRRK2 Kinase Inhibitor PF-06447475 in Human Nerve-Like Differentiated Cells Exposed to Oxidative Stress Stimuli: Implications for Parkinson's Disease. *Neurochem Res*, 41(10), 2675-2692. doi:10.1007/s11064-016-1982-1
- Meylan, E., & Tschopp, J. (2005). The RIP kinases: crucial integrators of cellular stress. *Trends Biochem Sci*, 30(3), 151-159. doi:10.1016/j.tibs.2005.01.003
- Michail, S., Bultron, G., & Depaolo, R. W. (2013). Genetic variants associated with Crohn's disease. *Appl Clin Genet*, 6, 25-32. doi:10.2147/TACG.S33966
- Michielan, A., & D'Inca, R. (2015). Intestinal Permeability in Inflammatory Bowel Disease: Pathogenesis, Clinical Evaluation, and Therapy of Leaky Gut. *Mediators Inflamm*, 2015, 628157. doi:10.1155/2015/628157

- Miklossy, J., Arai, T., Guo, J. P., Klegeris, A., Yu, S., McGeer, E. G., & McGeer, P. L. (2006). LRRK2 expression in normal and pathologic human brain and in human cell lines. *J Neuropathol Exp Neurol*, *65*(10), 953-963. doi:10.1097/01.jnen.0000235121.98052.54
- Miller, J. D., Peters, M., Oran, A. E., Beresford, G. W., Harrington, L., Boss, J. M., & Altman, J. D. (2002). CD94/NKG2 expression does not inhibit cytotoxic function of lymphocytic choriomeningitis virus-specific CD8+ T cells. *J Immunol*, *169*(2), 693-701. doi:10.4049/jimmunol.169.2.693
- Mishra, A. K., Mishra, S., Rajput, C., Ur Rasheed, M. S., Patel, D. K., & Singh, M. P. (2018). Cypermethrin Activates Autophagosome Formation Albeit Inhibits Autophagy Owing to Poor Lysosome Quality: Relevance to Parkinson's Disease. *Neurotox Res*, *33*(2), 377-387. doi:10.1007/s12640-017-9800-3
- Mizuta, I., Nishimura, M., Mizuta, E., Yamasaki, S., Ohta, M., Kuno, S., . . . Ota, M. (2001). Relation between the high production related allele of the interferon-gamma (IFN-gamma) gene and age at onset of idiopathic Parkinson's disease in Japan. *J Neurol Neurosurg Psychiatry*, *71*(6), 818-819. doi:10.1136/jnnp.71.6.818a
- Moehle, M. S., Daher, J. P., Hull, T. D., Boddu, R., Abdelmotilib, H. A., Mobley, J., . . . West, A. B. (2015). The G2019S LRRK2 mutation increases myeloid cell chemotactic responses and enhances LRRK2 binding to actin-regulatory proteins. *Hum Mol Genet*, *24*(15), 4250-4267. doi:10.1093/hmg/ddv157
- Moehle, M. S., Webber, P. J., Tse, T., Sukar, N., Standaert, D. G., DeSilva, T. M., . . . West, A. B. (2012). LRRK2 inhibition attenuates microglial inflammatory responses. *J Neurosci*, *32*(5), 1602-1611. doi:10.1523/JNEUROSCI.5601-11.2012
- Mogi, M., Harada, M., Kondo, T., Riederer, P., Inagaki, H., Minami, M., & Nagatsu, T. (1994). Interleukin-1 beta, interleukin-6, epidermal growth factor and transforming growth factor-alpha are elevated in the brain from parkinsonian patients. *Neurosci Lett*, *180*(2), 147-150. doi:10.1016/0304-3940(94)90508-8
- Mogi, M., Harada, M., Riederer, P., Narabayashi, H., Fujita, K., & Nagatsu, T. (1994). Tumor necrosis factor-alpha (TNF-alpha) increases both in the brain and in the cerebrospinal fluid from parkinsonian patients. *Neurosci Lett*, *165*(1-2), 208-210. doi:10.1016/0304-3940(94)90746-3
- Monfrini, E., & Di Fonzo, A. (2017). Leucine-Rich Repeat Kinase (LRRK2) Genetics and Parkinson's Disease. *Adv Neurobiol*, *14*, 3-30. doi:10.1007/978-3-319-49969-7_1
- More, S. V., Kumar, H., Kim, I. S., Song, S. Y., & Choi, D. K. (2013). Cellular and molecular mediators of neuroinflammation in the pathogenesis of Parkinson's disease. *Mediators Inflamm*, *2013*, 952375. doi:10.1155/2013/952375
- Mortera, P., & Herculano-Houzel, S. (2012). Age-related neuronal loss in the rat brain starts at the end of adolescence. *Front Neuroanat*, *6*, 45. doi:10.3389/fnana.2012.00045
- Mortiboys, H., Johansen, K. K., Aasly, J. O., & Bandmann, O. (2010). Mitochondrial impairment in patients with Parkinson disease with the G2019S mutation in LRRK2. *Neurology*, *75*(22), 2017-2020. doi:10.1212/WNL.0b013e3181ff9685
- Mount, M. P., Lira, A., Grimes, D., Smith, P. D., Faucher, S., Slack, R., . . . Park, D. S. (2007). Involvement of interferon-gamma in microglial-mediated loss of dopaminergic neurons. *J Neurosci*, *27*(12), 3328-3337. doi:10.1523/JNEUROSCI.5321-06.2007
- Mulak, A., & Bonaz, B. (2015). Brain-gut-microbiota axis in Parkinson's disease. *World J Gastroenterol*, *21*(37), 10609-10620. doi:10.3748/wjg.v21.i37.10609
- Mun, J. Y., Lee, W. Y., & Han, S. S. (2005). Effects of cypermethrin on the dopaminergic neurons in the progressive hemiparkinsonian rats. *Toxicol Mech Methods*, *15*(6), 399-404. doi:10.1080/15376520500194742
- Murch, S. H., Braegger, C. P., Walker-Smith, J. A., & MacDonald, T. T. (1993). Location of tumour necrosis factor alpha by immunohistochemistry in chronic inflammatory bowel disease. *Gut*, *34*(12), 1705-1709. doi:10.1136/gut.34.12.1705

- Muzes, G., Molnar, B., Tulassay, Z., & Sipos, F. (2012). Changes of the cytokine profile in inflammatory bowel diseases. *World J Gastroenterol*, *18*(41), 5848-5861. doi:10.3748/wjg.v18.i41.5848
- Nagatsu, T., Mogi, M., Ichinose, H., & Togari, A. (2000). Cytokines in Parkinson's disease. *J Neural Transm Suppl*(58), 143-151. Retrieved from <https://www.ncbi.nlm.nih.gov/pubmed/11128604>
- Nalls, M. A., Blauwendraat, C., Vallerga, C. L., Heilbron, K., Bandres-Ciga, S., Chang, D., . . . International Parkinson's Disease Genomics, C. (2019). Identification of novel risk loci, causal insights, and heritable risk for Parkinson's disease: a meta-analysis of genome-wide association studies. *Lancet Neurol*, *18*(12), 1091-1102. doi:10.1016/S1474-4422(19)30320-5
- Nalls, M. A., Pankratz, N., Lill, C. M., Do, C. B., Hernandez, D. G., Saad, M., . . . Singleton, A. B. (2014). Large-scale meta-analysis of genome-wide association data identifies six new risk loci for Parkinson's disease. *Nat Genet*, *46*(9), 989-993. doi:10.1038/ng.3043
- Nancey, S., Holvoet, S., Graber, I., Joubert, G., Philippe, D., Martin, S., . . . Kaiserlian, D. (2006). CD8+ cytotoxic T cells induce relapsing colitis in normal mice. *Gastroenterology*, *131*(2), 485-496. doi:10.1053/j.gastro.2006.05.018
- Natah, S. S., Mouihate, A., Pittman, Q. J., & Sharkey, K. A. (2005). Disruption of the blood-brain barrier during TNBS colitis. *Neurogastroenterol Motil*, *17*(3), 433-446. doi:10.1111/j.1365-2982.2005.00654.x
- Nelson, B. H. (2004). IL-2, regulatory T cells, and tolerance. *J Immunol*, *172*(7), 3983-3988. doi:10.4049/jimmunol.172.7.3983
- Ness, D., Ren, Z., Gardai, S., Sharpnack, D., Johnson, V. J., Brennan, R. J., . . . Olaharski, A. J. (2013). Leucine-rich repeat kinase 2 (LRRK2)-deficient rats exhibit renal tubule injury and perturbations in metabolic and immunological homeostasis. *PLoS One*, *8*(6), e66164. doi:10.1371/journal.pone.0066164
- Nichols, R. J., Dzamko, N., Hutti, J. E., Cantley, L. C., Deak, M., Moran, J., . . . Alessi, D. R. (2009). Substrate specificity and inhibitors of LRRK2, a protein kinase mutated in Parkinson's disease. *Biochem J*, *424*(1), 47-60. doi:10.1042/BJ20091035
- Nickol, A. D., & Bonventre, P. F. (1977). Anomalous high native resistance to athymic mice to bacterial pathogens. *Infect Immun*, *18*(3), 636-645. Retrieved from <https://www.ncbi.nlm.nih.gov/pubmed/412787>
- Nielsen, O. H., Kirman, I., Rudiger, N., Hendel, J., & Vainer, B. (2003). Upregulation of interleukin-12 and -17 in active inflammatory bowel disease. *Scand J Gastroenterol*, *38*(2), 180-185. doi:10.1080/00365520310000672
- Nishimura, M., Kuno, S., Kaji, R., Yasuno, K., & Kawakami, H. (2005). Glutathione-S-transferase-1 and interleukin-1beta gene polymorphisms in Japanese patients with Parkinson's disease. *Mov Disord*, *20*(7), 901-902. doi:10.1002/mds.20477
- Nishimura, M., Mizuta, I., Mizuta, E., Yamasaki, S., Ohta, M., Kaji, R., & Kuno, S. (2001). Tumor necrosis factor gene polymorphisms in patients with sporadic Parkinson's disease. *Neurosci Lett*, *311*(1), 1-4. doi:10.1016/s0304-3940(01)02111-5
- Nissen, S. K., Shrivastava, K., Schulte, C., Otzen, D. E., Goldeck, D., Berg, D., . . . Romero-Ramos, M. (2019). Alterations in Blood Monocyte Functions in Parkinson's Disease. *Mov Disord*, *34*(11), 1711-1721. doi:10.1002/mds.27815
- Niu, J., Yu, M., Wang, C., & Xu, Z. (2012). Leucine-rich repeat kinase 2 disturbs mitochondrial dynamics via Dynamin-like protein. *J Neurochem*, *122*(3), 650-658. doi:10.1111/j.1471-4159.2012.07809.x
- Novello, S., Arcuri, L., Dovero, S., Dutheil, N., Shimshek, D. R., Bezard, E., & Morari, M. (2018). G2019S LRRK2 mutation facilitates alpha-synuclein neuropathology in aged mice. *Neurobiol Dis*, *120*, 21-33. doi:10.1016/j.nbd.2018.08.018

- Nussbaum, R. L., & Ellis, C. E. (2003). Alzheimer's disease and Parkinson's disease. *N Engl J Med*, *348*(14), 1356-1364. doi:10.1056/NEJM2003ra020003
- Ogura, Y., Bonen, D. K., Inohara, N., Nicolae, D. L., Chen, F. F., Ramos, R., . . . Cho, J. H. (2001). A frameshift mutation in NOD2 associated with susceptibility to Crohn's disease. *Nature*, *411*(6837), 603-606. doi:10.1038/35079114
- Okayasu, I., Hatakeyama, S., Yamada, M., Ohkusa, T., Inagaki, Y., & Nakaya, R. (1990). A novel method in the induction of reliable experimental acute and chronic ulcerative colitis in mice. *Gastroenterology*, *98*(3), 694-702. doi:10.1016/0016-5085(90)90290-h
- Orr, C. F., Rowe, D. B., Mizuno, Y., Mori, H., & Halliday, G. M. (2005). A possible role for humoral immunity in the pathogenesis of Parkinson's disease. *Brain*, *128*(Pt 11), 2665-2674. doi:10.1093/brain/awh625
- Ozelius, L. J., Senthil, G., Saunders-Pullman, R., Ohmann, E., Deligtisch, A., Tagliati, M., . . . Bressman, S. B. (2006). LRRK2 G2019S as a cause of Parkinson's disease in Ashkenazi Jews. *N Engl J Med*, *354*(4), 424-425. doi:10.1056/NEJMc055509
- Padmanabhan, S., Lanz, T. A., Gorman, D., Wolfe, M., Joyce, A., Cabrera, C., . . . Merchant, K. (2020). An Assessment of LRRK2 Serine 935 Phosphorylation in Human Peripheral Blood Mononuclear Cells in Idiopathic Parkinson's Disease and G2019S LRRK2 Cohorts. *J Parkinsons Dis*. doi:10.3233/JPD-191786
- Paisan-Ruiz, C., Jain, S., Evans, E. W., Gilks, W. P., Simon, J., van der Brug, M., . . . Singleton, A. B. (2004). Cloning of the gene containing mutations that cause PARK8-linked Parkinson's disease. *Neuron*, *44*(4), 595-600. doi:10.1016/j.neuron.2004.10.023
- Paisan-Ruiz, C., Nath, P., Washecka, N., Gibbs, J. R., & Singleton, A. B. (2008). Comprehensive analysis of LRRK2 in publicly available Parkinson's disease cases and neurologically normal controls. *Hum Mutat*, *29*(4), 485-490. doi:10.1002/humu.20668
- Pamer, E. G. (2004). Immune responses to *Listeria monocytogenes*. *Nat Rev Immunol*, *4*(10), 812-823. doi:10.1038/nri1461
- Papachroni, K. K., Ninkina, N., Papapanagiotou, A., Hadjigeorgiou, G. M., Xiromerisiou, G., Papadimitriou, A., . . . Buchman, V. L. (2007). Autoantibodies to alpha-synuclein in inherited Parkinson's disease. *J Neurochem*, *101*(3), 749-756. doi:10.1111/j.1471-4159.2006.04365.x
- Parillaud, V. R., Lornet, G., Monnet, Y., Privat, A. L., Haddad, A. T., Brochard, V., . . . Lobsiger, C. S. (2017). Analysis of monocyte infiltration in MPTP mice reveals that microglial CX3CR1 protects against neurotoxic over-induction of monocyte-attracting CCL2 by astrocytes. *J Neuroinflammation*, *14*(1), 60. doi:10.1186/s12974-017-0830-9
- Parisiadou, L., Yu, J., Sgobio, C., Xie, C., Liu, G., Sun, L., . . . Cai, H. (2014). LRRK2 regulates synaptogenesis and dopamine receptor activation through modulation of PKA activity. *Nat Neurosci*, *17*(3), 367-376. doi:10.1038/nn.3636
- Park, H., Lee, J. Y., Shin, C. M., Kim, J. M., Kim, T. J., & Kim, J. W. (2015). Characterization of gastrointestinal disorders in patients with parkinsonian syndromes. *Parkinsonism Relat Disord*, *21*(5), 455-460. doi:10.1016/j.parkreldis.2015.02.005
- Park, J., Lee, J. W., Cooper, S. C., Broxmeyer, H. E., Cannon, J. R., & Kim, C. H. (2017). Parkinson disease-associated LRRK2 G2019S transgene disrupts marrow myelopoiesis and peripheral Th17 response. *J Leukoc Biol*, *102*(4), 1093-1102. doi:10.1189/jlb.1A0417-147RR
- Park, M., Ross, G. W., Petrovitch, H., White, L. R., Masaki, K. H., Nelson, J. S., . . . Abbott, R. D. (2005). Consumption of milk and calcium in midlife and the future risk of Parkinson disease. *Neurology*, *64*(6), 1047-1051. doi:10.1212/01.WNL.0000154532.98495.BF
- Park, S., Kim, J., Chun, J., Han, K., Soh, H., Kang, E. A., . . . Kim, J. S. (2019). Patients with Inflammatory Bowel Disease Are at an Increased Risk of Parkinson's Disease: A South Korean Nationwide Population-Based Study. *J Clin Med*, *8*(8). doi:10.3390/jcm8081191

- Parkinson, J. (1922). An essay on the shaking palsy. *Archives of Neurology and Psychiatry*, 7(6), 683-710. Retrieved from <Go to ISI>://WOS:000201539300002
- Perse, M., & Cerar, A. (2012). Dextran sodium sulphate colitis mouse model: traps and tricks. *J Biomed Biotechnol*, 2012, 718617. doi:10.1155/2012/718617
- Peter, I., Dubinsky, M., Bressman, S., Park, A., Lu, C., Chen, N., & Wang, A. (2018). Anti-Tumor Necrosis Factor Therapy and Incidence of Parkinson Disease Among Patients With Inflammatory Bowel Disease. *JAMA Neurol*, 75(8), 939-946. doi:10.1001/jamaneurol.2018.0605
- Petit, C. S., Barreau, F., Besnier, L., Gandille, P., Riveau, B., Chateau, D., . . . Thenet, S. (2012). Requirement of cellular prion protein for intestinal barrier function and mislocalization in patients with inflammatory bowel disease. *Gastroenterology*, 143(1), 122-132 e115. doi:10.1053/j.gastro.2012.03.029
- Pietrucci, D., Cerroni, R., Unida, V., Farcomeni, A., Pierantozzi, M., Mercuri, N. B., . . . Desideri, A. (2019). Dysbiosis of gut microbiota in a selected population of Parkinson's patients. *Parkinsonism Relat Disord*, 65, 124-130. doi:10.1016/j.parkreldis.2019.06.003
- Plowey, E. D., Cherra, S. J., 3rd, Liu, Y. J., & Chu, C. T. (2008). Role of autophagy in G2019S-LRRK2-associated neurite shortening in differentiated SH-SY5Y cells. *J Neurochem*, 105(3), 1048-1056. doi:10.1111/j.1471-4159.2008.05217.x
- Poly, T. N., Islam, M. M. R., Yang, H. C., & Li, Y. J. (2019). Non-steroidal anti-inflammatory drugs and risk of Parkinson's disease in the elderly population: a meta-analysis. *Eur J Clin Pharmacol*, 75(1), 99-108. doi:10.1007/s00228-018-2561-y
- Postuma, R. B., Berg, D., Stern, M., Poewe, W., Olanow, C. W., Oertel, W., . . . Deuschl, G. (2015). MDS clinical diagnostic criteria for Parkinson's disease. *Mov Disord*, 30(12), 1591-1601. doi:10.1002/mds.26424
- Postuma, R. B., Gagnon, J. F., Pelletier, A., & Montplaisir, J. (2013). Prodromal autonomic symptoms and signs in Parkinson's disease and dementia with Lewy bodies. *Mov Disord*, 28(5), 597-604. doi:10.1002/mds.25445
- Prigent, A., Gonzales, J., Durand, T., Le Berre-Scoul, C., Rolli-Derkinderen, M., Neunlist, M., & Derkinderen, P. (2019). Acute inflammation down-regulates alpha-synuclein expression in enteric neurons. *J Neurochem*, 148(6), 746-760. doi:10.1111/jnc.14656
- Priyadarshi, A., Khuder, S. A., Schaub, E. A., & Priyadarshi, S. S. (2001). Environmental risk factors and Parkinson's disease: a metaanalysis. *Environ Res*, 86(2), 122-127. doi:10.1006/enrs.2001.4264
- Priyadarshi, A., Khuder, S. A., Schaub, E. A., & Shrivastava, S. (2000). A meta-analysis of Parkinson's disease and exposure to pesticides. *Neurotoxicology*, 21(4), 435-440. Retrieved from <https://www.ncbi.nlm.nih.gov/pubmed/11022853>
- Puccini, J. M., Marker, D. F., Fitzgerald, T., Barbieri, J., Kim, C. S., Miller-Rhodes, P., . . . Gelbard, H. A. (2015). Leucine-rich repeat kinase 2 modulates neuroinflammation and neurotoxicity in models of human immunodeficiency virus 1-associated neurocognitive disorders. *J Neurosci*, 35(13), 5271-5283. doi:10.1523/JNEUROSCI.0650-14.2015
- Purlyte, E., Dhekne, H. S., Sarhan, A. R., Gomez, R., Lis, P., Wightman, M., . . . Alessi, D. R. (2019). Rab29 activation of the Parkinson's disease-associated LRRK2 kinase. *EMBO J*, 38(2). doi:10.15252/embj.2018101237
- Ramonet, D., Daher, J. P., Lin, B. M., Stafa, K., Kim, J., Banerjee, R., . . . Moore, D. J. (2011). Dopaminergic neuronal loss, reduced neurite complexity and autophagic abnormalities in transgenic mice expressing G2019S mutant LRRK2. *PLoS One*, 6(4), e18568. doi:10.1371/journal.pone.0018568
- Ray, S., & Liu, M. (2012). Current understanding of LRRK2 in Parkinson's disease: biochemical and structural features and inhibitor design. *Future Med Chem*, 4(13), 1701-1713. doi:10.4155/fmc.12.110

- Raynor, J., Lages, C. S., Shehata, H., Hildeman, D. A., & Chougnet, C. A. (2012). Homeostasis and function of regulatory T cells in aging. *Curr Opin Immunol*, 24(4), 482-487. doi:10.1016/j.coi.2012.04.005
- Reale, M., Greig, N. H., & Kamal, M. A. (2009). Peripheral chemo-cytokine profiles in Alzheimer's and Parkinson's diseases. *Mini Rev Med Chem*, 9(10), 1229-1241. doi:10.2174/138955709789055199
- Reale, M., Iarlori, C., Thomas, A., Gambi, D., Perfetti, B., Di Nicola, M., & Onofri, M. (2009). Peripheral cytokines profile in Parkinson's disease. *Brain Behav Immun*, 23(1), 55-63. doi:10.1016/j.bbi.2008.07.003
- Ren, L., Yi, J., Yang, J., Li, P., Cheng, X., & Mao, P. (2018). Nonsteroidal anti-inflammatory drugs use and risk of Parkinson disease: A dose-response meta-analysis. *Medicine (Baltimore)*, 97(37), e12172. doi:10.1097/MD.00000000000012172
- Resnikoff, H., Metzger, J. M., Lopez, M., Bondarenko, V., Mejia, A., Simmons, H. A., & Emborg, M. E. (2019). Colonic inflammation affects myenteric alpha-synuclein in nonhuman primates. *J Inflamm Res*, 12, 113-126. doi:10.2147/JIR.S196552
- Riederer, P., & Wuketich, S. (1976). Time course of nigrostriatal degeneration in parkinson's disease. A detailed study of influential factors in human brain amine analysis. *J Neural Transm*, 38(3-4), 277-301. doi:10.1007/bf01249445
- Rietdijk, C. D., Perez-Pardo, P., Garssen, J., van Wezel, R. J., & Kraneveld, A. D. (2017). Exploring Braak's Hypothesis of Parkinson's Disease. *Front Neurol*, 8, 37. doi:10.3389/fneur.2017.00037
- Ritz, B., Ascherio, A., Checkoway, H., Marder, K. S., Nelson, L. M., Rocca, W. A., . . . Gorell, J. (2007). Pooled analysis of tobacco use and risk of Parkinson disease. *Arch Neurol*, 64(7), 990-997. doi:10.1001/archneur.64.7.990
- Rodrigues-Sousa, T., Ladeirainha, A. F., Santiago, A. R., Carvalheiro, H., Raposo, B., Alarcao, A., . . . Souto-Carneiro, M. M. (2014). Deficient production of reactive oxygen species leads to severe chronic DSS-induced colitis in Ncf1/p47phox-mutant mice. *PLoS One*, 9(5), e97532. doi:10.1371/journal.pone.0097532
- Rosenkranz, D., Weyer, S., Tolosa, E., Gaenslen, A., Berg, D., Leyhe, T., . . . Stoltze, L. (2007). Higher frequency of regulatory T cells in the elderly and increased suppressive activity in neurodegeneration. *J Neuroimmunol*, 188(1-2), 117-127. doi:10.1016/j.jneuroim.2007.05.011
- Ross, G. W., Abbott, R. D., Petrovitch, H., Morens, D. M., Grandinetti, A., Tung, K. H., . . . White, L. R. (2000). Association of coffee and caffeine intake with the risk of Parkinson disease. *JAMA*, 283(20), 2674-2679. doi:10.1001/jama.283.20.2674
- Ross, O. A., O'Neill, C., Rea, I. M., Lynch, T., Gosal, D., Wallace, A., . . . Gibson, J. M. (2004). Functional promoter region polymorphism of the proinflammatory chemokine IL-8 gene associates with Parkinson's disease in the Irish. *Hum Immunol*, 65(4), 340-346. doi:10.1016/j.humimm.2004.01.015
- Ross, O. A., Soto-Ortolaza, A. I., Heckman, M. G., Aasly, J. O., Abahuni, N., Annesi, G., . . . Genetic Epidemiology Of Parkinson's Disease, C. (2011). Association of LRRK2 exonic variants with susceptibility to Parkinson's disease: a case-control study. *Lancet Neurol*, 10(10), 898-908. doi:10.1016/S1474-4422(11)70175-2
- Ross, O. A., Toft, M., Whittle, A. J., Johnson, J. L., Papapetropoulos, S., Mash, D. C., . . . Dickson, D. W. (2006). Lrrk2 and Lewy body disease. *Ann Neurol*, 59(2), 388-393. doi:10.1002/ana.20731
- Ross, O. A., Wu, Y. R., Lee, M. C., Funayama, M., Chen, M. L., Soto, A. I., . . . Wu, R. M. (2008). Analysis of Lrrk2 R1628P as a risk factor for Parkinson's disease. *Ann Neurol*, 64(1), 88-92. doi:10.1002/ana.21405

- Rouaud, T., Clairembault, T., Coron, E., Neunlist, M., Anheim, M., & Derkinderen, P. (2017). Enteric alpha-synuclein pathology in LRRK2-G2019S Parkinson's disease. *Parkinsonism Relat Disord*, *40*, 83-84. doi:10.1016/j.parkreldis.2017.05.001
- Rudyk, C., Dwyer, Z., Hayley, S., & membership, C. (2019). Leucine-rich repeat kinase-2 (LRRK2) modulates paraquat-induced inflammatory sickness and stress phenotype. *J Neuroinflammation*, *16*(1), 120. doi:10.1186/s12974-019-1483-7
- Rugbjerg, K., Friis, S., Ritz, B., Schernhammer, E. S., Korbo, L., & Olsen, J. H. (2009). Autoimmune disease and risk for Parkinson disease: a population-based case-control study. *Neurology*, *73*(18), 1462-1468. doi:10.1212/WNL.0b013e3181c06635
- Russo, I., Berti, G., Plotegher, N., Bernardo, G., Filograna, R., Bubacco, L., & Greggio, E. (2015). Leucine-rich repeat kinase 2 positively regulates inflammation and down-regulates NF-kappaB p50 signaling in cultured microglia cells. *J Neuroinflammation*, *12*, 230. doi:10.1186/s12974-015-0449-7
- Russo, I., Di Benedetto, G., Kaganovich, A., Ding, J., Mercatelli, D., Morari, M., . . . Greggio, E. (2018). Leucine-rich repeat kinase 2 controls protein kinase A activation state through phosphodiesterase 4. *J Neuroinflammation*, *15*(1), 297. doi:10.1186/s12974-018-1337-8
- Sadikot, R. T., Zeng, H., Azim, A. C., Joo, M., Dey, S. K., Breyer, R. M., . . . Christman, J. W. (2007). Bacterial clearance of *Pseudomonas aeruginosa* is enhanced by the inhibition of COX-2. *Eur J Immunol*, *37*(4), 1001-1009. doi:10.1002/eji.200636636
- Saijo, K., & Glass, C. K. (2011). Microglial cell origin and phenotypes in health and disease. *Nat Rev Immunol*, *11*(11), 775-787. doi:10.1038/nri3086
- Sairam, K., Saravanan, K. S., Banerjee, R., & Mohanakumar, K. P. (2003). Non-steroidal anti-inflammatory drug sodium salicylate, but not diclofenac or celecoxib, protects against 1-methyl-4-phenyl pyridinium-induced dopaminergic neurotoxicity in rats. *Brain Res*, *966*(2), 245-252. doi:10.1016/s0006-8993(02)04174-4
- Sanchez, G., Varaschin, R. K., Bueler, H., Marcogliese, P. C., Park, D. S., & Trudeau, L. E. (2014). Unaltered striatal dopamine release levels in young Parkin knockout, Pink1 knockout, DJ-1 knockout and LRRK2 R1441G transgenic mice. *PLoS One*, *9*(4), e94826. doi:10.1371/journal.pone.0094826
- Sanders, L. H., Laganier, J., Cooper, O., Mak, S. K., Vu, B. J., Huang, Y. A., . . . Schule, B. (2014). LRRK2 mutations cause mitochondrial DNA damage in iPSC-derived neural cells from Parkinson's disease patients: reversal by gene correction. *Neurobiol Dis*, *62*, 381-386. doi:10.1016/j.nbd.2013.10.013
- Sans, M., Kawachi, S., Soriano, A., Palacin, A., Morise, Z., Granger, D. N., . . . Panes, J. (2001). Brain endothelial adhesion molecule expression in experimental colitis. *Microcirculation*, *8*(2), 105-114. Retrieved from <https://www.ncbi.nlm.nih.gov/pubmed/11379790>
- Satake, W., Nakabayashi, Y., Mizuta, I., Hirota, Y., Ito, C., Kubo, M., . . . Toda, T. (2009). Genome-wide association study identifies common variants at four loci as genetic risk factors for Parkinson's disease. *Nat Genet*, *41*(12), 1303-1307. doi:10.1038/ng.485
- Saunders, J. A., Estes, K. A., Kosloski, L. M., Allen, H. E., Dempsey, K. M., Torres-Russotto, D. R., . . . Gendelman, H. E. (2012). CD4+ regulatory and effector/memory T cell subsets profile motor dysfunction in Parkinson's disease. *J Neuroimmune Pharmacol*, *7*(4), 927-938. doi:10.1007/s11481-012-9402-z
- Savica, R., Carlin, J. M., Grossardt, B. R., Bower, J. H., Ahlskog, J. E., Maraganore, D. M., . . . Rocca, W. A. (2009). Medical records documentation of constipation preceding Parkinson disease: A case-control study. *Neurology*, *73*(21), 1752-1758. doi:10.1212/WNL.0b013e3181c34af5
- Schapansky, J., Khasnavis, S., DeAndrade, M. P., Nardozi, J. D., Falkson, S. R., Boyd, J. D., . . . LaVoie, M. J. (2018). Familial knockin mutation of LRRK2 causes lysosomal dysfunction and accumulation of endogenous insoluble alpha-synuclein in neurons. *Neurobiol Dis*, *111*, 26-35. doi:10.1016/j.nbd.2017.12.005

- Schapansky, J., Nardoizzi, J. D., Felizia, F., & LaVoie, M. J. (2014). Membrane recruitment of endogenous LRRK2 precedes its potent regulation of autophagy. *Hum Mol Genet*, *23*(16), 4201-4214. doi:10.1093/hmg/ddu138
- Scheperjans, F., Aho, V., Pereira, P. A., Koskinen, K., Paulin, L., Pekkonen, E., . . . Auvinen, P. (2015). Gut microbiota are related to Parkinson's disease and clinical phenotype. *Mov Disord*, *30*(3), 350-358. doi:10.1002/mds.26069
- Schetters, S. T. T., Gomez-Nicola, D., Garcia-Vallejo, J. J., & Van Kooyk, Y. (2017). Neuroinflammation: Microglia and T Cells Get Ready to Tango. *Front Immunol*, *8*, 1905. doi:10.3389/fimmu.2017.01905
- Schildt, A., Walker, M. D., Dinelle, K., Miao, Q., Schulzer, M., O'Kusky, J., . . . Sossi, V. (2019). Single Inflammatory Trigger Leads to Neuroinflammation in LRRK2 Rodent Model without Degeneration of Dopaminergic Neurons. *J Parkinsons Dis*, *9*(1), 121-139. doi:10.3233/JPD-181446
- Schlachetzki, J. C. M., Prots, I., Tao, J., Chun, H. B., Saijo, K., Gosselin, D., . . . Winkler, J. (2018). A monocyte gene expression signature in the early clinical course of Parkinson's disease. *Sci Rep*, *8*(1), 10757. doi:10.1038/s41598-018-28986-7
- Schulte, T., Schols, L., Muller, T., Voitalla, D., Berger, K., & Kruger, R. (2002). Polymorphisms in the interleukin-1 alpha and beta genes and the risk for Parkinson's disease. *Neurosci Lett*, *326*(1), 70-72. doi:10.1016/s0304-3940(02)00301-4
- Seidler, S., Zimmermann, H. W., Bartneck, M., Trautwein, C., & Tacke, F. (2010). Age-dependent alterations of monocyte subsets and monocyte-related chemokine pathways in healthy adults. *BMC Immunol*, *11*, 30. doi:10.1186/1471-2172-11-30
- Shen, C. H., Chou, C. H., Liu, F. C., Lin, T. Y., Huang, W. Y., Wang, Y. C., & Kao, C. H. (2016). Association Between Tuberculosis and Parkinson Disease: A Nationwide, Population-Based Cohort Study. *Medicine (Baltimore)*, *95*(8), e2883. doi:10.1097/MD.0000000000002883
- Shen, X., Yang, H., Wu, Y., Zhang, D., & Jiang, H. (2017). Meta-analysis: Association of Helicobacter pylori infection with Parkinson's diseases. *Helicobacter*, *22*(5). doi:10.1111/hel.12398
- Sheng, Z., Zhang, S., Bustos, D., Kleinheinz, T., Le Pichon, C. E., Dominguez, S. L., . . . Zhu, H. (2012). Ser1292 autophosphorylation is an indicator of LRRK2 kinase activity and contributes to the cellular effects of PD mutations. *Sci Transl Med*, *4*(164), 164ra161. doi:10.1126/scitranslmed.3004485
- Sheu, J. J., Wang, K. H., Lin, H. C., & Huang, C. C. (2013). Psoriasis is associated with an increased risk of parkinsonism: a population-based 5-year follow-up study. *J Am Acad Dermatol*, *68*(6), 992-999. doi:10.1016/j.jaad.2012.12.961
- Shutinoski, B., Hakimi, M., Harmsen, I. E., Lunn, M., Rocha, J., Lengacher, N., . . . Schlossmacher, M. G. (2019). Lrrk2 alleles modulate inflammation during microbial infection of mice in a sex-dependent manner. *Sci Transl Med*, *11*(511). doi:10.1126/scitranslmed.aas9292
- Siddiqui, M. F., Rast, S., Lynn, M. J., Auchus, A. P., & Pfeiffer, R. F. (2002). Autonomic dysfunction in Parkinson's disease: a comprehensive symptom survey. *Parkinsonism Relat Disord*, *8*(4), 277-284. doi:10.1016/s1353-8020(01)00052-9
- Simon, D. K., Tanner, C. M., & Brundin, P. (2020). Parkinson Disease Epidemiology, Pathology, Genetics, and Pathophysiology. *Clin Geriatr Med*, *36*(1), 1-12. doi:10.1016/j.cger.2019.08.002
- Simon-Sanchez, J., Herranz-Perez, V., Olucha-Bordonau, F., & Perez-Tur, J. (2006). LRRK2 is expressed in areas affected by Parkinson's disease in the adult mouse brain. *Eur J Neurosci*, *23*(3), 659-666. doi:10.1111/j.1460-9568.2006.04616.x

- Simon-Sanchez, J., Schulte, C., Bras, J. M., Sharma, M., Gibbs, J. R., Berg, D., . . . Gasser, T. (2009). Genome-wide association study reveals genetic risk underlying Parkinson's disease. *Nat Genet*, *41*(12), 1308-1312. doi:10.1038/ng.487
- Singh, A. K., Tiwari, M. N., Dixit, A., Upadhyay, G., Patel, D. K., Singh, D., . . . Singh, M. P. (2011). Nigrostriatal proteomics of cypermethrin-induced dopaminergic neurodegeneration: microglial activation-dependent and -independent regulations. *Toxicol Sci*, *122*(2), 526-538. doi:10.1093/toxsci/kfr115
- Singh, A. K., Tiwari, M. N., Prakash, O., & Singh, M. P. (2012). A current review of cypermethrin-induced neurotoxicity and nigrostriatal dopaminergic neurodegeneration. *Curr Neuropharmacol*, *10*(1), 64-71. doi:10.2174/157015912799362779
- Singh, A. K., Tiwari, M. N., Upadhyay, G., Patel, D. K., Singh, D., Prakash, O., & Singh, M. P. (2012). Long term exposure to cypermethrin induces nigrostriatal dopaminergic neurodegeneration in adult rats: postnatal exposure enhances the susceptibility during adulthood. *Neurobiol Aging*, *33*(2), 404-415. doi:10.1016/j.neurobiolaging.2010.02.018
- Sloan, M., Alegre-Abarrategui, J., Potgieter, D., Kaufmann, A. K., Exley, R., Deltheil, T., . . . Wade-Martins, R. (2016). LRRK2 BAC transgenic rats develop progressive, L-DOPA-responsive motor impairment, and deficits in dopamine circuit function. *Hum Mol Genet*, *25*(5), 951-963. doi:10.1093/hmg/ddv628
- Smith, W. W., Pei, Z., Jiang, H., Dawson, V. L., Dawson, T. M., & Ross, C. A. (2006). Kinase activity of mutant LRRK2 mediates neuronal toxicity. *Nat Neurosci*, *9*(10), 1231-1233. doi:10.1038/nn1776
- Song, C. H., Fan, X., Exeter, C. J., Hess, E. J., & Jinnah, H. A. (2012). Functional analysis of dopaminergic systems in a DYT1 knock-in mouse model of dystonia. *Neurobiol Dis*, *48*(1), 66-78. doi:10.1016/j.nbd.2012.05.009
- Sossi, V., de La Fuente-Fernandez, R., Holden, J. E., Doudet, D. J., McKenzie, J., Stoessl, A. J., & Ruth, T. J. (2002). Increase in dopamine turnover occurs early in Parkinson's disease: evidence from a new modeling approach to PET 18 F-fluorodopa data. *J Cereb Blood Flow Metab*, *22*(2), 232-239. doi:10.1097/00004647-200202000-00011
- Soudja, S. M., Ruiz, A. L., Marie, J. C., & Lauvau, G. (2012). Inflammatory monocytes activate memory CD8(+) T and innate NK lymphocytes independent of cognate antigen during microbial pathogen invasion. *Immunity*, *37*(3), 549-562. doi:10.1016/j.immuni.2012.05.029
- Sroor, H. M., Hassan, A. M., Zenz, G., Valadez-Cosmes, P., Farzi, A., Holzer, P., . . . Reichmann, F. (2019). Experimental colitis reduces microglial cell activation in the mouse brain without affecting microglial cell numbers. *Sci Rep*, *9*(1), 20217. doi:10.1038/s41598-019-56859-0
- Stark, A. K., & Pakkenberg, B. (2004). Histological changes of the dopaminergic nigrostriatal system in aging. *Cell Tissue Res*, *318*(1), 81-92. doi:10.1007/s00441-004-0972-9
- Steenland, K., Hein, M. J., Cassinelli, R. T., 2nd, Prince, M. M., Nilsen, N. B., Whelan, E. A., . . . Schnorr, T. M. (2006). Polychlorinated biphenyls and neurodegenerative disease mortality in an occupational cohort. *Epidemiology*, *17*(1), 8-13. doi:10.1097/01.ede.0000190707.51536.2b
- Steger, M., Diez, F., Dhekne, H. S., Lis, P., Nirujogi, R. S., Karayel, O., . . . Mann, M. (2017). Systematic proteomic analysis of LRRK2-mediated Rab GTPase phosphorylation establishes a connection to ciliogenesis. *Elife*, *6*. doi:10.7554/eLife.31012
- Steger, M., Tonelli, F., Ito, G., Davies, P., Trost, M., Vetter, M., . . . Mann, M. (2016). Phosphoproteomics reveals that Parkinson's disease kinase LRRK2 regulates a subset of Rab GTPases. *Elife*, *5*. doi:10.7554/eLife.12813
- Stevens, C. H., Rowe, D., Morel-Kopp, M. C., Orr, C., Russell, T., Ranola, M., . . . Halliday, G. M. (2012). Reduced T helper and B lymphocytes in Parkinson's disease. *J Neuroimmunol*, *252*(1-2), 95-99. doi:10.1016/j.jneuroim.2012.07.015

- Su, Y. C., & Qi, X. (2013). Inhibition of excessive mitochondrial fission reduced aberrant autophagy and neuronal damage caused by LRRK2 G2019S mutation. *Hum Mol Genet*, 22(22), 4545-4561. doi:10.1093/hmg/ddt301
- Sulzer, D., Alcalay, R. N., Garretti, F., Cote, L., Kanter, E., Agin-Liebes, J., . . . Sette, A. (2017). T cells from patients with Parkinson's disease recognize alpha-synuclein peptides. *Nature*, 546(7660), 656-661. doi:10.1038/nature22815
- Takagawa, T., Kitani, A., Fuss, I., Levine, B., Brant, S. R., Peter, I., . . . Strober, W. (2018). An increase in LRRK2 suppresses autophagy and enhances Dectin-1-induced immunity in a mouse model of colitis. *Sci Transl Med*, 10(444). doi:10.1126/scitranslmed.aan8162
- Tan, E. K., Peng, R., Teo, Y. Y., Tan, L. C., Angeles, D., Ho, P., . . . Wu, R. M. (2010). Multiple LRRK2 variants modulate risk of Parkinson disease: a Chinese multicenter study. *Hum Mutat*, 31(5), 561-568. doi:10.1002/humu.21225
- Tanner, C. M., & Goldman, S. M. (1996). Epidemiology of Parkinson's disease. *Neurol Clin*, 14(2), 317-335. Retrieved from <https://www.ncbi.nlm.nih.gov/pubmed/8827174>
- Tanner, C. M., Kamel, F., Ross, G. W., Hoppin, J. A., Goldman, S. M., Korell, M., . . . Langston, J. W. (2011). Rotenone, paraquat, and Parkinson's disease. *Environ Health Perspect*, 119(6), 866-872. doi:10.1289/ehp.1002839
- Tansey, M. G., & Goldberg, M. S. (2010). Neuroinflammation in Parkinson's disease: its role in neuronal death and implications for therapeutic intervention. *Neurobiol Dis*, 37(3), 510-518. doi:10.1016/j.nbd.2009.11.004
- Thaler, A., Ash, E., Gan-Or, Z., Orr-Urtreger, A., & Giladi, N. (2009). The LRRK2 G2019S mutation as the cause of Parkinson's disease in Ashkenazi Jews. *J Neural Transm (Vienna)*, 116(11), 1473-1482. doi:10.1007/s00702-009-0303-0
- Thevenet, J., Pescini Gobert, R., Hooft van Huijsduijnen, R., Wiessner, C., & Sagot, Y. J. (2011). Regulation of LRRK2 expression points to a functional role in human monocyte maturation. *PLoS One*, 6(6), e21519. doi:10.1371/journal.pone.0021519
- Thomas, J. M., Li, T., Yang, W., Xue, F., Fishman, P. S., & Smith, W. W. (2016). 68 and FX2149 Attenuate Mutant LRRK2-R1441C-Induced Neural Transport Impairment. *Front Aging Neurosci*, 8, 337. doi:10.3389/fnagi.2016.00337
- Tiwari, M. N., Singh, A. K., Ahmad, I., Upadhyay, G., Singh, D., Patel, D. K., . . . Singh, M. P. (2010). Effects of cypermethrin on monoamine transporters, xenobiotic metabolizing enzymes and lipid peroxidation in the rat nigrostriatal system. *Free Radic Res*, 44(12), 1416-1424. doi:10.3109/10715762.2010.512041
- Ton, T. G., Heckbert, S. R., Longstreth, W. T., Jr., Rossing, M. A., Kukull, W. A., Franklin, G. M., . . . Checkoway, H. (2006). Nonsteroidal anti-inflammatory drugs and risk of Parkinson's disease. *Mov Disord*, 21(7), 964-969. doi:10.1002/mds.20856
- Tong, Y., Giaime, E., Yamaguchi, H., Ichimura, T., Liu, Y., Si, H., . . . Shen, J. (2012). Loss of leucine-rich repeat kinase 2 causes age-dependent bi-phasic alterations of the autophagy pathway. *Mol Neurodegener*, 7, 2. doi:10.1186/1750-1326-7-2
- Tong, Y., Pisani, A., Martella, G., Karouani, M., Yamaguchi, H., Pothos, E. N., & Shen, J. (2009). R1441C mutation in LRRK2 impairs dopaminergic neurotransmission in mice. *Proc Natl Acad Sci U S A*, 106(34), 14622-14627. doi:10.1073/pnas.0906334106
- Tong, Y., Yamaguchi, H., Giaime, E., Boyle, S., Kopan, R., Kelleher, R. J., 3rd, & Shen, J. (2010). Loss of leucine-rich repeat kinase 2 causes impairment of protein degradation pathways, accumulation of alpha-synuclein, and apoptotic cell death in aged mice. *Proc Natl Acad Sci U S A*, 107(21), 9879-9884. doi:10.1073/pnas.1004676107
- Travassos, L. H., Carneiro, L. A., Ramjeet, M., Hussey, S., Kim, Y. G., Magalhaes, J. G., . . . Philpott, D. J. (2010). Nod1 and Nod2 direct autophagy by recruiting ATG16L1 to the plasma membrane at the site of bacterial entry. *Nat Immunol*, 11(1), 55-62. doi:10.1038/ni.1823

- Tronel, C., Largeau, B., Santiago Ribeiro, M. J., Guilloteau, D., Dupont, A. C., & Arlicot, N. (2017). Molecular Targets for PET Imaging of Activated Microglia: The Current Situation and Future Expectations. *Int J Mol Sci*, *18*(4). doi:10.3390/ijms18040802
- Tsika, E., Nguyen, A. P., Dusonchet, J., Colin, P., Schneider, B. L., & Moore, D. J. (2015). Adenoviral-mediated expression of G2019S LRRK2 induces striatal pathology in a kinase-dependent manner in a rat model of Parkinson's disease. *Neurobiol Dis*, *77*, 49-61. doi:10.1016/j.nbd.2015.02.019
- Ueki, A., & Otsuka, M. (2004). Life style risks of Parkinson's disease: association between decreased water intake and constipation. *J Neurol*, *251 Suppl 7*, vii18-23. doi:10.1007/s00415-004-1706-3
- Umemura, A., Oeda, T., Tomita, S., Hayashi, R., Kohsaka, M., Park, K., . . . Sawada, H. (2014). Delirium and high fever are associated with subacute motor deterioration in Parkinson disease: a nested case-control study. *PLoS One*, *9*(6), e94944. doi:10.1371/journal.pone.0094944
- Umeno, J., Asano, K., Matsushita, T., Matsumoto, T., Kiyohara, Y., Iida, M., . . . Kubo, M. (2011). Meta-analysis of published studies identified eight additional common susceptibility loci for Crohn's disease and ulcerative colitis. *Inflamm Bowel Dis*, *17*(12), 2407-2415. doi:10.1002/ibd.21651
- van der Brug, M. P., Singleton, A., Gasser, T., & Lewis, P. A. (2015). Parkinson's disease: From human genetics to clinical trials. *Sci Transl Med*, *7*(305), 205ps220. doi:10.1126/scitranslmed.aaa8280
- van Wilgenburg, B., Browne, C., Vowles, J., & Cowley, S. A. (2013). Efficient, long term production of monocyte-derived macrophages from human pluripotent stem cells under partly-defined and fully-defined conditions. *PLoS One*, *8*(8), e71098. doi:10.1371/journal.pone.0071098
- Vescovini, R., Fagnoni, F. F., Telera, A. R., Bucci, L., Pedrazzoni, M., Magalini, F., . . . Sansoni, P. (2014). Naive and memory CD8 T cell pool homeostasis in advanced aging: impact of age and of antigen-specific responses to cytomegalovirus. *Age (Dordr)*, *36*(2), 625-640. doi:10.1007/s11357-013-9594-z
- Villaran, R. F., Espinosa-Oliva, A. M., Sarmiento, M., De Pablos, R. M., Arguelles, S., Delgado-Cortes, M. J., . . . Machado, A. (2010). Ulcerative colitis exacerbates lipopolysaccharide-induced damage to the nigral dopaminergic system: potential risk factor in Parkinson's disease. *J Neurochem*, *114*(6), 1687-1700. doi:10.1111/j.1471-4159.2010.06879.x
- Villumsen, M., Aznar, S., Pakkenberg, B., Jess, T., & Brudek, T. (2019). Inflammatory bowel disease increases the risk of Parkinson's disease: a Danish nationwide cohort study 1977-2014. *Gut*, *68*(1), 18-24. doi:10.1136/gutjnl-2017-315666
- Volles, M. J., & Lansbury, P. T., Jr. (2007). Relationships between the sequence of alpha-synuclein and its membrane affinity, fibrillization propensity, and yeast toxicity. *J Mol Biol*, *366*(5), 1510-1522. doi:10.1016/j.jmb.2006.12.044
- Volta, M., Cataldi, S., Beccano-Kelly, D., Munsie, L., Tatarnikov, I., Chou, P., . . . Milnerwood, A. J. (2015). Chronic and acute LRRK2 silencing has no long-term behavioral effects, whereas wild-type and mutant LRRK2 overexpression induce motor and cognitive deficits and altered regulation of dopamine release. *Parkinsonism Relat Disord*, *21*(10), 1156-1163. doi:10.1016/j.parkreldis.2015.07.025
- Volta, M., & Melrose, H. (2017). LRRK2 mouse models: dissecting the behavior, striatal neurochemistry and neurophysiology of PD pathogenesis. *Biochem Soc Trans*, *45*(1), 113-122. doi:10.1042/BST20160238
- von Campenhausen, S., Bornschein, B., Wick, R., Botzel, K., Sampaio, C., Poewe, W., . . . Dodel, R. (2005). Prevalence and incidence of Parkinson's disease in Europe. *Eur Neuropsychopharmacol*, *15*(4), 473-490. doi:10.1016/j.euroneuro.2005.04.007

- Wahner, A. D., Sinsheimer, J. S., Bronstein, J. M., & Ritz, B. (2007). Inflammatory cytokine gene polymorphisms and increased risk of Parkinson disease. *Arch Neurol*, *64*(6), 836-840. doi:10.1001/archneur.64.6.836
- Wakabayashi, K., Takahashi, H., Ohama, E., & Ikuta, F. (1990). Parkinson's disease: an immunohistochemical study of Lewy body-containing neurons in the enteric nervous system. *Acta Neuropathol*, *79*(6), 581-583. doi:10.1007/bf00294234
- Wakabayashi, K., Takahashi, H., Takeda, S., Ohama, E., & Ikuta, F. (1988). Parkinson's disease: the presence of Lewy bodies in Auerbach's and Meissner's plexuses. *Acta Neuropathol*, *76*(3), 217-221. doi:10.1007/bf00687767
- Walker, M. D., Dinelle, K., Kornelsen, R., Lee, N. V., Miao, Q., Adam, M., . . . Sossi, V. (2015). [11C]PBR28 PET imaging is sensitive to neuroinflammation in the aged rat. *J Cereb Blood Flow Metab*, *35*(8), 1331-1338. doi:10.1038/jcbfm.2015.54
- Walker, M. D., Volta, M., Cataldi, S., Dinelle, K., Beccano-Kelly, D., Munsie, L., . . . Sossi, V. (2014). Behavioral deficits and striatal DA signaling in LRRK2 p.G2019S transgenic rats: a multimodal investigation including PET neuroimaging. *J Parkinsons Dis*, *4*(3), 483-498. doi:10.3233/JPD-140344
- Wang, D., Xu, L., Lv, L., Su, L. Y., Fan, Y., Zhang, D. F., . . . Yao, Y. G. (2015). Association of the LRRK2 genetic polymorphisms with leprosy in Han Chinese from Southwest China. *Genes Immun*, *16*(2), 112-119. doi:10.1038/gene.2014.72
- Wang, K., Yuan, C. P., Wang, W., Yang, Z. Q., Cui, W., Mu, L. Z., . . . Liu, J. X. (2010). Expression of interleukin 6 in brain and colon of rats with TNBS-induced colitis. *World J Gastroenterol*, *16*(18), 2252-2259. doi:10.3748/wjg.v16.i18.2252
- Wang, X., Yan, M. H., Fujioka, H., Liu, J., Wilson-Delfosse, A., Chen, S. G., . . . Zhu, X. (2012). LRRK2 regulates mitochondrial dynamics and function through direct interaction with DLP1. *Hum Mol Genet*, *21*(9), 1931-1944. doi:10.1093/hmg/dds003
- Wang, Z., Arat, S., Magid-Slav, M., & Brown, J. R. (2018). Meta-analysis of human gene expression in response to Mycobacterium tuberculosis infection reveals potential therapeutic targets. *BMC Syst Biol*, *12*(1), 3. doi:10.1186/s12918-017-0524-z
- Weimers, P., Halfvarson, J., Sachs, M. C., Saunders-Pullman, R., Ludvigsson, J. F., Peter, I., . . . Olen, O. (2019). Inflammatory Bowel Disease and Parkinson's Disease: A Nationwide Swedish Cohort Study. *Inflamm Bowel Dis*, *25*(1), 111-123. doi:10.1093/ibd/izy190
- Weindel, C. G., Bell, S. L., Vail, K. J., West, K. O., Patrick, K. L., & Watson, R. O. (2020). LRRK2 maintains mitochondrial homeostasis and regulates innate immune responses to Mycobacterium tuberculosis. *Elife*, *9*. doi:10.7554/eLife.51071
- Wellcome Trust Case Control, C. (2007). Genome-wide association study of 14,000 cases of seven common diseases and 3,000 shared controls. *Nature*, *447*(7145), 661-678. doi:10.1038/nature05911
- West, A. B. (2017). Achieving neuroprotection with LRRK2 kinase inhibitors in Parkinson disease. *Exp Neurol*, *298*(Pt B), 236-245. doi:10.1016/j.expneurol.2017.07.019
- West, A. B., Cowell, R. M., Daher, J. P., Moehle, M. S., Hinkle, K. M., Melrose, H. L., . . . Volpicelli-Daley, L. A. (2014). Differential LRRK2 expression in the cortex, striatum, and substantia nigra in transgenic and nontransgenic rodents. *J Comp Neurol*, *522*(11), 2465-2480. doi:10.1002/cne.23583
- West, A. B., Moore, D. J., Biskup, S., Bugayenko, A., Smith, W. W., Ross, C. A., . . . Dawson, T. M. (2005). Parkinson's disease-associated mutations in leucine-rich repeat kinase 2 augment kinase activity. *Proc Natl Acad Sci U S A*, *102*(46), 16842-16847. doi:10.1073/pnas.0507360102
- West, A. B., Moore, D. J., Choi, C., Andrabi, S. A., Li, X., Dikeman, D., . . . Dawson, T. M. (2007). Parkinson's disease-associated mutations in LRRK2 link enhanced GTP-binding and kinase activities to neuronal toxicity. *Hum Mol Genet*, *16*(2), 223-232. doi:10.1093/hmg/ddl471

- West, M. J., Slomianka, L., & Gundersen, H. J. (1991). Unbiased stereological estimation of the total number of neurons in the subdivisions of the rat hippocampus using the optical fractionator. *Anat Rec*, *231*(4), 482-497. doi:10.1002/ar.1092310411
- Whitton, P. S. (2007). Inflammation as a causative factor in the aetiology of Parkinson's disease. *Br J Pharmacol*, *150*(8), 963-976. doi:10.1038/sj.bjp.0707167
- Wirdefeldt, K., Adami, H. O., Cole, P., Trichopoulos, D., & Mandel, J. (2011). Epidemiology and etiology of Parkinson's disease: a review of the evidence. *Eur J Epidemiol*, *26 Suppl 1*, S1-58. doi:10.1007/s10654-011-9581-6
- Wirtz, S., Neufert, C., Weigmann, B., & Neurath, M. F. (2007). Chemically induced mouse models of intestinal inflammation. *Nat Protoc*, *2*(3), 541-546. doi:10.1038/nprot.2007.41
- Witoelar, A., Jansen, I. E., Wang, Y., Desikan, R. S., Gibbs, J. R., Blauwendraat, C., . . . United Kingdom Brain Expression Consortium, I. (2017). Genome-wide Pleiotropy Between Parkinson Disease and Autoimmune Diseases. *JAMA Neurol*, *74*(7), 780-792. doi:10.1001/jamaneurol.2017.0469
- Wong, A. Y. W., Oikonomou, V., Paolicelli, G., De Luca, A., Pariano, M., Fric, J., . . . Zelante, T. (2018). Leucine-Rich Repeat Kinase 2 Controls the Ca(2+)/Nuclear Factor of Activated T Cells/IL-2 Pathway during Aspergillus Non-Canonical Autophagy in Dendritic Cells. *Front Immunol*, *9*, 210. doi:10.3389/fimmu.2018.00210
- Wood-Kaczmar, A., Gandhi, S., & Wood, N. W. (2006). Understanding the molecular causes of Parkinson's disease. *Trends Mol Med*, *12*(11), 521-528. doi:10.1016/j.molmed.2006.09.007
- Wyss-Coray, T., & Mucke, L. (2002). Inflammation in neurodegenerative disease--a double-edged sword. *Neuron*, *35*(3), 419-432. doi:10.1016/s0896-6273(02)00794-8
- Xie, X., Luo, X., Liu, N., Li, X., Lou, F., Zheng, Y., & Ren, Y. (2017). Monocytes, microglia, and CD200-CD200R1 signaling are essential in the transmission of inflammation from the periphery to the central nervous system. *J Neurochem*, *141*(2), 222-235. doi:10.1111/jnc.13972
- Xiong, Y., Dawson, T. M., & Dawson, V. L. (2017). Models of LRRK2-Associated Parkinson's Disease. *Adv Neurobiol*, *14*, 163-191. doi:10.1007/978-3-319-49969-7_9
- Yanamandra, K., Gruden, M. A., Casate, V., Meskys, R., Forsgren, L., & Morozova-Roche, L. A. (2011). alpha-synuclein reactive antibodies as diagnostic biomarkers in blood sera of Parkinson's disease patients. *PLoS One*, *6*(4), e18513. doi:10.1371/journal.pone.0018513
- Yang, F., Trolle Lagerros, Y., Bellocco, R., Adami, H. O., Fang, F., Pedersen, N. L., & Wirdefeldt, K. (2015). Physical activity and risk of Parkinson's disease in the Swedish National March Cohort. *Brain*, *138*(Pt 2), 269-275. doi:10.1093/brain/awu323
- Yang, J., Zhang, L., Yu, C., Yang, X. F., & Wang, H. (2014). Monocyte and macrophage differentiation: circulation inflammatory monocyte as biomarker for inflammatory diseases. *Biomark Res*, *2*(1), 1. doi:10.1186/2050-7771-2-1
- Yao, C., El Khoury, R., Wang, W., Byrd, T. A., Pehek, E. A., Thacker, C., . . . Chen, S. G. (2010). LRRK2-mediated neurodegeneration and dysfunction of dopaminergic neurons in a *Caenorhabditis elegans* model of Parkinson's disease. *Neurobiol Dis*, *40*(1), 73-81. doi:10.1016/j.nbd.2010.04.002
- Ye, S. M., & Johnson, R. W. (2001). An age-related decline in interleukin-10 may contribute to the increased expression of interleukin-6 in brain of aged mice. *Neuroimmunomodulation*, *9*(4), 183-192. doi:10.1159/000049025
- Yu, G. I., Ha, E., Park, S. H., Park, J. H., Jang, H. S., Bae, J. H., . . . Song, D. K. (2011). Association of tumor necrosis factor-alpha (TNF-alpha) promoter polymorphisms with overweight/obesity in a Korean population. *Inflamm Res*, *60*(12), 1099-1105. doi:10.1007/s00011-011-0372-z

- Yue, M., Hinkle, K. M., Davies, P., Trushina, E., Fiesel, F. C., Christenson, T. A., . . . Melrose, H. L. (2015). Progressive dopaminergic alterations and mitochondrial abnormalities in LRRK2 G2019S knock-in mice. *Neurobiol Dis*, *78*, 172-195. doi:10.1016/j.nbd.2015.02.031
- Yuzefpolskiy, Y., Baumann, F. M., Kalia, V., & Sarkar, S. (2015). Early CD8 T-cell memory precursors and terminal effectors exhibit equipotent in vivo degranulation. *Cell Mol Immunol*, *12*(4), 400-408. doi:10.1038/cmi.2014.48
- Zhang, F. R., Huang, W., Chen, S. M., Sun, L. D., Liu, H., Li, Y., . . . Liu, J. J. (2009). Genomewide association study of leprosy. *N Engl J Med*, *361*(27), 2609-2618. doi:10.1056/NEJMoa0903753
- Zhang, M., Yao, C., Cai, J., Liu, S., Liu, X. N., Chen, Y., . . . Wang, Y. (2019). LRRK2 is involved in the pathogenesis of system lupus erythematosus through promoting pathogenic antibody production. *J Transl Med*, *17*(1), 37. doi:10.1186/s12967-019-1786-6
- Zhang, P., Fan, Y., Ru, H., Wang, L., Magupalli, V. G., Taylor, S. S., . . . Wu, H. (2019). Crystal structure of the WD40 domain dimer of LRRK2. *Proc Natl Acad Sci U S A*, *116*(5), 1579-1584. doi:10.1073/pnas.1817889116
- Zhang, Q., Pan, Y., Yan, R., Zeng, B., Wang, H., Zhang, X., . . . Liu, Z. (2015). Commensal bacteria direct selective cargo sorting to promote symbiosis. *Nat Immunol*, *16*(9), 918-926. doi:10.1038/ni.3233
- Zhou, H., Huang, C., Tong, J., Hong, W. C., Liu, Y. J., & Xia, X. G. (2011). Temporal expression of mutant LRRK2 in adult rats impairs dopamine reuptake. *Int J Biol Sci*, *7*(6), 753-761. doi:10.7150/ijbs.7.753
- Zhu, F., Li, C., Gong, J., Zhu, W., Gu, L., & Li, N. (2019). The risk of Parkinson's disease in inflammatory bowel disease: A systematic review and meta-analysis. *Dig Liver Dis*, *51*(1), 38-42. doi:10.1016/j.dld.2018.09.017
- Zhu, L., Liu, W., Alkhouri, R., Baker, R. D., Bard, J. E., Quigley, E. M., & Baker, S. S. (2014). Structural changes in the gut microbiome of constipated patients. *Physiol Genomics*, *46*(18), 679-686. doi:10.1152/physiolgenomics.00082.2014
- Zimprich, A., Biskup, S., Leitner, P., Lichtner, P., Farrer, M., Lincoln, S., . . . Gasser, T. (2004). Mutations in LRRK2 cause autosomal-dominant parkinsonism with pleomorphic pathology. *Neuron*, *44*(4), 601-607. doi:10.1016/j.neuron.2004.11.005